# Dynamics of Geometrically Nonlinear Sliding Beams

by

Kamran Behdinan
B.A.Sc., K. N. Toosi University of Technology, 1985
M.A.Sc., Sharif University of Technology, 1988

A Dissertation Submitted in Partial Fulfillment of the Requirements for the Degree of

DOCTOR OF PHILOSOPHY

in the Department of Mechanical Engineering

We accept this dissertation as conforming to the required standard

Dr. B. Tabarrok, Supervisor (Mechanical Engineering)

Dr. M. Nahon, Department Member (Mechanical Engineering)

Dr. R. Podhorodeski, Department Member (Mechanical Engineering)

Dr. W-S. Lu, Outside Member (Electrical & Computer Engineering)

Dr. M.P. Païdoussis, External Examiner (Mechanical Engineering, McGill University)



University of Victoria

Supervisor: Dr. B. Tabarrok


## ABSTRACT

The elasto-dynamics of flexible frame structures is of interest in many areas of engineering. In certain structural systems the deflections can be large enough to warrant a nonlinear analysis. For example, offshore structures, long suspension bridges and other relatively slender structures used in space applications require a geometrically nonlinear analysis. In addition, if the structure has deployable elements, as in some space structures, the required analysis becomes even more complex. Typical examples are spacecraft antennae, radio telescopes, solar panels and space-based manipulators with deployable elements.

The main objective of the present work is to formulate the problem of sliding beams undergoing large rotations and small strains. Further we aim to develop efficient finite element technique for analysis of such complex systems. Finally we wish to examine the nature of the motion of sliding beams and point out its salient features.

We start with two well known approaches in the nonlinear finite element static analysis of highly flexible structures, namely, the updated Lagrangian and the consistent co-rotational methods and extend these techniques to dynamic analysis of geometrically nonlinear beam structures. We analyse several examples by the same methods and compare the performance of each for efficiency and accuracy.

Next, using McIver's extension of Hamilton's principle, we formulate the problem of geometrically flexible sliding beams by two different approaches. In the first the beam slides through a fixed rigid channel with a prescribed sliding motion. In this formulation which we refer to as the sliding beam formulation, the material points on the beam slide relative to a fixed channel. In the second formulation the material points on the fixed beam are observed by a moving observer on a sliding channel and the beam is axially at rest. The governing equations of motion for the two formulations describe the same physical problem and by mapping both to a fixed domain, using proper transformations, we show that the two sets of governing equations become identical.

It is not possible to find analytical solutions to our problem and we choose the Galerkin numerical method to obtain the transient response of the problem for the special case axially rigid beam. Next we follow a more elegant approach wherein we use the developed incremental nonlinear finite element approaches (the updated Lagrangian and the consistent co-rotational method) in conjunction with a variable time domain beam finite elements (where the number of elements is fixed and as mass enters the domain of interest, but the sizes of elements change in a prescribed manner in the undeformed configuration).

To verify the formulation and its computational implementation we analyse many examples and compare our findings with those reported in the literature when possible. We also use these illustrative examples to identify the importance of various terms such as axial flexibility and foreshortening effects. Finally we look into the problem of parametric resonance for the beam with periodically varying length and we show that the regions of stability obtained in the literature, using a linear analysis, do not hold when a more realistic nonlinear analysis is undertaken.

Examiners:

Dr. B. Tabarrok, Supervisor (Mechanical Engineering)

Dr. M. Nahon, Department Member (Mechanical Engineering)

Dr. R. Podhorodeski, Department Member (Mechanical Engineering)

Dr. W-S. Lu, Outside Member (Electrical & Computer Engineering)

Dr. M.P. Païdoussis, External Examiner (Mechanical Engineering,
McGill University)

# Table of Contents

# List of Figures

# Nomenclature

This list defines the symbols used throughout the thesis. The list does not include all the symbols and other symbols are defined as and when they occur. The reader will find some symbols to be assigned for more than one definition however the context in which a symbol is used is clearly pointed out in the text and no ambiguity should arise.

| | |
|---|---|
| $\mathbf{a}_1$, $\mathbf{a}_2$, $\mathbf{b}_1$, $\mathbf{b}_2$ | the axes lying in the cross sectional planes of node 1, 2 |
| $a_0$ to $a_7$ | Newmark time integration coefficients |
| $A$ | beam element cross sectional area |
| ${}_t\bar{\mathbf{A}}$ | incremental strain-displacement matrix in the local coordinates |
| $b$ | beam width |
| ${}_t\bar{\mathbf{B}}_l$ | incremental displacements coefficient matrix for the linear part of strain-displacement relations in local coordinates |
| ${}_t\bar{\mathbf{B}}_{nl}$ | incremental displacements coefficient matrix for the nonlinear part of virtual strain-displacement relations in local coordinates |
| $\mathbf{C}$ | damping matrix |
| $[c_{eq}]$ | element equivalent damping matrix |
| $[c_1]$, $[c_2]$ | element dynamic damping matrix |

| | |
|---|---|
| $\mathbf{C}(t)$ | time varying length of the beam inside the channel |
| $\mathbf{D}$ | element material property matrix |
| $\tilde{\mathbf{e}}_1, \tilde{\mathbf{e}}_2$ | co-rotational axis |
| $E$ | Young's modulus |
| $\tilde{\mathbf{E}}_1, \tilde{\mathbf{E}}_2$ | co-rotational axis at initial configuration |
| $\{f\}$ | element internal force vector |
| $\{\hat{f}\}$ | element internal force vector in the fixed domain |
| $\tilde{\mathbf{f}}$ | element internal force vector |
| $\{f_{eq}\}$ | equivalent sliding inertia force vector |
| $\mathbf{F}_i$ | forces without potential acting on the $i^{\text{th}}$ particle |
| $\mathbf{F}$ | internal force vector |
| $\lfloor f_2 \rfloor^T - \left\lfloor \dfrac{df_1}{dt} \right\rfloor^T$ | element inertia force vector due to sliding motion |
| g | gravitational acceleration |
| $\mathbf{g}_{21}^T, \mathbf{g}_{22}^T, \mathbf{g}_1^T$ | strain vectors related to co-rotational frame |
| $\mathbf{G}$ | strain-displacement matrix |
| $G$ | potential energy of the sliding beam in a uniform gravitational field |
| $h$ | beam height |
| $\mathcal{h}_{ik}$ | matrix of shape functions |
| $\mathcal{H}_{14}$ | component of linear shape functions vector |
| $\lfloor \mathcal{H}_2 \rfloor$ | standard Hermitian shape functions vector |
| $I$ | second moment of area |
| $\mathbf{I}_1, \mathbf{I}_2$ | global coordinate axes, unit vectors |

| | |
|---|---|
| $J$ | Jacobian determinant of the deformation map |
| $[k_{eq}]$ | element equivalent stiffness matrix |
| $[k_m]$ | element stiffness matrix, sliding motion effects |
| $[k_T]$ | element tangent stiffness matrix |
| $\mathbf{k}_{G2}, \mathbf{k}_{G3}$ | geometric tangent stiffness matrices |
| $\mathbf{K}_e, \mathbf{K}_g$ | first and second parts of the element tangent stiffness matrix |
| $\mathbf{k}_{t1}$ | material stiffness matrix |
| $\mathbf{k}_t$ | geometric tangent stiffness matrix |
| $\mathbf{k}_T$ | element tangent stiffness matrix |
| $[K_{eq}]$ | assembled equivalent stiffness matrix |
| $[\hat{k}_m]$ | element stiffness matrix in the fixed domain due to sliding motion |
| $[\hat{k}_{eq}]$ | element equivalent stiffness matrix in the fixed domain |
| $[\hat{k}_T]$ | element tangent stiffness matrix in the fixed domain |
| $l_o$ | initial length of the beam element |
| $l$ | length of the beam element |
| $l_c$ | current beam element length in co-rotational axes |
| $L_B$ | total length of the beam |
| $L$ | beam length |
| $L_1$ | linear part of the equation of motion of axially inextensible sliding beams |
| $\hat{l}(t)$ | element length in the undeformed configuration |
| $\hat{l}_i$ | location of element coordinate system with respect to system coordinate system in the fixed domain |

| | |
|---|---|
| $\hat{L}_i$ | location of element coordinate system with respect to system coordinate system |
| $\hat{L}(t)$ | time varying length of the beam in the undeformed configuration |
| $\mathcal{L}$ | Lagrangian function |
| $\mathcal{L}(\eta)$ | nondimensionalize linear part of the equation of motion of axially inextensible sliding beams |
| $\mathcal{L}_1^G$ | nondimensional additional linear terms due to gravity to be added to the equation of motion of axially inextensible sliding beams in uniform gravitational field |
| $[m]$ | element mass matrix |
| $m_i$ | mass of the $i^{th}$ particle |
| $M_1, M_2$ | nodal bending moments |
| $\mathbf{M}$ | mass matrix |
| $n$ | number of elements |
| $\mathbf{n}$ | normal to the control surface across which mass is transported |
| $\lfloor N \rfloor$ | vector of shape functions |
| $N_1^G$ | additional nonlinear terms due to gravity to be added to the equation of motion of axially inextensible sliding beam in uniform gravitational field |
| pi | $\pi$ |
| P | tip load |
| $P$ | element axial force |
| $q_j$ | modal coefficients |
| $[Q]$ | transformation matrix |

| | |
|---|---|
| $\mathbf{r}$ | element externally applied force vector in global coordinates |
| $\mathbf{r}_i$ | position vector of the $i^{\text{th}}$ particle |
| $\{r\}$, $\{R\}$ | element external force vector, assembled external force vector |
| $\mathbf{R}_m$ | position vector of material point $m$ |
| $\{\hat{r}\}$ | element applied load vector |
| ${}^{t+\Delta t}\bar{\mathbf{R}}$ | nodal applied force vector |
| $s_o(t)$ | open control surface at time $t$ |
| $S$ | curvilinear coordinate of a point on the centerline of the beam |
| ${}^{t}_{t}\mathbf{S}$ | stress vector at time $t$ in the coordinate axes |
| ${}^{t+\Delta t}_{t}\mathbf{S}$ | current second Piola-Kirchhoff vector |
| $\langle \bar{S} \rangle$ | element stress matrix |
| $\bar{S}_x$, $\bar{S}_{xy}$, $\bar{S}_{xz}$ | components of the stress vector $\mathbf{S}$ |
| $\mathcal{S}$ | stretched curvilinear coordinate |
| $\delta S_o$, $\delta S$ | the distance between two points lying on the centerline of the beam in the undeformed and deformed configurations |
| $t$ | time |
| $\Delta t$ | time increment |
| $\mathbf{T}_i$ | transformation matrix |
| $T_i^*$ | kinetic co-energy of the $i^{\text{th}}$ element |
| Theta | $\theta$ |
| $\mathbf{u}_1$, $\mathbf{u}_2$ | nodal displacement vector in global coordinate system |
| $u_1$, $u_2$ | displacements components of a material point on the centerline of the beam |

| | |
|---|---|
| $\mathbf{u}_{21}$ | relative displacement vector of node 2 with respect to node 1 in global coordinate system |
| ${}_{t}U_{i}$ | incremental displacement |
| $U_{i}(x, y, z)$ | displacement field |
| $\{\tilde{u}\}$ | nodal degrees of freedom vector |
| $\tilde{u}$ | beam element axial extension |
| ${}_{t}\bar{u}_{k}$ | incremental nodal point displacements |
| $\{\grave{u}\}$ | nodal variables |
| $\hat{u}_{1}, \hat{u}_{2}$ | components of the displacement vector of a material point on the centerline of the beam in the fixed domain: sliding beam formulation |
| $\grave{u}_{1}, \grave{u}_{2}$ | components of the displacement vector of a material point along the element axis |
| $\bar{U}(\zeta)$ | local axial stretch of any point on the centerline of the beam element |
| $\tilde{U}_{2}(\zeta)$ | local transverse displacement of any point on the centerline of the beam element |
| ${}_{t}\bar{U}_{io}$ | incremental displacement field within each element |
| $\frac{\partial\bar{u}_{i3}}{\partial^{t}\bar{x}_{1}}, \frac{\partial\bar{u}_{i2}}{\partial^{t}\bar{x}_{1}}$ | angular displacements of node $i$ with respect to $\bar{y}$ and $\bar{x}$ axes |
| $\mathcal{U}$ | velocity of the particle |
| $\mathcal{v}$ | nondimensional velocity |
| $\mathcal{v}_{i}$ | beam element volume |
| $v_{c}(t)$ | volume of the closed control volume at time $t$ |

| | |
|---|---|
| $v_o(t)$ | volume of the open control volume at time $t$ |
| $v_e$ | element volume |
| $\mathbf{V}_m$ | velocity of a mass point m on the centerline of the beam as seen by a moving observer |
| $\mathbf{V}_{rb}$ | velocity of a point on the centerline due to rigid body sliding motion of the beam |
| $V$ | prescribed sliding velocity of the beam |
| $\mathbf{V}_e$ | velocity of a point on the centerline due to elastic deformation of the beam |
| $\mathcal{V}$ | velocity of the open control surface |
| $\delta\tilde{W}$ | virtual work |
| ${}^{t+\Delta t}x_i$ | current coordinates |
| ${}^{t}x_i$ | coordinates for the last known equilibrium configuration |
| $x, y, z$ | coordinates of any material points in the undeformed configuration of the beam |
| $x_1, x_2$ | material point coordinates in the deformed configuration |
| $X_1$ | coordinate of a material point on the centerline of the beam in the undeformed configuration with respect to the material frame |
| $\bar{x}_1, \bar{x}_2$ | coordinates of a material point on the centerline of the beam in the deformed configuration with respect to the moving observer |
| $\chi_1$ | position along the element with respect to element coordinate system |
| $\mathcal{X}_1$ | coordinate of a material point along the element axis in the undeformed configuration with respect to the element local coordinate system |

| | |
|---|---|
| $\alpha$ | the angle between the tangent at a point along the centerline of the beam and the horizontal axis in chapter 3 |
| $\alpha, \beta$ | total nodal rotations in co-rotational formulation, chapter 2 |
| $\alpha, \delta$ | Newmark time integration constants |
| $\beta_i$ | roots of characteristic equation |
| $\varepsilon, \varepsilon_{\chi_1}$ | axial strain |
| $\varepsilon_{eff}$ | effective axial strain |
| $\varepsilon(\tilde{x})$ | rotated engineering strain |
| ${}_t\bar{\varepsilon}_{ij}$ | incremental Green-Lagrange strains |
| $\delta_t\bar{\varepsilon}$ | incremental virtual strain tensor |
| $\zeta$ | natural local coordinate along the beam axis |
| $\zeta_1, \zeta_2$ | damping coefficients |
| $\eta_1, \eta_2$ | stretched coordinates for the sliding beam formulation |
| $\eta$ | nondimensional transverse displacement |
| $\bar{\eta}_1, \bar{\eta}_2$ | stretched coordinates for the alternative formulation |
| $\theta_o$ | angular displacement |
| $\bar{\theta}_i$ | nodal angular displacements with respect to $\bar{z}$ axis |
| $\tilde{\theta}_1, \tilde{\theta}_2$ | nodal rotational degrees of freedom |
| $\tilde{\theta}_o$ | initial local slope |
| $\kappa$ | curvature due to transverse local displacements |
| $\xi$ | element natural coordinate |
| $\Pi$ | the strain energy of the beam |

| | |
|---|---|
| $\rho, \rho_o$ | mass density, mass density in the undeformed configuration |
| $\sigma$ | stress tensor |
| ${}^t\tau$ | Cauchy stress vector |
| $\boldsymbol{\tau}$ | unit vector tangent to the centerline of the beam at some material point |
| $\tau$ | nondimensional time |
| $\bar{\phi}$ | out of balance force vector |
| $\varphi_o$ | initial orientation of the beam |
| $\varphi$ | total orientation of the co-rotational axis |
| $\varphi_i$ | rigid body rotation of the co-rotational axis of the i$^{th}$ element |
| $\phi$ | out of balance force vector in global coordinates |
| $\wp_j$ | modal functions |
| $\chi_1, \chi_2$ | material point coordinates in the undeformed configuration |
| $\omega_i$ | instantaneous $i^{th}$ natural frequency of the beam |
| $\varpi_1$ | the first natural frequency of the beam at initial configuration |

## Acronyms

| | |
|---|---|
| CPU | central processing unit |
| 2D | two dimensional |
| 3D | three dimensional |
| CESM | co-rotational engineering strain measure |
| CGSM | co-rotational Green-Lagrange strain measure |
| Eng. | engineering strain measure |

| | |
|---|---|
| G.L. | Green-Lagrange strain measure |
| elm | element |
| inc. | increment |
| ODE | ordinary differential equation |
| d.o.f. | degree of freedom |
| CC | consistent co-rotational |
| UL | updated Lagrangian |
| FE | finite element |

## Operators

| | |
|---|---|
| $\delta$ | variational operator |
| $\Delta$ | increment operator |
| $D(\ )/Dt$ | material time derivative |
| $d(\ )/dt$ | the time derivative following a control volume |
| $\frac{\partial}{\partial x}$ , $\frac{\partial}{\partial t}$ | partial differentiation with respect to $x$ and $t$ |
| $(\ )'$ , $(\dot{\ })$ | partial differentiation with respect to $x$ and $t$ |

## Coordinate System Variable

| | |
|---|---|
| $(\ )$ | global coordinates |
| $(\tilde{\ })$ | variable in element co-rotational axes |
| $(\hat{\ })$ | variable in the fixed domain (sliding beam formulation) |
| $(\bar{\ })$ | variable in alternative formulation |
| $(\hat{\bar{\ }})$ | variable in the fixed domain (alternative formulation) |
| $(\grave{\ })$ | variable in sliding beam element |

ACKNOWLEDGEMENTS

I am grateful to my supervisor, Professor B. Tabarrok, for his unwavering attention, assistance, encouragement, and support throughout this research. I would like to thank Dr. M.C. Stylianou for many insightful discussions which directly contributed to the quality of this work. Professor J.B. Haddow, kindly, made himself available to periodically review my progress and gave me numerous precious suggestions. Many thanks to all friends at the Department who facilitated the progress of this work by sharing their technical know-how.

I gratefully acknowledge the support of the Ministry of Culture and Higher Education of the I.R.Iran for awarding me the scholarship to pursue my Ph.D. in University of Victoria.

Finally, I am deeply grateful to my family for their guidance, understanding and patience. To them I am indebted.

*To Nasrin,*
*without her love, patience and sacrifices*
*this*
*and much else*
*would not be possible.*

*To Tina and Asha,*
*for their love and patience.*

# Chapter 1

# Introduction

## 1.1 Problem Description and History

The main objective of the present work is to study the dynamics of flexible sliding beams undergoing large rotations and small strains, see Figure 1.1. Thus the problem is geometrically nonlinear and the nonlinearities arise due to significant rigid body rotations in the overall motion of the beam. To develop the ground work for this study we first consider the large deflection analysis of non-sliding beams. This is an active area of research and potentially of interest to structural and aerospace engineers. This leads to an ongoing broad area of nonlinear structural dynamics that is of interest to many researchers in the field.

### 1.1.1 Geometrically Nonlinear Flexible Structures: Statics

Specifically the analysis of flexible structures is of interest in such systems as offshore structures, long suspension bridges and other slender structures which may deflect significantly under loads. Recently renewed interest in this area of study has been motivated by the stringent requirements of the space industry. Structures used in space applications generally have low mass and high flexibility to the extent that in some cases, as in the Canadarm, they cannot support their own weight in 1g environment. For such flexible systems, large displacement behaviour should be included in any type of analysis.

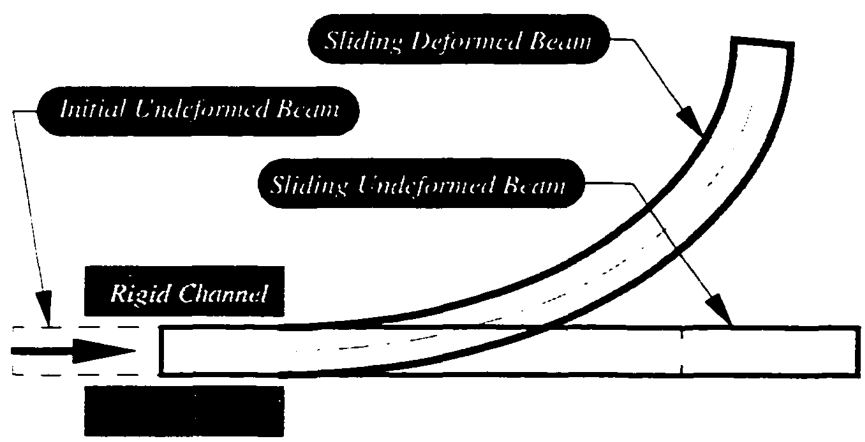


Figure 1.1: A Flexible Sliding Beam.

The subject of large deflections of slender beams has received considerable attention in the past. Specifically in the case of beams of constant length (the elastica), we may refer to Frisch-Fay, 1962, Holden, 1972, and Lau, 1982 and a survey of the relevant literature given by Schmidt and DaDeppo, 1971. For the elastica, elliptic integrals offer exact solutions. Mattiasson, 1981, presented accurate numerical results from large deflection analysis of beams and frames computed by elliptic integrals.

In the more general case, Stoker, 1968, showed that there exists a unique adjusted normal deformation which, when applied to the deformed body, will make the linear strain of the resulting combined deformation small; for then the linear theory is applicable in the neighborhood of a point on the centerline of the beam. Then he used this concept to exemplify the one and two dimensional elastica theory.

In structural analysis, when the equilibrium and kinematic relationships are written in the neighborhood of the undeformed (or original) configuration, the analysis is classified as first order. On the other hand, when the equilibrium and kinematic relationships are written for the deformed configuration, the analysis is referred to as second order. Unlike the first order analysis where the solution procedure is straight forward and relatively simple, in the second order analysis, solutions can normally be found only through iterations. Thus a converged solution is obtained in a step by step manner. At each increment the obtained equilibrium configuration is used to determine the equilibrium configuration in the next increment.

In structural analysis, in general, we have two types of nonlinearities: geometric and material nonlinearity. Geometrical nonlinearity, when small, can be taken into account by the use of stability stiffness functions in a beam-column formulation or by the use of a geometrical (or initial stress) stiffness matrix in a finite element formulation. However when geometric nonlinearities are large so that the current equilibrium configuration differs greatly from the unloaded configuration of the structure, then, a full nonlinear analysis must be undertaken since such an analysis is outside the limitations of the stability functions and the geometric stiffness matrix methods.

While the nonlinear analysis of cable nets (trusses) is by now quite common, frames are still the subject of some interest, e.g. Argyris et al., 1979, Bathe and Bolourchi, 1979, Simo, 1985, Simo and Vu-Quoc, 1986, Rankin and Brogan, 1986, Dvorkin et al., 1988, Meek and Loganathan, 1989, Spillers, 1990, Crisfield, 1990, Saje, 1990, Chen and Agar, 1993, Yang and Leu, 1994, Orth and Surana, 1994, Petrolito, 1995, Pai and Palazotto, 1996 and Crisfield and Moita, 1996. The reason for such prolific literature in this area is due to premature linearization, difficulty of dealing with the kinematics of finite rotations in three dimensions, inaccuracy in the solution and difficulty with the rate of convergence and finally omission of terms in the geometric stiffness matrix that cause significant problems, specifically in the stability analysis of structures. Among the methods developed for structural nonlinearities we will consider: the updated Lagrangian and the consistent co-rotational method because of their efficiency and popularity.

Bathe and Bolourchi, 1979, developed an updated Lagrangian and total Lagrangian formulation for large displacement and large rotation analysis of a three dimensional beam element. Further, they showed that the two formulations yield identical element stiffness matrices and nodal point force vectors. However, in their analysis, they proved that the updated Lagrangian formulation is computationally more effective. Because of premature linearization, their formulation does not include all the nonlinear effects. Also, the variation of the transformation matrix is not considered in their solution procedures. Thus their formulation fails for very large deflections of some problems such as a slender cantilever subjected to a large end moment. The computational cost of their formulation is also relatively high. Some other researchers have attempted to increase the efficiency of the Bathe and Bolourchi formulation, e.g. Chen and Agar, 1993, who presented a technique to express the geometric stiffness matrix either by a one dimensional integration of the stress resultants or a closed form computation of element-end forces.

The co-rotational method was first introduced by Wempner, 1969, and further developed by Belytschko and Hsieh, 1973, and Belytschko and Glaum, 1979. Further progress was made by: Rankin and Brogan, 1986, Hsiao, 1987, Nour-Omid and Rankin, 1991 and Crisfield et al., (1990, 1992, 1996). The adoption of co-rotational approach allows, at the element level, simple strain measures to be used and the consistent derivation of the tangent stiffness matrix and the out of balance force vector leads to improved efficiency and accuracy in the solution. The effect of the coordinate system on the accuracy of co-rotational formulation was also studied by Iura, 1994. He showed that numerical solutions obtained by the co-rotational formulation approach the solutions based on the theory of finite displacements with increasing number of elements. It was also shown that the convergence of numerical solutions obtained by the secant coordinates is faster than that by the tangent coordinates.

The pioneering work of Rankin and Brogan, 1986, in which a general approach applicable to any structural element was presented, freed the consistent co-rotational formulation from the specifics of any element. Earlier works on the consistent co-rotational formulation were element dependent. Further investigation on the use of projectors in finite rotation analysis and consistent linearization was undertaken and Crisfield and Moita developed the co-rotational method as a unified framework for solids, shells and beams in 1996. This method has shown good potential for geometrically nonlinear problems and its further development is needed for dynamic analysis of structures. This latter development is undertaken in the present study.

### 1.1.2 Geometrically Nonlinear Flexible Structures: Dynamics

Generally linear and nonlinear dynamic problems are classified, depending on the effect of the spectral characteristics of the excitation on the overall structural response, as wave propagation problems and inertial problems.

Wave propagation problems are those in which the behaviour at the wave front is of engineering importance, and in such cases it is the intermediate and high frequency structural modes that dominate the response throughout the time span of interest. Dynamic problems not classified as wave propagation are considered as inertial type. In this case the response is governed by a relatively small number of low frequency modes. Problems that fall into this category are seismic response and large deformations of elastic/elasto-plastic structures. These problems are often called structural dynamics problems.

Generally, wave propagation problems are best solved using an explicit time integration method whereas implicit time integration schemes are more effective for structural dynamics problems (see e.g. Dokainish and Subbaraj, 1989). Improvements in high speed digital computers has opened the way for more efficient time integration schemes for solution of dynamic transient problems, see Hughes and Belytschko, 1983. This has resulted in efficient algorithms in many commercially available FE programs such as, ANSYS, MARC, ADINA, NONSAP, NASTRAN, etc. (Fredriksso et al., 1983). In this respect we may refer to Hughes, 1976, Hilber et al., 1977, Zienkiewicz et al., 1980, Bathe, 1982, Belytschko and Hughes, 1983, Lopez-Almansa et al., 1988, Argyris and Mlejnek, 1991, Simo and Wong, 1991, Simo and Tarnow, 1992, Simo et al., 1992 (a,b), Chung and Lee, 1994, Crisfield and Shi, 1994, Tarnow and Simo, 1994, Simo and Tarnow, 1994, Simo et al., 1995, Leung and Mao, 1995 and Owren and Simonsen, 1995.

The unconditional stability of the many conventional implicit time integration schemes (e.g. Newmark direct time integration) for linear systems does not hold for nonlinear systems (see e.g. Argyris et al., 1991). For nonlinear analysis, the developed time integration methods are of the predictor/corrector iteration type used for nonlinear statics. The conventional methods often require small time steps to prevent blow up or locking in the solution (see Crisfield et al., 1994). Several researchers have attempted to overcome these difficulties, e.g., Haug et al., 1977, and Hughes et al., 1978, who used the Lagrangian multiplier to enforce an energy constraint.

In the solution procedures, the time integration schemes are completely divorced from the element methodology (with the exception of the provision of the mass matrix) and these schemes satisfy the dynamic equilibrium at the end of each time step. Recent attempts by Simo and Wong, 1991, Simo and Tarnow, 1992, Simo et al., 1992 and Crisfield and Shi, 1994 explore the idea of mid-point equilibrium as initially suggested by Hilber et al., 1977, and Zienkiewicz et al. 1980.

In the past two decades the dynamic behaviour of geometrically nonlinear flexible beams has been investigated by several approaches such as: the inertial frame approach (e.g. Bathe et al., 1975, and Geradin and Cardona, 1989), the floating frame approach (e.g. Kane and Levinson, 1981a,b), the geometrically-exact theory (e.g. Simo and Vu-Quoc, 1986 and 1988), the convected co-ordinate approach (e.g. Belytschko and Hsieh, 1973, and Belytschko et al., 1977) and the co-rotational approach (Hsiao and Jang, 1991, Elkaranshawy and Dokainish, 1995, and Iura and Atluri, 1995).

Because of the simple expression for the kinetic co-energy, the inertial frame approach has been frequently employed in the dynamic analysis of solids. Although the elastic deformations are small, the nonlinearity due to rigid-body motion of the beam must be considered in the kinematics of motion. Depending on the nonlinearities in the system, the linearization of equations of motion may introduce errors which may build up and ultimately result in solution instability. For this reason it may be necessary to iterate at each load step until, within the necessary assumptions on the variation of the material parameters and the numerical time integration, the equations of motion are satisfied to a prescribed tolerance.

The use of floating frame, relative to which the strains in the beams are measured, is motivated by the assumption of infinitesimal strains. This type of formulation leads to implicit, nonlinear and highly coupled equations of motion. In order to simplify the inertia operator, the geometrically-exact theory was developed which conceptually is similar to the inertia frame approach but uses a more advanced beam theory capable of accounting for large rotations of the beam.

In the convected co-ordinate technique and direct nodal force computational scheme, the large displacement effects are treated entirely by transformations of the displacement and force components between the global and convected element co-ordinates. The inertial and external forces are evaluated in the fixed global co-ordinates, while the internal forces are calculated from the stress components measured in the convected co-ordinates. The governing equations of motion are derived under the conditions that the local nodal forces of an element must be self-equilibrated. It is obvious that within the iterations, this condition does not always hold, since the out-of-balance forces do not vanish.

The co-rotational formulation provides a simple and expedient method for large displacement analysis avoiding the complexities of the Lagrangian methods. Standard linear beam theory is used with respect to a body-attached follower frame. The nonlinearity is taken into account by the rotation of this follower frame. The term consistent is used here to describe a general procedure in which virtual variations in local strains are related to virtual variations in the global displacements. This relationship is then used in the virtual work equation to determine the nodal out-of-balance force vector. Differentiation of this expression then leads directly to a consistent tangent stiffness matrix. Using this general procedure, the variation of all local/global transformation matrices is taken into account.

For large deflection dynamic analysis of Euler-Bernoulli beams, using the consistent co-rotational method, there exist no published formulations that take into consideration the inertial effects of the rotating mass matrix. Most researchers have used the element local mass matrices in the local co-rotational frame and transform them to the global co-ordinates during the assembly phase (e.g. Hsiao and Jang, 1991, Elkaranshawy and Dokainish, 1995). This effect becomes significant at high velocities and it has been discussed by researchers in the area of mechanism vibration, see Cleghorn et al., 1981.

### 1.1.3 Flexible Sliding Beams

The flexible sliding beam problem has been the topic of many publications in recent years. This is due to the high demand of such analysis in various industrial applications. Spacecraft antennae (Tabarrok et al., 1974), space based deployable structures and mobile deployable manipulators (Modi and Marom, 1993) are some applications of sliding beams in space industries. Other applications of this problem are associated with cable tramways, band saws, cold and hot rolling processes, magnetic tape drives and machine tools. In this respect we may refer to Mote, 1972, Mote and Wu, 1985, Wickert and Mote, 1988, Abrate, 1992 and Hwang and Perkins, 1994. A related problem is that of a fixed beam subjected to a sliding load such as trains moving on flexible guideway (see Vu-Quoc and Olsson, 1993, and Chang and Liu, 1996).

Applications of this class of moving materials in dynamics which indicates the motion of robot arms with prismatic joints has motivated many researchers in the area. To this end, we may refer to the works of Wang and Wei, 1987, Pan et al., 1990, Yuh and young, 1991 and Tadikonda and Baruh, 1992.

Another related problem is that of pipes conveying fluids. Although physically different, these problems have much in common with sliding beams. Literature on pipes conveying fluids is very extensive and an excellent survey of these problems is given by Païdoussis 1991. Recently, Païdoussis and his co-workers extended the problem of pipes conveying fluid to nonlinear analysis and studied the stability and the chaotic motion of cantilevered pipes (see Semler, 1991, Païdoussis and Semler, 1993, Li and Païdoussis, 1994 and Semler, Li and Païdoussis, 1994).

Most investigations of axially-moving beams deal with beams supported at two fixed points, and it is the transverse motion of the beam within the span that is of interest (Wickert and Mote, 1988). If such a beam is assumed to be axially rigid, then under these conditions, the mass of the system within the domain of interest is conserved for small-amplitude motions. But if the two support points are in motion or more simply the beam is cantilevered the mass will not be conserved.

A comprehensive derivation of the non-linear, coupled longitudinal and transverse equations of motion of the flexible extendible beam was given by Tabarrok et al., 1974, through Newton's Second Law. In addition, it was shown that for a constant axial velocity, oscillatory motions dominate the response during the initial stages of deployment and that, at least within the linear theory, the transverse deflection becomes unbounded with time. Their findings were confirmed by simulations using the assumed-modes technique. The same technique was also employed in an investigation by Cherchas and Gossain, 1974, on the dynamics of a large flexible solar array as it deploys from a spinning spacecraft. Several investigators have also examined the stability of beams under harmonic longitudinal motion for beams of constant length (Elmaraghy and Tabarrok, 1975) and variable length (Zajaczkowski and Lipinski, 1979, Zajaczkowski and Yamada, 1980). Regions of stability and instability in the excitation-amplitude and frequency parameter space were identified.

Recently, flexible extendible beams have gained prominence due to new applications in the area of robotics, specifically in the modeling of flexible links traveling through prismatic joints. Wang and Wei, 1987, used a modified Galerkin method to solve the equation of motion of an axially-moving beam. However, their derivation of the governing equation, through Newton's Second Law, leaves out certain terms and leads to an incorrect expression for the total energy of the system. Yuh and Young, 1991, used the assumed-modes method and compared their simulation results with those obtained experimentally. Their simulation results for cases involving rigid-body angular accelerations are not plausible on physical grounds, and are in disagreement with results obtained by Stylianou and Tabarrok, 1994. Buffinton, 1992, also used the assumed-modes technique to model the moving beam as an unconstrained body, and treated the beam's finite number of supports as kinematical constraints. Kim and Gibson, 1991, used the finite-element approach to model a sliding flexible link. However, the derivation of the complementary kinetic energy of the sliding flexible link, outlined by Kim, 1988, also leaves out certain terms. Stylianou and Tabarrok, 1994, used the finite element method and developed elements with time-varying domains to investigate the dynamics of the flexible extendible beams under more general configurations. Recently, Al-Bedoor and Khulief, 1996, used a transition element, i.e. an element which is partially housed inside the joint hub and with time dependent boundary conditions simulates the prismatic joint constraint. In their work the stiffness of the transition element changes with element length. The remainder of the beam was modelled by conventional finite elements. This method lacks generality and can be used for relatively slow sliding velocities and for short periods of time.

Most of the works cited are concerned with linear axially inextensible sliding beams. This assumption while plausible in most cases, restricts the generality of treatment. There is need to account for axial flexibility in a more realistic formulation. Also in some applications, e.g. space deployable structures or space craft antenna, the deployable element can undergo large displacements and rotations. There is therefore a need for nonlinear analysis of the problem.

Dynamics of sliding beams for large angle maneuvers was considered in a recent work by Vu-Quoc and Li,1995. They used the geometrically exact theory (as developed by Simo, 1985) to formulate two theoretically equivalent formulations: A full Lagrangian version, and an Eulerian Lagrangian version. Then they transformed the system equations from the time variable domain to a fixed domain via the introduction of stretched coordinates. A Galerkin projection was then used to discretize the governing equation of motion and some examples were solved to show the flapping phenomenon where the beam is retrieved.

## 1.2 Thesis Organisation

In chapter 2, we study the statics and dynamics of geometrically nonlinear beams that undergo large rotations but small strains. Two incremental nonlinear finite element methods are used, namely, the updated Lagrangian and the consistent co-rotational methods. We solve several problems with both approaches. Then we compare the results and make comments on the performance of each formulation.

Equations of motion for geometrically nonlinear flexible sliding beams are derived in chapter 3. Based on the Euler-Bernoulli beam theory, the governing equations of motion are given for small deformations through an extension of Hamilton's principle. In another perspective, we provide an alternative formulation wherein the beam is brought to rest and the channel assumes a prescribed sliding motion.

In chapter 4, we first examine the inextensible flexible sliding beam problem undergoing small deformations and transform its governing equation to a fixed domain subsequently and use Galerkin's approach to study the transient response of this problem. We then compare the obtained results with those reported in the literature. Then we extend our approach to the inextensible flexible sliding beams undergoing large amplitude vibrations and solve several examples to show the differences between the solutions obtained via linear and nonlinear solvers.

Chapter 5 is devoted to the finite element discretization of geometrically nonlinear flexible sliding beams. Here we use two approaches. In the first we transform the Lagrangian to the fixed domain by using the stretched coordinates and in the second we employ the variable-domain elements. The two techniques developed in chapter 2 are then used to account for geometrical nonlinearities in the problem.

In chapter 6 we integrate the incremental finite element equations in time to obtain the transient response of the system. Then we consider several examples to show the generality, reliability and performance of the formulations and their implementations. In the first set of examples we restrict the analysis to simple linear inextensible flexible sliding beams and we verify the results obtained by Stylianou, 1993. In the second set of examples, we solve the same problems with the nonlinear effects and comment on the differences between the linear and nonlinear solutions. Then we consider some problems with large deflections (free or forced vibrations) and compare the obtained results for the linear and nonlinear formulations. Finally we consider the case of parametric resonance and show that the unstable regions reported by Zajaczkowski et al., 1979, using a linear analysis do not hold for the nonlinear analysis.

Finally, in chapter 7, we conclude our work and make some suggestions for further research in this area of study.

# Chapter 2

# Nonlinear FE Static and Dynamic Analysis of Beams

The static and dynamic analysis of beams undergoing large deflections are investigated in this chapter. In most cases, for simplicity and better understanding of the basic concepts, we focus attention on two dimensional analysis of beams. The Euler-Bernoulli hypothesis is employed and the beam deforms with large rotations but small strains. We start with the static analysis using the updated Lagrangian and the consistent co-rotational techniques and then we extend both methods to dynamic analysis and obtain transient responses of beam systems. This chapter includes several examples illustrating the implementation and the performance of various formulations.

## 2.1 Nonlinear Finite Element Static Analysis

For the static analysis of beams undergoing large rotations under small strains, two methods are considered herein. The first is the updated Lagrangian formulation as developed by Bathe and Bolourchi, 1979, and the second is the consistent co-rotational method introduced by Crisfield, 1990. These methods are quite different and it is of interest to compare the performance of the two formulations. Such a comparison is carried out at the end of this section. Our objective in this work is twofold. First we will contribute to some aspects of formulations of these methods, particularly in the numerical implementation and second we will use these methods in later chapters for dynamic analysis. Thus in this chapter we lay out the pertinent concepts for large deformation analysis of beams.

### 2.1.1 Updated-Lagrangian Formulation for Beams

In this section an updated Lagrangian formulation is presented for the nonlinear large displacement analysis of beam elements. For sake of generality we consider the three dimensional case.

The essence of this method is the updating of the reference frame at each iteration so that:

$$ {}^{t+\Delta t}x_i = {}^{t}x_i + {}_{t}U_i \tag{2.1.1} $$

where ${}^{t+\Delta t}x_i$ identifies the current coordinates to be used for the new equilibrium configuration and ${}_{t}U_i$ is the incremental displacement from the last known equilibrium configuration to the current configuration.

Due to changes of frame, it is necessary to use a compact notation with clear and specific meanings. To this end we follow the notation introduced by Bathe, 1982. This notation requires symbols with pre and post superscripts and subscripts. Specially we will identify a variable $S$ as:

$$ {}^{t+\Delta t}_{t}S^{i}_{j} $$

where ${}^{t+\Delta t}S$ identifies $S$ at the current configuration at time $t+\Delta t$, ${}_{t}S$ implies $S$ measured at the last known configuration at time $t$, $S^{i}$ computes $S$ at iteration $i$ and $S_j$ defines the components of $S$ with respect to a coordinate system of interest.

#### 2.1.1.1 Displacement Field

In the absence of transverse shear deformations and warping effects, based on the Euler-Bernoulli hypothesis that the cross sections perpendicular to the centroid locus before bending remain plane and perpendicular to the deformed locus after bending and suffer no strains in their planes, the displacement field may be represented approximately by:

$$U_i(x, y, z) = \begin{Bmatrix} U_1(x, y, z) \\ U_2(x, y, z) \\ U_3(x, y, z) \end{Bmatrix} = \begin{Bmatrix} U_{1o} - y \dfrac{\partial U_{2o}}{\partial x} - z \dfrac{\partial U_{3o}}{\partial x} \\ U_{2o} - z\ \theta_o \\ U_{3o} + y\ \theta_o \end{Bmatrix} \tag{2.1.2}$$

where $x$, $y$, $z$ are the coordinates of any material point in the undeformed configuration of the beam measured from the reference axes with $x$ along the neutral axis of the beam and $y$ and $z$ along the principal axes of the beam's cross section. $U_{1o}$, $U_{2o}$ and $U_{3o}$ refer to the centroid displacements and $\theta_o$ is the angular displacement of a point located at radial distance $r(y, z)$ and axial distance $x$.

#### 2.1.1.2 Interpolation Functions

For the general three dimensional prismatic beam element, we consider two nodes with six degrees of freedom per node associated with an axial force, two shear forces, two bending moments and a torque.

The interpolation functions for incremental displacement field within each element, as a function of the incremental *nodal* displacement components $\bar{u}_k$, may be expressed as,

$${}_t\bar{U}_i = {}_t\bar{h}_{ik}\ {}_t\bar{u}_k \tag{2.1.3}$$

where $k = 1,\ldots,12$ (d.o.f.), i=1,2,3 (directions) and the ${}_t\bar{h}_{ik}$ are the interpolation functions corresponding to the local axis ${}^t\bar{x}_i$ and the ${}_t\bar{u}_k$ are the nodal point displacement increments measured with respect to the same local axes at time $t$ (see Figure 2.1.1). The nodal displacement vector for the beam is defined as:

$$
{}_t\bar{u}_k = {}_t\left\lfloor \bar{u}_{11} \quad \bar{u}_{12} \quad \bar{u}_{13} \quad \bar{\theta}_1 \quad \frac{\partial \bar{u}_{13}}{\partial^t \bar{x}_1} \quad \frac{\partial \bar{u}_{12}}{\partial^t \bar{x}_1} \quad \bar{u}_{21} \quad \bar{u}_{22} \quad \bar{u}_{23} \quad \bar{\theta}_2 \quad \frac{\partial \bar{u}_{23}}{\partial^t \bar{x}_1} \quad \frac{\partial \bar{u}_{22}}{\partial^t \bar{x}_1} \right\rfloor^T \tag{2.1.4}
$$

The above notation requires some explanation. The first of the double subscripts for $\bar{u}$ identifies the node of the beam and the second denotes the direction. Thus $\bar{u}_{13}$ is the displacement in the $\bar{x}_3$ direction for the first node of the element. We also point out that barred quantities refer to incremental description in the local coordinate system.

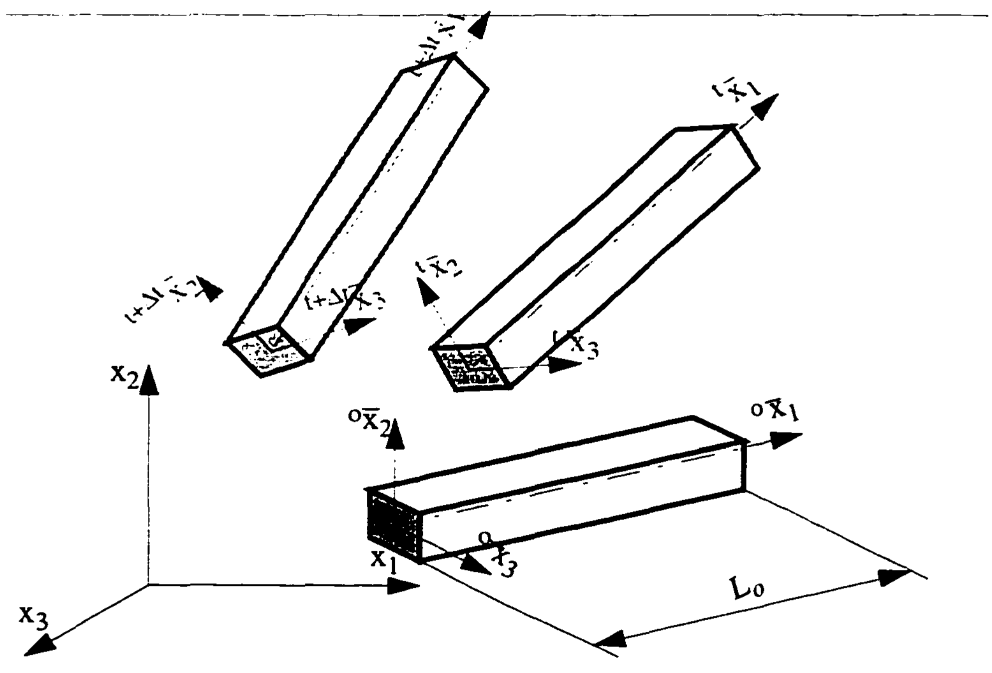


Figure 2.1.1: Updated Lagrangian Formulation: Three dimensional Beam element at different configurations in the Global Coordinate system.

Assuming cubic polynomials for flexural and linear for axial and torsional displacements of the centerline we need to express the displacements at points across the depth and width of the beam as required by equation (2.1.3). This can be done conveniently by introducing the following functions:

$$
\begin{aligned}
f_1 &= \frac{\bar{x}_1}{l} - \left(\frac{\bar{x}_1}{l}\right)^2 & f_2 &= 1 - \frac{4\bar{x}_1}{l} + 3\left(\frac{\bar{x}_1}{l}\right)^2 \\
f_3 &= \frac{2\bar{x}_1}{l} - 3\left(\frac{\bar{x}_1}{l}\right)^2 & f_4 &= 1 - 3\left(\frac{\bar{x}_1}{l}\right)^2 + 2\left(\frac{\bar{x}_1}{l}\right)^3 \\
f_5 &= \frac{\bar{x}_1}{l} - 2\left(\frac{\bar{x}_1}{l}\right)^2 + \left(\frac{\bar{x}_1}{l}\right)^3 & f_6 &= 3\left(\frac{\bar{x}_1}{l}\right)^2 - 2\left(\frac{\bar{x}_1}{l}\right)^3
\end{aligned}
\tag{2.1.5}
$$

Now the displacements of a point within the cross section of the beam may be expressed via equation (2.1.3) where ${}_t h_{ik}$ is given as follows:

$$
{}_t h_{ik} = {}_t\left[\begin{array}{cccccc}
1 - \frac{\bar{x}_1}{l} & \frac{6\bar{x}_2}{l} f_1 & \frac{6\bar{x}_3}{l} f_1 & 0 & \bar{x}_3 f_2 & -\bar{x}_2 f_2 \\
0 & f_4 & 0 & -\left(1 - \frac{\bar{x}_1}{l}\right)\bar{x}_3 & 0 & l f_5 \\
0 & 0 & f_4 & \left(1 - \frac{\bar{x}_1}{l}\right)\bar{x}_2 & -l f_5 & 0 \\
\frac{\bar{x}_1}{l} & -\frac{6\bar{x}_2}{l} f_1 & -\frac{6\bar{x}_3}{l} f_1 & 0 & -f_3\bar{x}_3 & f_3\bar{x}_2 \\
0 & f_6 & 0 & -\frac{\bar{x}_1}{l}\bar{x}_3 & 0 & -\bar{x}_1 f_1 \\
0 & 0 & f_6 & \frac{\bar{x}_1}{l}\bar{x}_2 & \bar{x}_1 f_1 & 0
\end{array}\right]
\tag{2.1.6}
$$

and $l$ is the length of the beam element.

#### 2.1.1.3 Nonlinear Kinematics

In our problem, the strains are small but because of large rotations, the geometry changes significantly requiring nonlinear strain-displacement relationships. One well established approach is to use the Green-Lagrange strain-displacement relations given by:

$$
{}_t\varepsilon_{ij} = \frac{1}{2}\left({}_t\bar{U}_{i,j} + {}_t\bar{U}_{j,i} + {}_t\bar{U}_{k,i}\ {}_t\bar{U}_{k,j}\right) \tag{2.1.7}
$$

(here we use the conventional notations in continuum mechanics). We may express ${}_t\varepsilon_{ij}$ in two parts, linear and nonlinear, as:

$$ {}_t\varepsilon_{ij} = {}_t\bar{e}_{ij} + {}_t\eta_{ij} \tag{2.1.8} $$

where for the incremental description the components of the linear part are given by:

$$ \begin{aligned} \bar{e}_{11} &= \frac{\partial \bar{U}_1}{\partial \bar{x}_1} \\ \bar{e}_{12} &= \frac{\partial \bar{U}_1}{\partial \bar{x}_2} + \frac{\partial \bar{U}_2}{\partial \bar{x}_1} \\ \bar{e}_{13} &= \frac{\partial \bar{U}_1}{\partial \bar{x}_3} + \frac{\partial \bar{U}_3}{\partial \bar{x}_1} \end{aligned} \tag{2.1.9} $$

and the components of the nonlinear part are expressed as:

$$ \begin{aligned} \eta_{11} &= \frac{1}{2}\left[\left(\frac{\partial \bar{U}_1}{\partial \bar{x}_1}\right)^2 + \left(\frac{\partial \bar{U}_2}{\partial \bar{x}_1}\right)^2 + \left(\frac{\partial \bar{U}_3}{\partial \bar{x}_1}\right)^2\right] \\ \eta_{12} &= \frac{1}{2}\left[\left(\frac{\partial \bar{U}_1}{\partial \bar{x}_1}\right)\left(\frac{\partial \bar{U}_1}{\partial \bar{x}_2}\right) + \left(\frac{\partial \bar{U}_3}{\partial \bar{x}_1}\right)\left(\frac{\partial \bar{U}_3}{\partial \bar{x}_2}\right)\right] \\ \eta_{13} &= \frac{1}{2}\left[\left(\frac{\partial \bar{U}_1}{\partial \bar{x}_1}\right)\left(\frac{\partial \bar{U}_1}{\partial \bar{x}_3}\right) + \left(\frac{\partial \bar{U}_2}{\partial \bar{x}_1}\right)\left(\frac{\partial \bar{U}_2}{\partial \bar{x}_3}\right)\right] \end{aligned} \tag{2.1.10} $$

By substituting equation (2.1.3) into equations (2.1.9) and (2.1.10), we may express equation (2.1.8) in a matrix form as:

$$ {}_t\boldsymbol{\varepsilon} = {}_t\mathbf{B}_l \; {}_t\bar{\mathbf{u}} + \frac{1}{2} \; {}_t\bar{\mathbf{A}} \; {}_t\bar{\boldsymbol{\theta}} \tag{2.1.11} $$

where:

$$ {}_t\mathbf{B}_l = \begin{bmatrix} {}_t\bar{h}_{11,1} & \cdots\cdots\cdots & {}_t\bar{h}_{1k,1} & \cdots\cdots\cdots \\ {}_t\bar{h}_{11,2} + {}_t\bar{h}_{21,1} & \cdots\cdots\cdots & {}_t\bar{h}_{1k,2} + {}_t\bar{h}_{2k,1} & \cdots\cdots\cdots \\ {}_t\bar{h}_{11,3} + {}_t\bar{h}_{31,1} & \cdots\cdots\cdots & {}_t\bar{h}_{1k,3} + {}_t\bar{h}_{3k,1} & \cdots\cdots\cdots \end{bmatrix} \tag{2.1.12} $$

$$ {}_t\bar{\boldsymbol{\theta}} = {}_t\left[\frac{\partial \bar{U}_1}{\partial^t\bar{x}_1} \quad \frac{\partial \bar{U}_2}{\partial^t\bar{x}_1} \quad \frac{\partial \bar{U}_3}{\partial^t\bar{x}_1} \quad \frac{\partial \bar{U}_1}{\partial^t\bar{x}_2} \quad \frac{\partial \bar{U}_3}{\partial^t\bar{x}_2} \quad \frac{\partial \bar{U}_1}{\partial^t\bar{x}_3} \quad \frac{\partial \bar{U}_2}{\partial^t\bar{x}_3}\right]^T \tag{2.1.13} $$

$$ {}_t\bar{\mathbf{A}} = {}_t\begin{bmatrix} \frac{\partial \bar{U}_1}{\partial^t\bar{x}_1} & \frac{\partial \bar{U}_2}{\partial^t\bar{x}_1} & \frac{\partial \bar{U}_3}{\partial^t\bar{x}_1} & 0 & 0 & 0 & 0 \\ \frac{\partial \bar{U}_1}{\partial^t\bar{x}_2} & 0 & \frac{\partial \bar{U}_3}{\partial^t\bar{x}_2} & \frac{\partial \bar{U}_1}{\partial^t\bar{x}_1} & \frac{\partial \bar{U}_3}{\partial^t\bar{x}_1} & 0 & 0 \\ \frac{\partial \bar{U}_1}{\partial^t\bar{x}_3} & \frac{\partial \bar{U}_2}{\partial^t\bar{x}_3} & 0 & 0 & 0 & \frac{\partial \bar{U}_1}{\partial^t\bar{x}_1} & \frac{\partial \bar{U}_2}{\partial^t\bar{x}_1} \end{bmatrix} \tag{2.1.14} $$

Now from equation (2.1.11) we obtain an expression for virtual strains as follows:

$$ \begin{aligned} \delta_t\bar{\varepsilon} &= \delta_t(\mathbf{B}_l\ \bar{\mathbf{u}}) + \frac{1}{2}\ \delta_t(\bar{\mathbf{A}}\ \bar{\theta}) \\ &= {}_t\mathbf{B}_l\ \delta_t\bar{\mathbf{u}} + \frac{1}{2}\ \delta_t\bar{\mathbf{A}}\ {}_t\bar{\theta} + \frac{1}{2}\ {}_t\bar{\mathbf{A}}\ \delta_t\bar{\theta} \end{aligned} \tag{2.1.15} $$

Using equations (2.1.13) and (2.1.14), we may express virtual strains in terms of nodal displacements as follows:

$$ \delta_t\bar{\varepsilon} = ({}_t\mathbf{B}_l + {}_t\bar{\mathbf{A}}\ {}_t\mathbf{B}_{nl})\,\delta_t\bar{\mathbf{u}} \tag{2.1.16} $$

where:

$$ {}_t\mathbf{B}_{nl} = \begin{bmatrix} {}_t\bar{h}_{11,1} \cdots\cdots\cdots {}_t\bar{h}_{1k,1} \cdots\cdots\cdots \\ {}_t\bar{h}_{21,1} \cdots\cdots\cdots {}_t\bar{h}_{2k,1} \cdots\cdots\cdots \\ {}_t\bar{h}_{31,1} \cdots\cdots\cdots {}_t\bar{h}_{3k,1} \cdots\cdots\cdots \\ {}_t\bar{h}_{11,2} \cdots\cdots\cdots {}_t\bar{h}_{1k,2} \cdots\cdots\cdots \\ {}_t\bar{h}_{31,2} \cdots\cdots\cdots {}_t\bar{h}_{3k,2} \cdots\cdots\cdots \\ {}_t\bar{h}_{11,3} \cdots\cdots\cdots {}_t\bar{h}_{1k,3} \cdots\cdots\cdots \\ {}_t\bar{h}_{21,3} \cdots\cdots\cdots {}_t\bar{h}_{2k,3} \cdots\cdots\cdots \end{bmatrix} \tag{2.1.17} $$

In the equations (2.1.12) and (2.1.17), we need to calculate the derivatives of the shape functions with respect to $\bar{x}_1$, $\bar{x}_2$ and $\bar{x}_3$, e.g.:

$$ {}_t\bar{h}_{11,1} = -\frac{1}{l} \qquad (2.1.18)$$

$$ {}_t\bar{h}_{12,1} = \frac{6\,{}^t\bar{x}_2}{l}\left(\frac{1}{l} - \frac{2\,{}^t\bar{x}_1}{l^2}\right) \qquad (2.1.19)$$

#### 2.1.1.4 Constitutive Equations

For small strain problems, the linear elastic constitutive relations take the form:

$$ {}^{t+\Delta t}_{\ \ \ \ t}\mathbf{S} = {}_t\mathbf{D}\,{}_t\varepsilon + {}^t_t\mathbf{S} \qquad (2.1.20)$$

where ${}^{t+\Delta t}_{\ \ \ \ t}\mathbf{S}$ is the current second Piola–Kirchhoff stress vector, ${}_t\mathbf{D}$ is the incremental stress–strain material property matrix and ${}_t\varepsilon$ is the incremental Green–Lagrange strain vector. ${}^t_t\mathbf{S}$ is the stress vector in the coordinate axes at time $t$ and is known from the previous step. Hence it is equivalent to the cauchy stress vector ${}^t\tau$. Then we can write equation (2.1.20) as:

$$ {}^{t+\Delta t}_{\ \ \ \ t}\mathbf{S} = {}_t\mathbf{D}\,{}_t\varepsilon + {}^t\tau \qquad (2.1.21)$$

It is worth pointing out that the Green Lagrange strains and the second Piola–Kirchhoff stress are invariant under rigid body translations and rotations.

#### 2.1.1.5 Equilibrium Equations

The equilibrium equations for a three dimensional beam element, in the local coordinate system at step $t$, may be obtained through the principle of virtual work:

$$ \int_{v_e} \delta\ {}^{t+\Delta t}_{\ \ \ \ t}\varepsilon\ {}^{t+\Delta t}_{\ \ \ \ t}\mathbf{S}\ {}^{t+\Delta t}dv - \delta\ {}^{t+\Delta t}\bar{\mathbf{u}}\ {}^{t+\Delta t}\mathbf{R} = 0 \qquad (2.1.22)$$

where ${}^{t+\Delta t}\mathbf{R}$ denotes the nodal applied force vector in the current coordinates at time $t+\Delta t$.

#### 2.1.1.6 Solution Procedure

For nonlinear structural systems, it is necessary to carry out the analysis in a series of load increments since the equilibrium configuration changes. The equilibrium and kinematic states of the structure at the end of the load increment are used to formulate the stiffness relationship for the solution of the next load increment. Thus, the solution of a nonlinear problem is obtained as a sequence of linearized analyses. Needless to say, the size of the load increment has a significant influence on the solution time and convergence characteristics of the problem. If the size of the load increment is too small, the number of load increments required to cover the load range will be large and considerable CPU time may be required to complete the analysis. On the other hand, if the size of the load increment is too large, the number of iterations required to obtain a solution for a given load step may be large. In some cases, the solution may even diverge.

Among the four commonly used solution schemes for nonlinear problems are: the load control method, the displacement control method, the arc length control method and the work control method. The load control method is chosen for the subject of this thesis. The advantage of this method is its easy implementation and applications to the majority of problems in nonlinear analysis.

The load control method can be applied with or without iterations. If the method is applied without iterations, it is referred to as the simple incremental method (Euler method). The major advantage of this method is its simplicity in application and its essential drawback is that errors tend to accumulate since no iterations are used to bring the calculated equilibrium path back to the true equilibrium path. This so-called drift-off error may become significant for highly nonlinear systems.To reduce the drift-off error, it is advisable to employ an iteration scheme within each load increment to correct for the discrepancy that exists between the external and the internal forces of the system. A convenient way to carry out this iteration is by the load control Newton-Raphson method.

In the load control Newton-Raphson method, iterations tend to eliminate the unbalanced forces at each load step. The presence of unbalanced forces indicates that equilibrium between external and internal forces is violated. This discrepancy is attributed to the errors that arise due to the use of the stiffness matrix developed from the past configuration of the structure and used in the current configuration. If these errors are not corrected, the calculated equilibrium path will drift off from the true equilibrium path. Of course the accuracy of extracting internal forces has a crucial effect on the computed force unbalances.

One obvious advantage of the Newton-Raphson iterative method is that in this approach the drift-off errors can be greatly reduced or eliminated. A drawback is its failure at a limit point such as that in snap-through problems where tangent stiffness matrix becomes singular preventing further advance in the solution.

Returning to equations (2.1.22), which are the elemental equilibrium equations, we first transform these equations to the global axes and assemble them to obtain the global equilibrium equations. These equations can then be solved iteratively by the Newton–Raphson method. At the element level, let us assume:

$$ {}^{t+\Delta t}_{\;\;t}\bar{\Phi}^{i} = \left. \int_{V_e} \left(\mathbf{B}_l + \bar{\mathbf{A}}^{i}\ \mathbf{B}_{nl}\right)^T \left[\mathbf{D}\left(\mathbf{B}_l\ \bar{\mathbf{u}}^{i} + \frac{1}{2}\bar{\mathbf{A}}^{i}\ \bar{\theta}^{i}\right) + {}^{t}\boldsymbol{\tau}\right] dv \right|_{t}^{t+\Delta t} - {}^{t+\Delta t}\mathbf{R} \tag{2.1.23} $$

as the residual term after $i^{th}$ iteration (out of balance force). Then, for the next step which is expected to yield the exact solution, we have by Taylor series expansion:

$$ {}^{t+\Delta t}_{\;\;t}\bar{\Phi}^{i+1} = {}^{t+\Delta t}_{\;\;t}\bar{\Phi}^{i} + \left.\frac{\partial \bar{\Phi}}{\partial \bar{\mathbf{u}}}\right|_{t}^{t+\Delta t}{}^{i} \Delta\bar{\mathbf{u}}^{i} \approx 0 \tag{2.1.24} $$

or:

$$ \left.\frac{\partial \bar{\Phi}}{\partial \bar{\mathbf{u}}}\right|_{t}^{t+\Delta t}{}^{i} \Delta\bar{\mathbf{u}}^{i} = -{}^{t+\Delta t}_{\;\;t}\bar{\Phi}^{i} \tag{2.1.25} $$

and the displacement vector after $(i+1)^{th}$ iteration can be computed as:

$$ {}^{t+\Delta t}\bar{\mathbf{u}}^{i+1} = {}^{t}\bar{\mathbf{u}}^{i} + \Delta\bar{\mathbf{u}}^{i} \tag{2.1.26} $$

The tangent stiffness matrix $\left.\frac{\partial \bar{\Phi}}{\partial \bar{\mathbf{u}}}\right|_{t}^{t+\Delta t}{}^{i}$ consists of two parts as follows:

$$\left. {}^{t+\Delta t}_{t} \frac{\partial \bar{\phi}^{i}}{\partial \bar{\mathbf{u}}} \right| = {}^{t+\Delta t}_{t}\mathbf{K}^{i}_{e} + {}^{t+\Delta t}_{t}\mathbf{K}^{i}_{g} \tag{2.1.27}$$

where

$${}^{t+\Delta t}_{t}\mathbf{K}^{i}_{e} = {}^{t+\Delta t}_{t}\left| \int_{v_e} \left( \bar{\mathbf{B}}_{l} + \bar{\mathbf{A}}^{i}\ \bar{\mathbf{B}}_{nl} \right)^{T} \frac{\partial}{\partial \bar{\mathbf{u}}} \left[ \mathbf{D}\left( \bar{\mathbf{B}}_{l}\ \bar{\mathbf{u}}^{i} + \frac{1}{2}\bar{\mathbf{A}}^{i}\ \bar{\theta}^{i} \right) + {}^{t}\bar{\boldsymbol{\tau}} \right] dv \right| \tag{2.1.28}$$

or

$${}^{t+\Delta t}_{t}\mathbf{K}^{i}_{e} = {}^{t+\Delta t}_{t}\left| \int_{v_e} \left( \bar{\mathbf{B}}_{l} + \bar{\mathbf{A}}^{i}\ \bar{\mathbf{B}}_{nl} \right)^{T} \mathbf{D} \left( \bar{\mathbf{B}}_{l} + \bar{\mathbf{A}}^{i}\ \bar{\mathbf{B}}_{nl} \right) dv \right| \tag{2.1.29}$$

and

$${}^{t+\Delta t}_{t}\mathbf{K}^{i}_{g} = {}^{t+\Delta t}_{t}\left| \int_{v_e} \frac{\partial}{\partial \bar{\mathbf{u}}} \left( \bar{\mathbf{B}}_{l} + \bar{\mathbf{A}}^{i}\ \bar{\mathbf{B}}_{nl} \right)^{T} \left[ \mathbf{D}\left( \bar{\mathbf{B}}_{l}\ \bar{\mathbf{u}}^{i} + \frac{1}{2}\bar{\mathbf{A}}^{i}\ \bar{\theta}^{i} \right) + {}^{t}\bar{\boldsymbol{\tau}} \right] dv \right| \tag{2.1.30}$$

or by using equations (2.1.11) and (2.1.21), we have:

$$\begin{aligned} {}^{t+\Delta t}_{t}\mathbf{K}^{i}_{g} &= {}^{t+\Delta t}_{t}\left| \int_{v_e} \frac{\partial}{\partial \bar{\mathbf{u}}} \left( \bar{\mathbf{B}}_{l} + \bar{\mathbf{A}}^{i}\ \bar{\mathbf{B}}_{nl} \right)^{T}\ \bar{S}\ dv \right| \\ &= {}^{t+\Delta t}_{t}\left| \int_{v_e} \bar{\mathbf{B}}^{T}_{nl}\ \frac{\partial \bar{\mathbf{A}}^{iT}}{\partial \bar{\mathbf{u}}}\ \bar{S}\ dv \right| \end{aligned} \tag{2.1.31}$$

Using equation (2.1.14) and rearranging the matrix $\frac{\partial \bar{\mathbf{A}}^{iT}}{\partial \bar{\mathbf{u}}}\ {}^{t+\Delta t}_{t}\bar{S}$, we obtain:

$${}^{t+\Delta t}_{t}\mathbf{K}^{i}_{g} = {}^{t+\Delta t}_{t}\left| \int_{v_e} \bar{\mathbf{B}}^{T}_{nl}\ \langle \bar{S}^{i} \rangle\ \frac{\partial}{\partial \bar{\mathbf{u}}} (\bar{\mathbf{B}}_{nl}\ \bar{\mathbf{u}})\ dv \right| \tag{2.1.32}$$

or

$${}^{t+\Delta t}_{t}\mathbf{K}^{i}_{g} = {}^{t+\Delta t}_{t}\left| \int_{v_e} \bar{\mathbf{B}}^{T}_{nl} \langle \bar{S}^{i} \rangle \bar{\mathbf{B}}_{nl} dv \right| \tag{2.1.33}$$

In equation (2.1.32), $\langle {}^{t+\Delta t}_{t}\bar{S}^{i} \rangle$ is the stress matrix. We may write $\langle {}^{t+\Delta t}_{t}\bar{S}^{i} \rangle$ as:

$$\langle {}^{t+\Delta t}_{\ t}\tilde{S}^{i} \rangle = {}^{t+\Delta t}_{\ t}\left\|\begin{bmatrix} \tilde{S}_{\bar{x}_1} & 0 & 0 & \tilde{S}_{\bar{x}_1\bar{x}_2} & 0 & \tilde{S}_{\bar{x}_1\bar{x}_3} & 0 \\ 0 & \tilde{S}_{\bar{x}_1} & 0 & 0 & 0 & 0 & \tilde{S}_{\bar{x}_1\bar{x}_3} \\ 0 & 0 & \tilde{S}_{\bar{x}_1} & 0 & \tilde{S}_{\bar{x}_1\bar{x}_2} & 0 & 0 \\ \tilde{S}_{\bar{x}_1\bar{x}_2} & 0 & 0 & 0 & 0 & 0 & 0 \\ 0 & 0 & \tilde{S}_{\bar{x}_1\bar{x}_2} & 0 & 0 & 0 & 0 \\ \tilde{S}_{\bar{x}_1\bar{x}_3} & 0 & 0 & 0 & 0 & 0 & 0 \\ 0 & \tilde{S}_{\bar{x}_1\bar{x}_3} & 0 & 0 & 0 & 0 & 0 \end{bmatrix}\right\|^{i} \qquad (2.1.34)$$

where $\tilde{S}_{\bar{x}_1}$, $\tilde{S}_{\bar{x}_1\bar{x}_2}$, $\tilde{S}_{\bar{x}_1\bar{x}_3}$ are the components of the current second Piola-Kirchhoff stress vector.

#### 2.1.1.7 Illustrative Examples

The following examples all involve the use of the modified Newton-Raphson iterative method in conjunction with a tangent stiffness matrix. The modified Newton-Raphson iteration involves fewer stiffness reformations than the full Newton-Raphson iteration, and uses the stiffness matrix of the last equilibrium configuration.

To carry out the integration required for computing the out of balance force vector and tangent stiffness matrix by the symbolic operator program MAPLE, we need to approximate the known Cauchy stress ${}^{t}\tau$. This stress may be approximated in different ways. In our investigations we found the best approximation through a fit of a trilinear shape function to the stress values at the four corners of the two faces of the prismatic beam elements. This shape function is the same as that used for the displacements across the cross sections of the beam.

The convergence criterion is based on the residual energy of the system, measured from out of balance forces $\phi_i$ and incremental displacements $\Delta u_i$ at each load increment as:

$$\phi_i \ \Delta u_i \leq 10^{-5} \qquad (2.1.35)$$

- **Cantilever Subjected to an End Moment**

This two dimensional example provides a severe test for inextensional bending. The initially straight cantilever is subjected to an end moment, as shown in Figure 2.1.2.

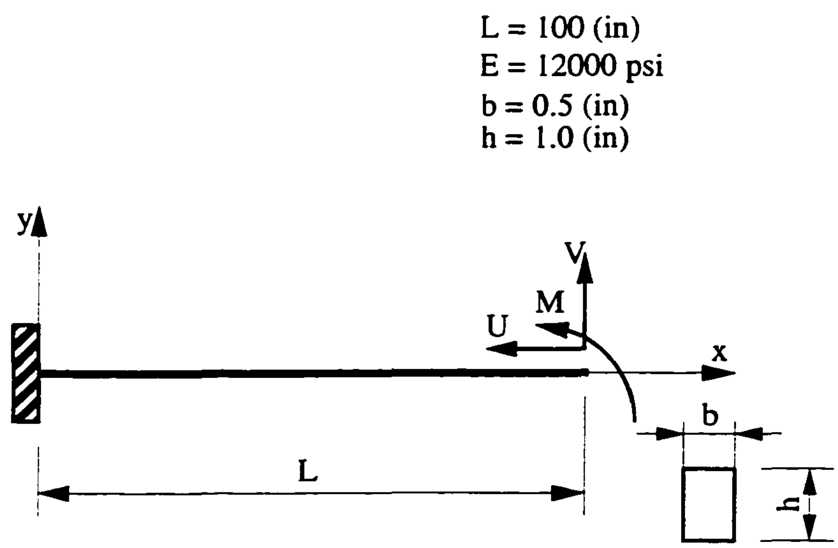


Figure 2.1.2: Cantilever Beam Subjected to an End Moment.

Using eight elements and sixty load increments, the results obtained were found to be in good agreement with the analytical solution (see Cook, 1981), Figures 2.1.3 and 2.1.4 (e.g. M = 1.8 (lb-in), V = 61.0 (in) as against the analytical solution 60.37 (in)). The superiority of these results can be seen when compared with those obtained by Bathe and Bolourchi, 1979. Figures 2.1.5 and 2.1.6 show the effect of the number of load increments and the number of elements used to model and solve this problem. It can be seen that by increasing the number of elements and load increments, the accuracy of the solution also increases but proportionally the cost of computations also increases. By increasing the end moment ($ML/2\pi EI \geq 0.5$), this method fails to yield an accurate solution, see Bathe and Bolourchi, 1979, and Crisfield's comments, 1990.

We also produced the same results using numerical integration (Newton-Cotes method) to form the out of balance force vector and the tangent stiffness matrices, and we found that the CPU time increases dramatically (by an order of magnitude compared with the explicit forming of the system matrices and vectors by MAPLE).

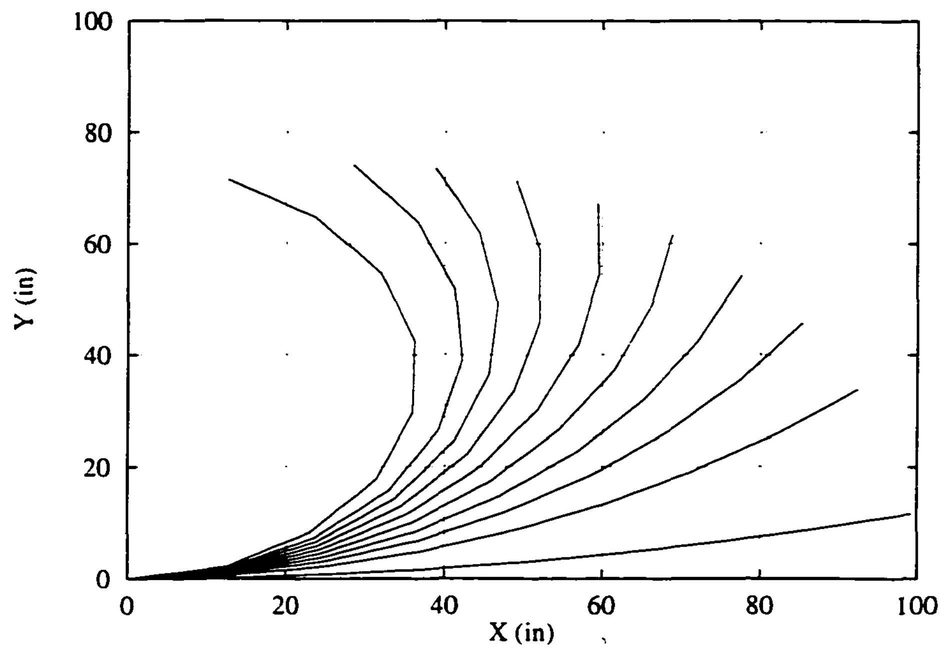


Figure 2.1.3: Cantilever Subjected to an End Moment: Beam Positions.

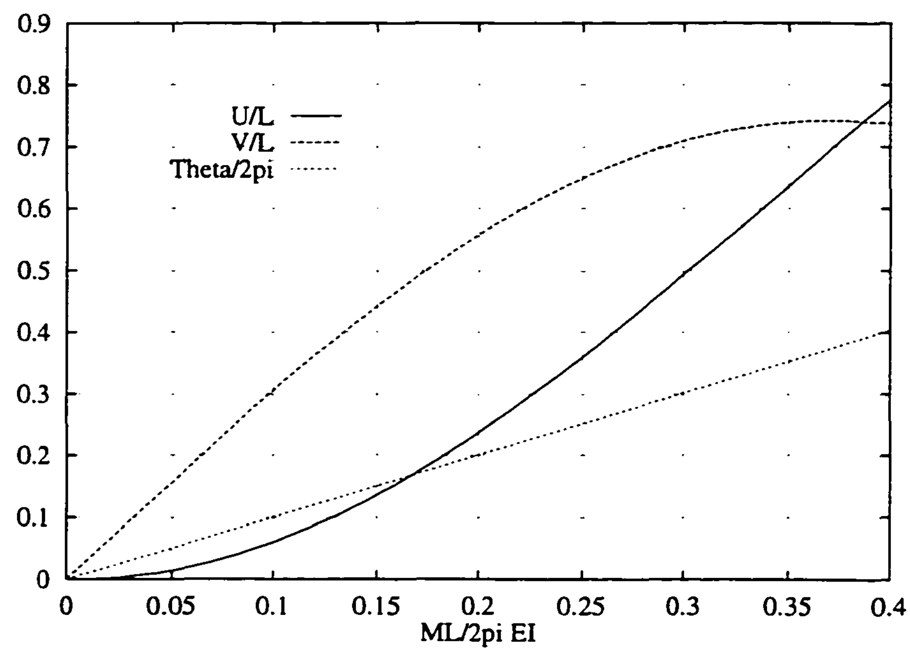


Figure 2.1.4: Cantilever Subjected to an End Moment: Tip Deflections and Slope, 8 Elements, 60 Load Increments.

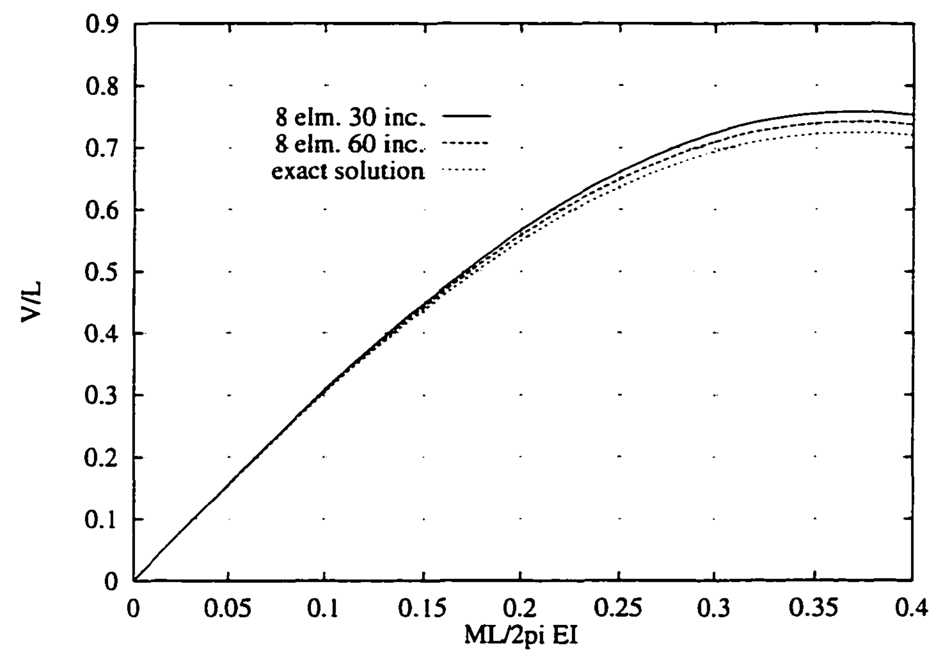


Figure 2.1.5: Cantilever Subjected to an End Moment: Transverse Tip Deflection, 8 Elements and 30 Load Increments, 8 Elements and 60 Load Increments, Exact Solution.

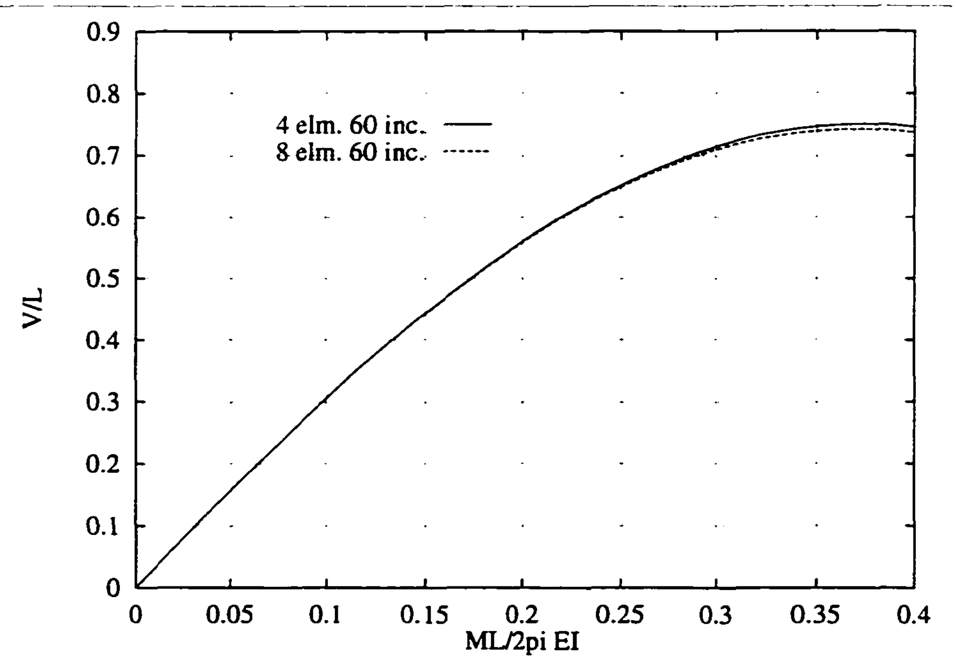


Figure 2.1.6: Cantilever Subjected to an End Moment: Transverse Deflection, 4 Elements and 60 Load Increments, 8 Elements and 60 Load Increments.

- **Cantilever Subjected to a Concentrated Tip Load**

For this problem a large deflection and moderate rotation analysis of a cantilever beam with a concentrated end load (Figure 2.1.7) was carried out and the results obtained are shown in Figures 2.1.8 and 2.1.9. The effects of increasing the number of load increments and elements are also investigated showing increased accuracy at the cost of increased CPU time. The obtained results show a 7% larger transverse tip deflection as compared with the results obtained by Bathe and Bolourchi, 1979 (which are the more accurate ones). This difference is due to the calculation of internal forces from the stiffness matrix rather than the element stresses.

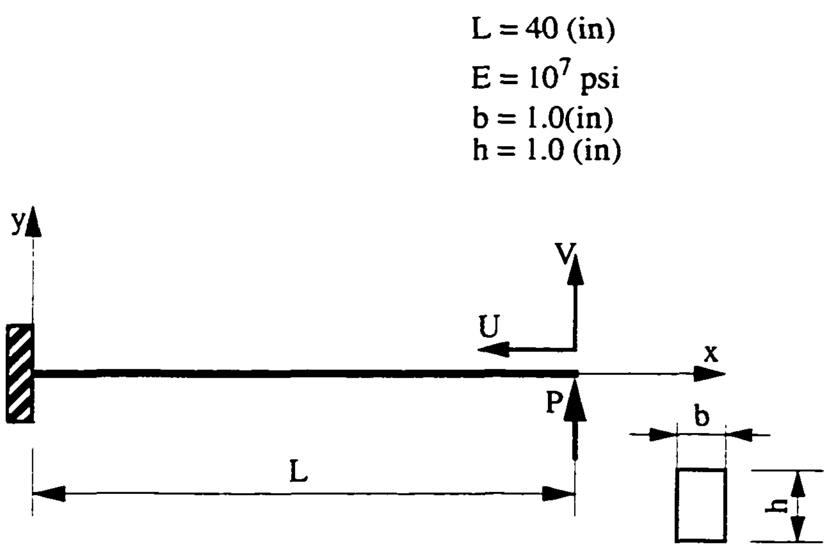


Figure 2.1.7: Cantilever Subjected to a Concentrated Tip Load

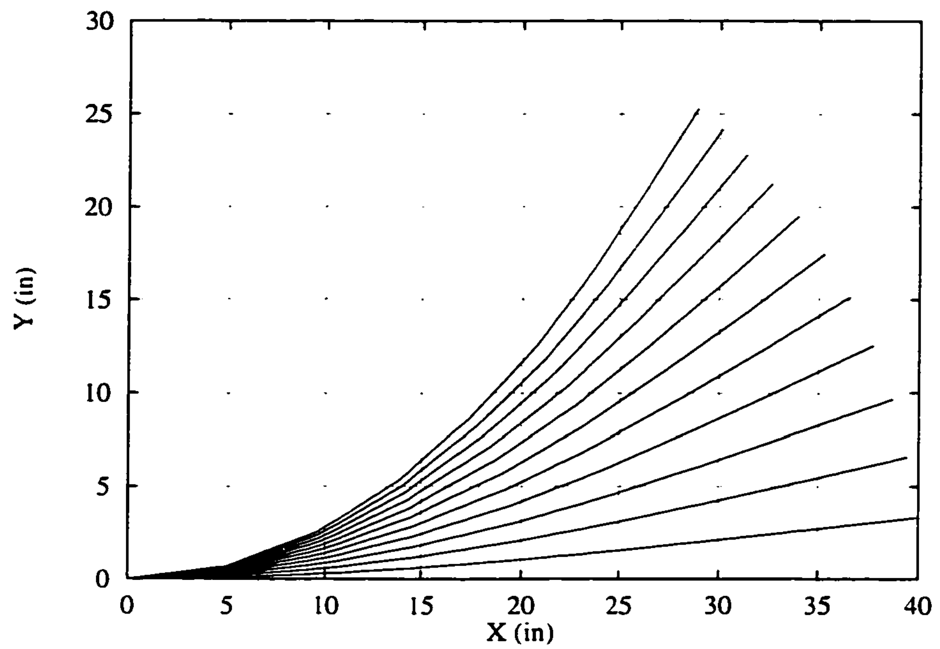


Figure 2.1.8: Cantilever Subjected to a Concentrated Tip Load: Beam Positions.

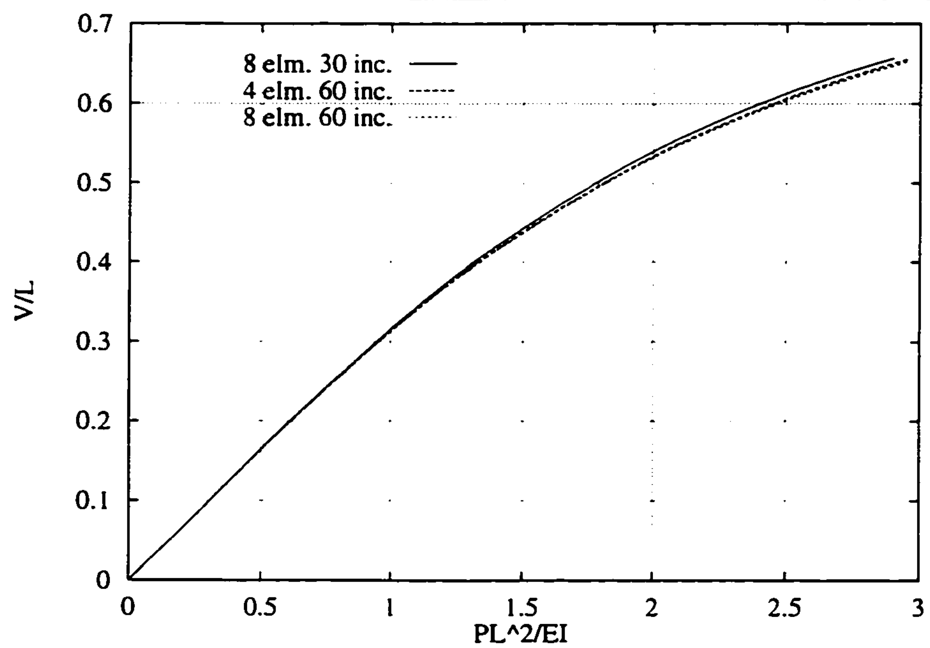


Figure 2.1.9: Cantilever Subjected to a Concentrated Tip Load: Transverse Tip Deflection, 4 Elements and 60 Load Increments, 8 Elements and 30 Load Increments, 8 Elements and 60 Load Increments.

- **Large Displacement 3D Analysis of a 45-Degree Bend**

In this case the large displacement response of a cantilever 45-degree bend subjected to a concentrated end load is considered (see Figure 2.1.10). The concentrated tip load is applied in the $z$-direction. The bend is approximated by eight equal size prismatic beam elements and the solution was carried out using sixty load increments. Figure 2.1.11 shows the results obtained which are in good agreement with those given by Bathe and Bolourchi, 1979 (U = 13.4 (in), V = 23.5 (in) and W = 53.4 (in)). The effects of using lower number of elements and load increments are also investigated and are shown in Figure 2.1.12. Again these effects are consistent with those discussed in the previous examples.

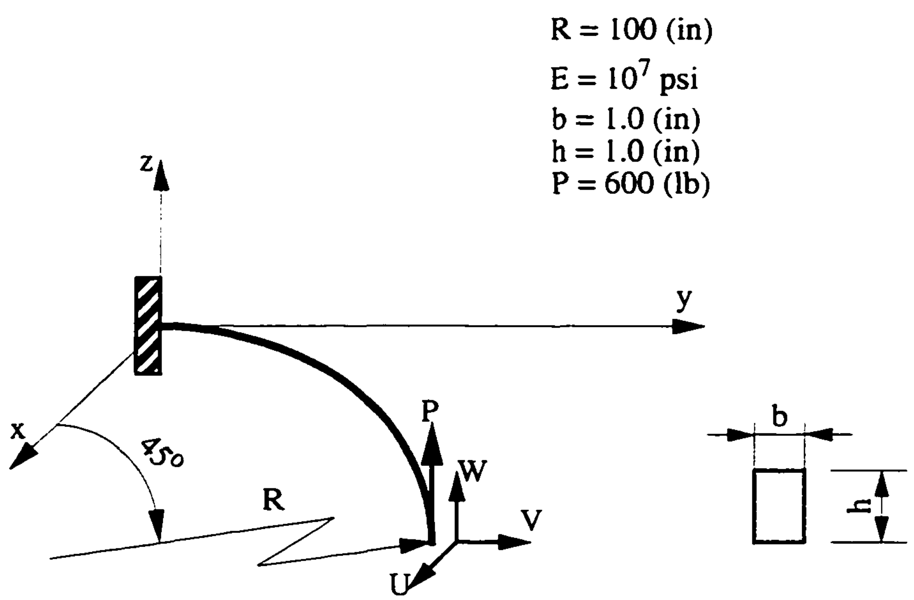


Figure 2.1.10: 3D 45-Degree Bend.

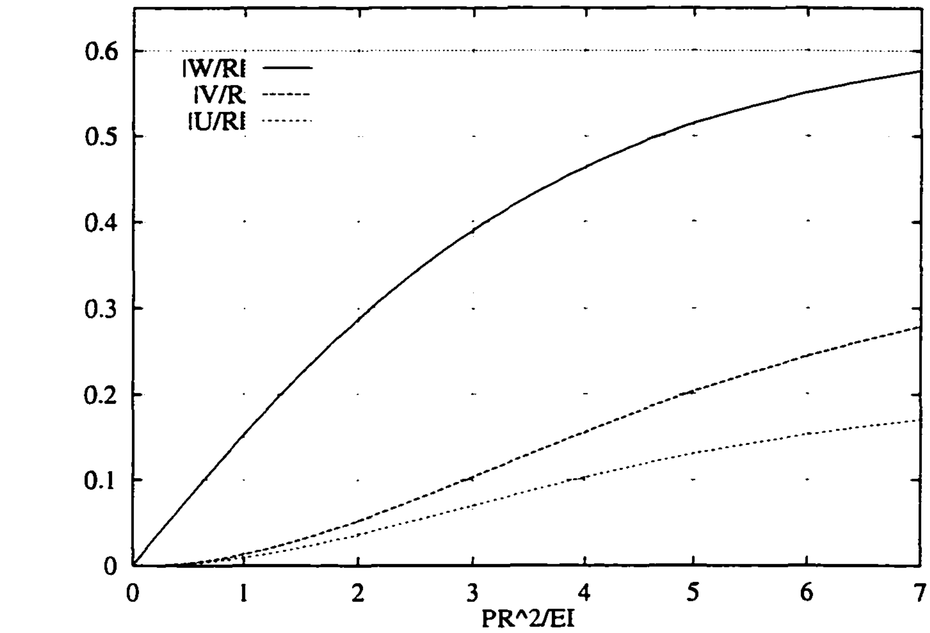


Figure 2.1.11: 3D 45-Degree Bend: Beam Tip Deflections.

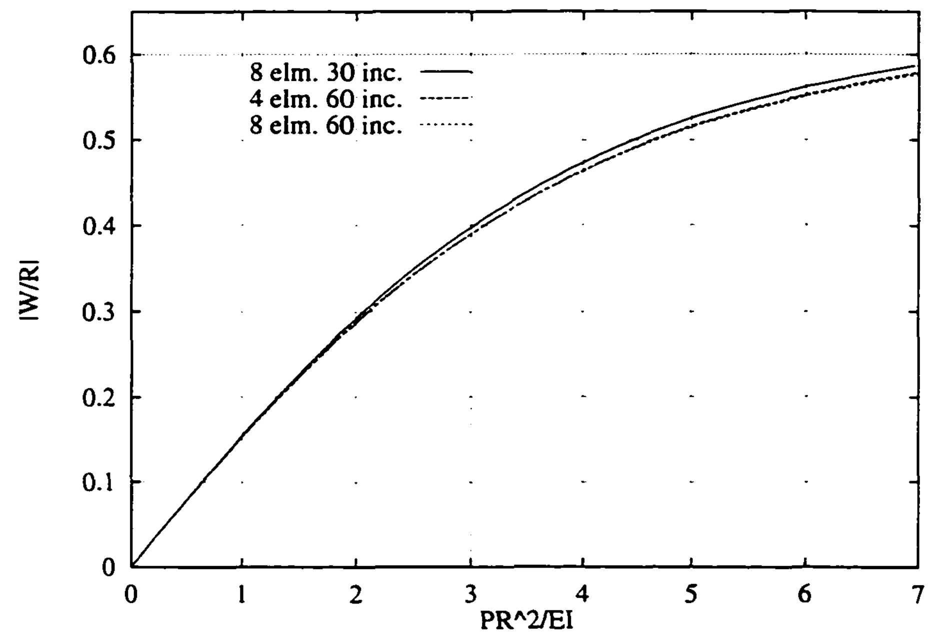


Figure 2.1.12: 3D 45-Degree Bend: Beam Tip Deflection in $z$-direction, 4 Elements and 60 Load Increments, 8 Elements and 30 Load Increments, 8 Elements and 60 Load Increments.

### 2.1.2 Consistent Co-Rotational Formulation for Planar Euler-Bernoulli Beam: Engineering Strain Measures

The term *co-rotational* has been used in a number of different contexts but will be taken here to specify the use of a single element frame that continuously rotates with the element and with respect to which small deformations (Engineering strain measure) or higher order strain measures can be applied. The nonlinearity in the system arises due to the rotation of the co-rotational frame. This approach is in contrast to the total or the updated Lagrangian methods wherein the reference configuration is fixed as the initial or the last equilibrium configuration respectively.

In this work, the term consistent refers to a general scheme whereby variations of the strain in the local coordinate system are related to the variations of the global displacements. With such a relationship established one can develop the (tangent) stiffness equation directly in terms of the global displacements.

The assumption of small strains allows one to use the engineering strain measures in the formulation. The element equations are obtained with respect to the co-rotational axes and are transformed to the global coordinate system through the consistent transformation matrices.

#### 2.1.2.1 Co-Rotational Element Kinematics and Constitutive Relations

Figure 2.1.13 shows the kinematic description of an element. A single body-attached coordinate frame follows the rigid body motion of the beam from its initial configuration $(\tilde{\mathbf{E}}_1, \tilde{\mathbf{E}}_2)$ to the current configuration $(\tilde{\mathbf{e}}_1, \tilde{\mathbf{e}}_2)$. The small deformation based on the engineering strain measures is defined with respect to this co-rotational frame and the nonlinearities are introduced through the rigid body rotation of this frame (see Crisfield, 1990). In this formulation rotational deformations are computed by updating a set of axes which define the orientation of the cross section at each node as the element deforms. The orientation of these axes relative to the co-rotational frame then gives the rotations due to deformations only. In this approach the strain displacement relations are introduced with respect to the local axes and therefore the restriction of the required small rotations for successive load increments is overcome. The obtained local displacements then may be used to evaluate the stresses and strains.

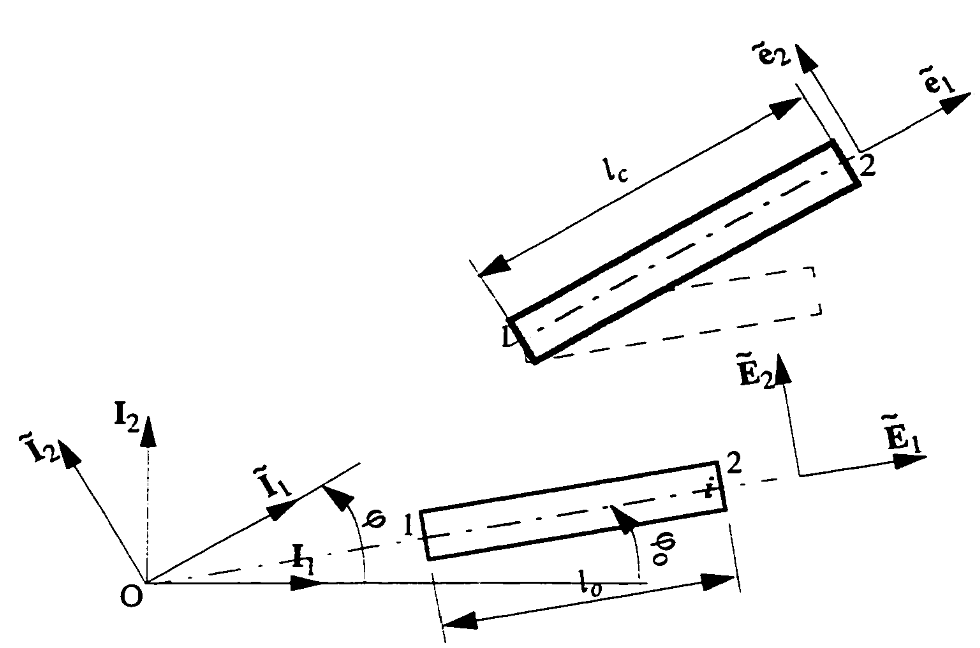


Figure 2.1.13: Consistent Co-rotational Formulation: Kinematics Description.

Linear and standard Hermitian shape functions in the co-rotational frame are used to model the axial and transverse displacement fields for the element, respectively. In keeping with the convention used in co-rotational formulation we will use the natural coordinate $\zeta$ $(=2\bar{x}/l_o - 1)$ to standardize the relevant integrations from -1 to 1. Thus the local axial extension and transverse displacement of any point on the centerline of the beam may be expressed as:

$$\tilde{U}(\zeta) = \mathcal{H}_{14} \quad (\tilde{u}_{21} - \tilde{u}_{11}) \tag{2.1.36}$$

and

$$\tilde{U}_2(\zeta) = \lfloor \mathcal{H}_2 \rfloor \; \{\tilde{u}\} \tag{2.1.37}$$

where

$$\mathcal{H}_{14} = \frac{1}{2}(1+\zeta) \tag{2.1.38}$$

and

$$\lfloor \mathcal{H}_2 \rfloor = \left\lfloor 0, \frac{\zeta^3}{4} - \frac{3}{4}\zeta + \frac{1}{2}, \frac{l_o}{8}\left(\zeta^3 - \zeta^2 - \zeta + 1\right), 0, \frac{1}{2} + \frac{3}{4}\zeta - \frac{\zeta^3}{4}, \frac{l_o}{8}\left(\zeta^3 + \zeta^2 - \zeta - 1\right)\right\rfloor \tag{2.1.39}$$

$l_o$ is the initial chord length of the beam element and

$$\{\bar{u}\} = \lfloor \bar{u}_{11} \quad \bar{u}_{12} \quad \bar{\theta}_1 \quad \bar{u}_{21} \quad \bar{u}_{22} \quad \bar{\theta}_2 \rfloor^T \tag{2.1.40}$$

are the nodal translational and local rotational degrees of freedom. The first and the fourth shape functions are set to zero since the axial effect is taken into consideration via equation (2.1.36).

Let the initial position vectors of nodes 1 and 2, with respect to the global coordinate axes be $\mathbf{x}_1$ and $\mathbf{x}_2$, respectively. The displacement vectors at these nodes may be denoted as $\mathbf{u}_1$ and $\mathbf{u}_2$ in the global coordinate system (see Figure 2.1.14). Then we define:

$$\mathbf{x}_{21} = \mathbf{x}_2 - \mathbf{x}_1 \tag{2.1.41}$$

and

$$\mathbf{u}_{21} = \mathbf{u}_2 - \mathbf{u}_1 \tag{2.1.42}$$

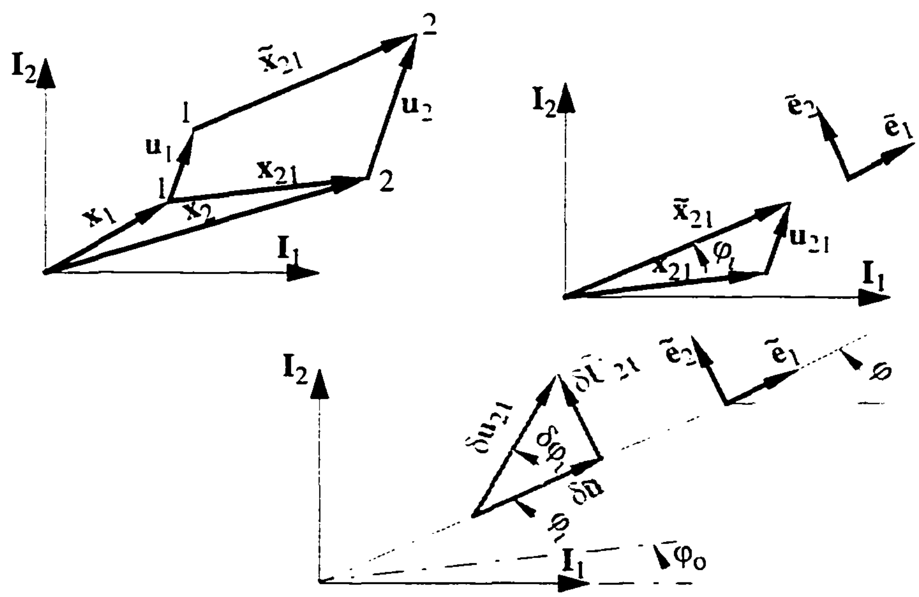

Figure 2.1.14: Consistent Co-rotational Formulation: Definition of Vectors.

Now we may express the net axial extension $\tilde{u} = \tilde{u}_{21} - \tilde{u}_{11}$ as:

$$\tilde{u} = l_c - l_o = \left[(\mathbf{x}_{21} + \mathbf{u}_{21})^T \ (\mathbf{x}_{21} + \mathbf{u}_{21})\right]^{\frac{1}{2}} - \left[\mathbf{x}_{21}^T \ \mathbf{x}_{21}\right]^{\frac{1}{2}} \tag{2.1.43}$$

where $l_c$ is the current chord length of the beam element. Belytschko and Hsieh, 1973, noted that the direct use of the above formula may result in large round-off errors. Following Belytschko and Hsieh we adopt:

$$\begin{aligned} \tilde{u} &= \frac{l_c^2 - l_o^2}{l_c + l_o} = \frac{1}{l_c + l_o}\left(\left[(\mathbf{x}_{21} + \mathbf{u}_{21})^T \ (\mathbf{x}_{21} + \mathbf{u}_{21})\right] - \left[\mathbf{x}_{21}^T \ \mathbf{x}_{21}\right]\right) \\ &= \frac{1}{l_c + l_o}\left[(2\mathbf{x}_{21} + \mathbf{u}_{21})^T \ \mathbf{u}_{21}\right] \end{aligned} \tag{2.1.44}$$

Now we may express the rotated engineering strain, i.e. strain subsequent to a rigid body rotation, (Crisfield, 1991), which is assumed to be constant over the length of the element, with respect to the co-rotational axes as:

$$\varepsilon(\tilde{x}) = \frac{d}{d\tilde{x}}\tilde{U}(\zeta) = \left(\frac{d}{d\zeta}\tilde{U}\right)\left(\frac{d\zeta}{d\tilde{x}}\right) \tag{2.1.45}$$

Given that:

$$\zeta = \frac{2\tilde{x}}{l_o} - 1 \qquad \text{where } (-1 \le \zeta \le 1) \quad \text{and} \quad (0 \le \tilde{x} \le l_o) \tag{2.1.46}$$

and using equations (2.1.36) and (2.1.38), we find:

$$\frac{d}{d\zeta}\tilde{U} = \frac{d\mathcal{H}_{14}}{d\zeta} = \frac{1}{2}\ (\tilde{u}_{21} - \tilde{u}_{11}) = \frac{1}{2}\ \tilde{u} \qquad \text{and} \qquad \frac{d\zeta}{d\tilde{x}} = \frac{2}{l_o} \tag{2.1.47}$$

Substituting equation (2.1.47) into equation (2.1.45), we obtain:

$$\varepsilon(\tilde{x}) = \frac{\tilde{u}}{l_o} \tag{2.1.48}$$

Note that in expression (2.1.45), the effect of element curvature on the axial strain is neglected. The axial force may also be expressed as:

$$P = EA \;\; \varepsilon(\bar{x}) \;\; = EA \;\; \frac{\bar{u}}{l_o} \tag{2.1.49}$$

where $E$ is the modulus of elasticity and $A$ is the cross sectional area of the beam.

We may obtain the curvature due to transverse local displacements as:

$$\kappa \equiv \frac{d^2\bar{U}_2}{d\bar{x}^2} \tag{2.1.50}$$

Using equations (2.1.37) and (2.1.39), we have:

$$\begin{aligned} \frac{d\bar{U}_2}{d\bar{x}} &= \left(\frac{d\bar{U}_2}{d\zeta}\right)\left(\frac{d\zeta}{d\bar{x}}\right) = \frac{1}{4}\begin{bmatrix} 3\zeta^2 - 2\zeta - 1 \\ 3\zeta^2 + 2\zeta - 1 \end{bmatrix}^T \begin{Bmatrix} \bar{\theta}_1 \\ \bar{\theta}_2 \end{Bmatrix} \\ \frac{d^2\bar{U}_2}{d\bar{x}^2} &= \frac{1}{l_o}\begin{bmatrix} 3\zeta - 1 \\ 3\zeta + 1 \end{bmatrix}^T \begin{Bmatrix} \bar{\theta}_1 \\ \bar{\theta}_2 \end{Bmatrix} \end{aligned} \tag{2.1.51}$$

where we have noted that in the co-rotational frame $\bar{u}_{12} = \bar{u}_{22} = 0$.

Now substituting equation (2.1.51) into (2.1.50), we may express the curvature as:

$$\kappa \equiv \frac{d^2\bar{U}_2}{d\bar{x}^2} = \frac{1}{l_o}\begin{bmatrix} 3\zeta - 1 \\ 3\zeta + 1 \end{bmatrix}^T \begin{Bmatrix} \bar{\theta}_1 \\ \bar{\theta}_2 \end{Bmatrix} \tag{2.1.52}$$

Let us consider the beam to be initially straight. The nodal rotations or slopes in the local coordinates are given by: (see Figure 2.1.15)

$$\begin{aligned} \bar{\theta}_1 &= -\arcsin(\mathbf{a}_2 \cdot \bar{\mathbf{e}}_1) \\ \bar{\theta}_2 &= -\arcsin(\mathbf{b}_2 \cdot \bar{\mathbf{e}}_1) \end{aligned} \tag{2.1.53}$$

where $\mathbf{a}_i$, $\mathbf{b}_i$ are the axes lying in the cross sectional planes of nodes 1 and 2, respectively, and $\bar{\mathbf{e}}_1$ is the unit vector along the co-rotational axis which passes through the nodes. These unit vectors may be defined as:

$$\begin{aligned} \mathbf{a}_1 &= [\cos(\alpha + \varphi_o), \sin(\alpha + \varphi_o)]^T \\ \mathbf{a}_2 &= [-\sin(\alpha + \varphi_o), \cos(\alpha + \varphi_o)]^T \end{aligned} \tag{2.1.54}$$

$$\mathbf{b}_1 = [\cos(\beta+\varphi_o), \sin(\beta+\varphi_o)]^T$$
$$\mathbf{b}_2 = [-\sin(\beta+\varphi_o), \cos(\beta+\varphi_o)]^T \tag{2.1.55}$$

$$\tilde{\mathbf{e}}_1 = \frac{1}{l_c}[\mathbf{x}_{21} + \mathbf{u}_{21}] \tag{2.1.56}$$

where $\alpha$, $\beta$ denote the total nodal rotations measured from the element axis in its initial configuration, i.e. the nodal rigid body rotations plus the nodal elastic rotations, (see Figure 2.1.15). $\varphi_o$ is the initial orientation of the beam. Under the assumption that normals to the cross sections remain normals after deformation, $\mathbf{a}_1$ and $\mathbf{b}_1$ remain normal to the cross sections at node 1 and 2, respectively.

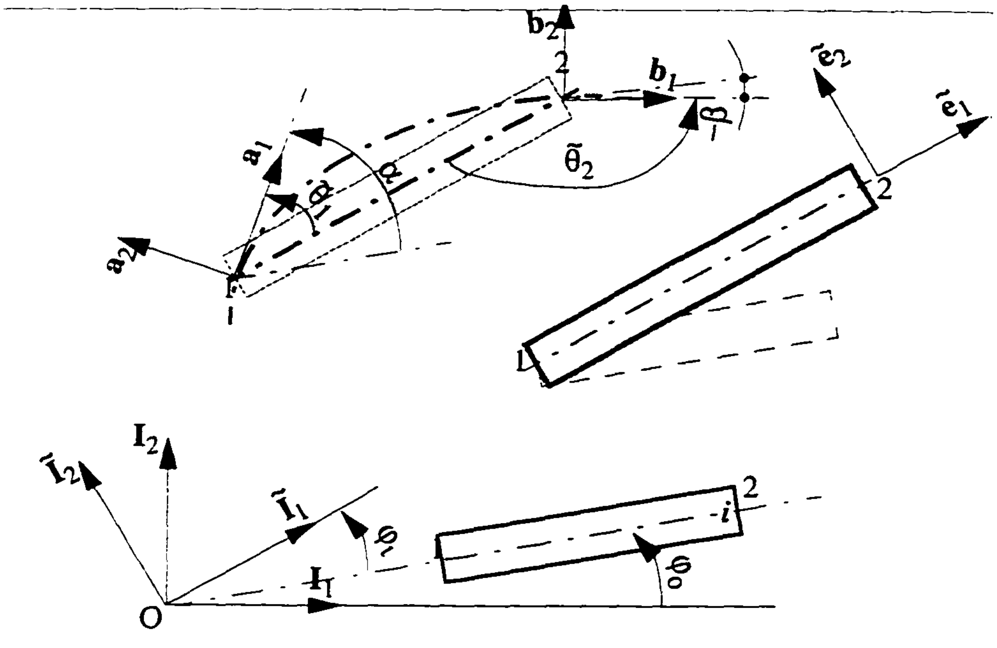

Figure 2.1.15: Consistent Co-rotational Formulation: Rigid body Motion and Elastic Deformation.

### 2.1.2.2 Virtual Displacements in the Local Frame

Using the geometry shown in Figure 2.1.14, the variation of axial extension and nodal slopes used in the principle of virtual work $\delta W = P\delta\tilde{u} + M_1\delta\tilde{\theta}_1 + M_2\delta\tilde{\theta}_2$, may be evaluated.

For element variation of axial extension we have:

$$\delta\tilde{u} = \tilde{\mathbf{e}}_1 \cdot \delta\mathbf{u}_{21} = \begin{bmatrix} \cos\varphi \\ \sin\varphi \end{bmatrix}^T \delta\mathbf{u}_{21} \qquad (2.1.57)$$

where $\varphi$ is the rigid body rotation of the co-rotational axes (see Figure 2.1.14). We intend to express the virtual quantities $\delta\tilde{u}$, $\delta\tilde{\theta}_1$ and $\delta\tilde{\theta}_2$ in terms of the nodal displacements and rotations in the global coordinates. To this end we write $\delta\tilde{u}$ as:

$$\delta\tilde{u} = \mathbf{g}_1^T \, \delta\mathbf{u} \qquad (2.1.58)$$

where

$$\mathbf{g}_1^T = \begin{bmatrix} -\cos\varphi & -\sin\varphi & 0 & \cos\varphi & \sin\varphi & 0 \end{bmatrix} \qquad (2.1.59)$$

and

$$\mathbf{u} = \begin{bmatrix} u_{11} & u_{12} & \alpha & u_{21} & u_{22} & \beta \end{bmatrix}^T \qquad (2.1.60)$$

Consider next the variations of the local elastic slopes. Using equation (2.1.53), we may obtain the variation of the local slopes as:

$$\delta\tilde{\theta}_1 = -\frac{1}{\cos\tilde{\theta}_1} (\delta\mathbf{a}_2 \cdot \tilde{\mathbf{e}}_1 + \mathbf{a}_2 \cdot \delta\tilde{\mathbf{e}}_1) \qquad (2.1.61)$$

Since

$$\delta\mathbf{a}_2 = -\mathbf{a}_1 \, \delta\alpha \qquad (2.1.62)$$

the first term in equation (2.1.61) may be expressed in terms of $\delta\mathbf{u}$ with $\mathbf{u}$ as given in equation (2.1.60). For the second term we find from equation (2.1.56):

$$\delta\tilde{\mathbf{e}}_1 = \delta\left(\frac{1}{l_c}\right)[\mathbf{x}_{21} + \mathbf{u}_{21}] + \frac{1}{l_c}(\delta\mathbf{u}_{21}) \qquad (2.1.63)$$

Since $\delta l_c = \delta\tilde{u}$, then we have

$$\begin{aligned}
\delta\tilde{\mathbf{e}}_1 &= -\frac{1}{l_c^2}[\mathbf{x}_{21}+\mathbf{u}_{21}]\,\delta\tilde{u} + \frac{1}{l_c}(\delta\mathbf{u}_{21}) \\
&= -\frac{1}{l_c^2}[\mathbf{x}_{21}+\mathbf{u}_{21}]\,(\tilde{\mathbf{e}}_1\cdot\delta\mathbf{u}_{21}) + \frac{1}{l_c}(\delta\mathbf{u}_{21}) \\
&= -\frac{1}{l_c}\;(\tilde{\mathbf{e}}_1\otimes\tilde{\mathbf{e}}_1)\,\delta\mathbf{u}_{21} + \frac{1}{l_c}\;\delta\mathbf{u}_{21} \\
&= \mathbf{A}\;\;\delta\mathbf{u}_{21}
\end{aligned} \tag{2.1.64}$$

where

$$\mathbf{A} = \frac{1}{l_c}[\mathbf{I}-\tilde{\mathbf{e}}_1\otimes\tilde{\mathbf{e}}_1] \tag{2.1.65}$$

The symbol $\otimes$ denotes the dyadic product of the two vectors.

In equation (2.1.65), **I** is a $(2\times 2)$ unit matrix. Now substituting equations (2.1.62) and (2.1.64) into equation (2.1.61), we obtain:

$$\delta\tilde{\theta}_1 = -\frac{1}{\cos\tilde{\theta}_1}\;(-\tilde{\mathbf{e}}_1\cdot\;\mathbf{a}_1\;\delta\alpha + \mathbf{a}_2\cdot\;\mathbf{A}\;\delta\mathbf{u}_{21}) \tag{2.1.66}$$

or

$$\delta\tilde{\theta}_1 = -\frac{1}{\cos\tilde{\theta}_1}\;\mathbf{g}_{21}\cdot\delta\mathbf{u} \tag{2.1.67}$$

where

$$\mathbf{g}_{21}^T = \lfloor -\mathbf{a}_2\;\mathbf{A} \quad -\tilde{\mathbf{e}}_1\cdot\mathbf{a}_1 \quad \mathbf{a}_2\;\mathbf{A} \quad 0 \rfloor \tag{2.1.68}$$

A similar expression can be found for $\delta\tilde{\theta}_2$:

$$\delta\tilde{\theta}_2 = -\frac{1}{\cos\tilde{\theta}_2}\;\mathbf{g}_{22}\cdot\delta\mathbf{u} \tag{2.1.69}$$

where

$$\mathbf{g}_{22}^T = \lfloor -\mathbf{b}_2\;\mathbf{A} \quad 0 \quad \mathbf{b}_2\;\mathbf{A} \quad -\tilde{\mathbf{e}}_1\cdot\mathbf{b}_1 \rfloor \tag{2.1.70}$$

Now using equations (2.1.57), (2.1.67) and (2.1.69), we may express the relationship between the local nodal virtual displacement vector and the global nodal displacement vector as:

$$\delta\tilde{\mathbf{u}} = \begin{Bmatrix} \delta\tilde{u} \\ \delta\tilde{\theta}_1 \\ \delta\tilde{\theta}_2 \end{Bmatrix} = \begin{bmatrix} \mathbf{g}_1^T \\ \mathbf{g}_2^T \end{bmatrix} \delta\mathbf{u} = \mathbf{G}^T \ \delta\mathbf{u} \tag{2.1.71}$$

where

$$\mathbf{g}_2 = \left[ -\frac{1}{\cos\tilde{\theta}_1} \ \mathbf{g}_{21}^T, \quad -\frac{1}{\cos\tilde{\theta}_2} \ \mathbf{g}_{22}^T \right] \tag{2.1.72}$$

### 2.1.2.3 Equilibrium Equations

The virtual work expression for internal forces may be written as:

$$\begin{aligned} \delta\tilde{W} &= P\delta\tilde{u} + M_1\delta\tilde{\theta}_1 + M_2\delta\tilde{\theta}_2 \\ &= \delta\tilde{\mathbf{u}}^T \ \tilde{\mathbf{f}} = \delta\mathbf{u}^T \ \mathbf{G} \ \tilde{\mathbf{f}} \end{aligned} \tag{2.1.73}$$

where

$$\tilde{\mathbf{f}} = \lfloor P \quad M_1 \quad M_2 \rfloor^T \tag{2.1.74}$$

and

$$\begin{Bmatrix} P \\ M_1 \\ M_2 \end{Bmatrix} = \frac{1}{l_o} \begin{bmatrix} EA & 0 & 0 \\ 0 & 4EI & 2EI \\ 0 & 2EI & 4EI \end{bmatrix} \begin{Bmatrix} \tilde{u} \\ \tilde{\theta}_1 \\ \tilde{\theta}_2 \end{Bmatrix} \tag{2.1.75}$$

Now we may use the principle of virtual work and obtain the element equilibrium equation in the global coordinate system, i.e.:

$$\mathbf{G} \ \tilde{\mathbf{f}} - \mathbf{r} = 0 \tag{2.1.76}$$

where $\mathbf{r}$ is the element externally applied force vector expressed in the global coordinates. The nodal out of balance force vector may be defined as:

$$\phi = \mathbf{G}\ \tilde{\mathbf{f}} - \mathbf{r} \tag{2.1.77}$$

For satisfaction of the equilibrium equation, $\phi$ must vanish. Before embarking on the numerical solution it is worth noting that $\phi$ is in general a function of $\tilde{\theta}_1$, $\tilde{\theta}_2$, $\tilde{u}$ and $\varphi$. However the source of nonlinearity is limited to the rotation of the co-rotational axes namely $\varphi$. In Appendix H we explicitly demonstrate the nonlinear dependence of the out of balance force $\phi$ in the orientation of the axis $\varphi$.

For implementation of the Newton-Raphson method we expand $\phi$ by Taylor series and find:

$$\delta\phi \cong \frac{\partial\phi}{\partial\mathbf{G}}\ \delta\mathbf{G} + \frac{\partial\phi}{\partial\tilde{\mathbf{f}}}\ \delta\tilde{\mathbf{f}} + \frac{\partial\phi}{\partial\mathbf{r}}\ \delta\mathbf{r} \tag{2.1.78}$$

For the case of conservative loading, the external load will not change in direction or magnitude, hence $\delta\mathbf{r} = 0$. Thus we have:

$$\delta\phi \cong \tilde{\mathbf{f}}\ \delta\mathbf{G} + \mathbf{G}\ \delta\tilde{\mathbf{f}}. \tag{2.1.79}$$

It remains to express $\delta\mathbf{G}$ and $\delta\tilde{\mathbf{f}}$ in terms of the primary variables $\tilde{\theta}_1$, $\tilde{\theta}_2$, $\tilde{u}$ and $\varphi$.

Consider first:

$$\delta\tilde{\mathbf{f}} = \frac{1}{l_o}\begin{bmatrix} EA & 0 & 0 \\ 0 & 4EI & 2EI \\ 0 & 2EI & 4EI \end{bmatrix}\ \delta\tilde{\mathbf{u}} = \mathbf{D}\ \delta\tilde{\mathbf{u}} = \mathbf{D}\ \mathbf{G}^T\ \delta\mathbf{u} \tag{2.1.80}$$

Thus:

$$\begin{aligned} \mathbf{G}\ \delta\tilde{\mathbf{f}} &= \mathbf{G}\ \mathbf{D}\ \mathbf{G}^T\ \delta\mathbf{u} \\ &= \mathbf{k}_{t1}\ \delta\mathbf{u} \end{aligned} \tag{2.1.81}$$

where

$$\mathbf{k}_{t1} = \mathbf{G}\ \mathbf{D}\ \mathbf{G}^T \tag{2.1.82}$$

and is called the material stiffness matrix.

Next consider the term $\tilde{\mathbf{f}}\ \delta\mathbf{G}$ which we write in expanded form as:

$$\tilde{\mathbf{f}}\ \delta\mathbf{G} = P\ \delta\mathbf{G}_1 + M_1\ \delta\mathbf{G}_2 + M_2\ \delta\mathbf{G}_3 \tag{2.1.83}$$

where $\mathbf{G}_1$, $\mathbf{G}_2$ and $\mathbf{G}_3$ are the first, second and third columns of the $\mathbf{G}$ matrix, respectively.

The so called geometric tangent stiffness matrix arises from the terms on the right hand side of equation (2.1.83).

Now we note from equation (2.1.71) that $\delta\mathbf{G}_1 = \delta\mathbf{g}_1$ and further that $\delta\mathbf{G}_1$ depends upon the orientation of the co-rotation axes, namely, $\varphi$. Thus from equation (2.1.59) we have:

$$\delta\mathbf{g}_1 = \begin{bmatrix}\sin\varphi & -\cos\varphi & 0 & -\sin\varphi & \cos\varphi & 0\end{bmatrix}^T \delta\varphi = \mathbf{Z}\ \delta\varphi \tag{2.1.84}$$

where

$$\mathbf{Z} = \begin{bmatrix}\sin\varphi & -\cos\varphi & 0 & -\sin\varphi & \cos\varphi & 0\end{bmatrix}^T \tag{2.1.85}$$

From Figure 2.1.14, we note that:

$$\delta\varphi = \delta\varphi_i = \frac{1}{l_c}\ (\bar{\mathbf{e}}_2 \cdot\ \delta\mathbf{u}_{21}) = \frac{1}{l_c}\begin{bmatrix}-\sin\varphi \\ \cos\varphi\end{bmatrix}^T \delta\mathbf{u}_{21} = \frac{1}{l_c}\ \mathbf{Z}^T\ \delta\mathbf{u} \tag{2.1.86}$$

Hence using equations (2.1.84) and (2.1.86), we obtain:

$$\delta\mathbf{G}_1 = \delta\mathbf{g}_1 = \mathbf{Z}\ \delta\varphi = \mathbf{k}_{t2}\ \delta\mathbf{u} \tag{2.1.87}$$

where

$$\mathbf{k}_{t2} = \frac{1}{l_c}\ \mathbf{Z}\ \mathbf{Z}^T \tag{2.1.88}$$

Consider next the evaluation $\delta\mathbf{G}_2$. From equations (2.1.68), (2.1.71) and (2.1.72), we have that:

$$\mathbf{G}_2 = -\frac{1}{\cos\bar{\theta}_1}\begin{bmatrix}-\mathbf{A}\ \mathbf{a}_2 & -\bar{\mathbf{e}}_1 \cdot \mathbf{a}_1 & \mathbf{A}\ \mathbf{a}_2 & 0\end{bmatrix}^T \tag{2.1.89}$$

where we have used the symmetry of $\mathbf{A}$.

For clarity of development, we write $\delta\mathbf{G}_2$ in two parts as:

$$\delta\mathbf{G}_2 = \delta\mathbf{G}_2{}^a + \delta\mathbf{G}_2{}^b \tag{2.1.90}$$

where

$$\delta\mathbf{G}_2{}^a = -\frac{1}{\cos\bar{\theta}_1}\delta\Big(\lfloor -\mathbf{A}\;\;\mathbf{a}_2 \quad -\tilde{\mathbf{e}}_1\cdot\mathbf{a}_1 \quad \mathbf{A}\;\;\mathbf{a}_2 \quad 0\rfloor^T\Big) \tag{2.1.91}$$

and

$$\delta\mathbf{G}_2{}^b = \delta\Big(-\frac{1}{\cos\bar{\theta}_1}\Big)\lfloor -\mathbf{A}\;\;\mathbf{a}_2 \quad -\tilde{\mathbf{e}}_1\cdot\mathbf{a}_1 \quad \mathbf{A}\;\;\mathbf{a}_2 \quad 0\rfloor^T \tag{2.1.92}$$

To evaluate the variation of the terms in the column vector, in $\delta\mathbf{G}_2{}^a$, we will examine one term at a time. Thus using equation (2.1.65), we may write:

$$\begin{aligned}
\delta\mathbf{A}\;\;\mathbf{a}_2 &= \Big\{-\frac{\delta l_c}{l_c^2}[\mathbf{I}-\tilde{\mathbf{e}}_1\otimes\tilde{\mathbf{e}}_1] + \frac{1}{l_c}[-\delta\tilde{\mathbf{e}}_1\otimes\tilde{\mathbf{e}}_1 - \tilde{\mathbf{e}}_1\otimes\delta\tilde{\mathbf{e}}_1]\Big\}\;\;\mathbf{a}_2 \\
&= \{-\frac{\delta\bar{u}}{l_c}\;\mathbf{A} + \frac{1}{l_c}[-\delta\tilde{\mathbf{e}}_1\otimes\tilde{\mathbf{e}}_1 - \tilde{\mathbf{e}}_1\otimes\delta\tilde{\mathbf{e}}_1]\}\;\;\mathbf{a}_2 \\
&= -\frac{1}{l_c}[(\tilde{\mathbf{e}}_1\cdot\delta\mathbf{u}_{21})\mathbf{A} + \mathbf{A}\;\;\delta\mathbf{u}_{21}\otimes\tilde{\mathbf{e}}_1 + \tilde{\mathbf{e}}_1\otimes\mathbf{A}\;\;\delta\mathbf{u}_{21}]\;\;\mathbf{a}_2
\end{aligned} \tag{2.1.93}$$

Now we may write:

$$\delta\mathbf{A}\;\;\mathbf{a}_2 = -\mathcal{A}\;\;\delta\mathbf{u}_{21} \tag{2.1.94}$$

where the matrix $\mathcal{A}$ is given by:

$$\mathcal{A} = \frac{1}{l_c}\;[(\mathbf{A}\;\;\mathbf{a}_2\otimes\tilde{\mathbf{e}}_1) + (\tilde{\mathbf{e}}_1\cdot\mathbf{a}_2)\mathbf{A} + (\tilde{\mathbf{e}}_1\otimes\mathbf{a}_2)\mathbf{A}] \tag{2.1.95}$$

We have already evaluated $\delta\tilde{\mathbf{e}}_1$ and $\delta\mathbf{a}_2$. Therefore using equations (2.1.62), (2.1.64), (2.1.65) and (2.1.94), one may show that:

$$\delta\mathbf{G}_2{}^a = \mathbf{k}_{t3}\;\;\delta\mathbf{u} \tag{2.1.96}$$

where

$$\mathbf{k}_{t3} = -\frac{1}{\cos\tilde{\theta}_1}\begin{bmatrix} -\mathcal{A} & \mathbf{A}\mathbf{a}_1 & \mathcal{A} & \mathbf{0} \\ \mathbf{a}_1\mathbf{A} & -\tilde{\mathbf{e}}_1\cdot\mathbf{a}_2 & -\mathbf{a}_1\mathbf{A} & 0 \\ \mathcal{A} & -\mathbf{A}\mathbf{a}_1 & -\mathcal{A} & \mathbf{0} \\ \mathbf{0} & 0 & \mathbf{0} & 0 \end{bmatrix} \tag{2.1.97}$$

It should be noted that $\mathcal{A} = \mathcal{A}^T$ and the geometric stiffness matrix $\mathbf{k}_{t3}$ is symmetric.

The variation of the term $1/\cos\tilde{\theta}_1$ in equation (2.1.92) can be expressed as:

$$\delta\left(\frac{1}{\cos\tilde{\theta}_1}\right) = \frac{\tan\tilde{\theta}_1}{\cos\tilde{\theta}_1}\,\delta\tilde{\theta}_1 = -\frac{\tan\tilde{\theta}_1}{\cos^2\tilde{\theta}_1}\,\mathbf{g}_{21}\cdot\delta\mathbf{u} \tag{2.1.98}$$

On substituting equation (2.1.98) into equation (2.1.92) and by using equation (2.1.89) we obtain:

$$\begin{aligned} \delta\mathbf{G}_2{}^b &= -\delta\left(\frac{1}{\cos\tilde{\theta}_1}\right)\lfloor -\mathbf{A}\,\mathbf{a}_2 \quad -\tilde{\mathbf{e}}_1\cdot\mathbf{a}_1 \quad \mathbf{A}\,\mathbf{a}_2 \quad 0\rfloor^T \\ &= \left(\frac{\tan\tilde{\theta}_1}{\cos^2\tilde{\theta}_1}\lfloor -\mathbf{A}\,\mathbf{a}_2 \quad -\tilde{\mathbf{e}}_1\cdot\mathbf{a}_1 \quad \mathbf{A}\,\mathbf{a}_2 \quad 0\rfloor^T\,\mathbf{g}_{21}^T\right)\delta\mathbf{u} \\ &= \left(\mathbf{G}_2\,\tan\tilde{\theta}_1\,\mathbf{G}_2^T\right)\delta\mathbf{u} \end{aligned} \tag{2.1.99}$$

Variation of the third term in equation (2.1.83) may also be evaluated in a similar manner leading to:

$$\delta\mathbf{G}_3{}^a = \mathbf{k}_{t4}\,\delta\mathbf{u} \tag{2.1.100}$$

where

$$\mathbf{k}_{t4} = -\frac{1}{\cos\tilde{\theta}_2}\begin{bmatrix} -\mathcal{B} & \mathbf{0} & \mathcal{B} & \mathbf{A}\mathbf{b}_1 \\ \mathbf{0} & 0 & \mathbf{0} & 0 \\ \mathcal{B} & \mathbf{0} & -\mathcal{B} & -\mathbf{A}\mathbf{b}_1 \\ \mathbf{b}_1\mathbf{A} & 0 & -\mathbf{b}_1\mathbf{A} & -\tilde{\mathbf{e}}_1\cdot\mathbf{b}_2 \end{bmatrix} \tag{2.1.101}$$

The matrix $\mathcal{B}$, given by:

$$\mathcal{B} = \frac{1}{l_c} \; [\,(\mathbf{A} \;\; \mathbf{b}_2 \otimes \tilde{\mathbf{e}}_1) + (\tilde{\mathbf{e}}_1 \cdot \mathbf{b}_2)\,\mathbf{A} + (\tilde{\mathbf{e}}_1 \otimes \mathbf{b}_2)\,\mathbf{A}] \tag{2.1.102}$$

and is related to node 2.

Also we have:

$$\delta \mathbf{G}_3{}^b = \left(\mathbf{G}_3 \;\; \tan\tilde{\theta}_2 \;\; \mathbf{G}_3^T\right)\delta\mathbf{u} \tag{2.1.103}$$

Using equations (2.1.100) and (2.1.103) and referring to equation (2.1.83), we obtain:

$$M_1 \;\; \delta\mathbf{G}_2{}^b + M_2 \;\; \delta\mathbf{G}_3{}^b = \mathbf{k}_{t5} \;\; \delta\mathbf{u} \tag{2.1.104}$$

where

$$\mathbf{k}_{t5} = \mathbf{g}_2 \begin{bmatrix} M_1 \tan\tilde{\theta}_1 & 0 \\ 0 & M_2 \tan\tilde{\theta}_2 \end{bmatrix} \mathbf{g}_2{}^T \tag{2.1.105}$$

Now the complete tangent stiffness matrix may be expressed as:

$$\mathbf{k}_T = \mathbf{k}_{t1} + P \;\; \mathbf{k}_{t2} + M_1 \;\; \mathbf{k}_{t3} + M_2 \;\; \mathbf{k}_{t4} + \mathbf{k}_{t5} \tag{2.1.106}$$

The obtained elemental equilibrium equations in the global coordinate system should be assembled to form the global system equilibrium equations. When these latter equations are solved iteratively the incremental displacements will be obtained.

### 2.1.3 Consistent Co-Rotational Formulation: Higher Order Strain Measures

Rather than using the co-rotational engineering strain which has been used in the basic consistent co-rotational finite element, we now introduce the Green-Lagrange strain measures with respect to a co-rotational frame which includes the effect of element curvature on the axial strain. This approach yields more accurate displacements for coarser meshes.

### 2.1.3.1 Strain Measures

The higher order strain measure in the a co-rotational frame, was first introduced by Belytschko and Glaum, 1979. For the Euler Bernoulli beam the axial Green Lagrange strain measures for the centerline, with respect to the co-rotational frame may be expressed as:

$$\varepsilon(\tilde{x}) = \frac{d}{d\tilde{x}}\tilde{U}(\zeta) + \frac{1}{2}\left(\frac{d}{d\tilde{x}}\tilde{U}(\zeta)\right)^2 + \frac{1}{2}\left(\frac{d}{d\tilde{x}}\tilde{U}_2(\zeta)\right)^2 \qquad (2.1.107)$$

This strain is independent of rigid body displacements and rotations.

Introducing the linear and cubic shape functions for the axial and transverse displacements, respectively, equation (2.1.107) may be expressed as:

$$\varepsilon(\tilde{x}) = \frac{\tilde{u}}{l_o} + \frac{1}{2}\left(\frac{\tilde{u}}{l_o}\right)^2 + \frac{1}{2}\lfloor \tilde{\theta}_1 \quad \tilde{\theta}_2 \rfloor\, \mathbf{d}\, \mathbf{d}^T \begin{Bmatrix} \tilde{\theta}_1 \\ \tilde{\theta}_2 \end{Bmatrix} \qquad (2.1.108)$$

where

$$\mathbf{d} = \frac{1}{4} \begin{Bmatrix} 3\zeta^2 - 2\zeta - 1 \\ 3\zeta^2 + 2\zeta - 1 \end{Bmatrix} \qquad (2.1.109)$$

and once again the lateral displacements are set to zero in the co-rotational axis.

Based on the defined shape functions, in order to remove, or at least ameliorate the membrane locking (see Cole, 1990), we replace the axial strain $\varepsilon(\tilde{x})$ with an effective axial strain $\varepsilon_{eff}$, define as:

$$\varepsilon_{eff} = \frac{1}{l_o} \int \varepsilon(\tilde{x}) \quad d\tilde{x} \qquad (2.1.110)$$

Hence the element is only able to accommodate a constant axial strain. Substituting equation (2.1.108) into equation (2.1.110) and using relation (2.1.109), we obtain:

$$\varepsilon_{eff} = \frac{\tilde{u}}{l_o} + \frac{1}{2}\left(\frac{\tilde{u}}{l_o}\right)^2 + \frac{1}{2}\lfloor \tilde{\theta}_1 \quad \tilde{\theta}_2 \rfloor \left(\frac{1}{l_o}\int_0^{l_o} \mathbf{d}\ \mathbf{d}^T\ d\tilde{x}\right) \begin{Bmatrix} \tilde{\theta}_1 \\ \tilde{\theta}_2 \end{Bmatrix}$$

$$= \frac{\tilde{u}}{l_o} + \frac{1}{2}\left(\frac{\tilde{u}}{l_o}\right)^2 + \frac{1}{60}\lfloor \tilde{\theta}_1 \quad \tilde{\theta}_2 \rfloor \begin{bmatrix} 4 & -1 \\ -1 & 4 \end{bmatrix} \begin{Bmatrix} \tilde{\theta}_1 \\ \tilde{\theta}_2 \end{Bmatrix} \tag{2.1.111}$$

From equations (2.1.71) and (2.1.111), we may obtain the variation of $\varepsilon_{eff}$ in terms of the nodal displacements as:

$$\delta\varepsilon_{eff} = \frac{1}{l_o}\left(1 + \frac{\tilde{u}}{l_o}\right) \mathbf{g}_1^T\ \delta\mathbf{u} + \frac{1}{30}\lfloor \tilde{\theta}_1 \quad \tilde{\theta}_2 \rfloor \begin{bmatrix} 4 & -1 \\ -1 & 4 \end{bmatrix} \mathbf{g}_2^T\ \delta\mathbf{u} \tag{2.1.112}$$

Also the variation of axial extension may be expressed as:

$$\delta\tilde{\underline{u}} = l_o\ \delta\varepsilon_{eff} = \left(1 + \frac{\tilde{u}}{l_o}\right) \mathbf{g}_1^T\ \delta\mathbf{u} + \frac{l_o}{30}\lfloor \tilde{\theta}_1 \quad \tilde{\theta}_2 \rfloor \begin{bmatrix} 4 & -1 \\ -1 & 4 \end{bmatrix} \mathbf{g}_2^T\ \delta\mathbf{u} \tag{2.1.113}$$

Therefore, the virtual local displacements may be expressed in terms of virtual global displacements as:

$$\delta\tilde{\mathbf{u}} = \begin{Bmatrix} \delta\tilde{\underline{u}} \\ \delta\tilde{\theta}_1 \\ \delta\tilde{\theta}_2 \end{Bmatrix} = \begin{bmatrix} \left(1 + \frac{\tilde{u}}{l_o}\right)\mathbf{g}_1^T + \frac{l_o}{30}\lfloor \tilde{\theta}_1 \quad \tilde{\theta}_2 \rfloor \begin{bmatrix} 4 & -1 \\ -1 & 4 \end{bmatrix} \mathbf{g}_2^T \\ \mathbf{g}_2^T \end{bmatrix} \delta\mathbf{u} = \mathbf{G}^T\ \delta\mathbf{u} \tag{2.1.114}$$

### 2.1.3.2 Equilibrium Equations

Referring to section 2.1.2.3, we may express the elemental equilibrium equation in the global coordinate system as:

$$\mathbf{G}\ \tilde{\mathbf{f}} - \mathbf{r} = 0 \tag{2.1.115}$$

where $\mathbf{G}\ \tilde{\mathbf{f}}$ is the nodal global internal force vector. The nodal out of balance force is then given by:

$$\phi = \mathbf{G}\ \tilde{\mathbf{f}} - \mathbf{r} \tag{2.1.116}$$

The solution of equation (2.1.115) follows the lines already outlined in section 2.1.2.3. The Taylor series expansion of the out of balance force vector $\phi$ is formally as derived earlier. The only change is in the evaluation of $\delta\mathbf{G}_1$. In this case we have:

$$\delta\mathbf{G}_1 = \left(1+\frac{\bar{u}}{l_o}\right)\delta\mathbf{g}_1 + \frac{\delta\bar{u}}{l_o}\ \mathbf{g}_1 + \frac{l_o}{30}\left(\delta\mathbf{g}_2\begin{bmatrix}4 & -1\\ -1 & 4\end{bmatrix}\begin{Bmatrix}\bar{\theta}_1\\ \bar{\theta}_2\end{Bmatrix} + \mathbf{g}_2\begin{bmatrix}4 & -1\\ -1 & 4\end{bmatrix}\begin{Bmatrix}\delta\bar{\theta}_1\\ \delta\bar{\theta}_2\end{Bmatrix}\right) \quad (2.1.117)$$

In the above expression, substituting the terms $\delta\bar{u}$, $\delta\mathbf{g}_1$ and $\delta\bar{\theta}$ from equations (2.1.58), (2.1.71) and (2.1.87) into equation (2.1.117), we obtain:

$$\delta\mathbf{G}_1 = \frac{1}{l_c}\left(1+\frac{\bar{u}}{l_o}\right)\mathbf{Z}\mathbf{Z}^T\delta\mathbf{u} + \frac{1}{l_o}\mathbf{g}_1\mathbf{g}_1^T\delta\mathbf{u} + \frac{l_o}{30}\lfloor \delta G_2 \quad \delta G_3\rfloor\begin{bmatrix}4 & -1\\ -1 & 4\end{bmatrix}\begin{Bmatrix}\bar{\theta}_1\\ \bar{\theta}_2\end{Bmatrix} +$$
$$\frac{l_o}{30}\ \mathbf{g}_2\begin{bmatrix}4 & -1\\ -1 & 4\end{bmatrix}\mathbf{g}_2^T\ \delta\mathbf{u} \quad (2.1.118)$$

Using equations (2.1.96), (2.1.100) and (2.1.103), the third term in equation (2.1.118) can be written as:

$$\frac{l_o}{30}\lfloor 4\delta G_2 - \delta G_3 \quad 4\delta G_3 - \delta G_2\rfloor\begin{Bmatrix}\bar{\theta}_1\\ \bar{\theta}_2\end{Bmatrix} = \frac{l_o}{30}\left[\,(4\bar{\theta}_1 - \bar{\theta}_2)\,\delta G_2 + (4\bar{\theta}_2 - \bar{\theta}_1)\,\delta G_3\right] \quad (2.1.119)$$
$$= \frac{l_o}{30}\left[\,(4\bar{\theta}_1 - \bar{\theta}_2)\,\mathbf{k}_{G2} + (4\bar{\theta}_2 - \bar{\theta}_1)\,\mathbf{k}_{G3}\right]\delta\mathbf{u}$$

where

$$\mathbf{k}_{G2} = \mathbf{k}_{t3} + \frac{\tan\bar{\theta}_1}{\cos\bar{\theta}_1^{\,2}}\ \mathbf{g}_{21}\ \mathbf{g}_{21}^T \quad (2.1.120)$$

and

$$\mathbf{k}_{G3} = \mathbf{k}_{t4} + \frac{\tan\bar{\theta}_2}{\cos\bar{\theta}_2^{\,2}}\ \mathbf{g}_{22}\ \mathbf{g}_{22}^T \quad (2.1.121)$$

Now we may express the complete form of the tangent stiffness matrix as:

$$\mathbf{k}_T = \mathbf{GDG}^T + \frac{P}{l_c}\left(1+\frac{\tilde{u}}{l_o}\right)\mathbf{ZZ}^T + \frac{P}{l_o}\ \mathbf{g}_1\ \mathbf{g}_1^T + \frac{Pl_o}{30}\ \mathbf{g}_2\begin{bmatrix}4 & -1\\ -1 & 4\end{bmatrix}\mathbf{g}_2^T +$$
$$\frac{Pl_o}{30}\ \left[(4\tilde{\theta}_1-\tilde{\theta}_2)\,\mathbf{k}_{G2} + (4\tilde{\theta}_2-\tilde{\theta}_1)\,\mathbf{k}_{G3}\right] + M_1\mathbf{k}_{t3} + M_2\mathbf{k}_{t4} + \mathbf{k}_{t5} \qquad (2.1.122)$$

#### 2.1.3.3 Illustrative Examples

In the following examples we use a 2D Euler-Bernoulli beam element and to obtain solutions we employ the full Newton-Raphson method. We compare the results obtained, using the co-rotational engineering strain measure, (CESM), with the results obtained using the co-rotational Green-Lagrange strain measures (CGSM), for accuracy and rate of convergence as the number of elements is increased. The convergence rate depends on the tangent stiffness matrix while the accuracy of solutions depends on the residual forces, see Iura, 1994. The system matrices and vectors are obtained explicitly using the MAPLE symbolic mathematical tool box. The convergence criterion used in all examples is based on the residual energy computed from the out of balance forces and the corresponding displacements at each load increment. Convergence is considered to have been achieved when the computed residual energy becomes less than $10^{-6}$ lb-in.

- **Cantilever Subjected to an End Moment**

In the first example an initially straight cantilever beam is subjected to an end moment of 7.85 lb-in, see Figure 2.1.2. The displacement history of the free end is shown in Figures 2.1.16, 2.1.17. In Figure 2.1.18 we have shown the nodal locations and the co-rotational axes for each element when the entire beam is modelled by 4, 8 and 16 elements. It can be seen that for a small number of elements, the CGSM yields more accurate results than the CESM. However, as the mesh is refined, the differences between the two results become less apparent. Also during the tests, it was observed that for 4 elements, using 6 and 10 load increments, CGSM needed 14 and 10 iterations per increment while CESM required 5 and 4 iterations per increment. Thus, for the CGSM, the rate of convergence is sensitive to the number of load increments and is higher than that for the CESM. This means that CGSM requires more CPU time (at least twice as long) than the CESM. Increasing the number of elements does not affect the rate of convergence.

The obtained results are identical to those reported by Crisfield, 1990, and Cole, 1990, and show excellent performance compared to results obtained by the updated Lagrangian method.

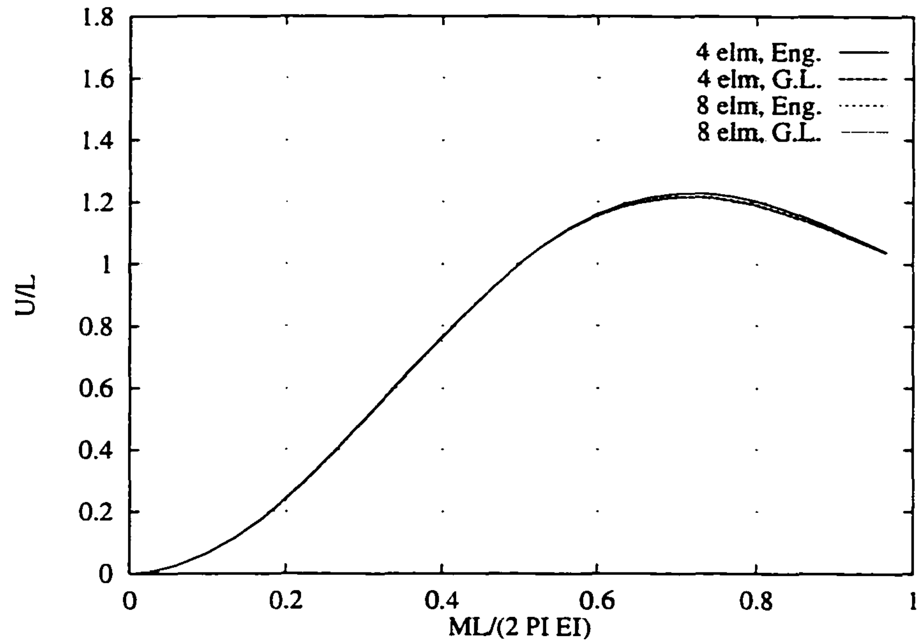


Figure 2.1.16: Non-Dimensional Horizontal Displacement of Free End.

- **Cantilever Subjected to a Concentrated Tip Load**

Next, we consider a cantilever beam subjected to a concentrated tip load of 5208.33 lb as shown in Figure 2.1.7. The tip displacement history shows the accuracy of the CGSM for 2 beam elements as compared to CESM, see Figures 2.1.19, 2.1.20 and 2.1.21. Again the CGSM needs more iterations per increment than the CESM (about 50% more), e.g. for 2 beam elements and 2 load increments, 9 and 6 iterations were required, respectively, showing the additional cost of computation for accurate solutions. The results are identical to those reported by Cole, 1990, and show outstanding performance compared to the updated Lagrangian method.

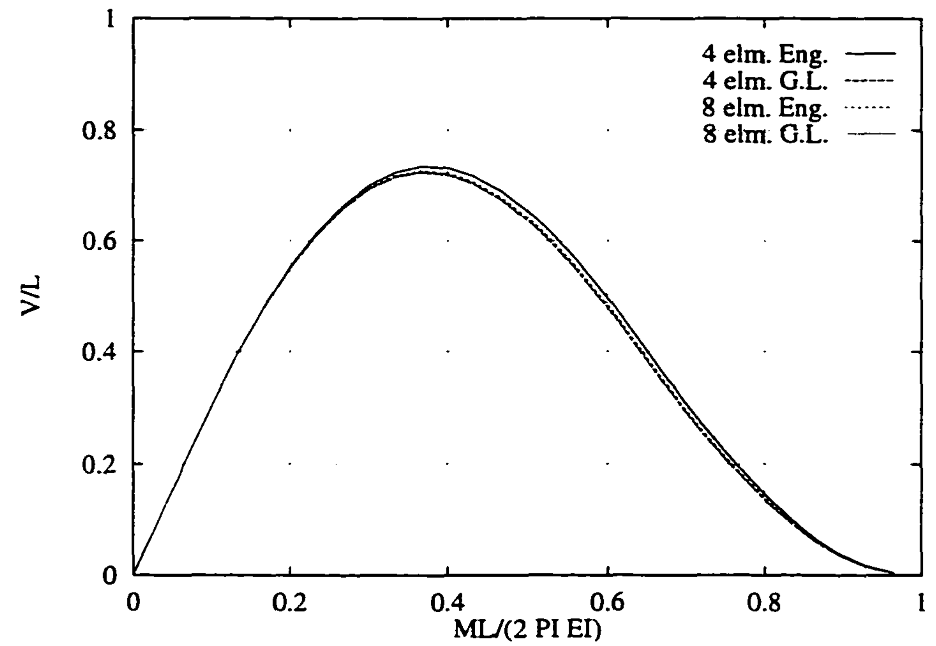


Figure 2.1.17: Non-Dimensional Vertical Displacement of Free End.

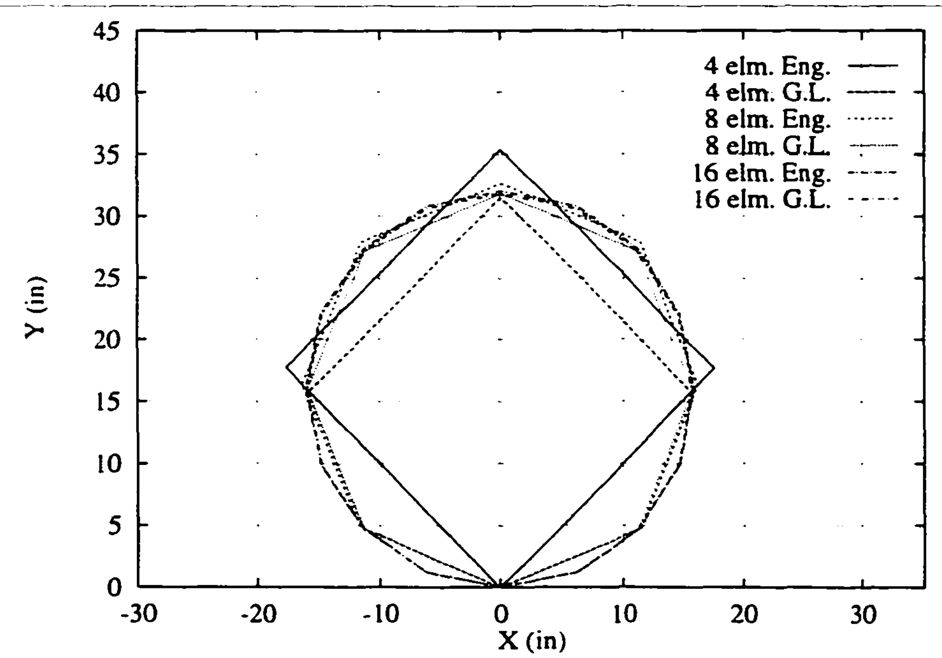


Figure 2.1.18: Nodal Positions and Co-rotational Axes.

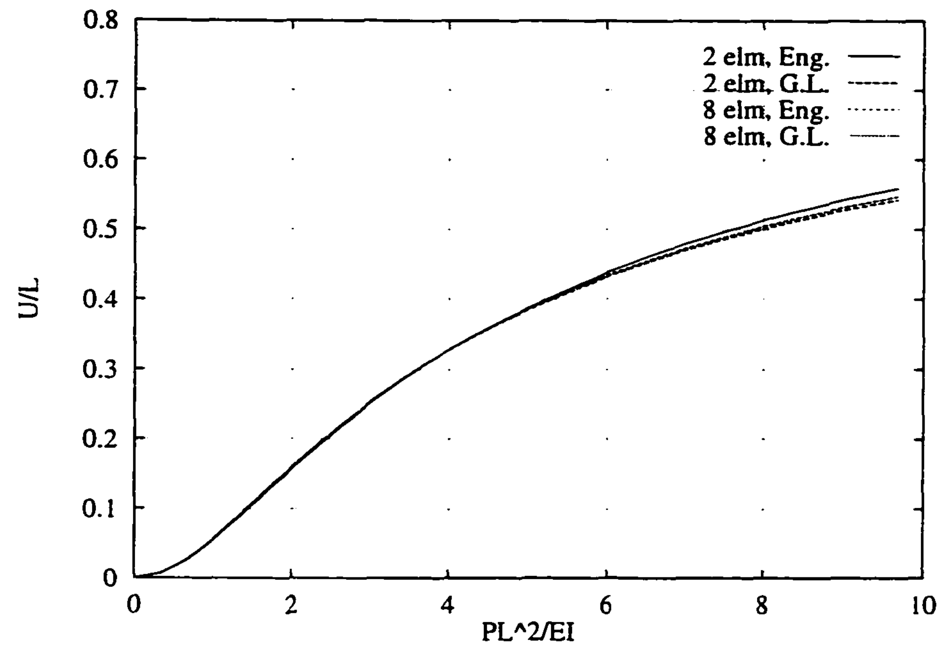


Figure 2.1.19: Non-Dimensional Horizontal Displacement of Free End.

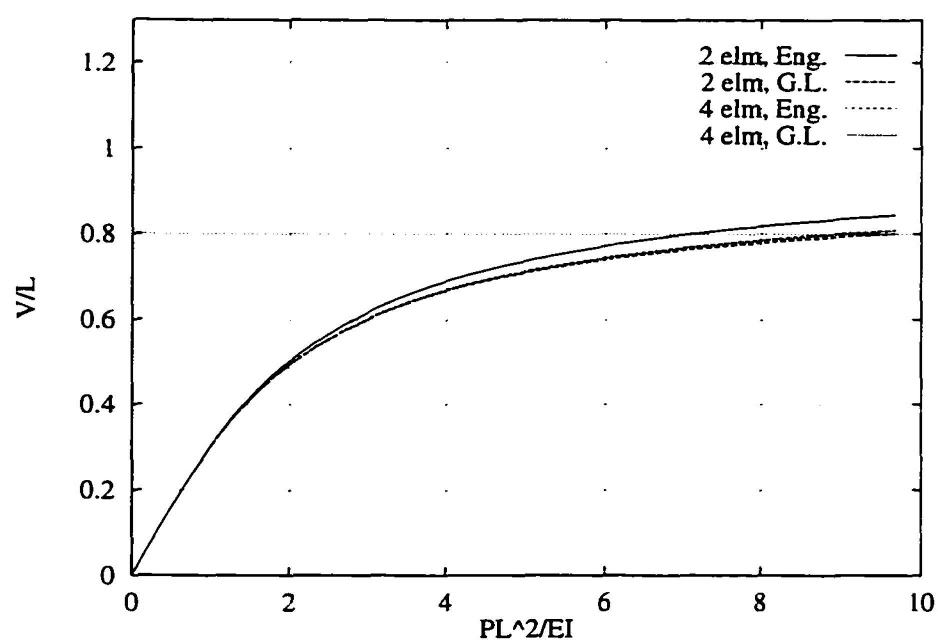


Figure 2.1.20: Non-Dimensional Vertical Displacement of Free End.

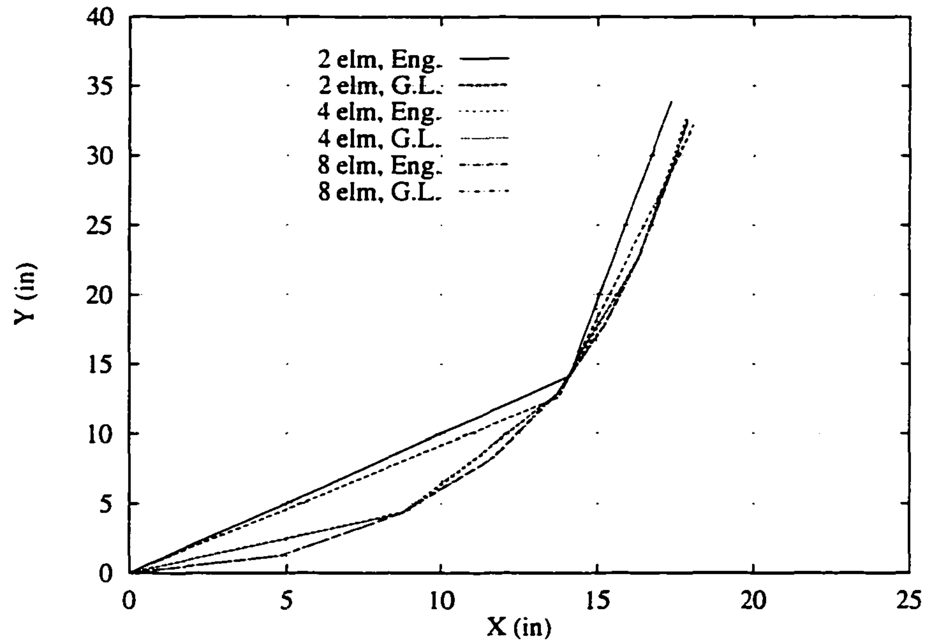


Figure 2.1.21: Nodal Positions and Co-rotational Axes.

- **Post Buckling Behaviour of a Cantilever**

Finally, we study the performance of the CGSM for the post buckling behaviour of an initially straight cantilever beam. The beam is loaded axially at the tip with 14323 lb. On the first load increment, a small transverse perturbation load of 14.323 lb is provided at the tip as shown in Figure 2.1.22. The results shown in Figures 2.1.23, 2.1.24 and 2.1.25 again demonstrate the accuracy of the CGSM as compared to the CESM, especially when a small number of elements are used. It is noted, once again, that as the mesh is refined, this difference becomes less apparent. Since each element in this problem is in general sensitive to the load increment size at each iteration, the rate of convergence is found to be almost the same for both formulations, e.g. 4 load increments and 5 to 7 iterations for each increment. The computed results are also identical to the results reported by Cole, 1990.

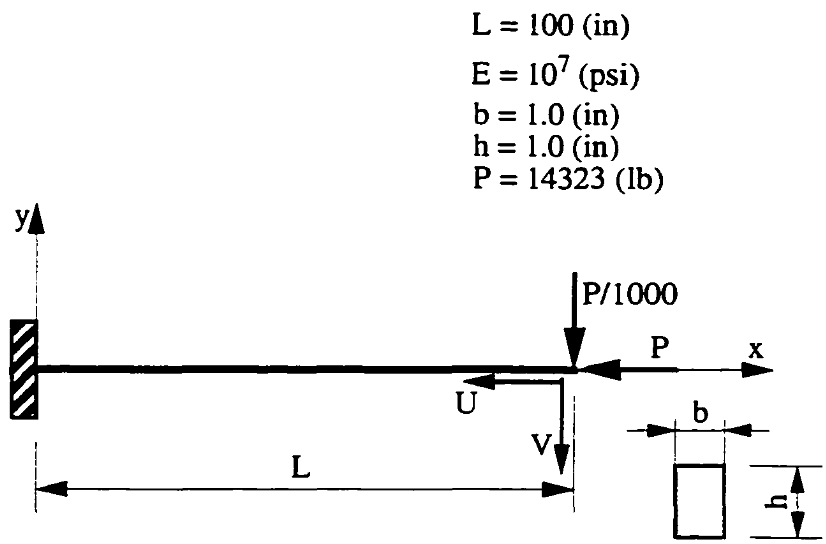


Figure 2.1.22: Post Buckling Behaviour of a Cantilever.

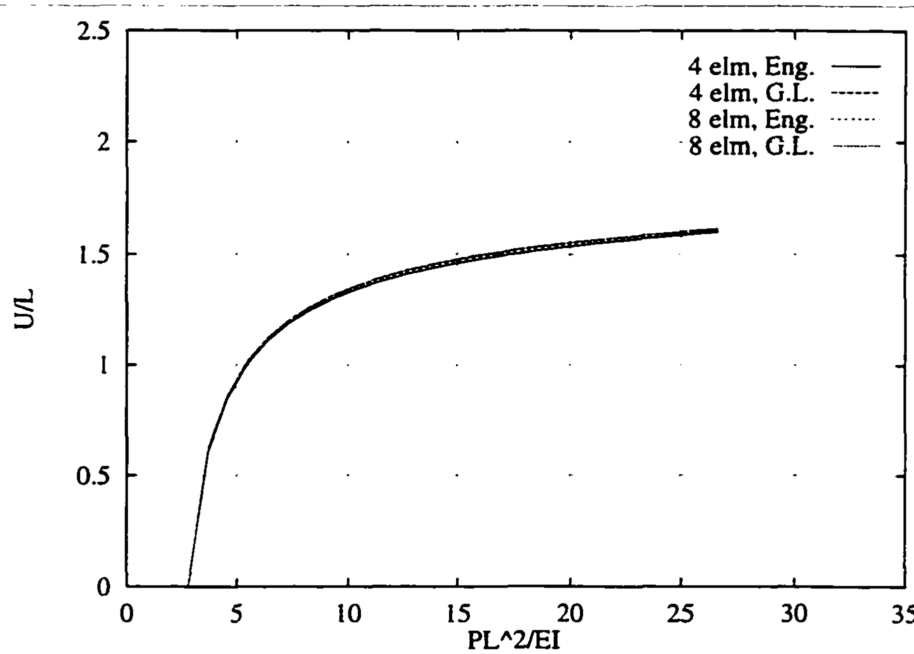


Figure 2.1.23: Non-Dimensional Horizontal Displacement of Free End.

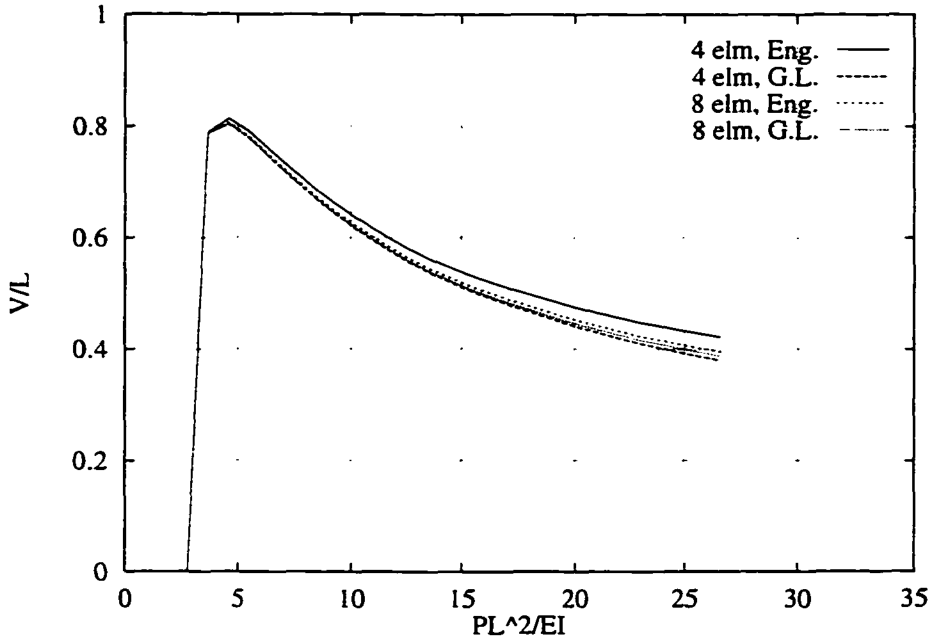


Figure 2.1.24: Non-Dimensional Vertical Displacement of Free End.

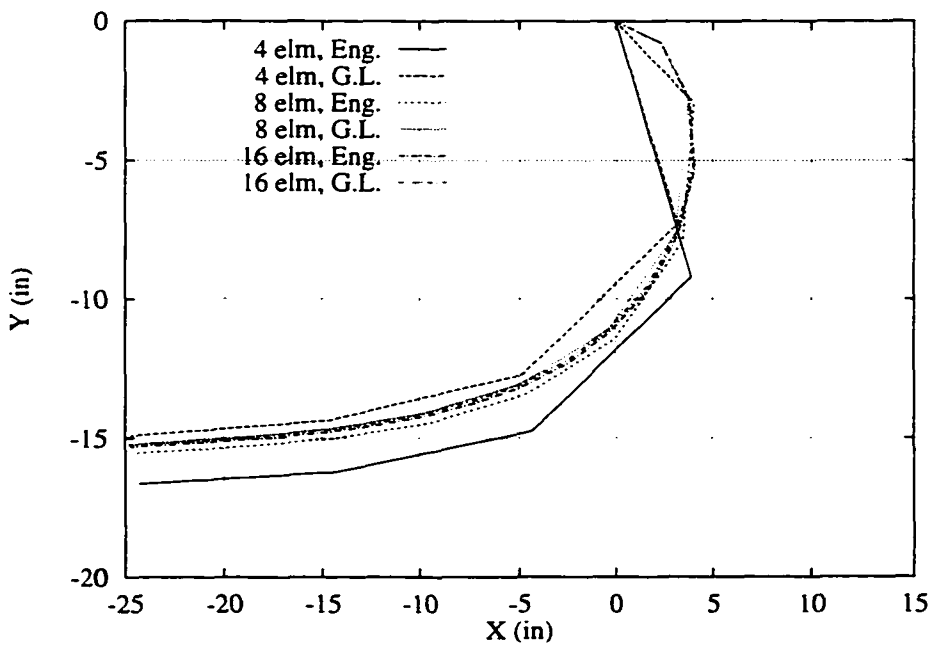


Figure 2.1.25: Nodal Positions and Co-rotational Axes.

## 2.2 Nonlinear Finite Element Dynamic Analysis

For the dynamic analysis of geometrically nonlinear beams undergoing large rotations and small deformation, we use the Newmark $\beta$ direct time integration scheme and implement it using the updated Lagrangian formulation (which is an inertial-frame type approach). We also implement the Newmark integration method using the consistent co-rotational formulation. Several examples are solved using both formulations and the results are compared.

### 2.2.1 Newmark $\beta$ Direct Time Integration for Nonlinear Systems: Updated Lagrangian Formulation

In the dynamic analysis, we need to add the inertia forces to the applied forces. Since the mass of the system must be conserved, the mass matrix should be evaluated prior to time integration for the updated Lagrangian formulation, using the initial configuration as reference. Employing the standard finite element formulation to evaluate the element mass matrix, the equation of motion for a nonlinear system at configuration $t + \Delta t$, in the global coordinate system, can be written as:

$$\mathbf{M}\ {}^{t+\Delta t}\frac{d^2\mathbf{u}}{dt^2} + \mathbf{C}\ {}^{t+\Delta t}\frac{d\mathbf{u}}{dt} + {}^{t+\Delta t}_{t+\Delta t}\mathbf{F}(\mathbf{u}) = {}^{t+\Delta t}\mathbf{R} \tag{2.2.1}$$

where $\mathbf{M}$ and $\mathbf{C}$ are the mass and damping matrices and $\mathbf{F}$ and $\mathbf{R}$ are the internal force and applied force vectors, respectively, and $\mathbf{u}$ is the nodal displacement vector. To obtain the solution of the nonlinear equation (2.2.1), we use the modified Newton-Raphson method. After neglecting the higher order terms, equation (2.2.1) at the $i^{th}$ iteration may be expressed as:

$$\mathbf{M}\ {}^{t+\Delta t}\frac{d^2\mathbf{u}}{dt^2}^{i} + \mathbf{C}\ {}^{t+\Delta t}\frac{d\mathbf{u}}{dt}^{i} + {}^{t}_{t}\mathbf{K}_T\ \Delta\mathbf{u}^i = {}^{t+\Delta t}\mathbf{R} - {}^{t+\Delta t}_{t+\Delta t}\mathbf{F}(\mathbf{u})^{i-1} \tag{2.2.2}$$

where ${}^{t}_{t}\mathbf{K}_T$ is the tangent stiffness matrix at configuration $t$ and $\Delta\mathbf{u}^i$ is the incremental displacement vector at iteration $i$.

The Newmark method which is a generalization of the linear acceleration method, proceeds as follows:

$$\begin{aligned}
\frac{{}^{t+\Delta t}d^2\mathbf{u}^i}{dt^2} &= a_0\left({}^{t+\Delta t}\mathbf{u}^i - {}^t\mathbf{u}\right) - a_2\,\frac{{}^t d\mathbf{u}}{dt} - a_3\,\frac{{}^t d^2\mathbf{u}}{dt^2} \\
&= a_0\left({}^{t+\Delta t}\mathbf{u}^{i-1} + \Delta\mathbf{u}^i - {}^t\mathbf{u}\right) - a_2\,\frac{{}^t d\mathbf{u}}{dt} - a_3\,\frac{{}^t d^2\mathbf{u}}{dt^2} \\
&= a_0\,\Delta\mathbf{u}^i + a_0\left({}^{t+\Delta t}\mathbf{u}^{i-1} - {}^t\mathbf{u}\right) - a_2\,\frac{{}^t d\mathbf{u}}{dt} - a_3\,\frac{{}^t d^2\mathbf{u}}{dt^2}
\end{aligned} \tag{2.2.3}$$

and

$$\begin{aligned}
\frac{{}^{t+\Delta t}d\mathbf{u}^i}{dt} &= \frac{{}^t d\mathbf{u}}{dt} + a_6\,\frac{{}^t d^2\mathbf{u}}{dt^2} + a_7\,\frac{{}^{t+\Delta t}d^2\mathbf{u}^i}{dt^2} \\
&= \frac{{}^t d\mathbf{u}}{dt} + a_6\,\frac{{}^t d^2\mathbf{u}}{dt^2} + a_7\Big[a_0\,\Delta\mathbf{u}^i + a_0\left({}^{t+\Delta t}\mathbf{u}^{i-1} - {}^t\mathbf{u}\right) - \\
&\qquad a_2\,\frac{{}^t d\mathbf{u}}{dt} - a_3\,\frac{{}^t d^2\mathbf{u}}{dt^2}\Big] \\
&= a_1\,\Delta\mathbf{u}^i + a_1\left({}^{t+\Delta t}\mathbf{u}^{i-1} - {}^t\mathbf{u}\right) - a_4\,\frac{{}^t d\mathbf{u}}{dt} - a_5\,\frac{{}^t d^2\mathbf{u}}{dt^2}
\end{aligned} \tag{2.2.4}$$

where

$$\begin{aligned}
a_0 &= \frac{1}{\alpha\Delta t^2}, & a_1 &= \frac{\delta}{\alpha\Delta t}, & a_2 &= \frac{1}{\alpha\Delta t} \\
a_3 &= \frac{1}{2\alpha} - 1, & a_4 &= \frac{\delta}{\alpha} - 1, & a_5 &= \frac{\Delta t}{2}\left(\frac{\delta}{\alpha} - 2\right) \\
a_6 &= \Delta t\,(1-\delta), & a_7 &= \delta\Delta t
\end{aligned} \tag{2.2.5}$$

For the linear system, it is well known that the Newmark time integration is unconditionally stable provided:

$$\alpha \geq \frac{1}{4}\left(\delta + \frac{1}{2}\right)^2 \qquad \text{and} \qquad \delta \geq \frac{1}{2} \tag{2.2.6}$$

Also unless $\delta$ is taken to be 0.5, the method introduces artificial damping, which can be negative (when $\delta < 0.5$). The Newmark method reduces to the constant average acceleration method when $\delta = 0.5$ and $\alpha = 0.25$ which is unconditionally stable.

However, in nonlinear structural dynamics, this method is not unconditionally stable (see e.g. Argyris and Mlejnek, 1991).

By substituting equations (2.2.3) and (2.2.4) into equation (2.2.2), we obtain:

$$\left(a_0\ \mathbf{M}+a_1\ \mathbf{C}+{}^{t}_{t}\mathbf{K}_T\right)\ \Delta\mathbf{u}^{i} = {}^{t+\Delta t}\mathbf{R}-{}^{t+\Delta t}_{t+\Delta t}\mathbf{F}(\mathbf{u})^{i-1} - \mathbf{M}\left[a_0\left({}^{t+\Delta t}\mathbf{u}^{i-1}-{}^{t}\mathbf{u}\right)-a_2\ \frac{{}^{t}d\mathbf{u}}{dt}-a_3\ \frac{{}^{t}d^2\mathbf{u}}{dt^2}\right] - \mathbf{C}\left[a_1\left({}^{t+\Delta t}\mathbf{u}^{i-1}-{}^{t}\mathbf{u}\right)-a_4\ \frac{{}^{t}d\mathbf{u}}{dt}-a_5\ \frac{{}^{t}d^2\mathbf{u}}{dt^2}\right] \tag{2.2.7}$$

### 2.2.2 Nonlinear Dynamic Analysis: Consistent Co-rotational Formulation

An Euler-Bernoulli beam undergoing large rotations in a plane is shown in Figure 2.2.1. Let $(\mathbf{I}_1, \mathbf{I}_2)$ be the fixed global coordinate frame and $(\mathbf{E}_1, \mathbf{E}_2)$ the frame attached to the initial configuration of the element. In the deformed configuration, we consider the co-rotational frame $(\tilde{\mathbf{e}}_1, \tilde{\mathbf{e}}_2)$ where $\tilde{\mathbf{e}}_1$ passes through the nodes of the beam element. The rigid body motion of the beam element can be determined from the motion of the co-rotational frame, and the small axial and transverse deformations of the beam element can be measured with respect to the co-rotational frame.

The position vector of an arbitrary material point $m$ on the centerline of the beam in the fixed coordinate system may be expressed as:

$$\mathbf{R}_m = \mathbf{R}_o + \mathbf{R}_i \tag{2.2.8}$$

Using the transformation matrix $\mathbf{T}_i$, it can be shown that:

$$\mathbf{R}_i = \mathbf{T}_i\ \tilde{\mathbf{R}}_i \tag{2.2.9}$$

where $\tilde{\mathbf{R}}_i$ is the transformed position vector in the co-rotational frame. Then the velocity of the material point $m$ can be obtained as:

$$\frac{d\mathbf{R}_m}{dt} = \frac{d\mathbf{T}_i}{dt}\ \tilde{\mathbf{R}}_i + \mathbf{T}_i\ \frac{d\tilde{\mathbf{R}}_i}{dt} \tag{2.2.10}$$

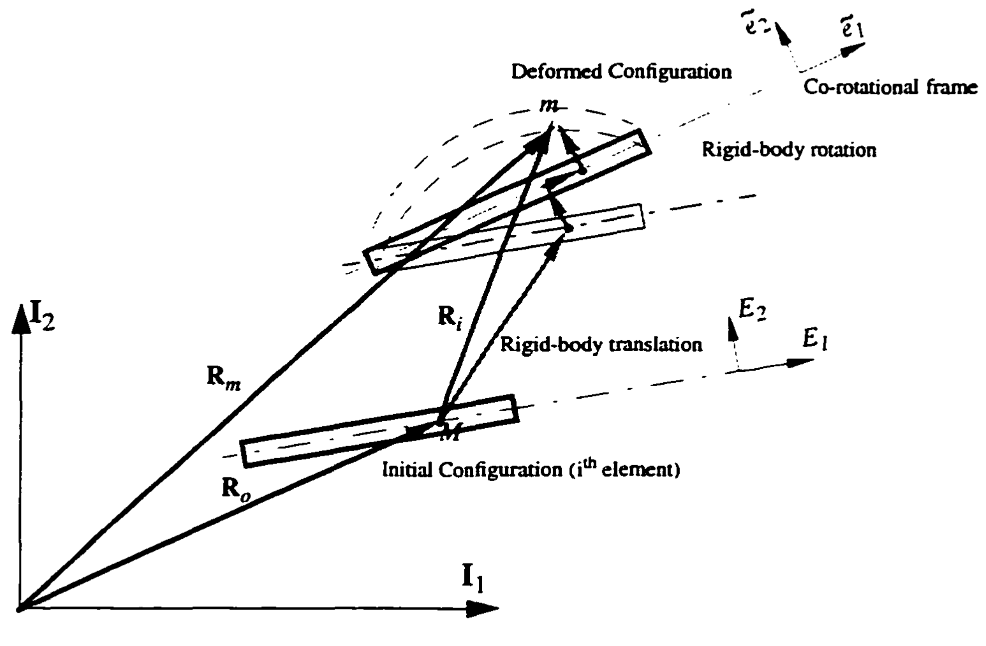


Figure 2.2.1: Co-rotational Frame for a Deformed Beam Element.

#### 2.2.2.1 Complementary Kinetic Energy

The kinetic co-energy of the $i^{th}$ element may be expressed as:

$$T_i^* = \frac{1}{2} \int_{v_i} \rho_{o_i} \left( \frac{d\mathbf{R}_m}{dt} \cdot \frac{d\mathbf{R}_m}{dt} \right) dv_i \tag{2.2.11}$$

where $\rho_{o_i}$ is the mass density of element $i$ per unit volume. Substituting equation (2.2.10) into equation (2.2.11), we obtain:

$$T_i^* = \frac{1}{2} \int_{v_i} \rho_{o_i} \left( \frac{d\mathbf{T}_i}{dt} \tilde{\mathbf{R}}_i + \mathbf{T}_i \frac{d\tilde{\mathbf{R}}_i}{dt} \right) \cdot \left( \frac{d\mathbf{T}_i}{dt} \tilde{\mathbf{R}}_i + \mathbf{T}_i \frac{d\tilde{\mathbf{R}}_i}{dt} \right) dv_i \tag{2.2.12}$$

or

$$T_i^* = \frac{1}{2}\left[\int_{v_i} \rho_{oi}\ \tilde{\mathbf{R}}_i^T \frac{d\mathbf{T}_i^T}{dt} \frac{d\mathbf{T}_i}{dt} \tilde{\mathbf{R}}_i\ dv_i + \int_{v_i} \rho_{oi}\ \tilde{\mathbf{R}}_i^T \frac{d\mathbf{T}_i^T}{dt} \mathbf{T}_i \frac{d\tilde{\mathbf{R}}_i}{dt}\ dv_i + \right.$$
$$\left. \int_{v_i} \rho_{oi} \frac{d\tilde{\mathbf{R}}_i^T}{dt} \mathbf{T}_i^T \frac{d\mathbf{T}_i}{dt} \tilde{\mathbf{R}}_i\ dv_i + \int_{v_i} \rho_{oi} \frac{d\tilde{\mathbf{R}}_i^T}{dt} \mathbf{T}_i^T \mathbf{T}_i \frac{d\tilde{\mathbf{R}}_i}{dt}\ dv_i \right] \tag{2.2.13}$$

To discretize the expression for the kinetic co-energy, linear and cubic interpolation functions for the axial and bending displacements have been used respectively allowing us to write:

$$\{\tilde{R}\} = [\mathcal{H}]\ \{\tilde{u}\} \tag{2.2.14}$$

and

$$\{\frac{d}{dt}\tilde{R}\} = [\mathcal{H}]\ \{\frac{d}{dt}\tilde{u}\} \tag{2.2.15}$$

where $[\mathcal{H}]$ is the shape functions matrix and $\{\tilde{u}\}$ is the nodal displacement vector. Substituting equations (2.2.14) and (2.2.15) into equation (2.2.13), the kinetic co-energy may be expressed in terms of the nodal variables in the co-rotational frame as:

$$T_i^* = \frac{1}{2}\left[\tilde{\mathbf{u}}_i^T\ \mathcal{F}_{1i}\ \tilde{\mathbf{u}}_i + \frac{d\tilde{\mathbf{u}}_i^T}{dt}\ \mathcal{F}_{2i}\ \frac{d\tilde{\mathbf{u}}_i}{dt} + \tilde{\mathbf{u}}_i^T\ \mathcal{F}_{3i}\ \frac{d\tilde{\mathbf{u}}_i}{dt} + \frac{d\tilde{\mathbf{u}}_i^T}{dt}\ \mathcal{F}_{4i}\ \tilde{\mathbf{u}}_i\right] \tag{2.2.16}$$

where

$$\mathcal{F}_{1i} = \int_{v_i} \rho_{oi}\ \mathcal{H}^T \frac{d\mathbf{T}_i^T}{dt} \frac{d\mathbf{T}_i}{dt}\ \mathcal{H}\ dv_i \tag{2.2.17}$$

$$\mathcal{F}_{2i} = \int_{v_i} \rho_{oi}\ \mathcal{H}^T\ \mathcal{H}\ dv_i \tag{2.2.18}$$

$$\mathcal{F}_{3i} = \int_{v_i} \rho_{oi}\ \mathcal{H}^T \frac{d\mathbf{T}_i^T}{dt}\ \mathbf{T}_i\ \mathcal{H}\ dv_i \tag{2.2.19}$$

$$\mathcal{F}_{4i} = \int_{v_i} \rho_{oi}\ \mathcal{H}^T\ \mathbf{T}_i^T \frac{d\mathbf{T}_i}{dt}\ \mathcal{H}\ dv_i \tag{2.2.20}$$

Now in order to obtain the kinetic co-energy in the global coordinate system, it is required to consider the variation of the transformation matrix. Thus we have:

$$\{\tilde{u}\} = [Q] \ \{u\} \tag{2.2.21}$$

then

$$\{\frac{d}{dt}\tilde{u}\} = [Q] \ \{\frac{du}{dt}\} + \left[\frac{dQ}{dt}\right] \ \{u\} \tag{2.2.22}$$

where $\mathbf{Q}$ is the transformation matrix which transforms the nodal displacements from the co-rotational frame to the global coordinate system.

Substituting expressions (2.2.21) and (2.2.22) into equation (2.2.16), we obtain:

$$T_i^* = \frac{1}{2}\left[\mathbf{u}_i^T \ \mathcal{m}_{1i} \ \mathbf{u}_i + \frac{d\mathbf{u}_i}{dt}^T \ \mathcal{m}_{2i} \ \frac{d\mathbf{u}_i}{dt} + \mathbf{u}_i^T \ \mathcal{m}_{3i} \ \frac{d\mathbf{u}_i}{dt} + \frac{d\mathbf{u}_i}{dt}^T \ \mathcal{m}_{4i} \ \mathbf{u}_i\right] \tag{2.2.23}$$

where

$$\mathcal{m}_{1i} = \frac{d\mathbf{Q}}{dt}^T \ \mathcal{F}_{2i} \ \frac{d\mathbf{Q}}{dt} + \mathbf{Q}^T \ \mathcal{F}_{1i} \ \mathbf{Q} + \mathbf{Q}^T \ \mathcal{F}_{3i} \ \frac{d\mathbf{Q}}{dt} + \frac{d\mathbf{Q}}{dt}^T \ \mathcal{F}_{4i} \ \mathbf{Q} \tag{2.2.24}$$

$$\mathcal{m}_{2i} = \mathbf{Q}^T \ \mathcal{F}_{2i} \ \mathbf{Q} \tag{2.2.25}$$

$$\mathcal{m}_{3i} = \frac{d\mathbf{Q}}{dt}^T \ \mathcal{F}_{2i} \ \mathbf{Q} + \mathbf{Q}^T \ \mathcal{F}_{3i} \ \mathbf{Q} \tag{2.2.26}$$

$$\mathcal{m}_{4i} = \mathbf{Q}^T \ \mathcal{F}_{2i} \ \frac{d\mathbf{Q}}{dt} + \mathbf{Q}^T \ \mathcal{F}_{4i} \ \mathbf{Q} \tag{2.2.27}$$

It is important to note that since the rigid body motion of an element is part of the overall motion of that element and is not prescribed, it is required to obtain the relation between the rigid body angular velocity and the acceleration of the element and the nodal global velocities and accelerations found in the process of solution.

Referring to equation (2.1.58), we may write:

$$\frac{d}{dt}\tilde{u} = \mathbf{g}_1^T \ \frac{d\mathbf{u}}{dt} \tag{2.2.28}$$

Also from equation (2.1.86), we have:

$$\frac{d\varphi}{dt} = \frac{1}{l_c} \mathbf{Z}^T \frac{d\mathbf{u}}{dt} \tag{2.2.29}$$

which relates the angular velocity of the rigid body motion of the beam element to the rate of change of nodal variables.

To obtain the angular acceleration of the element due to rigid body rotation, we obtain the time derivative of equation (2.2.29), as:

$$\frac{d^2\varphi}{dt^2} = -\frac{1}{l_c^2} \frac{dl_c}{dt} \mathbf{Z}^T \frac{d\mathbf{u}}{dt} + \frac{1}{l_c} \frac{d\mathbf{Z}^T}{dt} \frac{d\mathbf{u}}{dt} + \frac{1}{l_c} \mathbf{Z}^T \frac{d^2\mathbf{u}}{dt^2} \tag{2.2.30}$$

Using equations (2.1.43) and (2.1.85), (2.2.28) and (2.2.29), we have:

$$\frac{dl_c}{dt} = \frac{d}{dt}\tilde{u} = \mathbf{g}_1^T \frac{d\mathbf{u}}{dt} \tag{2.2.31}$$

and

$$\frac{d\mathbf{Z}^T}{dt} = -\frac{d\varphi}{dt} \mathbf{g}_1^T = -\frac{1}{l_c} \mathbf{Z}^T \frac{d\mathbf{u}}{dt} \mathbf{g}_1^T \tag{2.2.32}$$

Substituting relations (2.2.31) and (2.2.32) into equation (2.2.30), we obtain:

$$\frac{d^2\varphi}{dt^2} = \frac{1}{l_c} \mathbf{Z}^T \frac{d^2\mathbf{u}}{dt^2} - \frac{2}{l_c} \frac{d\varphi}{dt} \mathbf{g}_1^T \frac{d\mathbf{u}}{dt} \tag{2.2.33}$$

### 2.2.2.2 Element Lagrangian Function

Using the obtained element kinetic co-energy and the element strain energy $\Pi_i$, due to large overall motion, and considering the potential energy for the external forces acting on the element $\mathbf{r}$, we may express the element Lagrangian function as:

$$\mathcal{L}_i = \frac{1}{2}\left[\mathbf{u}_i^T \; m_{1i} \; \mathbf{u}_i + \frac{d\mathbf{u}_i^T}{dt} \; m_{2i} \frac{d\mathbf{u}_i}{dt} + \mathbf{u}_i^T \; m_{3i} \frac{d\mathbf{u}_i}{dt} + \frac{d\mathbf{u}_i^T}{dt} \; m_{4i} \; \mathbf{u}_i\right] - \Pi_i - \mathbf{r}^T \mathbf{u}_i \tag{2.2.34}$$

### 2.2.2.3 Discretized Equations of Motion

Using Hamilton's principle and piece-wise linearizing the equation of motion through the full Newton-Raphson method, the equation of motion at the $i^{th}$ iteration are obtained as:

$$ {}^{t+\Delta t}[m] \, {}^{t+\Delta t}\left\{\frac{d^2u}{dt^2}\right\}^i + {}^{t+\Delta t}[c_{eq}] \, {}^{t+\Delta t}\left\{\frac{du}{dt}\right\}^i + {}^{t+\Delta t}[k_{eq}]\,\{\Delta u\}^i = {}^{t+\Delta t}\{r\} - {}^{t+\Delta t}_{t+\Delta t}\{f\}^{i-1} \tag{2.2.35} $$

where

$$ [m] = [m_{2i}] \tag{2.2.36} $$

$$ [c_{eq}] = \left[\frac{dm_{2i}}{dt}\right] + [m_{3i}]^T - [m_{3i}] \tag{2.2.37} $$

is the equivalent damping matrix,

$$ [k_{eq}] = \left[\frac{dm_{3i}}{dt}\right]^T - [m_{1i}] + [k_T] \tag{2.2.38} $$

is the equivalent stiffness matrix. In the above expressions $\mathbf{f}$ and $\mathbf{k}_T$ are the element internal force vector and the tangent stiffness matrix and can be obtained from the element strain energy, i.e.:

$$ \{f\} = \left\{\frac{\partial \Pi_i}{\partial u_m}\right\} \tag{2.2.39} $$

$$ [k_T] = \left[\frac{\partial^2 \Pi_i}{\partial u_m \partial u_n}\right] \tag{2.2.40} $$

The sum effect of all the elements, after assembly process is obtained as:

$$ {}^{t+\Delta t}[M] \, {}^{t+\Delta t}\left\{\frac{d^2u}{dt^2}\right\}^i + {}^{t+\Delta t}[C_{eq}] \, {}^{t+\Delta t}\left\{\frac{du}{dt}\right\}^i + {}^{t+\Delta t}[K_{eq}]\,\{\Delta u\}^i = {}^{t+\Delta t}\{R\} - {}^{t+\Delta t}_{t+\Delta t}\{F\}^{i-1} \tag{2.2.41} $$

### 2.2.2.4 Illustrative Examples

We note that the iterative equations in the dynamic analysis, using the implicit time integration are of the same form as the equations that we considered in the static non-linear analysis, except that in the dynamic case both the coefficient matrices and the nodal force vector contain contributions from the inertia of the system. We can therefore directly conclude that all iterative solution strategies discussed for static analysis are also applicable to the dynamic analysis. However, since the inertia of the system renders its dynamic response, in general, more smooth than its static response, convergence of the iteration can, in general, be expected to be more rapid than in the static analysis. The reason for the better convergence characteristics in the dynamic analysis lies in the contributions of the mass matrix to the coefficient matrices. Indeed, this contribution becomes dominant when the time step is small.

It is also important to note that the iteration can be of utmost importance, since any error admitted in the incremental solution at a particular time directly affects, in a path-dependent manner, the solution at any subsequent time (see Bathe, 1982).

The numerical stability and accuracy of the Newmark direct time integration has been discussed extensively by Argyris et al., 1991, and Leong, 1992. Here we show the performance of this implicit time integration scheme in conjunction with the updated Lagrangian method by considering four simple truss problems:

- **Bathe Pendulum**

This problem has been discussed by Bathe, 1982, and Crisfield and Shi, 1994. The axially flexible pendulum is dropped from the horizontal position due to gravity, see Figure 2.2.2. Figure 2.2.3 shows the time history of the motion using time steps 0.01 $s$ (correct solution) and 0.05 $s$. It can be easily seen that using large time steps, the response converges to the wrong solution. This phenomenon was also noted by Bathe, 1986, and Crisfield and Shi and is referred as solution locking. The problem shows that even though the solution algorithm is numerically stable, there is a need to use small time steps if accuracy is to be maintained. This is the major weakness of the Newmark implicit time integration. Other improvements are also required to produce economic dynamic solution algorithms (e.g. see Crisfield and Shi and Simo and Tarnow, 1992). The effect of using an iterative procedure to obtain converged equilibrium positions is also shown in Figure 2.2.4 where the solid line is obtained with no iterations. It is also important to note that for this time integration to retain the required accuracy, it is required to use a tight convergency tolerance. Such an effect can also be seen in Figure 2.2.5.

$L = 120$ (in)

$E = 10^7$ (psi)

$A = 1$ ($in^2$)

$m = 1$ (slug)

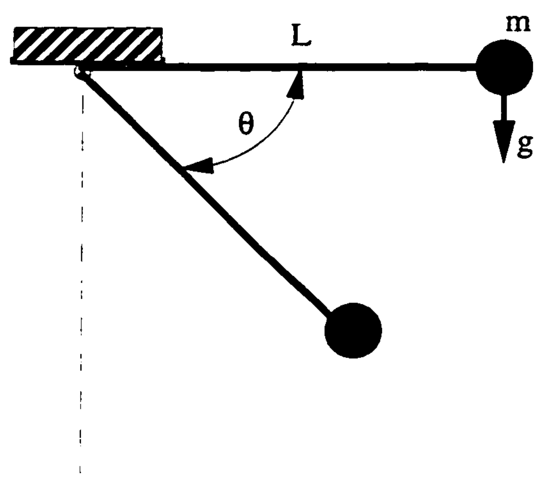


Figure 2.2.2: Bathe Pendulum.

- **Truss Element Under Impulse Loading: Snap Through Problem**

In this problem we consider a weightless truss element with a unit point mass attached at its free end as shown in Figure 2.2.6. The total nondimensionalized potential of the system, including the constant external force ($R$) and the spring, is given by:

$$\Pi = \frac{1}{2}\left(Y^2 + Y^3 + \frac{1}{4}Y^4\right) + \frac{1}{2}K\,Y^2 - P\,Y \qquad (2.2.42)$$

where

$$Y = \frac{y}{Y_o}, \quad K = \frac{K_s}{Y_o^2}\left(\frac{L^3}{EA}\right), \quad P = \frac{R}{Y_o^3}\left(\frac{L^3}{EA}\right) \text{ and } \Pi = \frac{\Pi}{Y_o^4}\left(\frac{L^3}{EA}\right) \qquad (2.2.43)$$

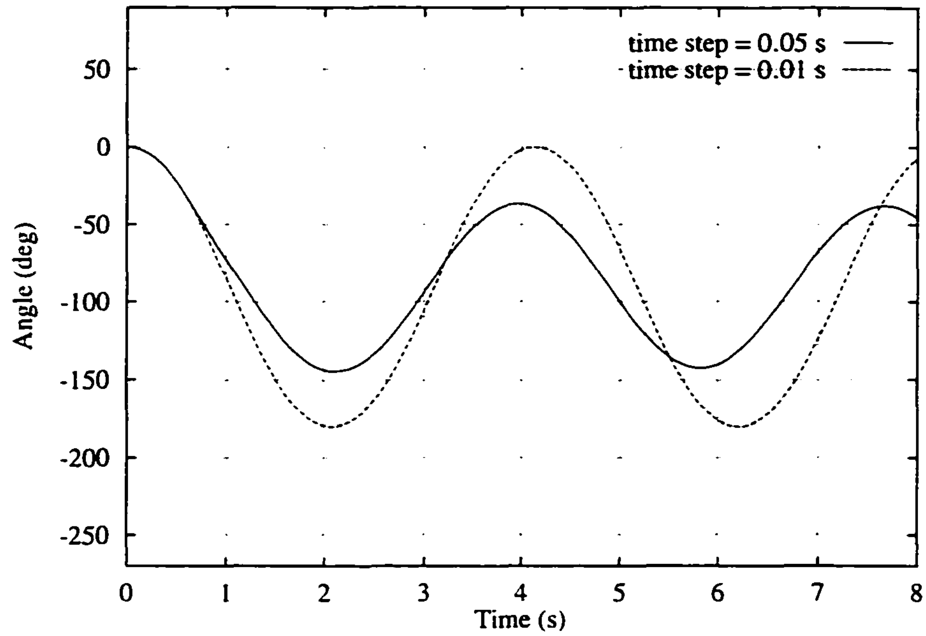


Figure 2.2.3: Bathe Pendulum: Time History.

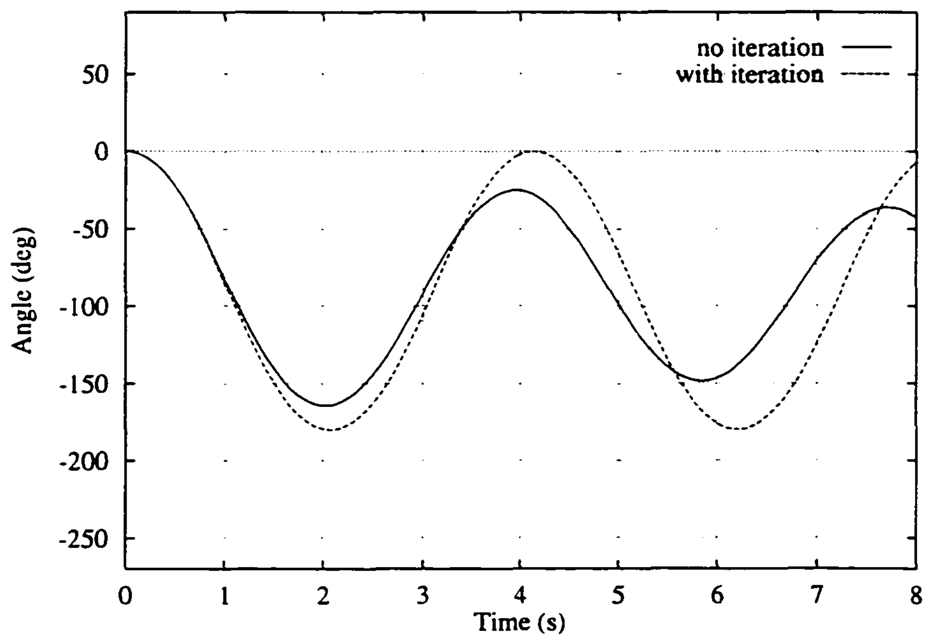


Figure 2.2.4: Bathe Pendulum: Time History, Effect of Iteration.

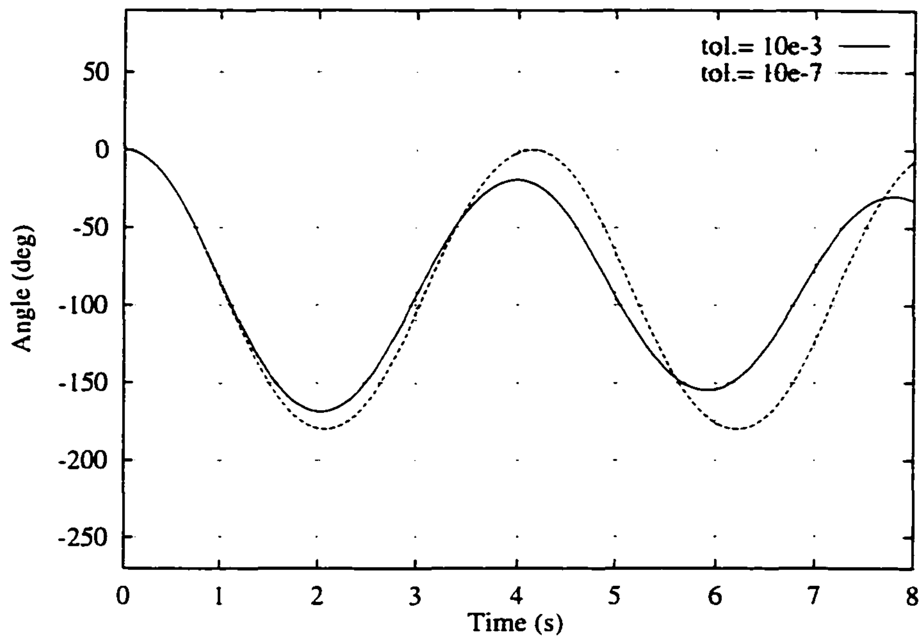


Figure 2.2.5: Bathe Pendulum: Time History, Effect of Tolerance.

Using equation (2.2.43), one may obtain the non-dimensionalized load-displacement curve under static equilibrium conditions with various values of spring stiffnesses, see Figure 2.2.7. Now an ideal impulse is applied at the free end of the truss. The phase diagrams of the system for various values of the spring stiffness and the initial kinetic co-energies are shown in Figures 2.2.8 to 2.2.10. It can be seen that for the zero spring stiffness when the ideal impulse is greater than the critical level (0.125), the system passes the unstable static equilibrium point (point $B$) and moves to the other static stable point (point $C$). This will result in a large amplitude vibrations enclosing points $A$, $B$ and $C$ (Figure 2.2.8).

For a spring stiffness of 0.125, if the initial kinetic co-energy is less than the critical energy level (0.21), the system only oscillates about the stable static equilibrium point $A$. When the energy level is greater than this critical level, again large amplitude oscillations occur enclosing both points $A$ and the neutral static equilibrium point $D$ (Figure 2.2.9). For the last case, when the spring stiffness is 0.5, the system oscillates around point A (statically stable) for all initial kinetic co-energies and therefore the system is always dynamically stable (see Figure 2.2.10).

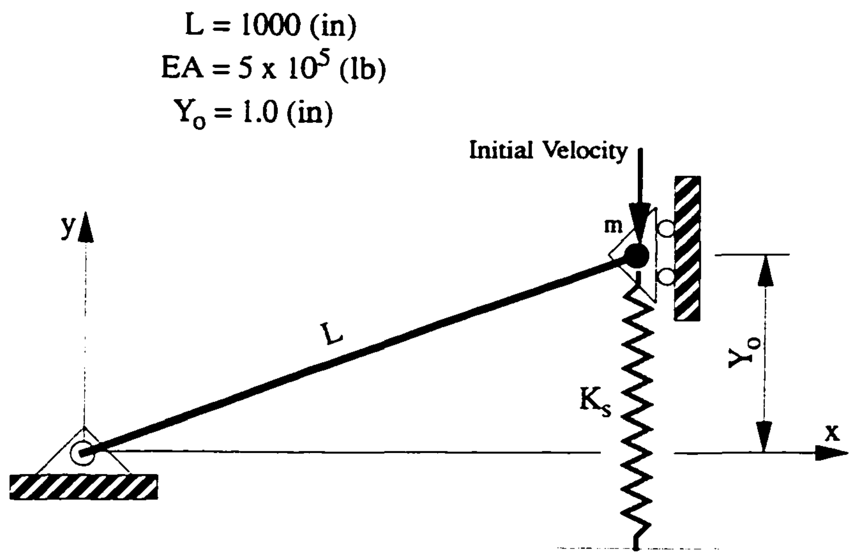


Figure 2.2.6: Snap Through Problem.

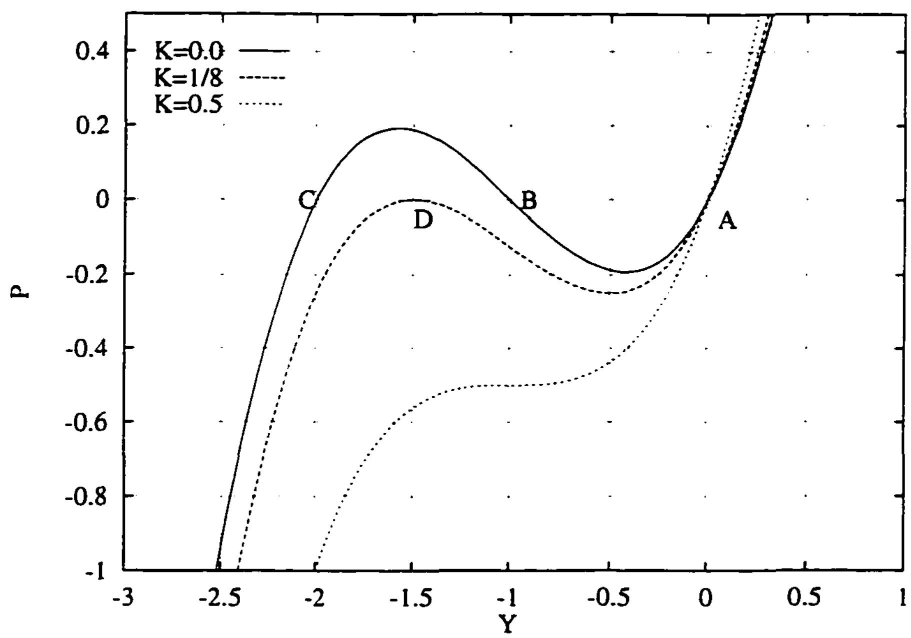


Figure 2.2.7: Static Equilibrium with varying Spring Stiffness.

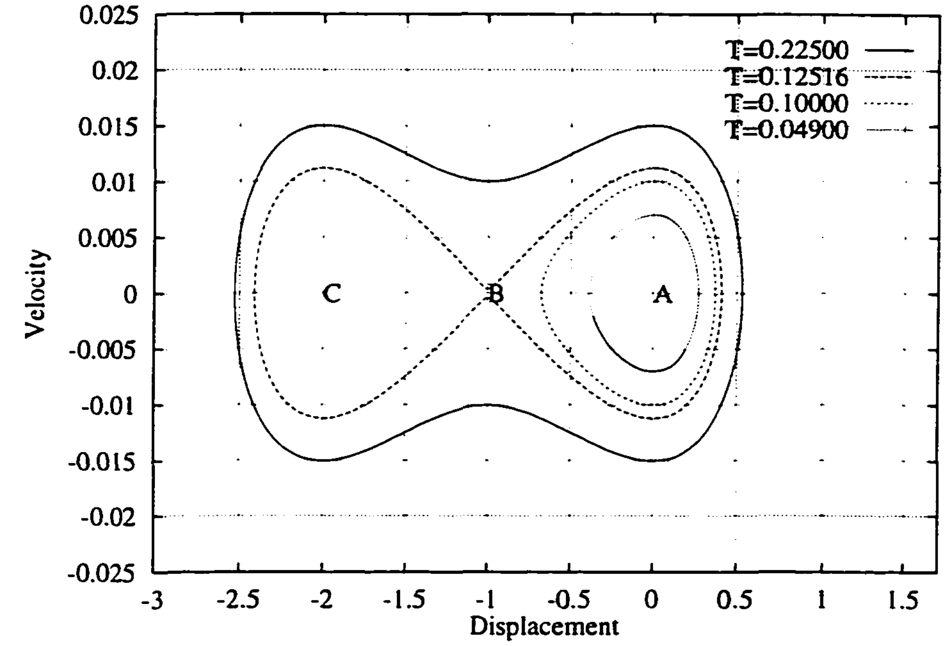


Figure 2.2.8: Phase Diagram, K=0.0.

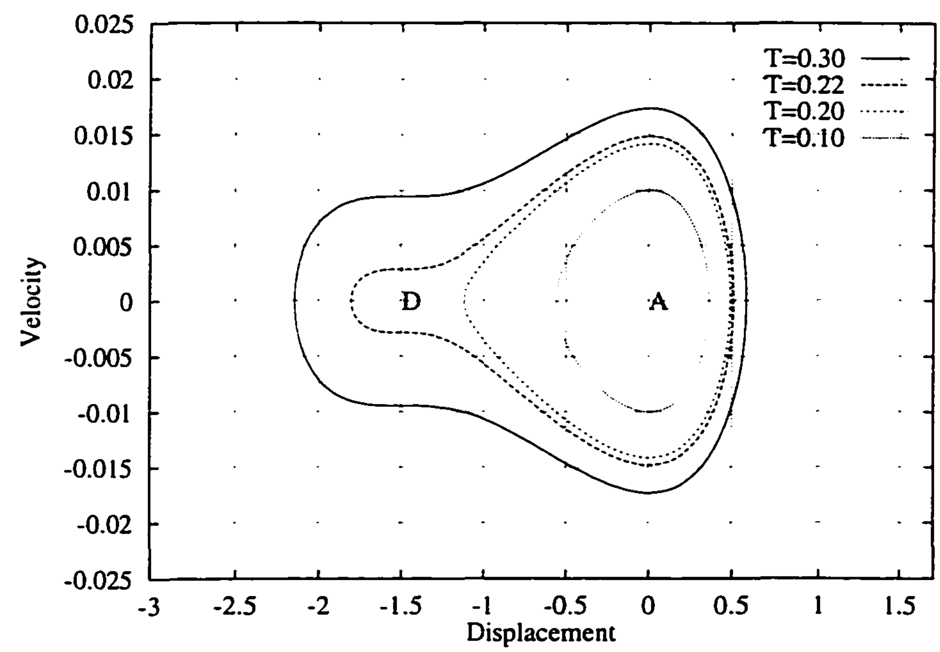


Figure 2.2.9: Phase Diagram, K=0.125.

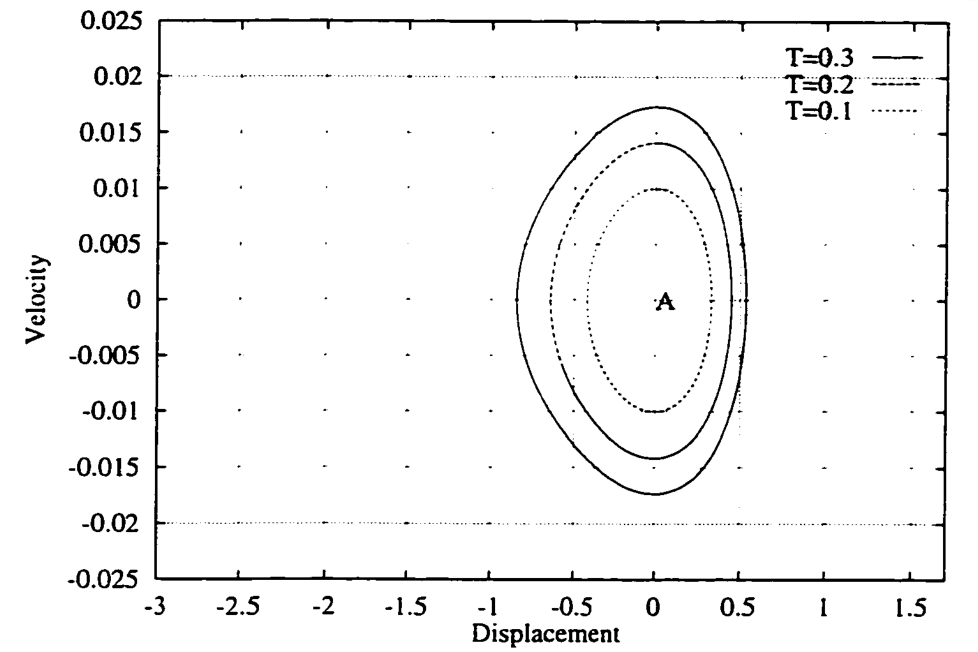


Figure 2.2.10: Phase Diagram, K=0.5.

- **Truss Element Under Impulse Loading: One d.o.f. Bifurcation**

The truss element shown in Figure 2.2.11 is assumed to be weightless with a unit point mass attached to its free end and initially lying on the $y$ axis. This system is known to exhibit limit point instability. The non-dimensionalized potential energy of the system is given by:

$$\Pi = (1 - \cos\theta)(1 + \cos\theta - 2P) \tag{2.2.44}$$

where

$$P = \frac{R}{K_s L} \quad \text{and} \quad \Pi = \frac{2\Pi}{K_s L^2} \tag{2.2.45}$$

The static equilibrium condition and the bifurcation point $A$ for this system are shown in Figure 2.2.12. An initial velocity is applied and the phase diagrams of the system under various initial kinetic co-energy levels, at zero eccentricity, are shown in Figure 2.2.13. Thus when the non-dimensionalized initial kinetic co-energy is less than the critical energy level 1.0, the system oscillates around the initial position. When the kinetic co-energy is greater than the critical energy level, then the system will be displaced in the positive (negative) angle direction with positive (negative) initial angular velocity.

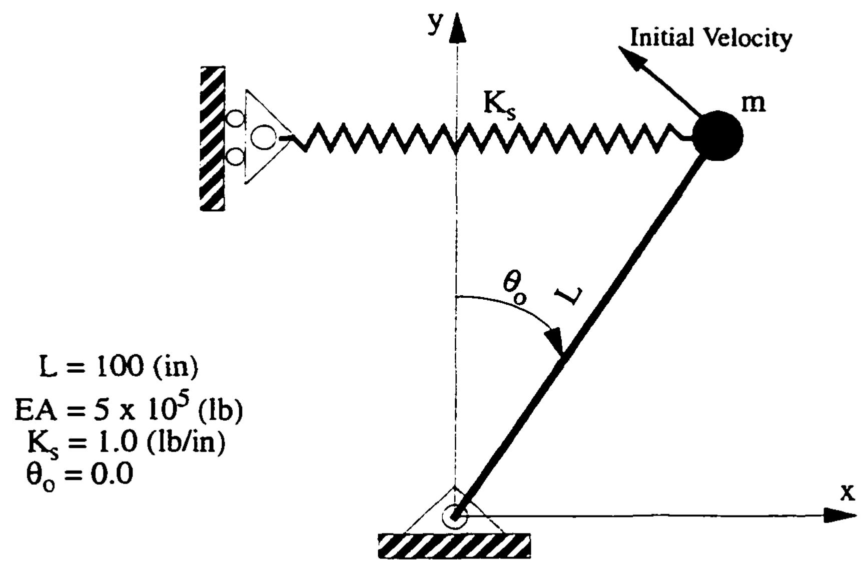


Figure 2.2.11: Bifurcation of a Single Degree of Freedom System.

The two previous examples have shown not only the physical side of these problems, but also the performance of time integration to achieve such results accurately. The obtained results are identical to those obtained by Leong, 1992. In the next example we return again to the effects of time step on the accuracy of solutions and consider the important issues of numerical stability and accuracy.

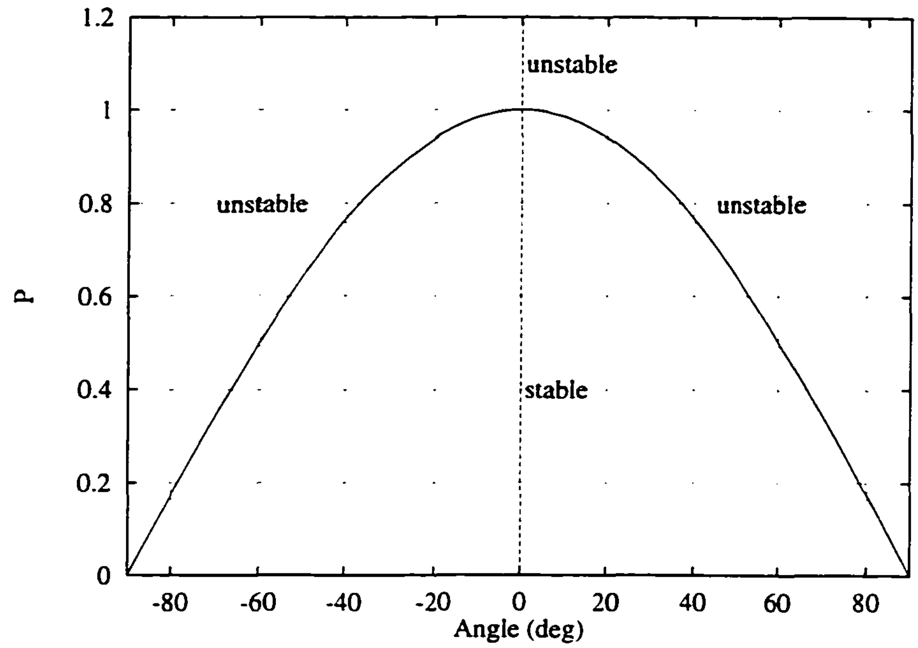


Figure 2.2.12: Static Equilibrium.

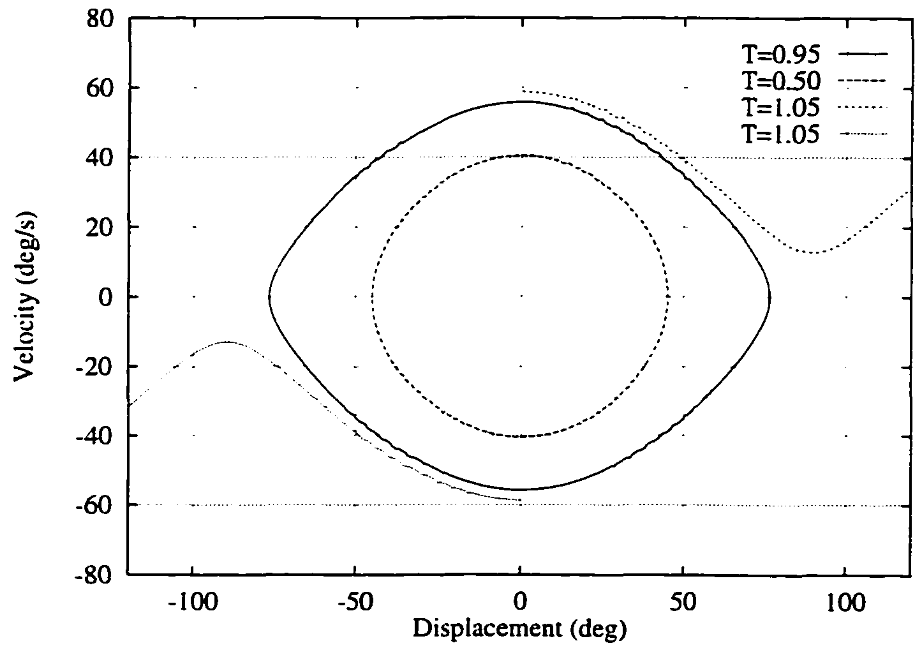


Figure 2.2.13: Phase Diagram Under Ideal Impulse.

- **Truss Element Under Impulse Loading: Two Degrees of Freedom Model**

This problem is the same as the previous one except that Young's modulus is taken as $5\times10^3$ psi. This adds another d.o.f. to the system due to the axial flexibility of the truss element. We consider the initial velocity of 70 in/sec which is lower than the critical velocity of 91.269 in/sec required for the truss to escape from the region where oscillations take place about the y axis. Using a time step of 0.01 s confirms such a response, Figures 2.2.14 and 2.2.15. Using larger time step, e.g. 0.1 *s*, leads to numerical instability as shown in Figures 2.2.14 and 2.2.16, implying an escape from the region of small vibrations. As shown by Crisfield and Shi, 1994, this is due to numerical instability and inaccuracy of the solution which converges to a false equilibrium position at each time step and after few time steps this yields to an artificial build up of energy in the system. This problem again emphasizes the fact that the implicit time integration methods which are unconditionally stable for linear systems, may be unstable in nonlinear systems and careful attention should be given to the time step to avoid numerical instability and inaccuracy. Evidently stable and accurate solutions can only be obtained at high computational costs, by this approach.

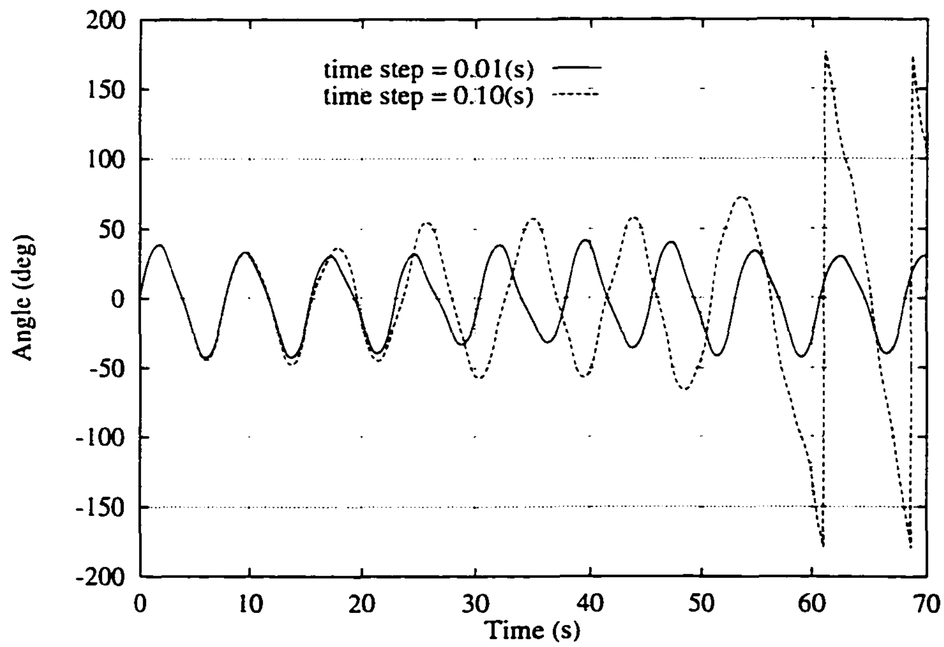


Figure 2.2.14: Time History.

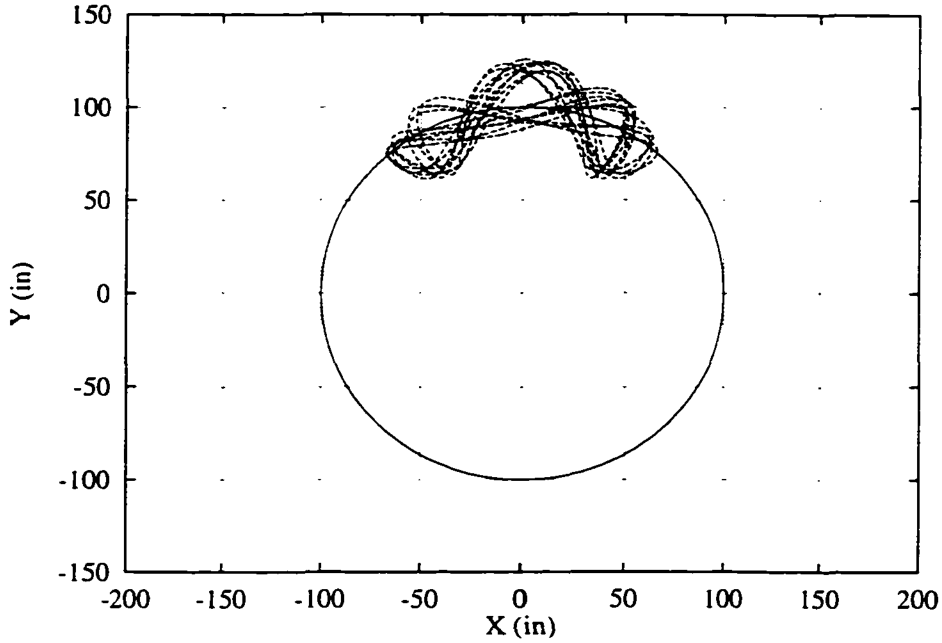


Figure 2.2.15: Trace of End Point: Time step 0.01 *s*.

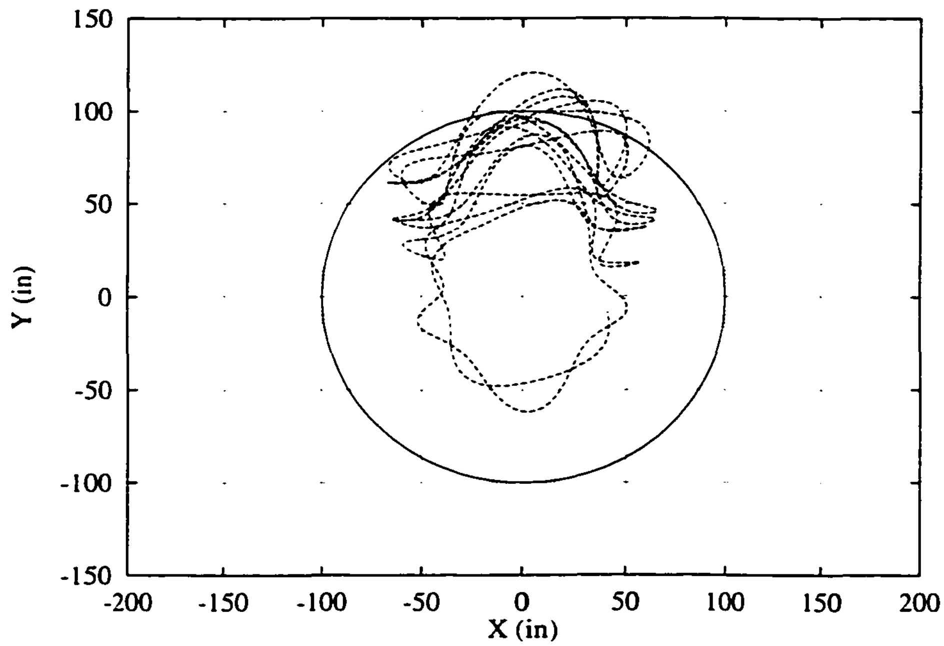


Figure 2.2.16: Trace of End Point: Time step 0.1 *s*.

In the following examples we solve for the displacement time history of a number of simple beam problems. These problems have been formulated using both the updated-Lagrangian and the consistent co-rotational methods. The updated-Lagrangian method uses the modified Newton-Raphson iterative method in conjunction with a tangential stiffness matrix. The consistent co-rotational method uses the full Newton-Raphson iterative method. The modified Newton-Raphson method uses the system matrices of the last equilibrium configuration and requires fewer mass, damping and stiffness reformations than the full Newton-Raphson method.

To carry out the integration required for computing the out-of-balance force vector and mass, damping and stiffness matrices, the symbolic operator program Maple was used, thereby decreasing the integration errors involved in numerical integration. In the case of the updated-Lagrangian formulation, an adaptive time-step size algorithm (Stylianou, 1993) was used. This algorithm has been found to be extremely efficient in decreasing the number of time integration steps for mildly nonlinear problems. Various convergence criteria have also been evaluated. It was found that the convergence criterion based on the residual energy, measured from the out-of-balance force and incremental displacement at each load increment, together with a tight tolerance ( $< 10^{-6}$) result in the least accumulation of error.

- **Undamped Clamped-Clamped Beam**

In this example an undamped clamped-clamped beam, subjected to a rectangular pulse loading as shown in Figures 2.2.17, is analysed. The displacement time histories determined by the two formulations (Figure 2.2.18) are in good agreement and are also in agreement with results reported by Rice and Ting, 1993. The updated Lagrangian method requires 250 time steps and the consistent co-rotational method uses 50 time step. The low number of time steps required for this problem is due to the fact that deflections under such load history still remain relatively small.

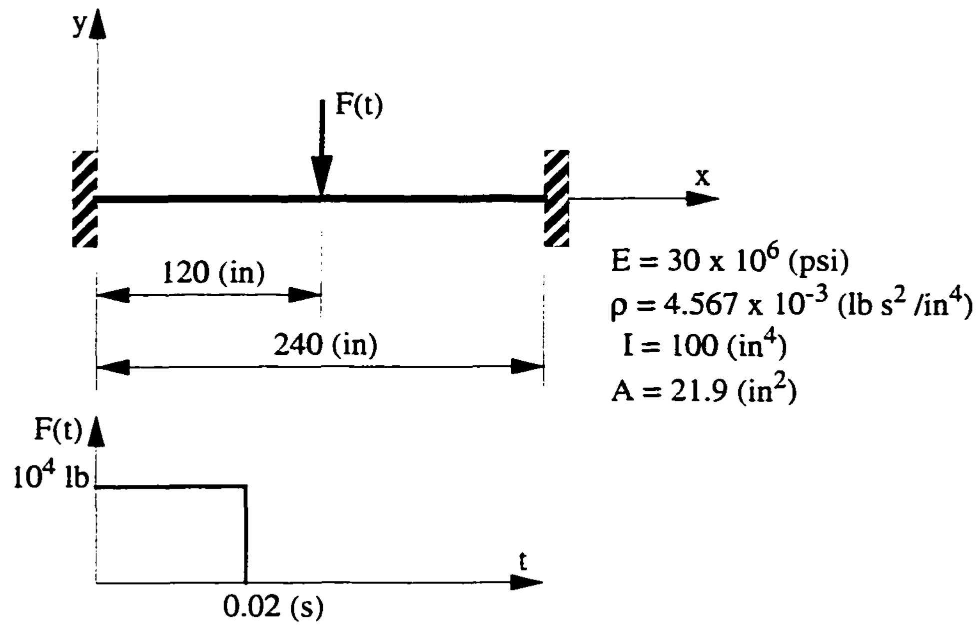


Figure 2.2.17: Beam Geometry and Load History.

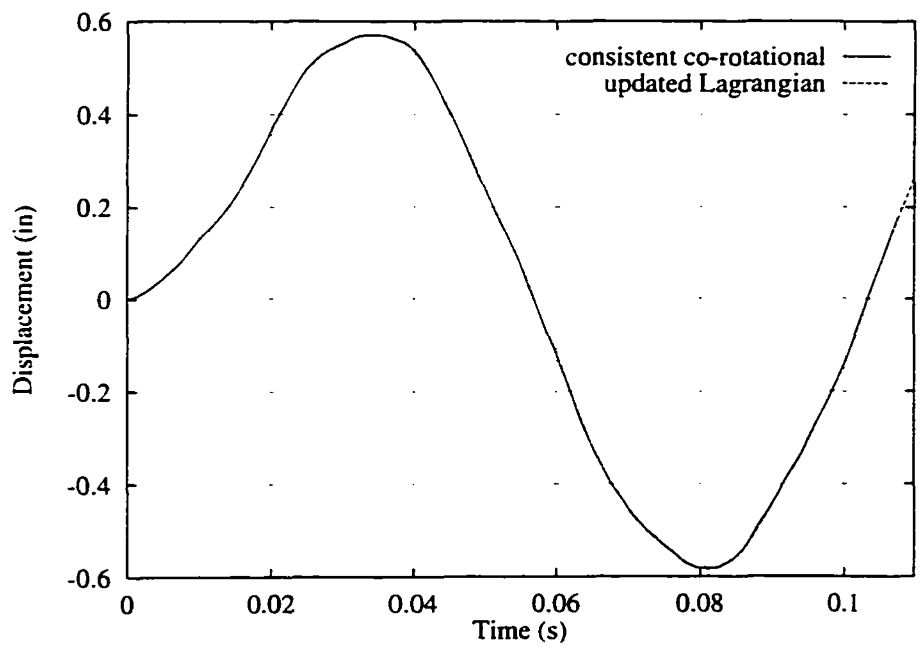


Figure 2.2.18: Mid-Span Displacement History.

- **Undamped Cantilever Under Ramp-Infinite Duration Load**

In this example we consider a cantilever beam under a ramp-infinite duration load as shown in Figure 2.2.19. For this problem 4 beam elements were used. Both formulations lead to the same response but in the updated Lagrangian method 627 time steps were needed while in the consistent co-rotational method with only 100 time steps convergence was assured (see Figure 2.2.20). This shows the efficiency of the latter formulation. The response obtained is in good agreement with those reported by Rice and Ting, 1993. Here it should be noted that using a tight tolerance for the program has a key role in preventing error accumulation in the follow-up time steps which in turn guarantee the accuracy of the solution.

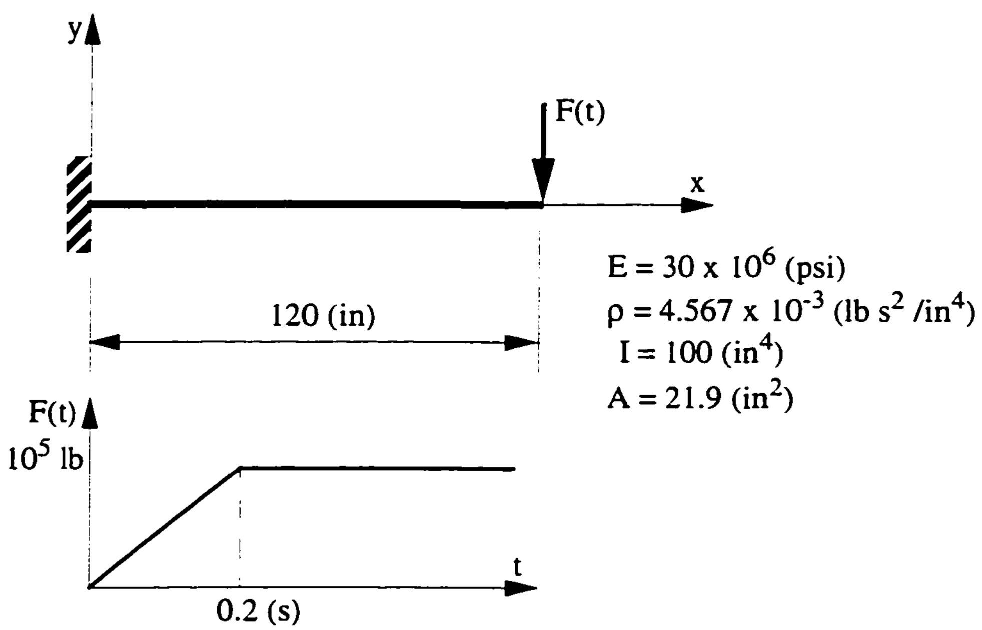


Figure 2.2.19: Beam Geometry and Load History.

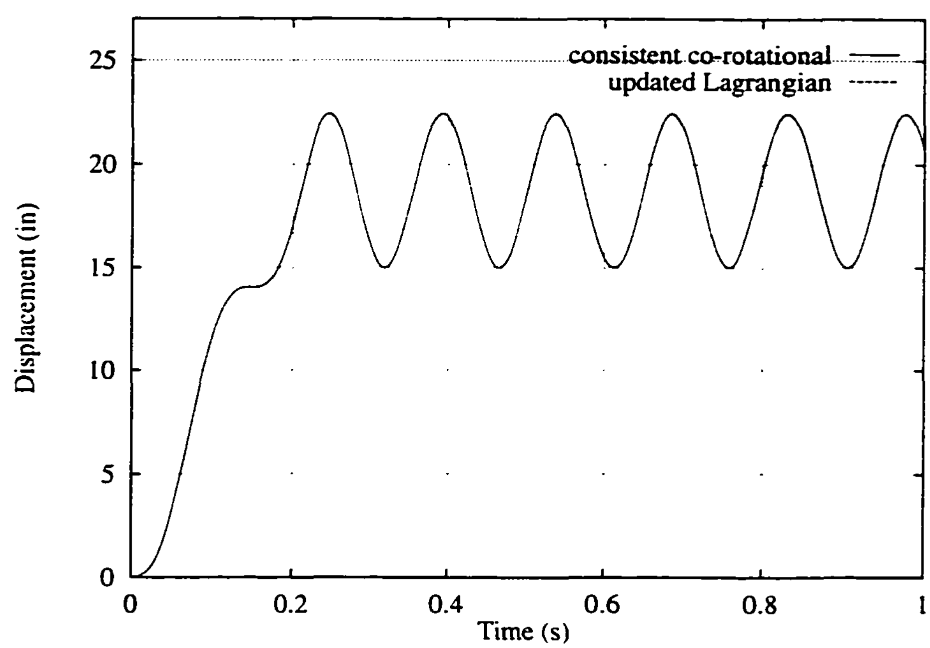


Figure 2.2.20: Time Response of the Tip.

- **Damped Cantilever Under Ramp-Ramp Load**

This problem involves a cantilever beam under a ramp-ramp load, as shown in Figure 2.2.21 (see also Simo and Vu-Quoc, 1986). Here a viscous damping coefficient of 10 lb/in/s was used at each translational degree of freedom. Four elements were used to model this problem. The results from the two formulations again show the same response, see Figure 2.2.22. The number of time steps required for converged solution was about the same as that in the previous example.

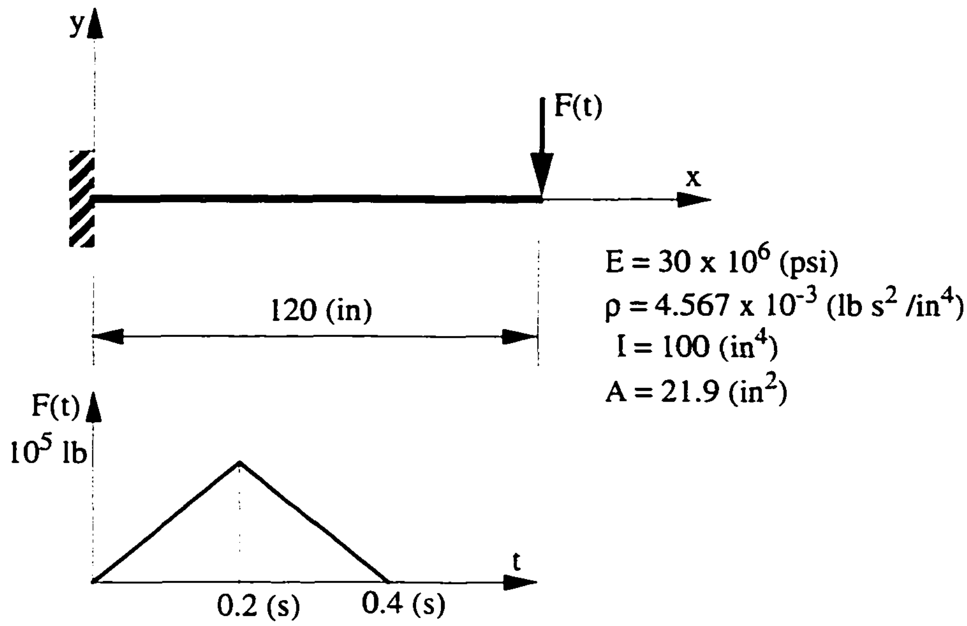


Figure 2.2.21: Beam Geometry and Load History.

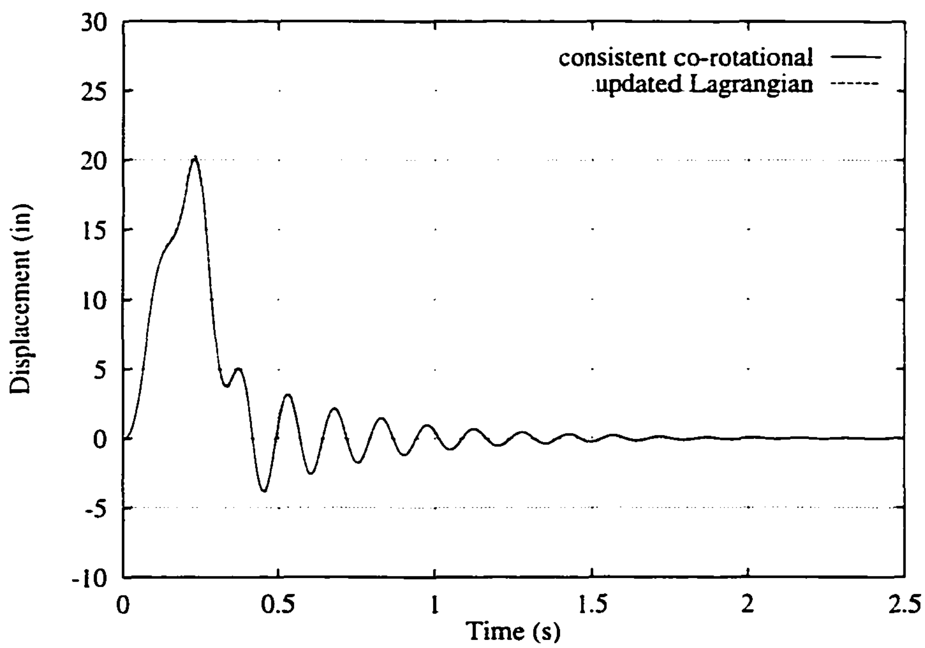


Figure 2.2.22: Tip Displacement History.

- **Damped Cantilever Subjected to Infinite Duration Load**

In this final example a cantilever beam is subjected to a tip load with an infinite duration as shown in Figures 2.2.23. This is a severe test for accuracy of the formulation and time integration. In this case, a viscous damping coefficient of 3 lb/in/s at each translational degree of freedom was used. The response is expected to converge to the static solution as time approaches infinity. However the updated-Lagrangian formulation shows a small offset compared with the consistent co-rotational method which converges correctly to the value of static solution, 24.3 (*in*), (Figure 2.2.24). A plausible explanation for the offset in the updated Lagrangian method is that in this formulation, conventionally the time rate of change of the rotation matrix of the element is not taken into account. That is, the system is modeled as instantaneous structures at each equilibrium configuration. This is the conventional updated Lagrangian method but this shortcoming may be overcome by a modification in its formulation. Since the final equilibrium depends on the response history of the system, the accumulation of errors at each time step leads to the observed discrepancy. In the case of highly nonlinear systems, such error accumulations is known to cause numerical instabilities and convergence failure.

It should also be noted that in the updated Lagrangian method 40000 time steps were required while in the consistent co-rotational method only 2000 time step were sufficient for convergence. This, once again, demonstrates the remarkable performance of the consistent co-rotational method in the dynamic analysis of geometrically nonlinear beams.

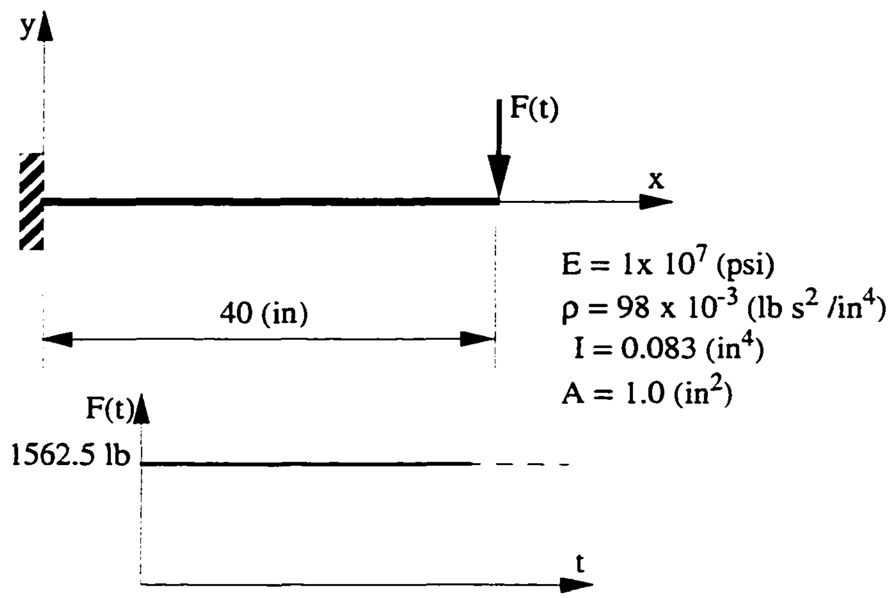


Figure 2.2.23: Beam Geometry and Load History.

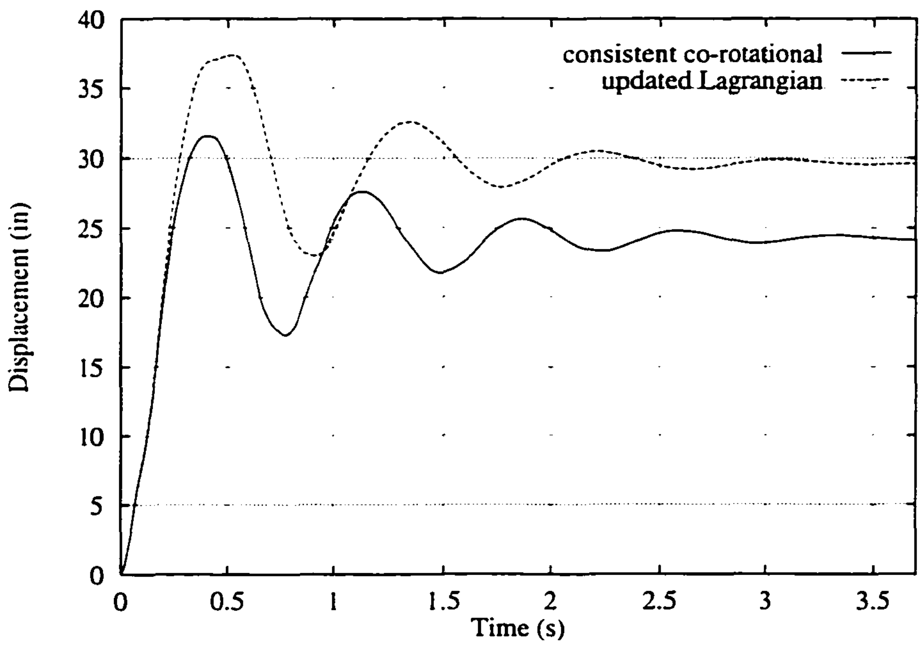


Figure 2.2.24: Tip Displacement History.

## 2.3 Conclusions

In this chapter, the general problem of static and dynamic analysis of geometrically nonlinear beams were considered. Two important formulations, namely the updated Lagrangian and the consistent co-rotational formulations, were used to obtain solutions for static and dynamic response of beam systems.

In the static and dynamic analysis, we found the consistent co-rotational method to be more powerful, accurate and efficient than the updated Lagrangian method. We also noted that the use of higher order strain measures will increase the accuracy of the solution but at the expense of increase computational costs. If the engineering strain measure is used the mesh must be refined for comparable accuracy.

In this chapter we used the load control algorithm for the examples analysed. Using the consistent co-rotational method for 3D systems requires careful attention to the rigid body rotation angles and forming the transformation matrix (where for efficiency it may be necessary to use the quaternion algebra, see Crisfield, 1990).

The developments in this chapter will be extensively used through out this thesis and in particular in the dynamic analysis of flexible sliding beams.

# Chapter 3

# Equations of Motion for Sliding Beams

Equations of motion for geometrically nonlinear flexible sliding beams, deployed or retrieved through prismatic joints, are derived in this chapter. The sliding motion of beams in a fixed channel can be brought about either by a constant density axial force field or by an axial force applied at the root of the beams. The beams can undergo large rotations in a plane. Based on the assumptions of Euler-Bernoulli beam theory, the equations of motion are derived for small deformations through an extension of Hamilton's principle. In the latter part of this chapter, we provide an alternative formulation wherein the beam is brought to rest and the channel assumes a prescribed velocity.

## 3.1 Sliding Beam Formulation

The natural way to formulate the flexible sliding beam problem is to view the beam sliding through a rigid channel and undergoing large overall motion when it has emerged from the channel. Thus at any instant, three different configurations can be distinguished, namely: the initial undeformed or material configuration in the channel, the spatially fixed intermediate configuration and the sliding deformed configuration.

The intermediate configuration is an artifice introduced for purposes of formulation. That is, the beam does not follow a sequence of configurations from within the channel to the intermediate and finally to the deformed configuration. Rather to describe the deformed configuration we need an undeformed reference configuration and it is for this purpose that the intermediate configuration is introduced.

The intermediate configuration can be seen as an Eulerian domain with respect to the translating undeformed beam and a Lagrangian domain with respect to the current deformed beam. The intermediate configuration is a fixed spatial configuration used as reference for the deformed state. In this configuration the boundary extends in time that is this configuration has a moving boundary.

The mapping from the material configuration to the intermediate configuration is a prescribed sliding rigid body motion along the channel axis. This can be seen by looking at the material point $M$ that passes by inertially fixed points and at time $t$ coincides with $\bar{m}$. Then, the deformation from the intermediate configuration to the current configuration is a Lagrangian description from the inertially fixed point $\bar{m}$ to the spatial point $m$, see Figure 3.1.1.

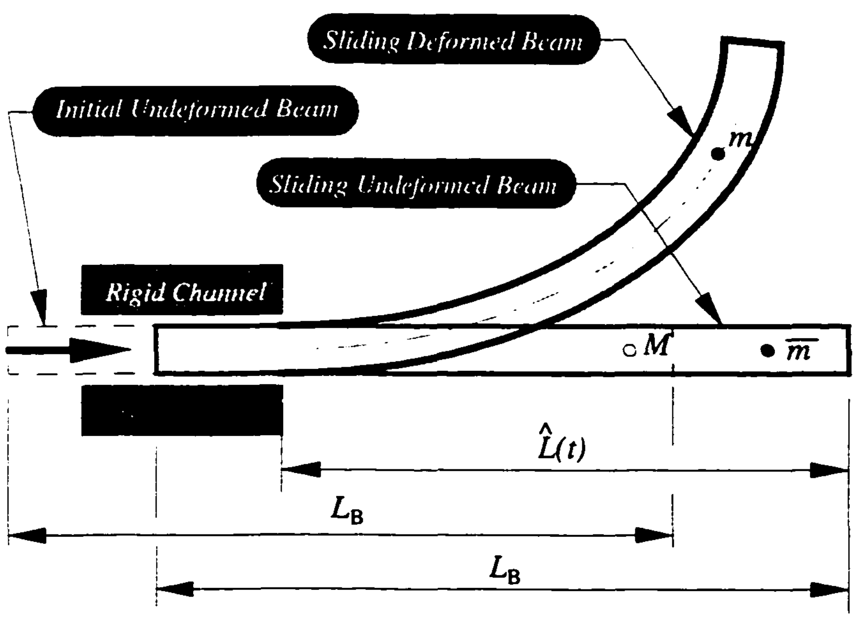


Figure 3.1.1: Sliding beam: initial undeformed, sliding undeformed and deformed configurations.

Viewing the sliding beam as a system of changing mass, we assume that the part of the beam inside the channel is non-deformable and has a prescribed motion. Thus, the task is to determine the motion of the beam as it emerges from the channel.

### 3.1.1 Kinematic Descriptions

Following the basic development by Semler et al., 1994, the distance, $\delta S_o$, between two points lying on the centerline of the beam in the undeformed state may be written as:

$$(\delta S_o)^2 = (\delta\chi_1)^2 + (\delta\chi_2)^2 \tag{3.1.1}$$

and the distance, $\delta S$, between the same two points after deformation is given by:

$$(\delta S)^2 = (\delta x_1)^2 + (\delta x_2)^2 \tag{3.1.2}$$

where $x_1 = x_1(\chi_1, \chi_2)$ and $x_2 = x_2(\chi_1, \chi_2)$.

Therefore, the change of distance between these two points is given by:

$$(\delta S)^2 - (\delta S_o)^2 = (\delta x_1)^2 + (\delta x_2)^2 - \left[(\delta\chi_1)^2 + (\delta\chi_2)^2\right] \tag{3.1.3}$$

For the beam initially lying along the $\mathbf{I}_1$ axis $(\delta S_o = \delta\chi_1, \delta\chi_2 = 0)$ :

$$\delta x_1 = \frac{\partial x_1}{\partial \chi_1}\,\delta\chi_1, \qquad \delta x_2 = \frac{\partial x_2}{\partial \chi_1}\,\delta\chi_1 \tag{3.1.4}$$

Hence, equation (3.1.2) may be expressed as:

$$\delta S = \sqrt{\left(\frac{\partial x_1}{\partial \chi_1}\right)^2 + \left(\frac{\partial x_2}{\partial \chi_1}\right)^2}\;\delta\chi_1 \tag{3.1.5}$$

and equation (3.1.3) may be written as:

$$(\delta S)^2 - (\delta S_o)^2 = \left[\left(\frac{\partial x_1}{\partial \chi_1}\right)^2 + \left(\frac{\partial x_2}{\partial \chi_1}\right)^2 - 1\right]\;(\delta\chi_1)^2 \tag{3.1.6}$$

For the axially inextensible beam, $\delta S = \delta S_o$, and for this case we find the inextensibility condition from equation (3.1.6) as:

$$\left(\frac{\partial x_1}{\partial \chi_1}\right)^2 + \left(\frac{\partial x_2}{\partial \chi_1}\right)^2 = 1 \tag{3.1.7}$$

It will be also useful to express the above conditions in terms of displacement components of the centerline $u_1$, $u_2$, see Figure 3.1.2.

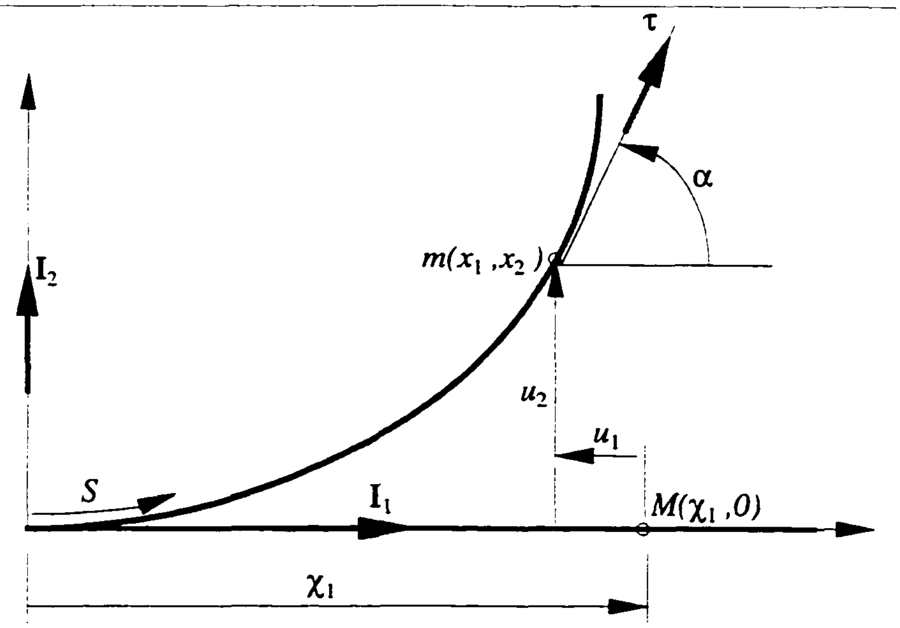


Figure 3.1.2: Centerline Kinematics of a deformed beam.

Noting that:

$$u_1 = x_1 - \chi_1 \tag{3.1.8}$$

$$u_2 = x_2 \tag{3.1.9}$$

where for our case along the centerline $\chi_2 = 0$, then:

$$\frac{\partial x_1}{\partial \chi_1} = \frac{\partial u_1}{\partial \chi_1} + 1 \tag{3.1.10}$$

and

$$\frac{\partial x_2}{\partial \chi_1} = \frac{\partial u_2}{\partial \chi_1} \tag{3.1.11}$$

Therefore, equations (3.1.5), (3.1.6) and (3.1.7) may be rewritten in terms of the displacements as:

$$\delta S = \sqrt{\left(\frac{\partial u_1}{\partial \chi_1} + 1\right)^2 + \left(\frac{\partial u_2}{\partial \chi_1}\right)^2}\ \delta \chi_1 \tag{3.1.12}$$

$$(\delta S)^2 - (\delta S_o)^2 = \left[\left(\frac{\partial u_1}{\partial \chi_1} + 1\right)^2 + \left(\frac{\partial u_2}{\partial \chi_1}\right)^2 - 1\right]\ (\delta \chi_1)^2 \tag{3.1.13}$$

and

$$\left(\frac{\partial u_1}{\partial \chi_1} + 1\right)^2 + \left(\frac{\partial u_2}{\partial \chi_1}\right)^2 = 1 \tag{3.1.14}$$

In general for the axially extensible beam $\delta S \neq \delta S_o$ and the axial strain $\varepsilon$ of the centerline may be defined through the engineering strain definition as:

$$\delta S = (1 + \varepsilon)\, \delta \chi_1 \tag{3.1.15}$$

or

$$\frac{\partial \chi_1}{\partial S} = \frac{1}{1 + \varepsilon} \tag{3.1.16}$$

Substituting the above expression into equations (3.1.5) and (3.1.12), the following relations are obtained:

$$1 + \varepsilon = \sqrt{\left(\frac{\partial x_1}{\partial \chi_1}\right)^2 + \left(\frac{\partial x_2}{\partial \chi_1}\right)^2} \tag{3.1.17}$$

$$1 + \varepsilon = \sqrt{\left(\frac{\partial u_1}{\partial \chi_1} + 1\right)^2 + \left(\frac{\partial u_2}{\partial \chi_1}\right)^2} \tag{3.1.18}$$

If $\alpha$ is the angle between the tangent at a point along the centerline of the beam and the $\mathbf{I}_1$ axis, Figure 3.1.2, then the curvature of the beam's centerline may be expressed as:

$$\kappa = \frac{\partial\alpha}{\partial S} \tag{3.1.19}$$

Now using equation (3.1.16), we may write:

$$\kappa = \frac{\partial\alpha}{\partial\chi_1}\frac{\partial\chi_1}{\partial S} = \frac{1}{1+\varepsilon}\frac{\partial\alpha}{\partial\chi_1} \tag{3.1.20}$$

To express $\kappa$ in terms of the displacement components, we proceed to relate $\dfrac{\partial\alpha}{\partial\chi_1}$ to the displacements. From the centerline curve, we have that:

$$\cos\alpha = \frac{\partial x_1}{\partial S} = \frac{\partial x_1}{\partial\chi_1}\frac{\partial\chi_1}{\partial S} = \frac{1}{1+\varepsilon}\left(1+\frac{\partial u_1}{\partial\chi_1}\right) \tag{3.1.21}$$

and

$$\sin\alpha = \frac{\partial x_2}{\partial S} = \frac{\partial x_2}{\partial\chi_1}\frac{\partial\chi_1}{\partial S} = \frac{1}{1+\varepsilon}\frac{\partial u_2}{\partial\chi_1} \tag{3.1.22}$$

Differentiating equations (3.1.22) with respect to $\chi_1$, we obtain:

$$\frac{\partial\alpha}{\partial\chi_1}\cos\alpha = \frac{\dfrac{\partial^2 u_2}{\partial\chi_1^2}(1+\varepsilon) - \dfrac{\partial u_2}{\partial\chi_1}\dfrac{\partial\varepsilon}{\partial\chi_1}}{(1+\varepsilon)^2} \tag{3.1.23}$$

Substituting for $\cos\alpha$ from equation (3.1.21) and using the relation (3.1.18), equation (3.1.23) becomes:

$$\frac{\partial\alpha}{\partial\chi_1} = \frac{\dfrac{\partial^2 u_2}{\partial\chi_1^2}\left[\left(\dfrac{\partial u_1}{\partial\chi_1}+1\right)^2+\left(\dfrac{\partial u_2}{\partial\chi_1}\right)^2\right] - \dfrac{\partial u_2}{\partial\chi_1}\left[\dfrac{\partial^2 u_1}{\partial\chi_1^2}\left(\dfrac{\partial u_1}{\partial\chi_1}+1\right)+\dfrac{\partial u_2}{\partial\chi_1}\dfrac{\partial^2 u_1}{\partial\chi_1^2}\right]}{(1+\varepsilon)^2\left(\dfrac{\partial u_1}{\partial\chi_1}+1\right)} \tag{3.1.24}$$

which upon simplification, results in:

$$\frac{\partial\alpha}{\partial\chi_1} = \left(\frac{1}{1+\varepsilon}\right)^2\left[\frac{\partial^2 u_2}{\partial\chi_1^2}\left(1+\frac{\partial u_1}{\partial\chi_1}\right) - \frac{\partial u_2}{\partial\chi_1}\frac{\partial^2 u_1}{\partial\chi_1^2}\right] \tag{3.1.25}$$

For the axially inextensible beam where $\varepsilon = 0$, using relations (3.1.10) and (3.1.11), equation (3.1.25) can be rewritten as:

$$\frac{\partial\alpha}{\partial\chi_1} = \frac{\partial^2 x_2}{\partial S^2}\frac{\partial x_1}{\partial S} - \frac{\partial^2 x_1}{\partial S^2}\frac{\partial x_2}{\partial S} \tag{3.1.26}$$

Further, using the inextensibility condition (3.1.7) and noting that in this case $\partial S = \partial\chi_1$, it can easily be shown that:

$$\begin{aligned} \frac{\partial x_1}{\partial S} &= \sqrt{1 - \left(\frac{\partial x_2}{\partial S}\right)^2} \\ \frac{\partial^2 x_1}{\partial S^2} &= \frac{-\dfrac{\partial^2 x_2}{\partial S^2}\dfrac{\partial x_2}{\partial S}}{\sqrt{1 - \left(\dfrac{\partial x_2}{\partial S}\right)^2}} \end{aligned} \tag{3.1.27}$$

Now substituting relations (3.1.27) into equation (3.1.26), we may express the curvature for the axially inextensible beam as:

$$\kappa = \frac{\partial\alpha}{\partial S} = \frac{\dfrac{\partial^2 x_2}{\partial S^2}}{\sqrt{1 - \left(\dfrac{\partial x_2}{\partial S}\right)^2}} \tag{3.1.28}$$

Alternatively, using the expressions:

$$\begin{aligned} \frac{\partial x_2}{\partial x_1} &= \frac{1}{\sqrt{1 - \left(\dfrac{\partial x_2}{\partial S}\right)^2}}\frac{\partial x_2}{\partial S} \\ \frac{\partial^2 x_2}{\partial x_1{}^2} &= \frac{1}{\left[1 - \left(\dfrac{\partial x_2}{\partial S}\right)^2\right]^2}\frac{\partial^2 x_2}{\partial S^2} \end{aligned} \tag{3.1.29}$$

the more familiar case when $x_2 = x_2(x_1)$, the Eulerian description of the curvature may be derived as:

$$\kappa = \frac{\dfrac{\partial^2 x_2}{\partial x_1^2}}{\sqrt{\left[1 + \left(\dfrac{\partial x_2}{\partial x_1}\right)^2\right]^3}} \tag{3.1.30}$$

## 3.1.2 Equation of Motion for Axially Inextensible Flexible Sliding Beams

Deflection of the sliding beam may be large, hence nonlinear terms of up to third order will be retained in the governing equation of the beam.

### 3.1.2.1 Extended Hamilton's Principle

Evidently sliding beams are systems of changing mass, that is generally the number of particles in the system at time $t_1$ are different from that at time $t_2$. Hamilton's principle, in its classical form applies to systems of particles that retain their identity and number, i.e. the same particle system is considered at times $t_1$ and $t_2$. Hence, to apply Hamilton's principle to the flexible sliding beam problem some modifications, related to the identity and aggregate of particles, are necessary.

It should be noted that the use of Hamilton's principle for the axially rigid sliding cantilever beams has been discussed by Tabarrok et al., 1974, and the following is an alternative approach in formulating the motion of sliding beams. The new approach sheds further light on this dynamically rich problem.

As noted earlier, the sliding beam problem has some features of flow, conventionally described by Eulerian formulations. There have been a number of studies to extend Hamilton's principle to "flow" problems, e.g. Veubeke, 1974, Leech, 1977, and Dost and Tabarrok, 1979. In these studies the difficult task of following the particles, as against monitoring changes at specific points in space, is recognized and discussed. For the sliding beam problem, the Lagrangian description, with its focus on the particles, can still be used even though the number of particles in the system is not fixed.

This problem of changing mass was addressed by McIver, 1973, in a remarkable development. In the following we review the salient points in McIver's formulation.

From D'Alembert principle, we have for a system of $N$ particles:

$$\sum_{i=1}^{N}\left(m_i\frac{D^2\mathbf{r}_i}{Dt^2}+\frac{\partial\Pi}{\partial\mathbf{r}_i}-\mathbf{F}_i\right)\cdot\delta\mathbf{r}_i = 0 \tag{3.1.31}$$

Where $\Pi = \Pi(\mathbf{r}_1, \mathbf{r}_2, \ldots, \mathbf{r}_N)$ is the potential energy of the particles, $\mathbf{F}_i$ denotes the forces without potentials acting on the $i^{th}$ particle, $\mathbf{r}_i$ is the position vector of this particle of mass $m_i$ and $\delta\mathbf{r}_i$ is a virtual displacement. $D(\;)/Dt$ is the material time derivative following the particle. We note that:

$$\sum_{i=1}^{N}\left(\frac{\partial\Pi}{\partial\mathbf{r}_i}\right)\cdot\delta\mathbf{r}_i = \delta\Pi \tag{3.1.32}$$

and

$$\sum_{i=1}^{N}(\mathbf{F}_i)\cdot\delta\mathbf{r}_i = \delta W \tag{3.1.33}$$

and

$$\sum_{i=1}^{N}\left(m_i\frac{D^2\mathbf{r}_i}{Dt^2}\right)\cdot\delta\mathbf{r}_i = \frac{D}{Dt}\left[\sum_{i=1}^{N}\left(m_i\frac{D\mathbf{r}_i}{Dt}\right)\cdot\delta\mathbf{r}_i\right]-\sum_{i=1}^{N}\left(m_i\frac{D\mathbf{r}_i}{Dt}\right)\cdot\delta\frac{D\mathbf{r}_i}{Dt} \tag{3.1.34}$$

or

$$\sum_{i=1}^{N}\left(m_i\frac{D^2\mathbf{r}_i}{Dt^2}\right)\cdot\delta\mathbf{r}_i = \frac{D}{Dt}\left[\sum_{i=1}^{N}\left(m_i\frac{D\mathbf{r}_i}{Dt}\right)\cdot\delta\mathbf{r}_i\right]-\delta T^* \tag{3.1.35}$$

where $T^*$ is the kinetic co-energy of the particles. Substituting from equations (3.1.32), (3.1.33) and (3.1.35) into equation (3.1.31), we may express D'Alembert's principle as:

$$\delta\mathcal{L}+\delta W-\frac{D}{Dt}\left[\sum_{i=1}^{N}\left(m_i\frac{D\mathbf{r}_i}{Dt}\right)\cdot\delta\mathbf{r}_i\right] = 0 \tag{3.1.36}$$

where $\mathcal{L} = T^* - \Pi$ is the Lagrangian of the system.

Starting from this point, McIver, considered a generalization from a discrete to a continuous system. In keeping with the precepts of conservation of mass and preservation of the identity of particles, McIver expressed equation (3.1.36) as:

$$\delta \mathcal{L}_c + \delta W - \frac{D}{Dt}\left( \int_{v_c(t)} (\rho \mathcal{U}) \cdot \delta \mathbf{r} \; dv \right) = 0 \tag{3.1.37}$$

where $\rho$ denotes the density and $\mathcal{U}$ is the velocity of the material point at time $t$ and $\mathcal{L}_c$ and $\delta W$ are the Lagrangian of the system and the virtual work performed by the generalized forces undergoing virtual displacements. The subscript $c$ denotes a fixed material system enclosed in a volume $v_c$.

Hamilton's principle is obtained by integrating equation (3.1.37) with respect to time over a time interval $t_1$ to $t_2$, yielding:

$$\delta \int_{t_1}^{t_2} \mathcal{L}_c \; dt + \int_{t_1}^{t_2} \delta W \; dt - \left. \int_{v_c(t)} (\rho \mathcal{U}) \cdot \delta \mathbf{r} \; dv \right|_{t_1}^{t_2} = 0 \tag{3.1.38}$$

If we now impose the requirement that at time $t_1$ and $t_2$ the configuration be prescribed, i.e. $\delta \mathbf{r} = 0$, then the last term in equation (3.1.38) drops out, leaving:

$$\delta \int_{t_1}^{t_2} \mathcal{L}_c \; dt + \int_{t_1}^{t_2} \delta W \; dt = 0 \tag{3.1.39}$$

Now to proceed from a closed material system to an open system we invoke Reynold's transport theorem which states that:

$$\frac{d}{dt} \int_{v_o(t)} (\;)\, dv = \frac{D}{Dt} \int_{v_c(t)} (\;)\, dv + \int_{s_o(t)} ((\;)\,(\mathcal{V} - \mathcal{U}) \cdot \mathbf{n})\, dS \tag{3.1.40}$$

In the above expression, $v_o(t)$ is the open control volume with the moving control surface $s_o(t)$ which advances with the velocity $\mathcal{V} \cdot \mathbf{n}$, in the outward normal direction $\mathbf{n}$ and across which mass is transported. The control volume $v_o(t)$ is pervious to the particles and thus the system is not necessarily of constant mass or, if of constant mass, it need not always contain the same set of particles. At instant $t$, the open control volume, $v_o(t)$, coincides with the closed control volume $v_c(t)$ with the boundary $s_c(t)$ for which $\mathcal{V}\cdot\mathbf{n} = \mathcal{U}\cdot\mathbf{n}$, see Figure 3.1.3.

It is important to be clear about the operators $d(\ )/dt$ and $D(\ )/Dt$. The operator $d(\ )/dt$ refers to the time derivative following a control volume whether of constant mass or not. It is obvious that when the control volume contains the same particles, i.e. it is the so called material control volume, then this derivative is equivalent to the material time derivative $D(\ )/Dt$.

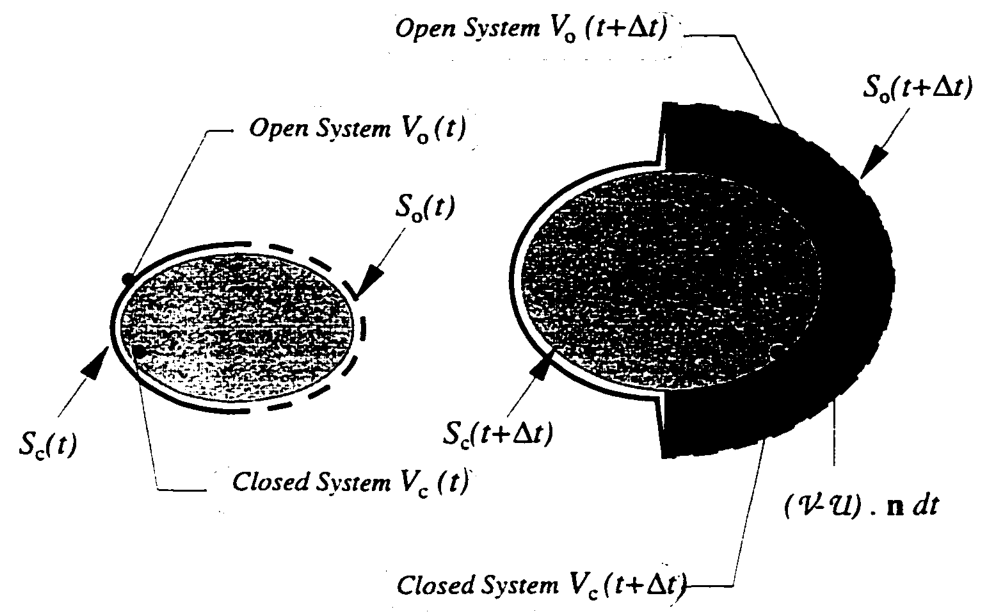


Figure 3.1.3: System of changing mass: open and closed control volumes.

Using Reynold's transport theorem (3.1.40), the virtual work equation for a system of changing mass, can be written as:

$$\delta\mathcal{L}_o + \delta W - \frac{d}{dt}\int_{v_o(t)} \rho\,(\mathcal{U}\cdot\delta\mathbf{r})\,dv + \int_{s_o(t)} [\rho\,(\mathcal{U}\cdot\delta\mathbf{r})\,(\mathcal{V}-\mathcal{U})\cdot\mathbf{n}]\,ds = 0 \quad (3.1.41)$$

where in the Lagrangian $\mathcal{L}_o$ of the open system mass is not fixed.

Now integrating with respect to time over the interval $t_1$, $t_2$ and again requiring the system configurations at $t_1$, $t_2$ be prescribed, the extended form of Hamilton's principle for a system of changing mass can be expressed as:

$$\delta\int_{t_1}^{t_2} \mathcal{L}_o dt + \int_{t_1}^{t_2} \delta W dt + \int_{t_1}^{t_2} dt \int_{s_o(t)} [\rho(\mathcal{U}\cdot\delta\mathbf{r})(\mathcal{V}-\mathcal{U})\cdot\mathbf{n}]\,ds = 0 \tag{3.1.42}$$

where $\delta W$ is the virtual work performed by the non-potential forces acting on the same system. If we only consider the contribution of virtual work due to surface tractions acting on the open and closed boundary of the system, then the extended Hamilton's principle for a system of changing mass becomes:

$$\delta\int_{t_1}^{t_2} \mathcal{L}_o dt + \int_{t_1}^{t_2} dt \int_{s_c(t)} (\sigma\cdot\mathbf{n})\cdot\delta\mathbf{r}ds + \int_{t_1}^{t_2} dt \int_{s_o(t)} ([\sigma + \rho\,\mathcal{U}(\mathcal{V}-\mathcal{U})]\cdot\mathbf{n})\cdot\delta\mathbf{r}ds = 0 \tag{3.1.43}$$

where $\sigma$ is the stress tensor and $\sigma\cdot\mathbf{n}$ represents the surface traction vector.

It should be noted that not all virtual displacement distributions are permissible. The virtual displacements should, not only satisfy the imposed geometrical constraints ensuring that there is no contribution of virtual work due to constraint forces, but must also satisfy the conservation of mass.

It is also worth noting that Hamilton's principle for closed systems for which there are no non-potential forces, is an extremum principle. This is not the case for systems of changing mass. This follows from the term accounting for changing mass in equation (3.1.42) which is in the form of a virtual work expression. In certain cases, by choosing particular boundary velocities, it is possible to render Hamilton's principle for a system of changing mass, a stationary principle, see McIver, 1973.

Returning to the sliding beam problem which is a system of changing mass, we apply the extended Hamilton's principle to obtain the governing equation of motion.

Figure 3.1.4 shows open and closed control volumes we choose for the sliding beam. At the tip of the beam the velocity of the material point is equal to the velocity of the moving boundary, i.e. $\mathcal{V}_{Tip} - \mathcal{U}_{Tip} = 0$. For simplicity, the only type of surface traction considered is a prescribed tip load independent of displacements. Hence, its virtual work can be expressed as a total differential.

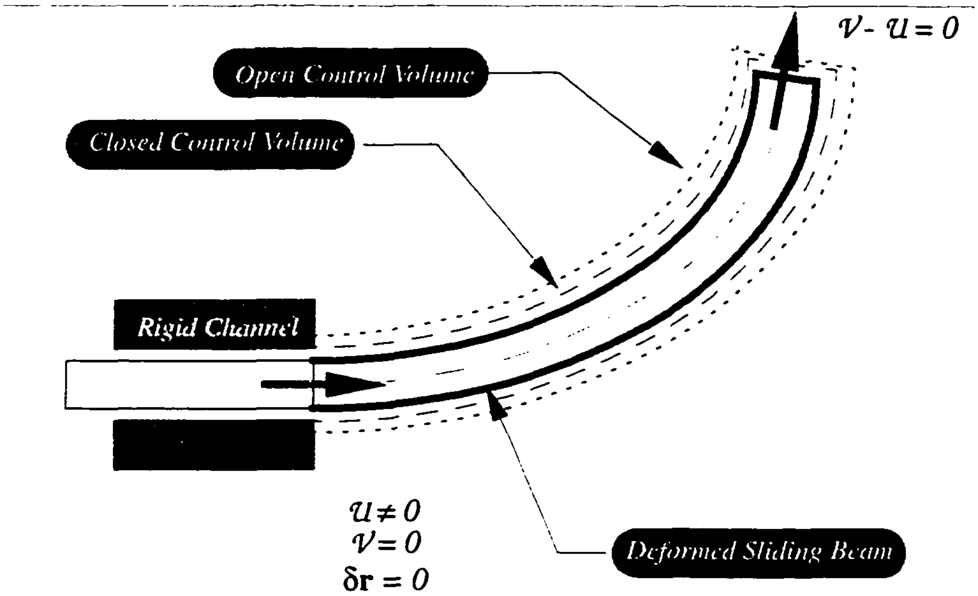


Figure 3.1.4: Sliding beam: open and closed control volumes.

At the root, the control surface does not move, but the material point on the centerline of the beam, has the velocity $\mathcal{U}_{root}$. Here, we invoke our previous assumption on the motion of the beam being prescribed inside the channel where the beam is considered rigid. This precludes the existence of a non-conservative force at the root (see equation (3.1.43)). Now, since the lateral deflection and the slope of the beam (for a cantilever support) at the root are prescribed as zero, virtual displacements vanish at the wall and there is no virtual work contribution from the wall reaction shear force and moment.

Implementing the above statements into equation (3.1.43), the extended Hamilton's principle for the sliding beam, outside the channel, with the variable length $L(t)$ can be expressed as:

$$\delta \int_{t_1}^{t_2} \mathcal{L}_o \, dt = 0 \tag{3.1.44}$$

which is the form of Hamilton's principle used by Tabarrok et al., 1974.

### 3.1.2.2 Complementary Kinetic Energy

In the absence of rotary inertia effects, the velocity of point $m$, on the centerline of the sliding beam, Figure 3.1.5, is made of two parts:

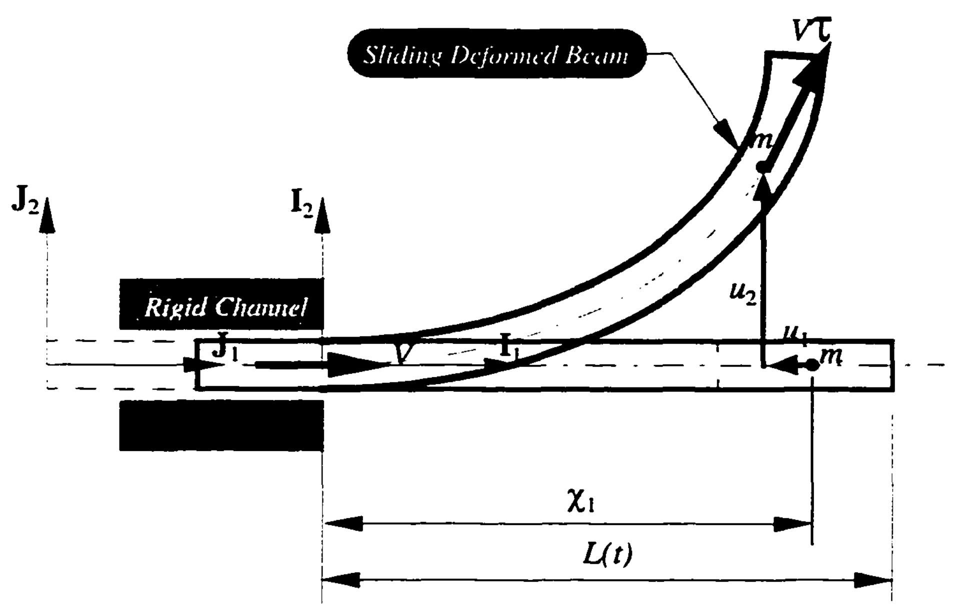


Figure 3.1.5: Axially inextensible sliding beam undergoing large overall motion: Kinematics of deformation.

- 1- Due to rigid body sliding motion of the beam:

$$\mathbf{V}_{rb} = V\boldsymbol{\tau} = V\frac{\partial x_1}{\partial S}\,\mathbf{I}_1 + V\frac{\partial x_2}{\partial S}\,\mathbf{I}_2 \tag{3.1.45}$$

where $V$ is the prescribed sliding velocity of the beam and $\boldsymbol{\tau}$ is the unit vector tangent to the centerline of the beam at the same material point.

- 2- Due to elastic deformation:

$$\mathbf{V}_e = \frac{\partial u_1}{\partial t}\mathbf{I}_1 + \frac{\partial u_2}{\partial t}\mathbf{I}_2 \tag{3.1.46}$$

or

$$\mathbf{V}_e = \frac{\partial x_1}{\partial t}\mathbf{I}_1 + \frac{\partial x_2}{\partial t}\mathbf{I}_2 \tag{3.1.47}$$

Therefore, the kinetic co-energy for the sliding beam may be written as:

$$T^* = \int_0^{L(t)} \frac{1}{2}\rho A \left[\left(\frac{\partial x_1}{\partial t} + V\frac{\partial x_1}{\partial S}\right)^2 + \left(\frac{\partial x_2}{\partial t} + V\frac{\partial x_2}{\partial S}\right)^2\right] dS \tag{3.1.48}$$

### 3.1.2.3 Strain Energy

For an axially inextensible beam $(\varepsilon = 0)$ in the case of large rotations and small strains, the strain energy was given by Stoker, 1968, as:

$$\Pi = \int_0^{L(t)} \frac{EI}{2}\kappa^2\, dS \tag{3.1.49}$$

where $I$ is the appropriate second moment of area and $E$ is the young's modulus of the beam material. Now, substituting for the curvature from equation (3.1.28), the strain energy correct to $o(\varepsilon^4)$ may be expressed as:

$$\Pi = \int_0^{L(t)} \frac{EI}{2}\left(\frac{\partial^2 x_2}{\partial S^2}\right)^2 \left[1 + \left(\frac{\partial x_2}{\partial S}\right)^2\right] dS \tag{3.1.50}$$

### 3.1.2.4 Lagrangian

For a flexible sliding beam which undergoes large overall motion and is axially inextensible, using equations (3.1.48) and (3.1.50), the Lagrangian can be expressed as:

$$\begin{aligned}\mathcal{L}_o &= T^* - \Pi \\ &= \int_0^{L(t)} \frac{1}{2}\rho A \left[\left(\frac{\partial x_1}{\partial t} + V\frac{\partial x_1}{\partial S}\right)^2 + \left(\frac{\partial x_2}{\partial t} + V\frac{\partial x_2}{\partial S}\right)^2\right] dS - \\ &\quad \int_0^{L(t)} \frac{EI}{2}\left(\frac{\partial^2 x_2}{\partial S^2}\right)^2 \left[1 + \left(\frac{\partial x_2}{\partial S}\right)^2\right] dS\end{aligned} \tag{3.1.51}$$

### 3.1.2.5 Equation of Motion

After many straightforward but tedious manipulations, the governing equation of motion for an axially inextensible flexible sliding beam, in the absence of traction and body forces, may be obtained as the stationary condition of the extended Hamilton's principle (3.1.44) as follows: (the details of the derivation are given in Appendix A)

In the domain:

$$\begin{aligned}&\rho A\left(\frac{\partial^2 x_2}{\partial t^2} + 2V\frac{\partial^2 x_2}{\partial t \partial S}\left[1 + \left(\frac{\partial x_2}{\partial S}\right)^2\right] + V^2\frac{\partial^2 x_2}{\partial S^2}\left[1 + \left(\frac{\partial x_2}{\partial S}\right)^2\right] + \right.\\ &\qquad \left.\frac{\partial V}{\partial t}\frac{\partial^2 x_2}{\partial S^2}(L - S)\left[1 + \frac{3}{2}\left(\frac{\partial x_2}{\partial S}\right)^2\right]\right) + \\ &EI\left(\frac{\partial^4 x_2}{\partial S^4}\left[1 + \left(\frac{\partial x_2}{\partial S}\right)^2\right] + \left(\frac{\partial^2 x_2}{\partial S^2}\right)^3 + 4\frac{\partial x_2}{\partial S}\frac{\partial^2 x_2}{\partial S^2}\frac{\partial^3 x_2}{\partial S^3}\right) + \\ &\rho A\frac{\partial x_2}{\partial S}\int_0^S\left[\frac{\partial x_2}{\partial S}\frac{\partial^3 x_2}{\partial t^2 \partial S} + \left(\frac{\partial^2 x_2}{\partial t \partial S}\right)^2\right] dS - \\ &\rho A\frac{\partial^2 x_2}{\partial S^2}\int_S^{L(t)}\int_0^S\left[\frac{\partial x_2}{\partial S}\frac{\partial^3 x_2}{\partial t^2 \partial S} + \left(\frac{\partial^2 x_2}{\partial t \partial S}\right)^2\right] dS\, dS - \\ &\rho A\frac{\partial^2 x_2}{\partial S^2}\int_S^{L(t)}\left[\frac{1}{2}\frac{\partial V}{\partial t}\left(\frac{\partial x_2}{\partial S}\right)^2 + 2V\frac{\partial x_2}{\partial S}\frac{\partial^2 x_2}{\partial t \partial S} + V^2\frac{\partial x_2}{\partial S}\frac{\partial^2 x_2}{\partial S^2}\right] dS = 0\end{aligned} \tag{3.1.52}$$

At the boundaries:

$$EI\left\{\frac{\partial^3 x_2}{\partial S^3}\left[1+\frac{1}{2}\left(\frac{\partial x_2}{\partial S}\right)^2\right]+\left(\frac{\partial^2 x_2}{\partial S^2}\right)^2\frac{\partial x_2}{\partial S}\right\}\delta x_2\Bigg|_0^{L(t)} = 0$$

$$EI\,\frac{\partial^2 x_2}{\partial S^2}\left[1+\frac{1}{2}\left(\frac{\partial x_2}{\partial S}\right)^2\right]\delta\left(\frac{\partial x_2}{\partial S}\right)\Bigg|_0^{L(t)} = 0 \tag{3.1.53}$$

Equation (3.1.52) is a nonlinear partial integro-differential equation and does not admit a general closed-form solution. Equations (3.1.53) provide all the boundary conditions, namely the essential boundary conditions for prescribed kinematic variables and the corresponding natural boundary conditions for force variables.

Removing terms of second and higher order, we obtain the following linear equation of motion:

$$\rho A\left[\frac{\partial^2 x_2}{\partial t^2}+2V\frac{\partial^2 x_2}{\partial t\partial S}+V^2\frac{\partial^2 x_2}{\partial S^2}+\frac{\partial V}{\partial t}\frac{\partial^2 x_2}{\partial S^2}(L-S)\right]+EI\,\frac{\partial^4 x_2}{\partial S^4} = 0 \tag{3.1.54}$$

which expresses the dynamic equilibrium for the linear axially inextensible flexible sliding beam first derived by Tabarrok et al., 1974.

### 3.1.2.6 Sliding Beam in Uniform Gravitational Field

The potential energy of the flexible sliding beam in a uniform gravitational field $g$ along $x_1$, is given by:

$$G = \rho A g\int_0^{L(t)} x_1\, dS \tag{3.1.55}$$

For the inextensible case, the inclusion of the potential energy due to gravity gives rise to two additional terms on the left hand side of the governing equation of motion (3.1.52), namely:

$$\rho A g\,\frac{\partial x_2}{\partial S}\left[1+\frac{1}{2}\left(\frac{\partial x_2}{\partial S}\right)^2\right]-\rho A g\,\frac{\partial^2 x_2}{\partial S^2}(L-S)\left[1+\frac{3}{2}\left(\frac{\partial x_2}{\partial S}\right)^2\right]$$

### 3.1.3 Equation of Motion for Axially Extensible Flexible Sliding Beams

In this case, the beam is axially extensible, i.e. $\varepsilon \neq 0$, and we need to account for transverse *and* axial motions. Thus for the axially flexible sliding beam two nonlinear coupled partial differential equations are to be derived.

It is important to note that the discussion in Section 3.1.2.1 remains valid and the equations of motion may be obtained from the extended Hamilton's principle as given in equation (3.1.44).

#### 3.1.3.1 Complementary Kinetic Energy

The velocity of a material point on the centerline of the beam can be expressed as, Figure 3.1.6:

$$\frac{dx}{dt} = \frac{dx_1}{dt} I_I + \frac{dx_2}{dt} I_2 \tag{3.1.56}$$

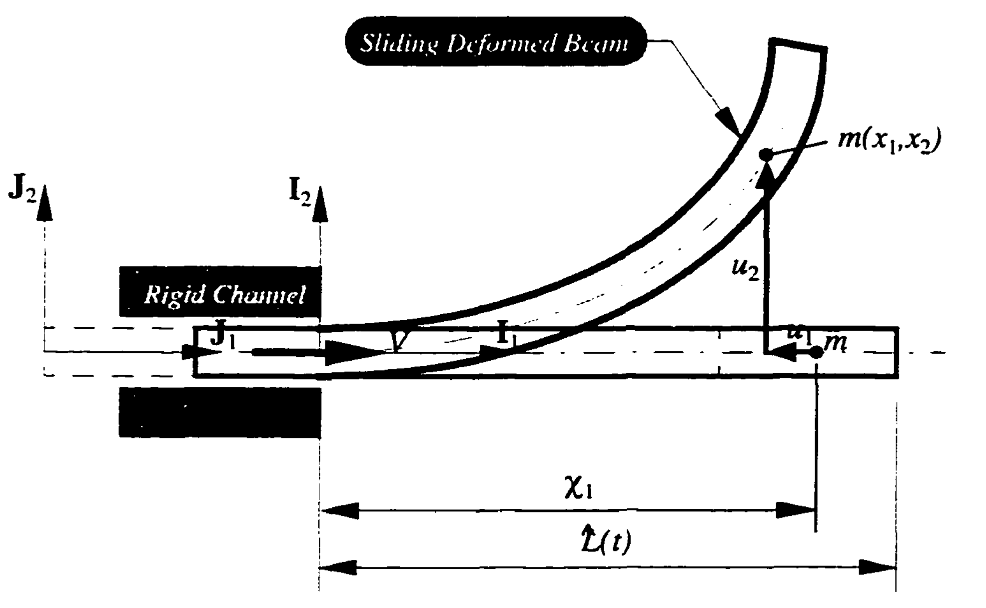


Figure 3.1.6: Flexible sliding beam undergoing large overall motion: Kinematics of deformation.

Now, substituting the relations (3.1.8) and (3.1.9) into equation (3.1.56), we obtain:

$$\frac{dx}{dt} = \left(\frac{d\chi_1}{dt} + \frac{\partial u_1}{\partial \chi_1}\frac{\partial \chi_1}{\partial t} + \frac{\partial u_1}{\partial t}\right) I_1 + \left(\frac{\partial u_2}{\partial \chi_1}\frac{\partial \chi_1}{\partial t} + \frac{\partial u_2}{\partial t}\right) I_2 \tag{3.1.57}$$

where $\frac{\partial \chi_I}{\partial t}$ is the prescribed velocity $V$ of the beam. Equation (3.1.57) may be simplified to:

$$\frac{dx}{dt} = \left[\frac{\partial u_1}{\partial t} + V\left(1 + \frac{\partial u_1}{\partial \chi_1}\right)\right] I_1 + \left[\frac{\partial u_2}{\partial t} + V\frac{\partial u_2}{\partial \chi_1}\right] I_2 \tag{3.1.58}$$

which describes the velocity of a material point on the centerline of the beam. Using equation (3.1.58), the kinetic co-energy of the sliding beam may be expressed as:

$$T^* = \int_0^{\hat{L}(t)} \frac{1}{2}\rho_o A \left\{\left[\frac{\partial u_1}{\partial t} + V\left(1 + \frac{\partial u_1}{\partial \chi_1}\right)\right]^2 + \left[\frac{\partial u_2}{\partial t} + V\frac{\partial u_2}{\partial \chi_1}\right]^2\right\} d\chi_1 \tag{3.1.59}$$

where $\hat{L}(t)$ is the length of the protruding part of the undeformed sliding beam and $\rho_o$ is the mass density of the undeformed beam.

### 3.1.3.2 Strain Energy

For an axially flexible beam undergoing large overall motions with finite rotations and small strains, Stoker, 1968, has shown that if shear is neglected, the axial strain may be expressed as:

$$\varepsilon_{\chi_1} = \varepsilon - (1 + \varepsilon)\kappa\chi_2 \tag{3.1.60}$$

Then an increment of the strain energy is taken to be:

$$d\Pi = \frac{Eb}{2}\varepsilon_{\chi_1}^2 \, d\chi_1 d\chi_2 \tag{3.1.61}$$

where $b$ is the width of the beam. Now one can express the strain energy of the beam as:

$$\Pi = \int_{-\frac{h}{2}}^{\frac{h}{2}} \int_0^{\hat{L}(t)} \frac{Eb}{2} [\varepsilon - (1+\varepsilon)\kappa\chi_2]^2 \; d\chi_1 d\chi_2 \tag{3.1.62}$$

where $h$ is the height of the beam's cross section. After simplifying the above relation, the strain energy becomes:

$$\Pi = \int_0^{\hat{L}(t)} \frac{E}{2} \left[A\varepsilon^2 + I(1+\varepsilon)^2 \kappa^2\right] \; d\chi_1 \tag{3.1.63}$$

where $A$ is the undeformed cross sectional area of the beam. Expressing $\varepsilon$ and $\kappa$ via equations (3.1.18), (3.1.20) and (3.1.25), we may write the strain energy in terms of the displacement components as follows:

$$\begin{aligned} \Pi = & \int_0^{\hat{L}(t)} \frac{1}{2} EA \left[\frac{\partial u_1}{\partial \chi_1} + \frac{1}{2}\left(\frac{\partial u_2}{\partial \chi_1}\right)^2\right]^2 d\chi_1 + \\ & \int_0^{\hat{L}(t)} \frac{1}{2} EI \left[\left(\frac{\partial^2 u_2}{\partial \chi_1^2}\right)^2 - 2\left(\frac{\partial^2 u_2}{\partial \chi_1^2}\right)^2 \frac{\partial u_1}{\partial \chi_1} - 2\left(\frac{\partial^2 u_2}{\partial \chi_1^2}\right)^2 \left(\frac{\partial u_2}{\partial \chi_1}\right)^2 - \right. \\ & \left. 2\frac{\partial u_2}{\partial \chi_1} \frac{\partial^2 u_2}{\partial \chi_1^2} \frac{\partial^2 u_1}{\partial \chi_1^2}\right] d\chi_1 \end{aligned} \tag{3.1.64}$$

### 3.1.3.3 Lagrangian

For the flexible sliding beam, undergoing large overall motion, the Lagrangian may be expressed as:

$$\mathcal{L}_o = \int_0^{\hat{L}(t)} \frac{1}{2}\rho_o A \left\{\left[\frac{\partial u_1}{\partial t} + V\left(1 + \frac{\partial u_1}{\partial \chi_1}\right)\right]^2 + \left[\frac{\partial u_2}{\partial t} + V\frac{\partial u_2}{\partial \chi_1}\right]^2\right\} d\chi_1 -$$
$$\int_0^{\hat{L}(t)} \frac{1}{2}EA \left[\frac{\partial u_1}{\partial \chi_1} + \frac{1}{2}\left(\frac{\partial u_2}{\partial \chi_1}\right)^2\right]^2 d\chi_1 -$$
$$\int_0^{\hat{L}(t)} \frac{1}{2}EI \left[\left(\frac{\partial^2 u_2}{\partial \chi_1^2}\right)^2 - 2\left(\frac{\partial^2 u_2}{\partial \chi_1^2}\right)^2 \frac{\partial u_1}{\partial \chi_1} - 2\left(\frac{\partial^2 u_2}{\partial \chi_1^2}\right)^2\left(\frac{\partial u_2}{\partial \chi_1}\right)^2 - \right.$$
$$\left. 2\frac{\partial u_2}{\partial \chi_1}\frac{\partial^2 u_2}{\partial \chi_1^2}\frac{\partial^2 u_1}{\partial \chi_1^2}\right] d\chi_1 \tag{3.1.65}$$

The Lagrangian in equation (3.1.65) is a second order functional with two independent variables $(\chi_1, t)$ and two dependent functions $(u_1, u_2)$ .

### 3.1.3.4 Equations of Motion

Rather than carrying out the variations in Hamilton's functional, we may first obtain the general Euler-Lagrange equations of a functional of second order in $u_1(\chi_1, t)$ and $u_2(\chi_1, t)$ (see Appendix B) and then substitute the required Lagrangian (3.1.65) into these Euler-Lagrange equations. After this is done, one obtains:

In the domain:

$$\rho_o A\left[\frac{\partial^2 u_1}{\partial t^2} + \frac{\partial V}{\partial t}\left(1 + \frac{\partial u_1}{\partial \chi_1}\right) + 2V\frac{\partial^2 u_1}{\partial t \partial \chi_1} + V^2\frac{\partial^2 u_1}{\partial \chi_1^2}\right] -$$
$$EA\left[\frac{\partial^2 u_1}{\partial \chi_1^2} + \frac{\partial u_2}{\partial \chi_1}\frac{\partial^2 u_2}{\partial \chi_1^2}\right] - EI\left[\frac{\partial^2 u_2}{\partial \chi_1^2}\frac{\partial^3 u_2}{\partial \chi_1^3} + \frac{\partial u_2}{\partial \chi_1}\frac{\partial^4 u_2}{\partial \chi_1^4}\right] = 0 \tag{3.1.66}$$

$$\rho_o A\left[\frac{\partial^2 u_2}{\partial t^2}+\frac{\partial V}{\partial t}\frac{\partial u_2}{\partial \chi_1}+2V\frac{\partial^2 u_2}{\partial t\partial \chi_1}+V^2\frac{\partial^2 u_2}{\partial \chi_1^{\,2}}\right]-$$
$$EA\left[\frac{\partial u_1}{\partial \chi_1}\frac{\partial^2 u_2}{\partial \chi_1^{\,2}}+\frac{\partial u_2}{\partial \chi_1}\frac{\partial^2 u_1}{\partial \chi_1^{\,2}}+\frac{3}{2}\left(\frac{\partial u_2}{\partial \chi_1}\right)^2\frac{\partial^2 u_2}{\partial \chi_1^{\,2}}\right]-$$
$$EI\left[3\frac{\partial^3 u_1}{\partial \chi_1^{\,3}}\frac{\partial^2 u_2}{\partial \chi_1^{\,2}}+2\frac{\partial u_1}{\partial \chi_1}\frac{\partial^4 u_2}{\partial \chi_1^{\,4}}+\frac{\partial u_2}{\partial \chi_1}\frac{\partial^4 u_1}{\partial \chi_1^{\,4}}+\right.$$
$$2\left(\frac{\partial u_2}{\partial \chi_1}\right)^2\frac{\partial^4 u_2}{\partial \chi_1^{\,4}}+8\frac{\partial u_2}{\partial \chi_1}\frac{\partial^2 u_2}{\partial \chi_1^{\,2}}\frac{\partial^3 u_2}{\partial \chi_1^{\,3}}+ \tag{3.1.67}$$
$$\left.2\left(\frac{\partial^2 u_2}{\partial \chi_1^{\,2}}\right)^3+4\frac{\partial^3 u_2}{\partial \chi_1^{\,3}}\frac{\partial^2 u_1}{\partial \chi_1^{\,2}}\quad-\frac{\partial^4 u_2}{\partial \chi_1^{\,4}}\right] = 0$$

At the boundaries:

$$\left\{EA\left[\frac{\partial u_1}{\partial \chi_1}+\frac{1}{2}\left(\frac{\partial u_2}{\partial \chi_1}\right)^2\right]+EI\frac{\partial u_2}{\partial \chi_1}\frac{\partial^3 u_2}{\partial \chi_1^{\,3}}\right\}\delta u_1\Bigg|_0^{\hat{L}(t)} = 0$$
$$EI\frac{\partial u_2}{\partial \chi_1}\frac{\partial^2 u_2}{\partial \chi_1^{\,2}}\,\delta\left(\frac{\partial u_1}{\partial \chi_1}\right)\Bigg|_0^{\hat{L}(t)} = 0 \tag{3.1.68}$$

$$\left\{EA\ \frac{\partial u_2}{\partial\chi_1}\left[\frac{\partial u_1}{\partial\chi_1}+\frac{1}{2}\left(\frac{\partial u_2}{\partial\chi_1}\right)^2\right]-\right.$$

$$EI\left[\frac{\partial^3 u_2}{\partial\chi_1^3}-2\frac{\partial^3 u_2}{\partial\chi_1^3}\ \frac{\partial u_1}{\partial\chi_1}-2\frac{\partial^2 u_2}{\partial\chi_i^2}\ \frac{\partial^2 u_1}{\partial\chi_1^2}-\right.$$

$$2\frac{\partial^3 u_2}{\partial\chi_1^3}\left(\frac{\partial u_2}{\partial\chi_1}\right)^2-2\left(\frac{\partial^2 u_2}{\partial\chi_1^2}\right)^2\ \frac{\partial u_2}{\partial\chi_1}-$$

$$\left.\left.\frac{\partial u_2}{\partial\chi_1}\ \frac{\partial^3 u_1}{\partial\chi_1^3}\right]\right\}\ \delta u_2\Bigg|_0^{\hat{L}(t)} = 0 \tag{3.1.69}$$

$$\left\{EI\left[\frac{\partial^2 u_2}{\partial\chi_1^2}-2\frac{\partial^2 u_2}{\partial\chi_1^2}\ \frac{\partial u_1}{\partial\chi_1}-2\frac{\partial^2 u_2}{\partial\chi_1^2}\left(\frac{\partial u_2}{\partial\chi_1}\right)^2-\right.\right.$$

$$\left.\left.\frac{\partial u_2}{\partial\chi_1}\ \frac{\partial^2 u_1}{\partial\chi_1 2}\right]\right\}\ \delta\left(\frac{\partial u_2}{\partial\chi_1}\right)\Bigg|_0^{\hat{L}(t)} = 0$$

Equations (3.1.66) and (3.1.67) are two nonlinear, coupled partial differential equations which describe the dynamics of an axially extensible flexible sliding beam undergoing large overall motion. Once again, these complex equations do not admit closed form solutions. However, through numerical techniques one can obtain approximate solutions for these governing equations. These will be discussed in the following chapters. Equations (3.1.68) and (3.1.69) express the kinematic and natural boundary conditions of the beam.

In the next section, we consider an alternative formulation wherein the beam remains fixed (no axial motion) and the channel moves with a prescribed velocity along the beam.

## 3.2 Alternative Formulation – The Sliding Channel

In the sliding beam problem the beam emerges with a prescribed velocity from a rigid channel which is at rest. The inertial reference frame is attached to the channel and the motion is observed by an inertial observer placed, say, on the channel. Now we superimpose a translational velocity on the system with the intent of bringing the beam to rest. Then the channel and the observer will move with this imposed velocity. In the following we will obtain the equations of motion of the system as seen by the same observer which is now moving.

It is important to note that in this case the reference axes attached to the moving channel is not, in general, an inertial frame. The exception occurs when the superimposed translational velocity is constant. Then the moving axes is an acceptable inertial frame and it is related to the original fixed inertial frame through a Galelean transformation. Now we will take the initial undeformed configuration which is fixed in space as the material configuration. The part inside the channel is assumed to be rigid and the protruding part undergoes large overall motion with a moving boundary with respect to the material frame, see Figure 3.2.1.

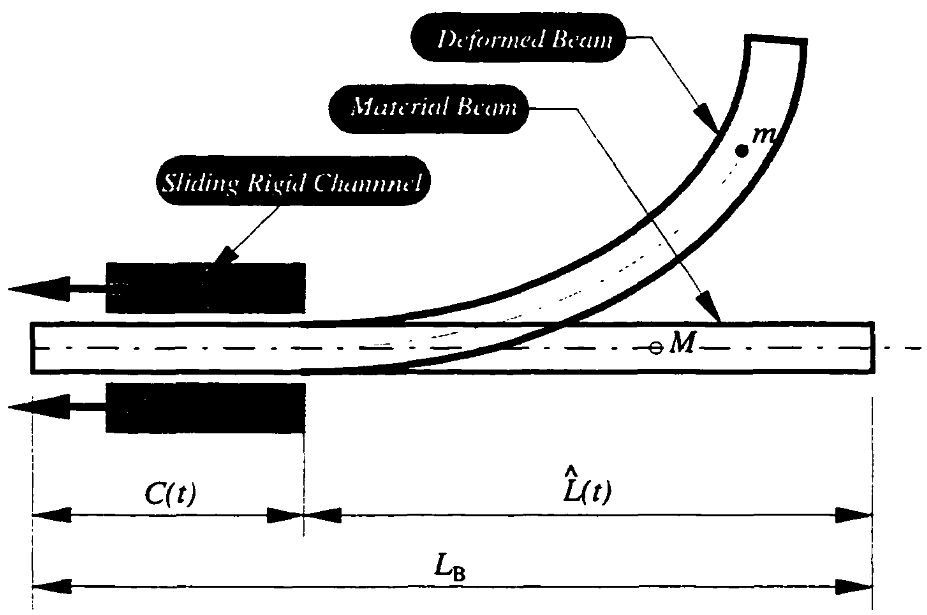


Figure 3.2.1: Sliding channel: Material and spatial configurations.

Evidently, the defined material configuration has the role of the Lagrangian domain with respect to the deformed configuration. In this case, the structural deformation is described by a mapping, which is time dependent, from the material configuration to the deformed configuration.

### 3.2.1 Kinematic Descriptions

As noted earlier we will obtain the differential equation of motion as seen by an observer O moving with the channel.

If we consider the beam to be initially lying along the $\mathbf{J}_1$ axis (Figure 3.2.2), then the length of the beam inside the channel is given by:

$$\mathbf{C}(t) = [L_B - L(t)]\,\mathbf{J}_1 \tag{3.2.1}$$

where $L_B$ is the total length of the beam and $L(t)$ is the time varying length of the beam outside the channel.

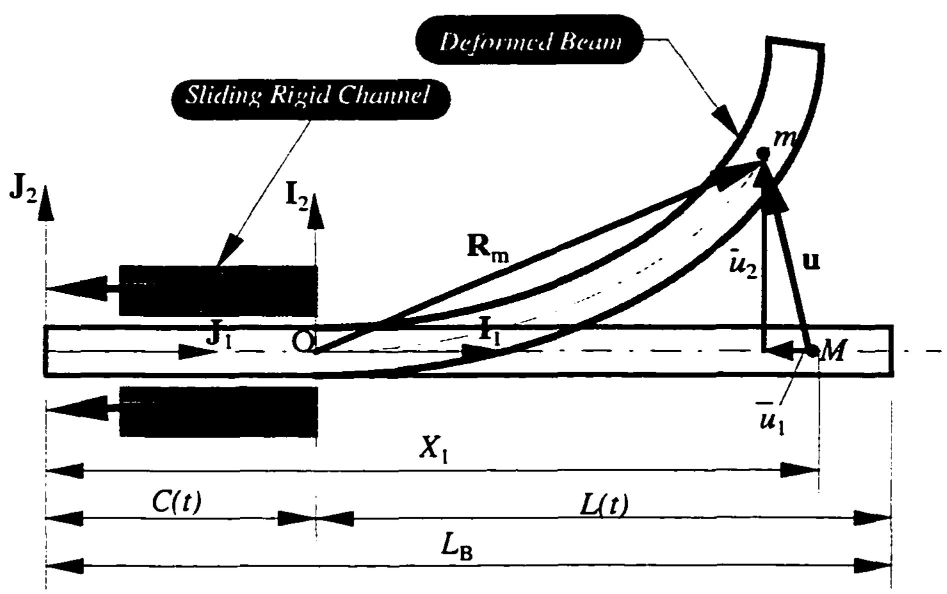


Figure 3.2.2: Axially inextensible beam with sliding channel undergoing large overall motion: Kinematics of the deformation.

The deformation from the material configuration to the deformed configuration is a Lagrangian description; thus a point $M$ on the centerline of the undeformed beam maps to a new position $m$ in the deformed configuration. Since the part of the beam inside the channel is considered to be rigid, we may refer the displacement vector $\bar{\mathbf{u}}(X_1, t)$, from $M$ to $m$, to the spatial frame $\mathbf{I}_1$ and $\mathbf{I}_2$. Now one may define the position vector of a point $m$ on the centerline of the deformed beam as (Figure 3.2.2):

$$\mathbf{R}_m = [X_1 - C(t)]\mathbf{I}_1 + \bar{\mathbf{u}} \tag{3.2.2}$$

## 3.2.2 Equation of Motion Obtained from Alternative Formulation

In Section 3.1.2, only terms up to the third order will be retained in the governing equations of motion.

### 3.2.2.1 Extended Hamilton's principle

Since the boundary is moving and the length of the beam outside the channel changes with time, this problem can also be viewed as a system of changing mass. Following the discussion in Section 3.1.2.1, we obtain the governing equation of motion for the moving boundary problem via extended Hamilton's principle.

Figure 3.2.3 shows the open and closed control volumes for the problem at hand. At the tip of the beam the velocity of the moving open control surface is equal to the velocity of the material points. Once again, we assume that the virtual work of possible prescribed traction forces at the tip is expressed as a total differential.

At the root, we have a moving boundary with a prescribed sliding velocity; therefore the open control surface has the prescribed velocity $\mathcal{V}_{root}$. Since the beam is considered axially fixed, the material point on the centerline at the root of the beam, is motionless. Also, it should be noted that the beam is considered to be axially rigid inside the channel and the lateral deflection and slope are prescribed at the root. Hence, there are no virtual work terms from the reaction forces at the root. Under these conditions the extended Hamilton's principle takes the form given in equation (3.1.44).

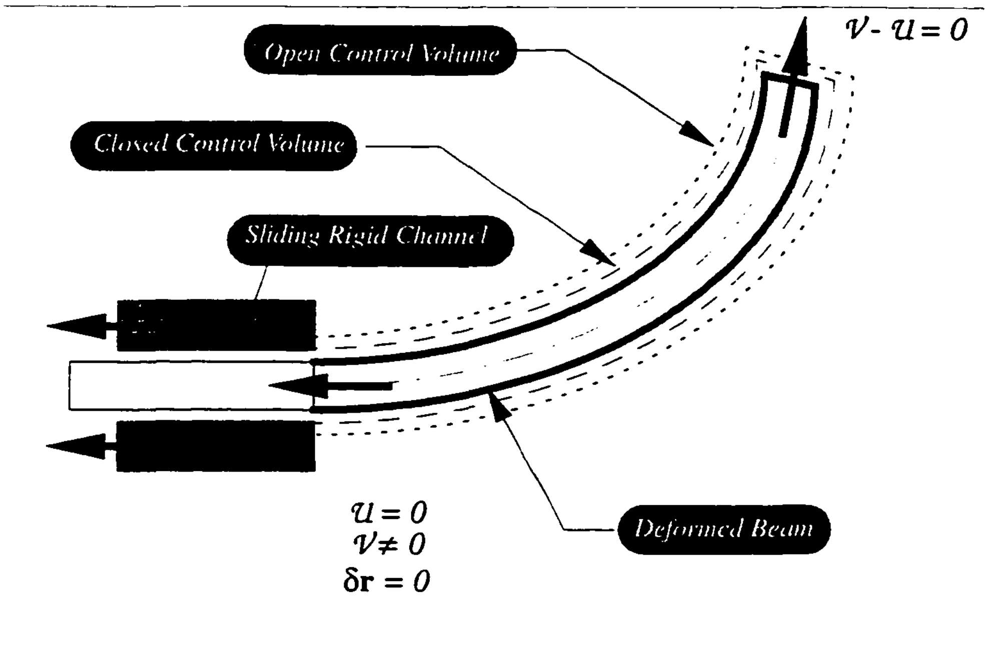


Figure 3.2.3: Sliding channel: Open and closed control volumes.

#### 3.2.2.2 Complementary Kinetic Energy

As seen by the observer on the moving channel (see Figure 3.2.2), the velocity of a mass point $m(x_1, x_2)$ on the centerline of the beam in the deformed configuration may be obtained by differentiating equation (3.2.2) i.e.:

$$\mathbf{V}_m = \frac{\partial \mathbf{R}_m}{\partial t} = -\frac{\partial C}{\partial t}\mathbf{I}_1 + \frac{\partial}{\partial t}\bar{\mathbf{u}} \tag{3.2.3}$$

or

$$\mathbf{V}_m = \left(V + \frac{\partial \bar{u}_1}{\partial t}\right)\mathbf{I}_1 + \frac{\partial \bar{u}_2}{\partial t}\mathbf{I}_2 \tag{3.2.4}$$

Thus, the kinetic co-energy with reference to the moving axes $\mathbf{I}_1$, $\mathbf{I}_2$ for the part of the beam outside the channel can be expressed as:

$$T^* = \int_{C(t)}^{L_B} \frac{1}{2}\rho A \left[\left(V + \frac{\partial \bar{u}_1}{\partial t}\right)^2 + \left(\frac{\partial \bar{u}_2}{\partial t}\right)^2\right] dX_1 \tag{3.2.5}$$

or in terms of the spatial coordinates $(\bar{x}_1, \bar{x}_2)$ , using the relations:

$$\begin{aligned} \bar{x}_1 &= X_1 - C(t) + \bar{u}_1 \\ \bar{x}_2 &= \bar{u}_2 \end{aligned} \tag{3.2.6}$$

the kinetic co-energy may be expressed as:

$$T^* = \int_{C(t)}^{L_B} \frac{1}{2}\rho A \left[ \left(\frac{\partial \bar{x}_1}{\partial t}\right)^2 + \left(\frac{\partial \bar{x}_2}{\partial t}\right)^2 \right] dX_1 \tag{3.2.7}$$

### 3.2.2.3 Strain Energy

For an axially inextensible beam, the expression for the strain energy is as given in equation (3.1.50), namely:

$$\Pi = \int_{C(t)}^{L_B} \frac{EI}{2} \left( \frac{\partial^2 \bar{x}_2}{\partial S^2} \right)^2 \left[ 1 + \left( \frac{\partial \bar{x}_2}{\partial S} \right)^2 \right] dS \tag{3.2.8}$$

### 3.2.2.4 Lagrangian

The Lagrangian for an axially inextensible beam undergoing large deflections with a moving boundary can now be expressed as:

$$\begin{aligned} \mathcal{L}_o = & \int_{C(t)}^{L_B} \frac{1}{2}\rho A \left[ \left(\frac{\partial \bar{x}_1}{\partial t}\right)^2 + \left(\frac{\partial \bar{x}_2}{\partial t}\right)^2 \right] dS - \\ & \int_{C(t)}^{L_B} \frac{EI}{2} \left( \frac{\partial^2 \bar{x}_2}{\partial S^2} \right)^2 \left[ 1 + \left( \frac{\partial \bar{x}_2}{\partial S} \right)^2 \right] dS \end{aligned} \tag{3.2.9}$$

where due to inextensibility condition we have used the relation $dX_1 = dS$.

### 3.2.2.5 Equation of Motion

Substituting the Lagrangian into the extended Hamilton's principle and carrying out the indicated variation, we obtain the governing equation of motion of the axially inextensible flexible beam with time dependent moving boundary as:

In the domain:

$$\rho A\frac{\partial^2 \bar{x}_2}{\partial t^2} + EI\left(\frac{\partial^4 \bar{x}_2}{\partial S^4}\left[1+\left(\frac{\partial \bar{x}_2}{\partial S}\right)^2\right] + \left(\frac{\partial^2 \bar{x}_2}{\partial S^2}\right)^3 + 4\,\frac{\partial \bar{x}_2}{\partial S}\,\frac{\partial^2 \bar{x}_2}{\partial S^2}\,\frac{\partial^3 \bar{x}_2}{\partial S^3}\right) +$$
$$\rho A\,\frac{\partial \bar{x}_2}{\partial S}\int_{C(t)}^{S}\left[\frac{\partial \bar{x}_2}{\partial S}\,\frac{\partial^3 \bar{x}_2}{\partial t^2 \partial S} + \left(\frac{\partial^2 \bar{x}_2}{\partial t \partial S}\right)^2\right]dS - \tag{3.2.10}$$
$$\rho A\,\frac{\partial^2 \bar{x}_2}{\partial S^2}\int_{S}^{L_B}\int_{C(t)}^{S}\left[\frac{\partial \bar{x}_2}{\partial S}\,\frac{\partial^3 \bar{x}_2}{\partial t^2 \partial S} + \left(\frac{\partial^2 \bar{x}_2}{\partial t \partial S}\right)^2\right]dS\;dS = 0$$

At the boundaries:

$$EI\left\{\frac{\partial^3 \bar{x}_2}{\partial S^3}\left[1+\frac{1}{2}\left(\frac{\partial \bar{x}_2}{\partial S}\right)^2\right] + \left(\frac{\partial^2 \bar{x}_2}{\partial S^2}\right)^2\frac{\partial \bar{x}_2}{\partial S}\right\}\delta \bar{x}_2\Bigg|_{C(t)}^{L_B} = 0$$
$$EI\,\frac{\partial^2 \bar{x}_2}{\partial S^2}\left[1+\frac{1}{2}\left(\frac{\partial \bar{x}_2}{\partial S}\right)^2\right]\delta\left(\frac{\partial \bar{x}_2}{\partial S}\right)\Bigg|_{C(t)}^{L_B} = 0 \tag{3.2.11}$$

Equation (3.2.10) is a nonlinear partial integro-differential equation. It will be noted that this equation appears simpler than that obtained for the sliding beam given in equation (3.1.52). This justifies the advantages of the new formulation. Since the beam is fixed, there are no convective terms in the kinetic co-energy. Accordingly this formulation may be considered as a full Lagrangian formulation. Equation (3.2.11) gives the kinematic and natural boundary conditions of the system. Details of the derivation of the above equations may be found in Appendix C.

### 3.2.3 Equation of Motion for Axially Extensible Flexible Beams with Sliding Boundaries-Alternative Formulation

For the axially extensible beam, $\varepsilon \neq 0$, two nonlinear coupled equations are expected. The extended Hamilton's principle in the form used in the previous section will also be used for this problem.

### 3.2.3.1 Complementary Kinetic Energy

The Kinetic co-energy is as obtained in Section 3.1.3.1 and may be rewritten as, see Figure 3.2.4:

$$T^* = \int_{C(t)}^{L_B} \frac{1}{2}\rho_o A \left[\left(V + \frac{\partial \bar{u}_1}{\partial t}\right)^2 + \left(\frac{\partial \bar{u}_2}{\partial t}\right)^2\right] dX_1 \tag{3.2.12}$$

It should be noted that in this case, $\bar{u}_I(X_1, t)$ and $\bar{u}_2(X_1, t)$ are independent.

### 3.2.3.2 Strain Energy

The expression in equation (3.1.64) may also be used for the strain energy of the deformed beam outside the moving channel:

$$\begin{aligned}\Pi = & \int_{C(t)}^{L_B} \frac{1}{2}EA \left[\frac{\partial \bar{u}_1}{\partial X_1} + \frac{1}{2}\left(\frac{\partial \bar{u}_2}{\partial X_1}\right)^2\right] dX_1 + \\ & \int_{C(t)}^{L_B} \frac{1}{2}EI \left[\left(\frac{\partial^2 \bar{u}_2}{\partial X_1^2}\right)^2 - 2\left(\frac{\partial^2 \bar{u}_2}{\partial X_1^2}\right)^2 \frac{\partial \bar{u}_1}{\partial X_1} - 2\left(\frac{\partial^2 \bar{u}_2}{\partial X_1^2}\right)^2 \left(\frac{\partial \bar{u}_2}{\partial X_1}\right)^2 - \right. \\ & \left. 2\frac{\partial \bar{u}_2}{\partial X_1} \frac{\partial^2 \bar{u}_2}{\partial X_1^2} \frac{\partial^2 \bar{u}_1}{\partial X_1^2}\right] dX_1\end{aligned} \tag{3.2.13}$$

### 3.2.3.3 Lagrangian

For the axially extensible flexible beam with sliding boundaries, the Lagrangian may be expressed as:

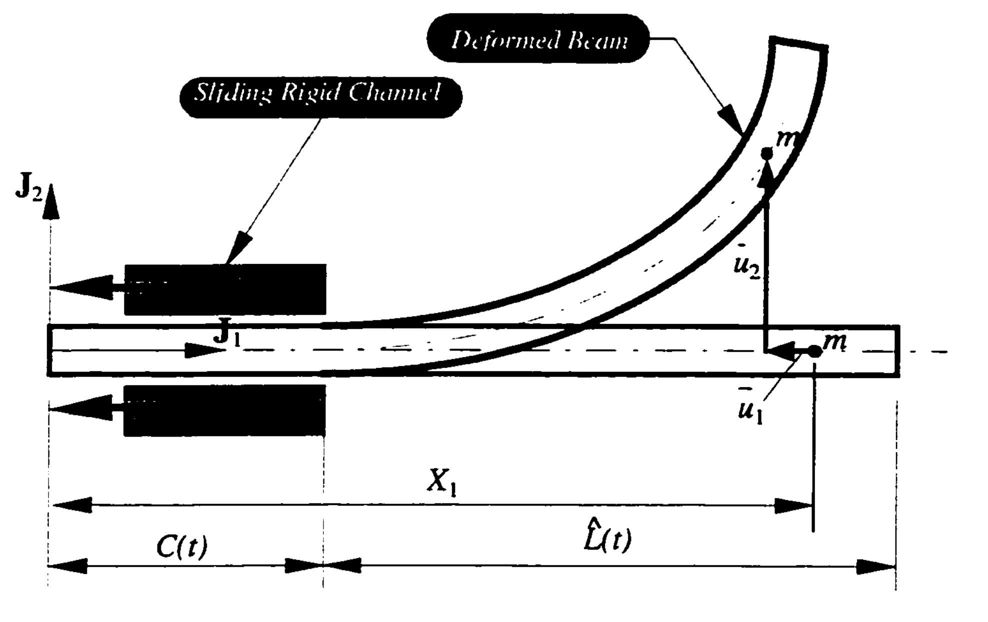


Figure 3.2.4: Flexible beam with sliding channel undergoing large overall motion: Kinematics of deformation.

$$\begin{aligned}
\mathcal{L}_o = & \int_{C(t)}^{L_B} \frac{1}{2}\rho_o A \left\{ \left[\frac{\partial \bar{u}_1}{\partial t} + V\right]^2 + \left[\frac{\partial \bar{u}_2}{\partial t}\right]^2 \right\} dX_1 - \\
& \int_{C(t)}^{L_B} \frac{1}{2} EA \left[\frac{\partial \bar{u}_1}{\partial X_1} + \frac{1}{2}\left(\frac{\partial \bar{u}_2}{\partial X_1}\right)^2\right]^2 dX_1 - \\
& \int_{C(t)}^{L_B} \frac{1}{2} EI \left[\left(\frac{\partial^2 \bar{u}_2}{\partial X_1^2}\right)^2 - 2\left(\frac{\partial^2 \bar{u}_2}{\partial X_1^2}\right)^2 \frac{\partial \bar{u}_1}{\partial X_1} - 2\left(\frac{\partial^2 \bar{u}_2}{\partial X_1^2}\right)^2 \left(\frac{\partial \bar{u}_2}{\partial X_1}\right)^2 - \right. \\
& \left. 2\frac{\partial \bar{u}_2}{\partial X_1} \frac{\partial^2 \bar{u}_2}{\partial X_1^2} \frac{\partial^2 \bar{u}_1}{\partial X_1^2}\right] dX_1
\end{aligned} \qquad (3.2.14)$$

### 3.2.3.4 Equation of Motion

Since the Lagrangian is a second order functional with two independent variables $(X_1, t)$ and two dependent functions $(\bar{u}_1(X_1, t), \bar{u}_2(X_1, t))$, two coupled Euler-Lagrange equations are obtained from the stationary conditions of Hamilton's principle. Such a derivation can be found in Appendix B. Substituting the Lagrangian from (3.2.14) into the Euler-Lagrange equations, one obtains:

In the domain:

$$\rho_o A\left[\frac{\partial^2 \bar{u}_1}{\partial t^2}+\frac{\partial V}{\partial t}\right]-EA\left[\frac{\partial^2 \bar{u}_1}{\partial X_1{}^2}+\frac{\partial \bar{u}_2}{\partial X_1}\frac{\partial^2 \bar{u}_2}{\partial X_1{}^2}\right]-EI\left[\frac{\partial^2 \bar{u}_2}{\partial X_1{}^2}\frac{\partial^3 \bar{u}_2}{\partial X_1{}^3}+\frac{\partial \bar{u}_2}{\partial X_1}\frac{\partial^4 \bar{u}_2}{\partial X_1{}^4}\right]=0 \qquad (3.2.15)$$

$$\begin{aligned}
&\rho_o A\left[\frac{\partial^2 \bar{u}_2}{\partial t^2}\right]-\\
&EA\left[\frac{\partial \bar{u}_1}{\partial X_1}\frac{\partial^2 \bar{u}_2}{\partial X_1{}^2}+\frac{\partial \bar{u}_2}{\partial X_1}\frac{\partial^2 \bar{u}_1}{\partial X_1{}^2}+\frac{3}{2}\left(\frac{\partial \bar{u}_2}{\partial X_1}\right)^2\frac{\partial^2 \bar{u}_2}{\partial X_1{}^2}\right]-\\
&EI\left[3\frac{\partial^3 \bar{u}_1}{\partial X_1{}^3}\frac{\partial^2 \bar{u}_2}{\partial X_1{}^2}+2\frac{\partial \bar{u}_1}{\partial X_1}\frac{\partial^4 \bar{u}_2}{\partial X_1{}^4}+\frac{\partial \bar{u}_2}{\partial X_1}\frac{\partial^4 \bar{u}_1}{\partial X_1{}^4}+\right.\\
&\quad 2\left(\frac{\partial \bar{u}_2}{\partial X_1}\right)^2\frac{\partial^4 \bar{u}_2}{\partial X_1{}^4}+8\frac{\partial \bar{u}_2}{\partial X_1}\frac{\partial^2 \bar{u}_2}{\partial X_1{}^2}\frac{\partial^3 \bar{u}_2}{\partial X_1{}^3}+\\
&\quad \left.2\left(\frac{\partial^2 \bar{u}_2}{\partial X_1{}^2}\right)^3+4\frac{\partial^3 \bar{u}_2}{\partial X_1{}^3}\frac{\partial^2 \bar{u}_1}{\partial X_1{}^2}-\frac{\partial^4 \bar{u}_2}{\partial X_1{}^4}\right]=0
\end{aligned} \qquad (3.2.16)$$

At the boundaries:

$$\begin{aligned}
&\left\{EA\left[\frac{\partial \bar{u}_1}{\partial X_1}+\frac{1}{2}\left(\frac{\partial \bar{u}_2}{\partial X_1}\right)^2\right]+EI\,\frac{\partial \bar{u}_2}{\partial X_1}\frac{\partial^3 \bar{u}_2}{\partial X_1{}^3}\right\}\delta\bar{u}_1\Bigg|_{C(t)}^{L_B}=0\\
&EI\,\frac{\partial \bar{u}_2}{\partial X_1}\frac{\partial^2 \bar{u}_2}{\partial X_1{}^2}\,\delta\left(\frac{\partial \bar{u}_1}{\partial X_1}\right)\Bigg|_{C(t)}^{L_B}=0
\end{aligned} \qquad (3.2.17)$$

$$\left\{EA\ \frac{\partial\bar{u}_2}{\partial X_1}\left[\frac{\partial\bar{u}_1}{\partial X_1}+\frac{1}{2}\left(\frac{\partial\bar{u}_2}{\partial X_1}\right)^2\right]-\right.$$

$$EI\left[\frac{\partial^3\bar{u}_2}{\partial X_1^{\,3}}-2\frac{\partial^3\bar{u}_2}{\partial X_1^{\,3}}\ \frac{\partial\bar{u}_1}{\partial X_1}-2\frac{\partial^2\bar{u}_2}{\partial X_1^{\,2}}\ \frac{\partial^2\bar{u}_1}{\partial X_1^{\,2}}-\right.$$

$$2\frac{\partial^3\bar{u}_2}{\partial X_1^{\,3}}\left(\frac{\partial\bar{u}_2}{\partial X_1}\right)^2-2\left(\frac{\partial^2\bar{u}_2}{\partial X_1^{\,2}}\right)^2\ \frac{\partial\bar{u}_2}{\partial X_1}-$$

$$\left.\left.\frac{\partial\bar{u}_2}{\partial X_1}\ \frac{\partial^3\bar{u}_1}{\partial X_1^{\,3}}\right]\right\}\ \delta\bar{u}_2\Bigg|_{C(t)}^{L_B}=0 \tag{3.2.18}$$

$$\left\{EI\left[\frac{\partial^2\bar{u}_2}{\partial X_1^{\,2}}-2\frac{\partial^2\bar{u}_2}{\partial X_1^{\,2}}\ \frac{\partial\bar{u}_1}{\partial X_1}-2\frac{\partial^2\bar{u}_2}{\partial X_1^{\,2}}\left(\frac{\partial\bar{u}_2}{\partial X_1}\right)^2-\right.\right.$$

$$\left.\left.\frac{\partial\bar{u}_2}{\partial X_1}\ \frac{\partial^2\bar{u}_1}{\partial X_1^{\,2}}\right]\right\}\ \delta\left(\frac{\partial\bar{u}_2}{\partial X_1}\right)\Bigg|_{C(t)}^{L_B}=0$$

Equations (3.2.15) and (3.2.16) are nonlinear coupled partial differential equations describing the dynamics of the flexible beam with a moving boundary. Equations (3.2.17) and (3.2.18) provide the consistent kinematic and force boundary conditions for the same problem.

## 3.3 Comparison of Two Formulations

Since the two formulations describe the motion of the same physical system, they are related through a transformation. The required transformation, relates the material and intermediate coordinates (Figures 3.1.5 and 3.2.4) and is given by:

$$\begin{aligned} X_1 &= \chi_1 + C(t) \\ X_2 &= \chi_2 \end{aligned} \tag{3.3.1}$$

In one formulation, namely the sliding beam, the equations contain convective acceleration terms whereas in the other there are no convective accelerations.

Also, we have seen that the two formulations lead to nonlinear equations of motion defined on the variable time domain $(0, L(t))$ for the sliding beam and $(C(t), L_B)$ for the alternative formulation. It is interesting to map the equations of the two formulations to a fixed domain at time *t, i.e.:*

$$\bar{\mathbf{u}}(X_1, t) \rightarrow \hat{\bar{\mathbf{u}}}(\hat{\eta}_1(X_1, t), t) \tag{3.3.2}$$

and

$$\mathbf{u}(\chi_1(X_1, t), t) \rightarrow \hat{\mathbf{u}}(\eta_1(X_1, t), t) \tag{3.3.3}$$

To this end we write for the sliding beam formulation:

$$\begin{aligned} \eta_1 &= \frac{\chi_1}{L(t)} && \text{where } (0 < \eta_1 \leq 1) \\ \eta_2 &= \chi_2 && \text{where } \left(-\frac{h}{2} < \eta_2 \leq \frac{h}{2}\right) \end{aligned} \tag{3.3.4}$$

or for mapping back:

$$\begin{aligned} \chi_1 &= L(t)\,\eta_1 && \text{where } (0 < \chi_1 \leq L(t)) \\ \chi_2 &= \eta_2 && \text{where } \left(-\frac{h}{2} < \chi_2 \leq \frac{h}{2}\right) \end{aligned} \tag{3.3.5}$$

For the alternative formulation, to obtain the governing equation of motion in the fixed domain, we use the transformation:

$$\begin{aligned} \hat{\eta}_1 &= \frac{X_1 - C(t)}{L(t)} && \text{where } (0 < \hat{\eta}_1 \leq 1) \\ \hat{\eta}_2 &= X_2 && \text{where } \left(-\frac{h}{2} < \hat{\eta}_2 \leq \frac{h}{2}\right) \end{aligned} \tag{3.3.6}$$

or for mapping back,

$$\begin{aligned} X_1 &= L(t)\,\hat{\eta}_1 + C(t) && \text{where } (C(t) < X_1 \leq L_B) \\ X_2 &= \hat{\eta}_2 && \text{where } \left(-\frac{h}{2} < X_2 \leq \frac{h}{2}\right) \end{aligned} \tag{3.3.7}$$

Substituting transformation (3.3.4) for the sliding beam formulation into equations (3.1.66) and (3.1.67), we find the transformed equations as follows:

$$
\begin{aligned}
&\rho_o A \left[ L^2 \frac{\partial^2 \hat{u}_1}{\partial t^2} + L^2 \frac{\partial V}{\partial t} + 2LV(1-\eta_1)\frac{\partial^2 \hat{u}_2}{\partial t \partial \eta_1} + V^2(1-\eta_1)^2 \frac{\partial^2 \hat{u}_1}{\partial \eta_1^2} + \right. \\
&\qquad \left. (1-\eta_1)\left(L \frac{\partial V}{\partial t} - 2V^2\right) \frac{\partial \hat{u}_1}{\partial \eta_1} \right] - \\
&EA \left[ \frac{\partial^2 \hat{u}_1}{\partial \eta_1^2} + \frac{1}{L} \left( \frac{\partial \hat{u}_2}{\partial \eta_1} \frac{\partial^2 \hat{u}_2}{\partial \eta_1^2} \right) \right] - \frac{EI}{L^3} \left[ \frac{\partial^2 \hat{u}_2}{\partial \eta_1^2} \frac{\partial^3 \hat{u}_2}{\partial \eta_1^3} + \frac{\partial \hat{u}_2}{\partial \eta_1} \frac{\partial^4 \hat{u}_2}{\partial \eta_1^4} \right] = 0
\end{aligned}
\tag{3.3.8}
$$

and

$$
\begin{aligned}
&\rho_o A \left[ L^2 \frac{\partial^2 \hat{u}_2}{\partial t^2} + 2LV(1-\eta_1)\frac{\partial^2 \hat{u}_2}{\partial t \partial \eta_1} + V^2(1-\eta_1)^2 \frac{\partial^2 \hat{u}_2}{\partial \eta_1^2} + \right. \\
&\qquad \left. (1-\eta_1)\left(L \frac{\partial V}{\partial t} - 2V^2\right) \frac{\partial \hat{u}_2}{\partial \eta_1} \right] - \\
&\frac{EA}{L} \left[ \frac{\partial \hat{u}_1}{\partial \eta_1} \frac{\partial^2 \hat{u}_2}{\partial \eta_1^2} + \frac{\partial \hat{u}_2}{\partial \eta_1} \frac{\partial^2 \hat{u}_1}{\partial \eta_1^2} + \frac{3}{2L}\left(\frac{\partial \hat{u}_2}{\partial \eta_1}\right)^2 \frac{\partial^2 \hat{u}_2}{\partial \eta_1^2} \right] - \\
&\frac{EI}{L^2} \left[ \frac{3}{L} \frac{\partial^3 \hat{u}_1}{\partial \eta_1^3} \frac{\partial^2 \hat{u}_2}{\partial \eta_1^2} + \frac{2}{L} \frac{\partial \hat{u}_1}{\partial \eta_1} \frac{\partial^4 \hat{u}_2}{\partial \eta_1^4} + \frac{1}{L} \frac{\partial \hat{u}_2}{\partial \eta_1} \frac{\partial^4 \hat{u}_1}{\partial \eta_1^4} + \right. \\
&\qquad \frac{2}{L^2} \left(\frac{\partial \hat{u}_2}{\partial \eta_1}\right)^2 \frac{\partial^4 \hat{u}_2}{\partial \eta_1^4} + \frac{8}{L^2} \frac{\partial \hat{u}_2}{\partial \eta_1} \frac{\partial^2 \hat{u}_2}{\partial \eta_1^2} \frac{\partial^3 \hat{u}_2}{\partial \eta_1^3} + \\
&\qquad \left. \frac{2}{L^2} \left(\frac{\partial^2 \hat{u}_2}{\partial \eta_1^2}\right)^3 + \frac{4}{L} \frac{\partial^3 \hat{u}_2}{\partial \eta_1^3} \frac{\partial^2 \hat{u}_1}{\partial \eta_1^2} - \frac{\partial^4 \hat{u}_2}{\partial \eta_1^4} \right] = 0
\end{aligned}
\tag{3.3.9}
$$

It remains now to use the equation (3.3.6) for the alternative formulation into equations (3.2.15) and (3.2.16) to obtain the equation of motion for this problem in the fixed domain. Not surprisingly these latter equations turn up identical to equations (3.3.8) and (3.3.9). This result confirms the self consistency of the two formulations. Details of derivations can be found in Appendix D.

## 3.4 Conclusions

This chapter has provided a comprehensive formulation for the sliding beam and an alternative formulation. Nonlinearities due to large deflections have been considered in these formulations. The governing equations and the related boundary conditions were obtained as stationary conditions of the extended Hamilton's principle.

The Euler-Lagrange equations for both problems yield nonlinear partial differential equations for which closed form solutions do not exist. We have demonstrated consistency in the two formulations.

In both formulations, we have considered the special case of the axially inextensible beams. Such a constraint leads to a single nonlinear partial integro-differential equation which in the case of the sliding beam problem, after eliminating the higher order terms, yields the well known linear sliding beam equation of motion.

Clearly the governing equations of motion are too complicated to solve analytically. In the following chapters, we will explore numerical solutions for such dynamical systems. Amongst such approaches are the versatile finite element formulations and the semi-analytical Galerkin's methods.

# Chapter 4

# Transient Response of Sliding Beams: Galerkin's Method

In chapter 3, the equations of motion for the sliding beam problem were obtained by two formulations; by allowing the beam to move in a rigid and fixed channel and by holding the beam fixed and allowing the channel to move along the beam. Also by mapping the two formulations to the fixed domain, it was shown that the Eulerian-Lagrangian formulation (sliding beam formulation) and the full Lagrangian formulation (sliding channel formulation) lead to the same equation of motion. The fixed domain provides a very effective means for obtaining solutions for this complex problem.

In this chapter, we first examine the axially rigid sliding beam problem undergoing small deformations and transform its governing equation and boundary conditions to the fixed domain and use the well known Galerkin's approach to study the transient response of this problem. We then compare the obtained results with those in the literature (e.g. Stylianou and Tabarrok, 1994). Subsequently we extend our approach to the nonlinear axially inextensible sliding beams undergoing large deflections.

## 4.1 Axially Inextensible Flexible Sliding Beams in Fixed Domain

To transform the equation of motion of the axially inextensible beam to a fixed domain, we start by mapping the Lagrangian of the system and then using Hamilton's principle we obtain the equation of motion in the fixed domain. We begin from the Lagrangian of the nonlinear system and subsequently linearize the system to facilitate a comparison with the results for the linear system reported in the literature.

### 4.1.1 Lagrangian in the Fixed Domain

From equation (3.1.51), the Lagrangian for the axially inextensible flexible sliding beam may be written as:

$$\begin{aligned} \mathcal{L}_o &= T^* - \Pi \\ &= \int_0^{L(t)} \frac{1}{2}\rho A \left[\left(\frac{\partial x_1}{\partial t} + V\frac{\partial x_1}{\partial S}\right)^2 + \left(\frac{\partial x_2}{\partial t} + V\frac{\partial x_2}{\partial S}\right)^2\right] dS - \\ &\quad \int_0^{L(t)} \frac{EI}{2}\left(\frac{\partial^2 x_2}{\partial S^2}\right)^2 \left[1 + \left(\frac{\partial x_2}{\partial S}\right)^2\right] dS \end{aligned} \tag{4.1.1}$$

Substituting the relations derived from the inextensibility condition (see Appendix A):

$$\frac{\partial x_1}{\partial S} = \sqrt{1 - \left(\frac{\partial x_2}{\partial S}\right)^2} \cong 1 - \frac{1}{2}\left(\frac{\partial x_2}{\partial S}\right)^2 \tag{4.1.2}$$

and

$$\frac{\partial x_1}{\partial t} = -\int_0^S \frac{\partial x_2}{\partial S}\left[1 + \frac{1}{2}\left(\frac{\partial x_2}{\partial S}\right)^2\right] \frac{\partial^2 x_2}{\partial t \partial S}\, dS \tag{4.1.3}$$

into equation (4.1.1), we obtain:

$$\mathcal{L}_o = \int_0^{L(t)} \frac{1}{2}\rho A \left\{ \left[ -\int_0^{S} \frac{\partial x_2}{\partial S} \left[ 1 + \frac{1}{2}\left(\frac{\partial x_2}{\partial S}\right)^2 \right] \frac{\partial^2 x_2}{\partial t \partial S}\, dS + V\left[ 1 - \frac{1}{2}\left(\frac{\partial x_2}{\partial S}\right)^2 \right] \right]^2 + \left(\frac{\partial x_2}{\partial t} + V\frac{\partial x_2}{\partial S}\right)^2 \right\} dS - \int_0^{L(t)} \frac{EI}{2}\left(\frac{\partial^2 x_2}{\partial S^2}\right)^2 \left[ 1 + \left(\frac{\partial x_2}{\partial S}\right)^2 \right] dS \tag{4.1.4}$$

In order to map equation (4.1.4) onto the fixed domain, we need the following transformation:

$$\mathcal{S} = \frac{S}{L} \qquad (\text{where} \quad 0 \le \mathcal{S} \le 1) \tag{4.1.5}$$

where $L = L(t)$ is the time varying length of the beam outside the channel and $\mathcal{S}$, $t$ are the independent variables. Transformation (4.1.5) shows that a fixed point in space $S$ (through which particles pass) does not map to a fixed point in space $\mathcal{S}$, see Figure 4.1.1.

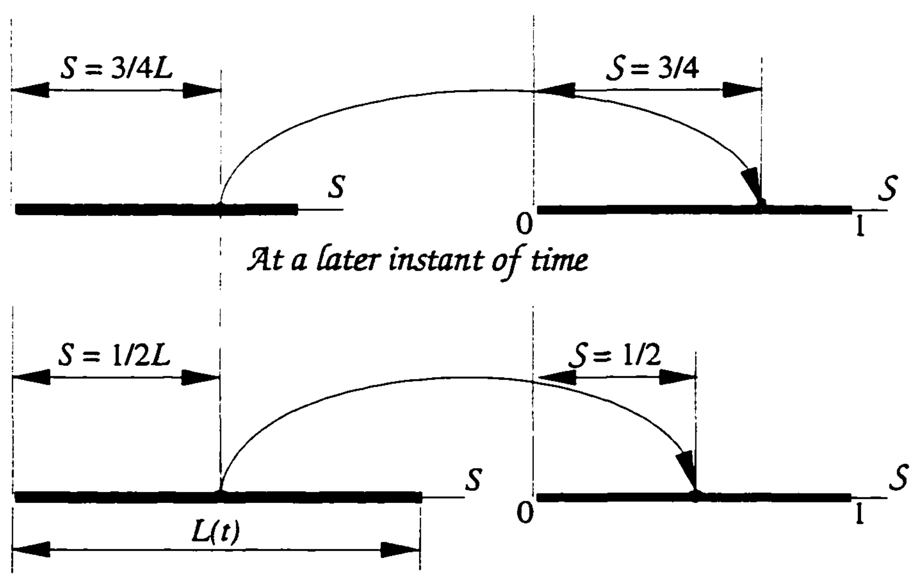


Figure 4.1.1: Mapping a fixed point in S to a moving point in $\mathcal{S}$.

From equation (4.1.5), we deduce that at time $t$:

$$
\begin{aligned}
dS &= L \; d\mathcal{S} \\
\frac{\partial x_2}{\partial S} &= \frac{\partial \hat{x}_2}{\partial \mathcal{S}} \; \frac{\partial \mathcal{S}}{\partial S} = \frac{1}{L} \; \frac{\partial \hat{x}_2}{\partial \mathcal{S}} \\
\frac{\partial^2 x_2}{\partial S^2} &= \frac{\partial}{\partial \mathcal{S}}\left( \frac{1}{L} \; \frac{\partial \hat{x}_2}{\partial \mathcal{S}} \right) = \frac{1}{L^2} \; \frac{\partial^2 \hat{x}_2}{\partial \mathcal{S}^2}
\end{aligned}
\tag{4.1.6}
$$

where

$$
x_2 (S, t) \equiv \hat{x}_2 (\mathcal{S}(S, t), t) \tag{4.1.7}
$$

We note that the partial operator $\partial (\;\;) / \partial t$ in the $S$ space provides the time rate of change at a fixed (Eulerian) point $S$. That is, as various particles pass this point, $\partial (\;\;) / \partial t|_S$ provides a measure of the changes occurring at this point over the passage of time. We have also noted that the fixed Eulerian point $S$ transforms to a *moving* point $\mathcal{S}$ in the $\mathcal{S}$ space. Hence, the $\partial (\;\;) / \partial t$ operator must be transformed as follows:

$$
\left.\frac{\partial}{\partial t}(\;\;)\right|_S = \frac{\partial}{\partial \mathcal{S}}(\;\;) \; \frac{\partial \mathcal{S}}{\partial t} + \left.\frac{\partial}{\partial t}(\;\;)\right|_{\mathcal{S}} \tag{4.1.8}
$$

Accordingly, we have:

$$
\frac{\partial x_2}{\partial t} = \frac{\partial \hat{x}_2}{\partial \mathcal{S}} \; \frac{\partial \mathcal{S}}{\partial t} + \frac{\partial \hat{x}_2}{\partial t} \tag{4.1.9}
$$

and

$$
\frac{\partial^2 x_2}{\partial t^2} = \frac{\partial^2 \mathcal{S}}{\partial t^2} \; \frac{\partial \hat{x}_2}{\partial \mathcal{S}} + 2 \frac{\partial \mathcal{S}}{\partial t} \; \frac{\partial^2 \hat{x}_2}{\partial t \partial \mathcal{S}} + \left( \frac{\partial \mathcal{S}}{\partial t} \right)^2 \; \frac{\partial^2 \hat{x}_2}{\partial \mathcal{S}^2} + \frac{\partial^2 \hat{x}_2}{\partial t^2} \tag{4.1.10}
$$

From (4.1.5), it follows that:

$$
\frac{\partial \mathcal{S}}{\partial t} = - \frac{1}{L^2} \; \frac{\partial L}{\partial t} \; S = - \frac{V}{L^2} \; S = - \frac{V}{L} \; \mathcal{S} \tag{4.1.11}
$$

and then:

$$\frac{\partial^2 S}{\partial t^2}=\frac{-L\ \frac{\partial V}{\partial t}S+V^2S-V\frac{\partial S}{\partial t}\ L}{L^2}=\frac{-L\ \frac{\partial V}{\partial t}S+V^2S-V\left(-\frac{V}{L}\ S\right)\ L}{L^2}$$
$$=\frac{2V^2S-L\ \frac{\partial V}{\partial t}S}{L^2} \tag{4.1.12}$$

Substituting equations (4.1.11) and (4.1.12) into equations (4.1.9) and (4.1.10), we obtain the following two relations:

$$\frac{\partial x_2}{\partial t}=-\frac{V}{L}S\ \frac{\partial \hat{x}_2}{\partial S}+\frac{\partial \hat{x}_2}{\partial t} \tag{4.1.13}$$

and

$$\frac{\partial^2 x_2}{\partial t^2}=\frac{2V^2S-L\ \frac{\partial V}{\partial t}S}{L^2}\ \frac{\partial \hat{x}_2}{\partial S}+2\left(-\frac{V}{L}\ S\right)\ \frac{\partial^2 \hat{x}_2}{\partial t\partial S}+\left(-\frac{V}{L}\ S\right)^2\ \frac{\partial^2 \hat{x}_2}{\partial S^2}+\frac{\partial^2 \hat{x}_2}{\partial t^2} \tag{4.1.14}$$

Also using relation (4.1.6), we may write:

$$\frac{\partial^2 x_2}{\partial t\partial S}=\frac{\partial}{\partial S}\left(\frac{1}{L}\ \frac{\partial \hat{x}_2}{\partial S}\right)\ \frac{\partial S}{\partial t}+\frac{\partial}{\partial t}\left(\frac{1}{L}\ \frac{\partial \hat{x}_2}{\partial S}\right)$$
$$=-\frac{V}{L^2}\ S\ \frac{\partial^2 \hat{x}_2}{\partial S^2}+\frac{1}{L}\ \frac{\partial^2 \hat{x}_2}{\partial t\partial S}-\frac{V}{L^2}\ \frac{\partial \hat{x}_2}{\partial S} \tag{4.1.15}$$

By substituting relations (4.1.13), (4.1.14) and (4.1.15) into equation (4.1.4), the Lagrangian of the sliding flexible beam at instant $t$, in the fixed domain, can finally be expressed as:

$$\hat{\mathcal{L}}_o = \int_0^1 \frac{1}{2}\rho A \left\{ \left[ -\int_0^S \frac{1}{L} \frac{\partial \hat{x}_2}{\partial S} \left[ 1 + \frac{1}{2L^2}\left(\frac{\partial \hat{x}_2}{\partial S}\right)^2 \right] \left( -\frac{V}{L^2} S \frac{\partial^2 \hat{x}_2}{\partial S^2} + \frac{1}{L} \frac{\partial^2 \hat{x}_2}{\partial t \partial S} - \right.\right.\right.$$

$$\left.\left. \frac{V}{L^2} \frac{\partial \hat{x}_2}{\partial S} \right) L dS + V\left( 1 - \frac{1}{2L^2}\left(\frac{\partial \hat{x}_2}{\partial S}\right)^2 \right) \right]^2 + \tag{4.1.16}$$

$$\left. \left( -\frac{V}{L} S \frac{\partial \hat{x}_2}{\partial S} + \frac{\partial \hat{x}_2}{\partial t} + \frac{V}{L} \frac{\partial \hat{x}_2}{\partial S} \right)^2 \right\} L dS \; -$$

$$\int_0^1 \frac{EI}{2L^3} \left( \frac{\partial^2 \hat{x}_2}{\partial S^2} \right)^2 \left[ 1 + \frac{1}{L^2}\left(\frac{\partial \hat{x}_2}{\partial S}\right)^2 \right] dS$$

For the linear case, in the absence of shortening effect, the Lagrangian (4.1.16) may be simplified to the following simple form:

$$\mathcal{L}_{oL} = \int_0^1 \left\{ \frac{1}{2}\rho A \left[ \frac{V}{L}(1-S)\frac{\partial \hat{x}_2}{\partial S} + \frac{\partial \hat{x}_2}{\partial t} \right]^2 - \frac{EI}{2L^4}\left( \frac{\partial^2 \hat{x}_2}{\partial S^2} \right)^2 \right\} L dS \tag{4.1.17}$$

### 4.1.2 Equation of Motion for Linear Axially Inextensible Flexible Sliding Beams in Fixed Domain

Using the Lagrangian (4.1.17) in Hamilton's principle:

$$\delta \int_{t_1}^{t_2} \mathcal{L}_{oL} \; dt = 0 \tag{4.1.18}$$

and carrying out the variations (see Appendix E), the equation of motion for the linear axially inextensible flexible sliding beam, in the fixed domain, and in the absence of shortening effect can be expressed as:

$$\rho A \left\{ \frac{\partial^2 \hat{x}_2}{\partial t^2} + \frac{2V}{L}(1-S)\frac{\partial^2 \hat{x}_2}{\partial t \partial S} + \frac{V^2}{L^2}(1-S)^2 \frac{\partial^2 \hat{x}_2}{\partial S^2} + \left[\frac{2V^2}{L^2}S - \frac{2V^2}{L^2} + \frac{1}{L}\frac{\partial V}{\partial t} - \frac{1}{L}\frac{\partial V}{\partial t}S\right]\frac{\partial \hat{x}_2}{\partial S} \right\} + \frac{EI}{L^4}\frac{\partial^4 \hat{x}_2}{\partial S^4} = 0 \tag{4.1.19}$$

Now, we need to account for the shortening effect. The term shortening effect has been used by various researchers with slightly different meanings. It can be seen that as the beam deflects in bending material points on the beam will have not only a lateral deflection along $x_2$ but also a secondary motion along the $x_1$ axis. There will be a kinetic co-energy associated with this secondary motion which we must take into account. It is to be noted that this secondary motion takes place even when the beam is considered axially inextensible. We consider the additional kinetic co-energy term as:

$$\mathcal{L}_{add} = \int_0^{L(t)} \frac{1}{2}\rho A \left[ -\int_0^S \frac{\partial x_2}{\partial S}\frac{\partial^2 x_2}{\partial t \partial S}\, dS + V \right]^2 dS \tag{4.1.20}$$

Here, one may use the Leibniz rule to integrate equation (4.1.20). After setting aside the boundary terms and noting the prescribed terms, the additional Lagrangian term that contributes to the equation of motion may be expressed as:

$$\mathcal{L}_{add} = \int_0^{L(t)} \frac{1}{2}\rho A \frac{\partial V}{\partial t}(L-S)\left(\frac{\partial x_2}{\partial S}\right)^2 dS \tag{4.1.21}$$

Using relations (4.1.6), equation (4.1.21) may also be transformed to the fixed domain and is given by:

$$\hat{\mathcal{L}}_{add} = \int_0^1 \frac{1}{2}\rho A \frac{\partial V}{\partial t}(1-S)\left(\frac{\partial \hat{x}_2}{\partial S}\right)^2 dS \tag{4.1.22}$$

Now adding $\hat{\mathcal{L}}_{add}$ to $\hat{\mathcal{L}}_{oL}$ and carrying out the variation, the comprehensive form of equation of motion for linear sliding flexible beam, including the shortening effect, in the fixed domain is obtained as:

$$\rho A\left\{\frac{\partial^2\hat{x}_2}{\partial t^2}+\frac{2V}{L}(1-\mathcal{S})\frac{\partial^2\hat{x}_2}{\partial t\partial\mathcal{S}}+\left[\frac{V^2}{L^2}(1-\mathcal{S})^2+\frac{1}{L}\frac{\partial V}{\partial t}(1-\mathcal{S})\right]\frac{\partial^2\hat{x}_2}{\partial\mathcal{S}^2}+\right.$$
$$\left.\left[\frac{2V^2}{L^2}\mathcal{S}-\frac{2V^2}{L^2}-\frac{1}{L}\frac{\partial V}{\partial t}\mathcal{S}\right]\frac{\partial\hat{x}_2}{\partial\mathcal{S}}\right\}+\frac{EI}{L^4}\frac{\partial^4\hat{x}_2}{\partial\mathcal{S}^4}=0 \tag{4.1.23}$$

Solution of the above equation and its geometric and natural boundary conditions as derived in chapter 3, leads to the transient response of the linear sliding flexible beams.

### 4.1.3 Solution Procedure: Galerkin's Method

One way of solving equation (4.1.23), is to use the Galerkin's method. To this end we first transform the governing equation of motion into a non-dimensional form. Introducing the non-dimensional quantities:

$$\eta=\frac{\hat{x}_2}{L_o}\quad,\quad\tau=\left(\frac{EI}{\rho A}\right)^{\frac{1}{2}}\frac{t}{L_o^2}$$
$$v=\left(\frac{\rho A}{EI}\right)^{\frac{1}{2}}VL_o\quad,\quad\text{where}\quad L(t)=L_o\,l(t) \tag{4.1.24}$$

and using the relations (4.1.24) in equation (4.1.23), after some manipulations, the dimensionless governing equation of motion is obtained as:

$$\frac{\partial^2\eta}{\partial\tau^2}+\frac{2v(1-\mathcal{S})}{l}\frac{\partial^2\eta}{\partial\tau\partial\mathcal{S}}+\left[\frac{v^2(1-\mathcal{S})^2}{l^2}+\frac{1}{l}\frac{\partial v}{\partial\tau}(1-\mathcal{S})\right]\frac{\partial^2\eta}{\partial\mathcal{S}^2}-$$
$$\frac{1}{l^2}\left[l\frac{\partial v}{\partial\tau}\mathcal{S}+(2-2\mathcal{S})v^2\right]\frac{\partial\eta}{\partial\mathcal{S}}+\frac{1}{l^4}\frac{\partial^4\eta}{\partial\mathcal{S}^4}=0 \tag{4.1.25}$$

To obtain a solution, we express $\eta$ in terms of modal functions $\wp_j(\mathcal{S})$ as follows:

$$\eta(\mathcal{S},\tau)=\sum_{j=1}^{N}\wp_j(\mathcal{S})\;q_j(\tau) \tag{4.1.26}$$

where $q_j(\tau)$ are the unknown modal coefficients. Substituting from (4.1.26) into (4.1.25) and using Galerkin's method, we obtain a set of ODE's in time part of the solution $q_j(\tau)$ . For the moment it must be implicitly assumed that the solution $\eta$ converges to the true solution as $N \to \infty$. On physical grounds one can anticipate that for problems with the majority of energy at low frequencies, the motion in low modes will predominate and that such an approximation will thus converge rapidly onto the true solution. Substituting the relation in (4.1.26) into equation (4.1.25) and following Galerkin's method, i.e. multiplying the residual obtained by $\wp_i(\mathcal{S})$ and integrating over the beam length (0,1), we may obtain the second order ODEs as:

$$\ddot{q}_i + a_{ij}\ \dot{q}_j + b_{ij}\ q_j = 0 \tag{4.1.27}$$

where

$$a_{ij} = \int_0^1 \frac{2v}{l}\ (1-\mathcal{S})\ \wp_i\ \frac{\partial \wp_j}{\partial \mathcal{S}}\ d\mathcal{S} \tag{4.1.28}$$

and

$$\begin{aligned} b_{ij} = \int_0^1 \wp_i \Bigg\{ & \left[\frac{v^2}{l^2}(1-\mathcal{S})^2 + \frac{1}{l}\ \frac{\partial v}{\partial \tau}(1-\mathcal{S})\right]\frac{\partial^2 \wp_j}{\partial \mathcal{S}^2} - \\ & \frac{1}{l^2}\left[l\ \frac{\partial v}{\partial \tau}\ \mathcal{S} + 2(1-\mathcal{S})\ \ v^2\right]\frac{\partial \wp_j}{\partial \mathcal{S}} + \frac{1}{l^4}\ \frac{\partial^4 \wp_j}{\partial \mathcal{S}^4}\Bigg\} d\mathcal{S} \end{aligned} \tag{4.1.29}$$

The coefficients $a_{ij}$ and $b_{ij}$ are time dependent making the governing equations of motion non-autonomous. It is important to note the significant advantage of deriving these equations in the fixed domain since for the computation of $a_{ij}$ and $b_{ij}$ the space dependent eigenfunctions of the beam instead of time and space dependent eigenfunctions, as used by other researchers (e.g. Tabarrok et al., 1974 and Al-Bedoor and Khulief, 1996), may be used.

### 4.1.4 Time Integration of System Equations

To integrate the system equations (4.1.27) in time and obtain the transient response of the system, it is required to define a proper set of comparison functions (Meirovitch, 1967). For an axially rigid flexible sliding beam emerging from a fixed rigid channel, the ortho-normal eigenfunctions of the stationary cantilever provide a convenient set of comparison functions in the following form:

$$\wp_i = \cos\beta_i\eta - \cosh\beta_i\eta - \frac{\cos\beta_i + \cosh\beta_i}{\sin\beta_i + \sinh\beta_i}(\sin\beta_i\eta - \sinh\beta_i\eta) \qquad (4.1.30)$$

where the eigenvalues $\beta_i$ are the roots of the characteristic equation:

$$1 + \cos\beta_i \cosh\beta_i = 0 \qquad (4.1.31)$$

Since in the fixed domain the comparison functions are only space dependent, by substituting equation (4.1.30) into relations (4.1.28) and (4.1.29) and using the MAPLE symbolic program, we can integrate and determine the matrices $a_{ij}$ and $b_{ij}$ as functions of prescribed velocity of the sliding beam and the instantaneous length of the beam.

With the matrices $a_{ij}$ and $b_{ij}$ at hand, we may now integrate the set of ODEs in equation (4.1.27) and obtain the transient response of the system. This has been done using the IMSL/DIVPRK routine.

To validate the equations and their solutions, we consider some examples studied by Stylianou, 1993. These cases were also investigated experimentally and simulated by Yuh and Young, 1991. To compare results we need to define a non-negative, structural damping force proportional to $\dot{q}_j$. Such a damping coefficient was determined experimentally by Yuh and Young. In this case of variable length beam, the damping coefficient becomes length dependent. Stylianou calculated an equivalent Rayleigh damping coefficient for his discretized equations and was able to compare his results with the experimental responses determined by Yuh and Young. For our formulation of the sliding beam, *in the fixed domain*, it is not evident how the damping coefficient (which is inserted in the discretized equations and does not appear in the partial differential equation) should be calculated. An indirect and relatively easy approach is to "guess" a damping coefficient and on comparison of results with those of Stylianou, adjust the coefficient for excellent agreement for small amplitude oscillations. Once this is accomplished, the same coefficient may be used for large amplitude of oscillations.

#### 4.1.4.1 Spaghetti and Reverse Spaghetti Problems: Quadratic Sliding Motion

Let us consider a quadratic sliding motion as:

$$L(t) = L_o + V_o \; t + \frac{a_o \; t^2}{2} \tag{4.1.32}$$

In the case of the reverse spaghetti problem i.e. beam extruding from a channel, we examine a constant velocity extrusion with the initial length $L_o = 0.4255\,(m)$ and velocity $V_o = 0.0410\,(m/s)$. The beam properties are given as follows: $\rho = 3144.3858\,(kg/m^3)$, $E = 68.96\times10^9\,(N/m^2)$, $A = 4.3434\times10^{-5}\,(m^2)$ and $I = 1.059\times10^{-11}\,(m^4)$. The time history of the tip deflection is given in Figure 4.1.2, which is in good agreement with the results obtained in test case #2 by Stylianou, 1993.

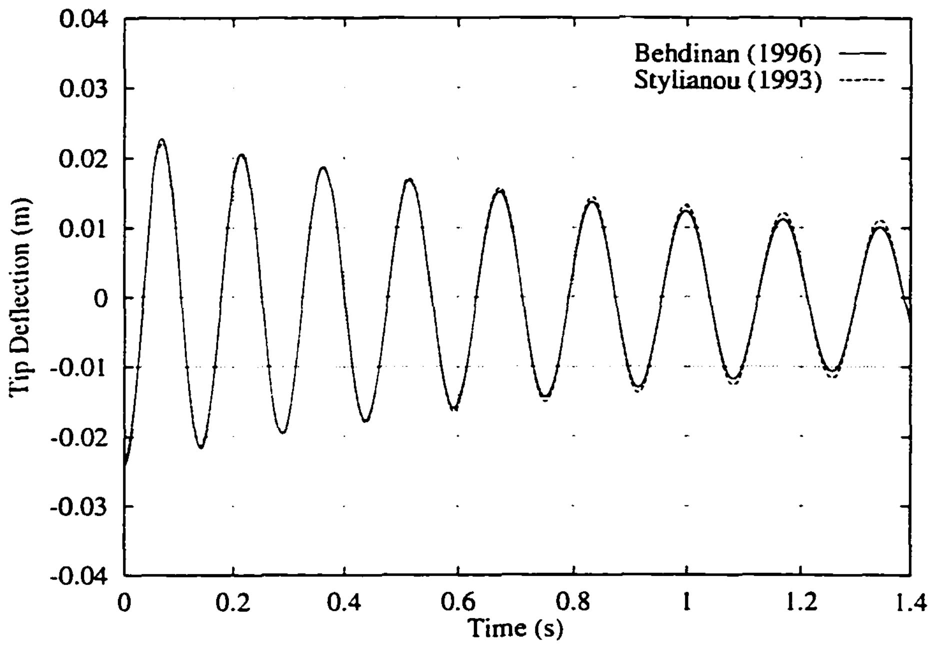


Figure 4.1.2: Reverse Spaghetti Problem: Constant Velocity Extrusion.

For the spaghetti problem i.e. beam retracting into a channel, we consider a constant acceleration retracting beam with the initial length $L_o = 0.521\,(m)$ and velocity $V_o = -0.0300\,(m/s)$ and constant acceleration $a_o = -0.0540\,(m/s^2)$. Figure 4.1.3

shows the tip response of the beam which is in good agreement with the results obtained in test case #3 of Stylianou, 1993.

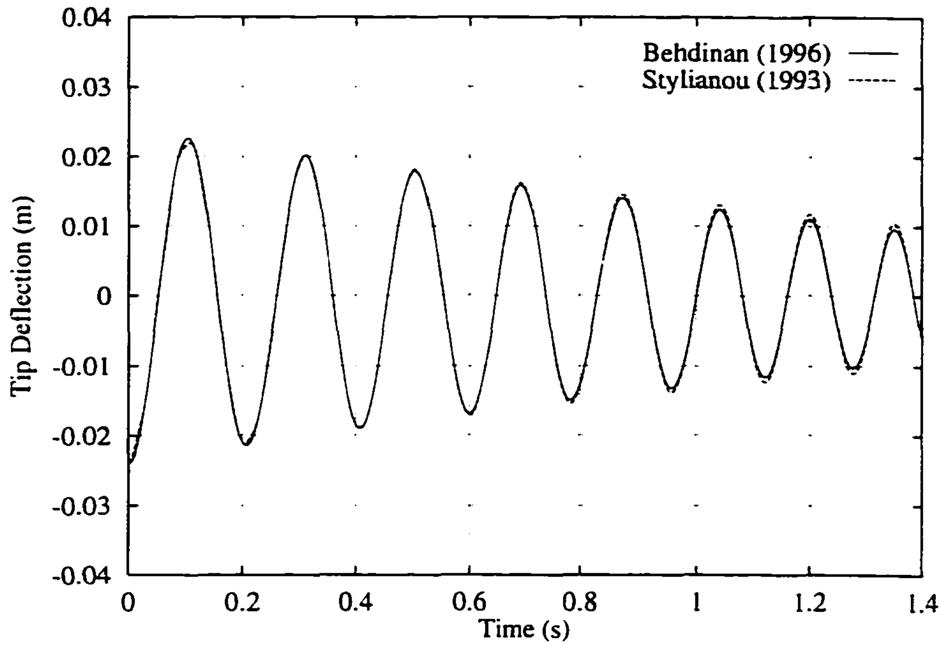


Figure 4.1.3: Spaghetti Problem: Constant Acceleration retraction.

#### 4.1.4.2 Spaghetti and Reverse Spaghetti Problems: Repositional Motion

For these simulations, the beam's length is described by:

$$L(t) = L_o + \frac{c_o}{t_o}\left[t - \frac{t_o}{2\pi}\sin\left(\frac{2\pi t}{t_o}\right)\right] \tag{4.1.33}$$

where in the case of the extrusion $L_o = 0.35\,(m)$ , $c_o = 0.7\,(m)$ and $t_o = 1.2\,(s)$ and for retraction these parameters are given as: $L_o = 1.05\,(m)$ , $c_o = -0.7\,(m)$ and $t_o = 1.2\,(s)$ . Equation (4.1.33) allows us to consider axial motions made up of a constant and an oscillatory part. For the oscillatory part it is of interest to examine frequencies higher and lower than the fundamental natural frequency of the beam at the initial configuration, for the retraction case, and the final configuration, for the extrusion case. The results are given in Figures 4.1.4 and 4.1.5 which are again in good agreement with those obtained in simulation #1 and #2 by Stylianou, 1993.

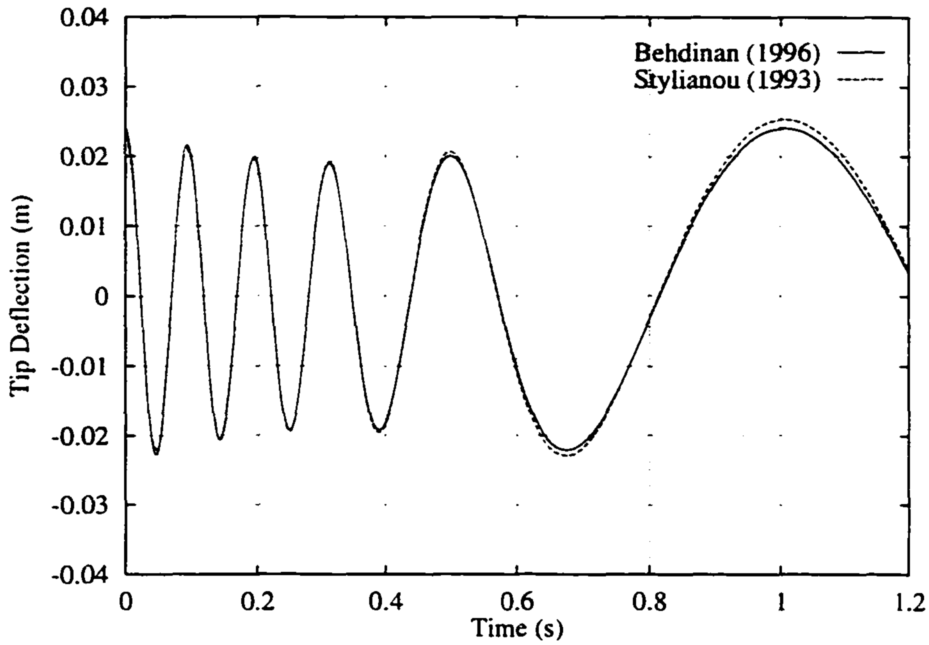


Figure 4.1.4: Reverse Spaghetti Problem: Low Frequency Extrusion.

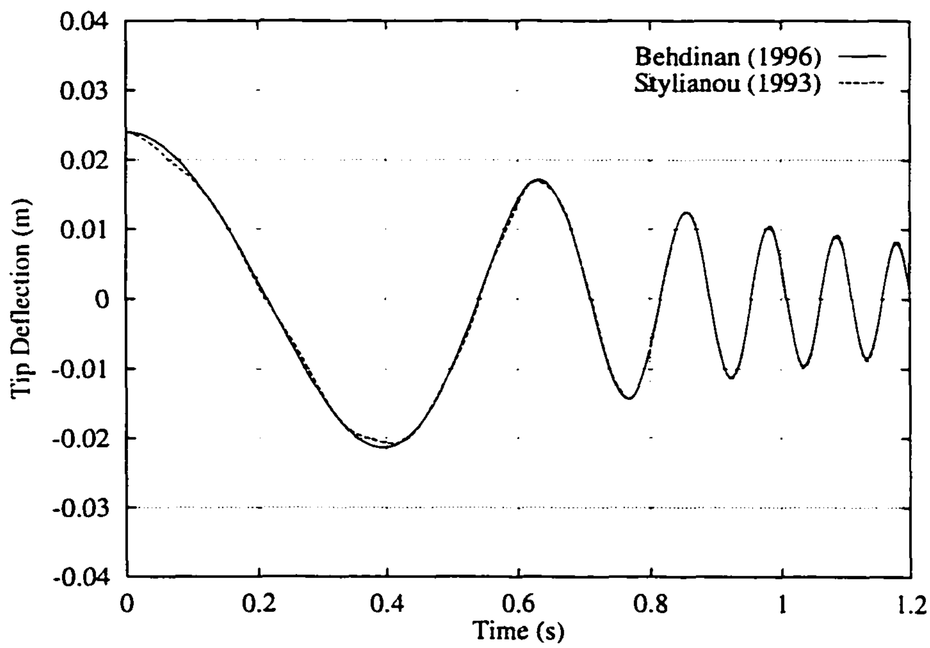


Figure 4.1.5: Spaghetti Problem: Low Frequency Retraction.

In the case of high frequency oscillation where the period of oscillation $t_o = 0.2\,(s)$, with the same parameters, the results shown in Figures 4.1.6 and 4.1.7 are in good qualitative agreement as with those obtained in simulation cases #5 and #7 by Yuh and Young, 1991.

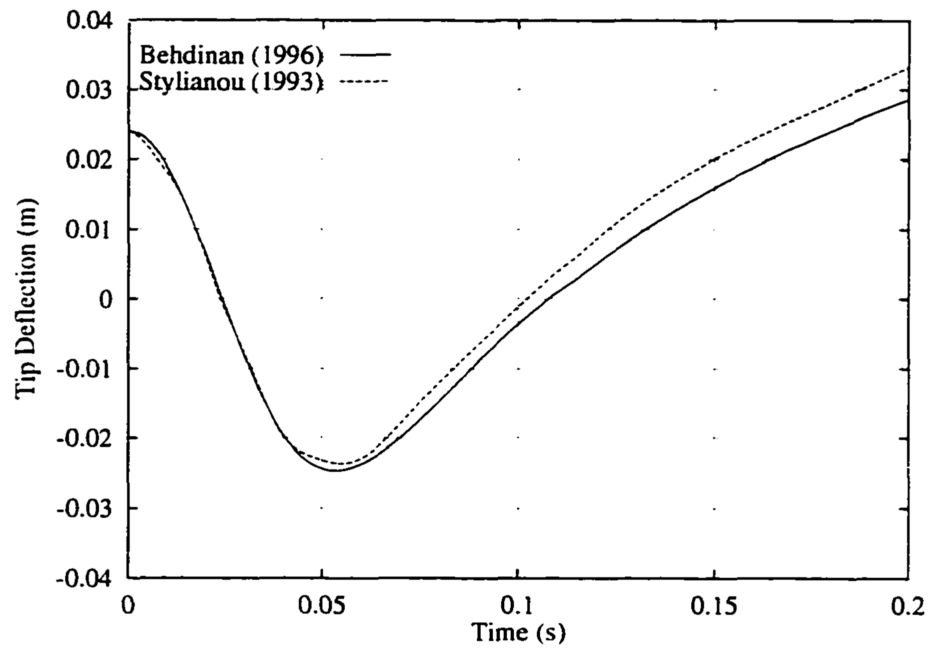


Figure 4.1.6: Reverse Spaghetti Problem: High Frequency Extrusion.

#### 4.1.4.3 Reverse Spaghetti Problem: High Frequency Perturbation

It is possible to attenuate the transverse oscillations of flexible sliding beams by introducing a high frequency, low amplitude perturbation to the otherwise constant-velocity axial motion. This was addressed by Golnaraghi, 1991, and Stylianou, 1993.

In this case the time varying length of the beam can be expressed as:

$$L(t) = L_o(1 + \varepsilon \sin\hat{\omega}t) + V_o t \tag{4.1.34}$$

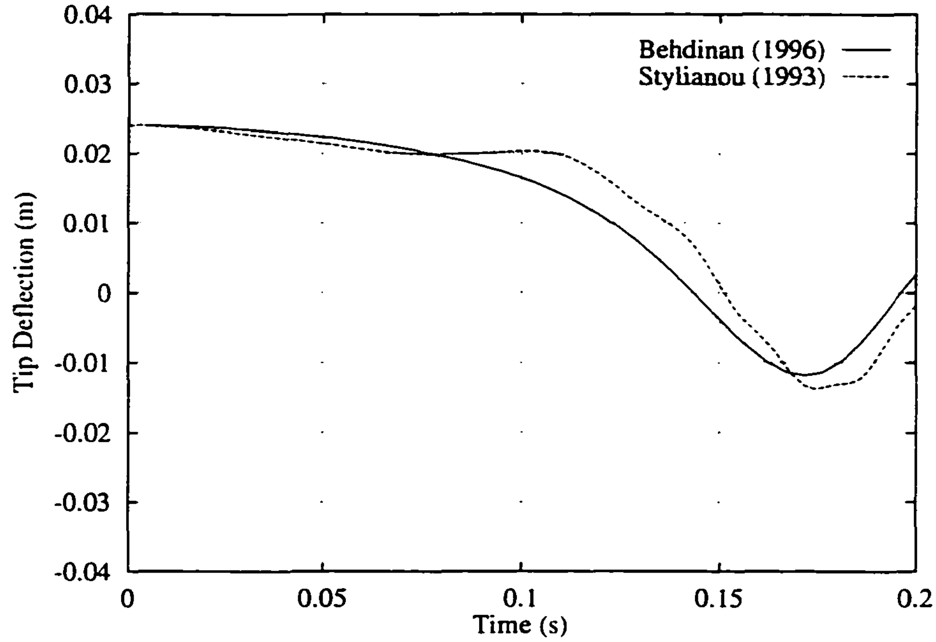


Figure 4.1.7: Spaghetti Problem: High Frequency Retraction.

Zajaczkowski and Lipinski, 1979, used Bolotin's approach (Bolotin, 1964) to obtain the region of stability and instability for this problem. Based on the perturbation parameters $\varepsilon$ and $\sqrt{\omega_1/2\hat{\omega}}$, where $\omega_1$ is the instantaneous fundamental natural frequency of the sliding beam, we may have stable or unstable response. Here we consider the following parameters in the stable region: $L_o = 0.4255 \quad (m)$, $\varepsilon = 0.0133$ and $\hat{\omega} = 11\omega_1$. Figure 4.1.8 shows the resulting suppression of oscillation.

These simulations clearly demonstrate the change in frequency and more importantly the amplitude of the oscillations due to the changing length of the beam.

## 4.2 Nonlinear Axially Inextensible Flexible Sliding Beams in Fixed Domain

To study the transient response of the nonlinear axially inextensible beam, we map the governing equation of motion to the fixed domain and then using Galerkin's approach we discretize the system equations and obtain a set of ODEs in $q_i(\tau)$ coefficients. Returning to equation (4.1.26), we then obtain the response of the system in the fixed domain. Subsequently we may transform the response to the physical i.e. variable domain.

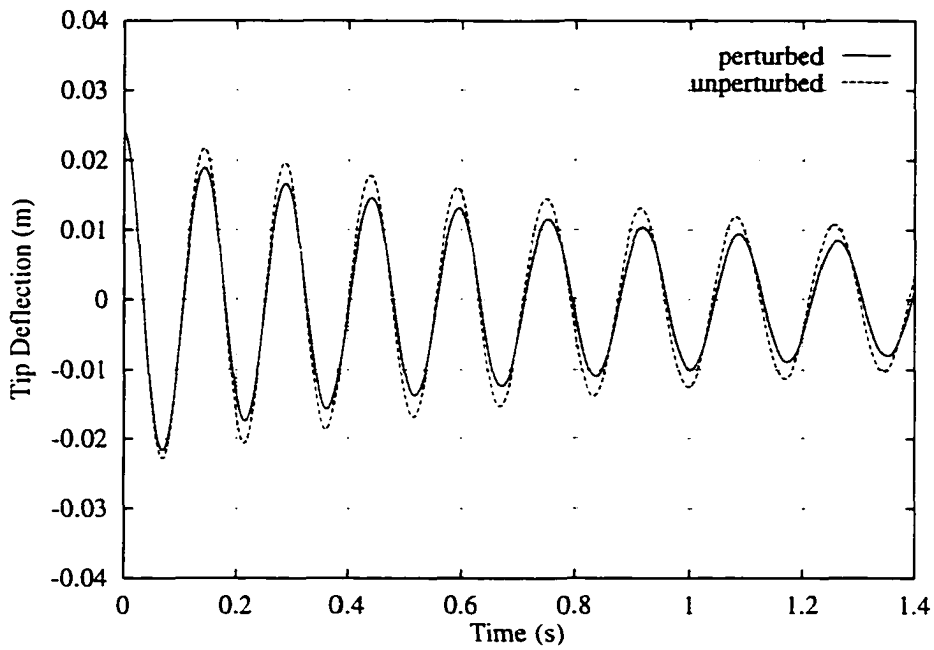


Figure 4.1.8: Reverse Spaghetti Problem: High Frequency Perturbation.

### 4.2.1 Nonlinear Equation of Motion of Inextensible Flexible Sliding Beams in the Fixed Domain

Here as in section 4.1, we need to use a one to one mapping from time variable domain to the fixed domain. Employing the transformation defined in equation (4.1.5) and using the relations (4.1.6), (4.1.13), (4.1.14) and (4.1.15) in the equation of motion of axially inextensible sliding beam given in (3.1.52), we obtain:

$$L_1 + N_1 + N_2 = 0 \tag{4.2.1}$$

where:

$$L_1 = \rho A \left\{ \frac{\partial^2 \hat{x}_2}{\partial t^2} + \frac{2V}{L}(1-S)\frac{\partial^2 \hat{x}_2}{\partial t \partial S} + \left[ \frac{V^2}{L^2}(1-S)^2 + \frac{1}{L}\frac{\partial V}{\partial t}(1-S) \right] \frac{\partial^2 \hat{x}_2}{\partial S^2} + \right.$$
$$\left. \left[ \frac{2V^2}{L^2} S - \frac{2V^2}{L^2} - \frac{1}{L}\frac{\partial V}{\partial t} S \right] \frac{\partial \hat{x}_2}{\partial S} \right\} + \frac{EI}{L^4}\frac{\partial^4 \hat{x}_2}{\partial S^4} \tag{4.2.2}$$

and

$$N_1 = \rho A \left\{ \frac{2V}{L^3}\left(\frac{\partial \hat{x}_2}{\partial S}\right)^2 \frac{\partial^2 \hat{x}_2}{\partial t \partial S} + \left[ \frac{-2V^2 S}{L^4} + \frac{3}{2L^3}\frac{\partial V}{\partial t}(1-S) + \frac{V^2}{L^4} \right] \left(\frac{\partial \hat{x}_2}{\partial S}\right)^2 \frac{\partial^2 \hat{x}_2}{\partial S^2} - \right.$$
$$\left. \frac{2V^2}{L^4}\left(\frac{\partial \hat{x}_2}{\partial S}\right)^3 \right\} + \frac{EI}{L^6}\left[ \frac{\partial^4 \hat{x}_2}{\partial S^4}\left(\frac{\partial \hat{x}_2}{\partial S}\right)^2 + 4\,\frac{\partial \hat{x}_2}{\partial S}\frac{\partial^2 \hat{x}_2}{\partial S^2}\frac{\partial^3 \hat{x}_2}{\partial S^3} + \left(\frac{\partial^2 \hat{x}_2}{\partial S^2}\right)^3 \right] \tag{4.2.3}$$

$$
\begin{aligned}
N_2 = {} & \frac{1}{L}\frac{\partial\hat{x}_2}{\partial S}\int_0^S \rho A\left[\left(\frac{-VS}{L^2}\frac{\partial^2\hat{x}_2}{\partial S^2}+\frac{1}{L}\frac{\partial^2\hat{x}_2}{\partial t\partial S}-\frac{V}{L^2}\frac{\partial\hat{x}_2}{\partial S}\right)^2+\frac{1}{L^2}\frac{\partial\hat{x}_2}{\partial S}\right. \\
& \left(\frac{2V^2-L\frac{\partial V}{\partial t}}{L^2}\frac{\partial\hat{x}_2}{\partial S}+\frac{4V^2S-L\frac{\partial V}{\partial t}S}{L^2}\frac{\partial^2\hat{x}_2}{\partial S^2}-\frac{2V}{L}\frac{\partial^2\hat{x}_2}{\partial t\partial S}-\right. \\
& \left.\left.\frac{2VS}{L}\frac{\partial^3\hat{x}_2}{\partial t\partial S^2}+\frac{V^2S^2}{L^2}\frac{\partial^3\hat{x}_2}{\partial S^3}+\frac{\partial^3\hat{x}_2}{\partial t^2\partial S}\right)\right]L\,dS- \\
& \frac{1}{L^2}\frac{\partial^2\hat{x}_2}{\partial S^2}\left\{\int_S^1\int_0^S \rho A\left[\left(\frac{-VS}{L^2}\frac{\partial^2\hat{x}_2}{\partial S^2}+\frac{1}{L}\frac{\partial^2\hat{x}_2}{\partial t\partial S}-\frac{V}{L^2}\frac{\partial\hat{x}_2}{\partial S}\right)^2+\frac{1}{L^2}\frac{\partial\hat{x}_2}{\partial S}\right.\right. \\
& \left(\frac{2V^2-L\frac{\partial V}{\partial t}}{L^2}\frac{\partial\hat{x}_2}{\partial S}+\frac{4V^2S-L\frac{\partial V}{\partial t}S}{L^2}\frac{\partial^2\hat{x}_2}{\partial S^2}-\right. \\
& \frac{2V}{L}\frac{\partial^2\hat{x}_2}{\partial t\partial S}-\frac{2VS}{L}\frac{\partial^3\hat{x}_2}{\partial t\partial S^2}+\frac{V^2S^2}{L^2}\frac{\partial^3\hat{x}_2}{\partial S^3}+ \\
& \left.\left.\frac{\partial^3\hat{x}_2}{\partial t^2\partial S}\right)\right]L^2\,dS\,dS+ \\
& \int_S^1\rho A\left[\frac{1}{2L^2}\frac{\partial V}{\partial t}\left(\frac{\partial\hat{x}_2}{\partial S}\right)^2+\frac{2V}{L}\frac{\partial\hat{x}_2}{\partial S}\left(\frac{-VS}{L^2}\frac{\partial^2\hat{x}_2}{\partial S^2}+\frac{1}{L}\frac{\partial^2\hat{x}_2}{\partial t\partial S}-\right.\right. \\
& \left.\left.\left.\frac{V}{L^2}\frac{\partial\hat{x}_2}{\partial S}\right)+\frac{V^2}{L^3}\frac{\partial\hat{x}_2}{\partial S}\frac{\partial^2\hat{x}_2}{\partial S^2}\right]L\,dS\right\}
\end{aligned}
\tag{4.2.4}
$$

In equation (4.2.1), $L_1$, $N_1$ and $N_2$ contain linear, nonlinear and nonlinear integral terms, respectively.

Introducing the non-dimensional quantities in (4.1.24), we may express the non-dimensional form of the governing equation of motion for the inextensible sliding beam, in the fixed domain, as:

$$\mathcal{L}(\eta) + \mathcal{N}_1(\eta) + \mathcal{N}_2(\eta) = 0 \tag{4.2.5}$$

where

$$\begin{aligned}\mathcal{L}(\eta) = {} & \frac{\partial^2 \eta}{\partial \tau^2} + \frac{2v}{l}(1-\mathcal{S})\frac{\partial^2 \eta}{\partial \tau \partial \mathcal{S}} + \left[\frac{v^2}{l^2}(1-\mathcal{S})^2 + \frac{1}{l}\frac{\partial v}{\partial t}(1-\mathcal{S})\right]\frac{\partial^2 \eta}{\partial \mathcal{S}^2} + \\ & \left[\frac{2v^2}{l^2}\mathcal{S} - \frac{2v^2}{l^2} - \frac{1}{l}\frac{\partial v}{\partial t}\mathcal{S}\right]\frac{\partial \eta}{\partial \mathcal{S}}\Bigg\} + \frac{1}{l^4}\frac{\partial^4 \eta}{\partial \mathcal{S}^4}\end{aligned} \tag{4.2.6}$$

and

$$\begin{aligned}\mathcal{N}_1(\eta) = {} & \frac{2v}{l^3}\left(\frac{\partial \eta}{\partial \mathcal{S}}\right)^2 \frac{\partial^2 \eta}{\partial \tau \partial \mathcal{S}} + \left[\frac{-2v^2\mathcal{S}}{l^4} + \frac{3}{2l^3}\frac{\partial v}{\partial t}(1-\mathcal{S}) + \frac{v^2}{l^4}\right]\left(\frac{\partial \eta}{\partial \mathcal{S}}\right)^2 \frac{\partial^2 \eta}{\partial \mathcal{S}^2} - \\ & \frac{2v^2}{l^4}\left(\frac{\partial \eta}{\partial \mathcal{S}}\right)^3 + \frac{1}{l^6}\left[\frac{\partial^4 \eta}{\partial \mathcal{S}^4}\left(\frac{\partial \eta}{\partial \mathcal{S}}\right)^2 + 4\frac{\partial \eta}{\partial \mathcal{S}}\frac{\partial^2 \eta}{\partial \mathcal{S}^2}\frac{\partial^3 \eta}{\partial \mathcal{S}^3} + \left(\frac{\partial^2 \eta}{\partial \mathcal{S}^2}\right)^3\right]\end{aligned} \tag{4.2.7}$$

and

$$
\begin{aligned}
\mathcal{N}_2 = {} & \frac{\partial \eta}{\partial S} \int_0^S \Bigg[ \left( \frac{-vS}{l^2} \frac{\partial^2 \eta}{\partial S^2} + \frac{1}{l} \frac{\partial^2 \eta}{\partial \tau \partial S} - \frac{v}{l^2} \frac{\partial \eta}{\partial S} \right)^2 + \frac{1}{l^2} \frac{\partial \eta}{\partial S} \\
& \left( \frac{2v^2 - l \dfrac{\partial v}{\partial t}}{l^2} \frac{\partial \eta}{\partial S} + \frac{4v^2 S - l \dfrac{\partial v}{\partial t} S}{l^2} \frac{\partial^2 \eta}{\partial S^2} - \frac{2v}{l} \frac{\partial^2 \eta}{\partial \tau \partial S} - \right. \\
& \left. \frac{2vS}{l} \frac{\partial^3 \eta}{\partial \tau \partial S^2} + \frac{v^2 S^2}{l^2} \frac{\partial^3 \eta}{\partial S^3} + \frac{\partial^3 \eta}{\partial \tau^2 \partial S} \right) \Bigg] dS - \\
& \frac{\partial^2 \eta}{\partial S^2} \Bigg\{ \int_S^1 \int_0^S \Bigg[ \left( \frac{-vS}{l^2} \frac{\partial^2 \eta}{\partial S^2} + \frac{1}{l} \frac{\partial^2 \eta}{\partial \tau \partial S} - \frac{v}{l^2} \frac{\partial \eta}{\partial S} \right)^2 + \frac{1}{l^2} \frac{\partial \eta}{\partial S} \\
& \left( \frac{2v^2 - l \dfrac{\partial v}{\partial t}}{l^2} \frac{\partial \eta}{\partial S} + \frac{4v^2 S - l \dfrac{\partial v}{\partial t} S}{l^2} \frac{\partial^2 \eta}{\partial S^2} - \right. \\
& \frac{2v}{l} \frac{\partial^2 \eta}{\partial \tau \partial S} - \frac{2vS}{l} \frac{\partial^3 \eta}{\partial \tau \partial S^2} + \frac{v^2 S^2}{l^2} \frac{\partial^3 \eta}{\partial S^3} + \\
& \left. \frac{\partial^3 \eta}{\partial \tau^2 \partial S} \right) \Bigg] dS\, dS + \\
& \int_S^1 \Bigg[ \frac{1}{2l^3} \frac{\partial v}{\partial \tau} \left( \frac{\partial \eta}{\partial S} \right)^2 + \frac{2v}{l^2} \frac{\partial \eta}{\partial S} \left( \frac{-vS}{l^2} \frac{\partial^2 \eta}{\partial S^2} + \frac{1}{l} \frac{\partial^2 \eta}{\partial \tau \partial S} - \right. \\
& \left. \frac{v}{l^2} \frac{\partial \eta}{\partial S} \right) + \frac{v^2}{l^4} \frac{\partial \eta}{\partial S} \frac{\partial^2 \eta}{\partial S^2} \Bigg] dS \Bigg\}
\end{aligned}
\tag{4.2.8}
$$

The nonlinear terms

$$\int_0^{S} \frac{\partial\eta}{\partial S} \frac{\partial^3\eta}{\partial\tau^2\partial S}\, dS \qquad \text{and} \qquad \int_S^1 \int_0^{S} \frac{\partial\eta}{\partial S} \frac{\partial^3\eta}{\partial\tau^2\partial S}\, dS\, dS$$

create some difficulties in the conventional solution procedures for dynamical systems. In most cases the equations of motion have linear second order time derivative inertia terms. One approach for dealing with these terms has been proposed by Li and Païdoussis, 1994. In this approach one approximates these troublesome terms by first noting that while the beam deflection can be large, from practical point of view, only the values of deflection much smaller than the length of the beam, i.e. $\eta \ll 1$, need be considered. To identify the relative magnitudes of various terms, we replace $\eta$ by $\sqrt{\varepsilon}\ \eta$, where $\varepsilon \ll 1$, in equation (4.2.5). This leads to:

$$\mathcal{L}(\eta) + \varepsilon\ \mathcal{N}_1(\eta) + \varepsilon\ \mathcal{N}_2(\eta) = 0 \tag{4.2.9}$$

It is now evident that the nonlinear terms are considerably smaller than the linear terms. Thus as a first approximation we may solve:

$$\mathcal{L}(\eta) = 0 \tag{4.2.10}$$

and from this expression we may isolate the term $\frac{\partial^2\eta}{\partial\tau^2}$ in equation (4.2.10) and obtain expressions for

$$\int_0^{S} \frac{\partial\eta}{\partial S} \frac{\partial^3\eta}{\partial\tau^2\partial S}\, dS \qquad \text{and} \qquad \int_S^1 \int_0^{S} \frac{\partial\eta}{\partial S} \frac{\partial^3\eta}{\partial\tau^2\partial S}\, dS\, dS$$

as follows:

$$\int_0^S \frac{\partial\eta}{\partial S}\frac{\partial^3\eta}{\partial\tau^2\partial S}\,dS = -\int_0^S \left\{\frac{2v}{l}(1-S)\frac{\partial\eta}{\partial S}\frac{\partial^3\eta}{\partial\tau\partial S^2} - \frac{2v}{l}\frac{\partial\eta}{\partial S}\frac{\partial^2\eta}{\partial\tau\partial S} - \right.$$
$$\left[\frac{1}{l}\frac{\partial v}{\partial\tau}(1+S) + \frac{4v^2}{l^2}(1-S)\right]\frac{\partial\eta}{\partial S}\frac{\partial^2\eta}{\partial S^2} +$$
$$\left[\frac{1}{l}\frac{\partial v}{\partial\tau} + \frac{v^2}{l^2}(1-S)\right](1-S)\frac{\partial\eta}{\partial S}\frac{\partial^3\eta}{\partial S^3} - \tag{4.2.11}$$
$$\left.\frac{1}{l^2}\left(l\frac{\partial v}{\partial\tau} - 2v^2\right)\left(\frac{\partial\eta}{\partial S}\right)^2 + \frac{1}{l^4}\frac{\partial\eta}{\partial S}\frac{\partial^5\eta}{\partial S^5}\right\} dS$$

The other nonlinear term may be obtained by integrating equation (4.2.11) from $S$ to 1.

Substituting the transformed nonlinear inertial term into equation (4.2.9) and returning to the original variable $\eta$, after very laborious manipulations, we obtain the nonlinear partial integro-differential equation of motion of the inextensible flexible sliding beam as:

$$\frac{\partial^2\eta}{\partial\tau^2} + \frac{2v}{l}(1-S)\frac{\partial^2\eta}{\partial\tau\partial S} + \left[\frac{v^2}{l^2}(1-S)^2 + \frac{1}{l}\frac{\partial v}{\partial t}(1-S)\right]\frac{\partial^2\eta}{\partial S^2} +$$
$$\left[\frac{2v^2}{l^2}S - \frac{2v^2}{l^2} - \frac{1}{l}\frac{\partial v}{\partial t}S\right]\frac{\partial\eta}{\partial S} + \frac{1}{l^4}\frac{\partial^4\eta}{\partial S^4} + \mathcal{N}(\eta) = 0 \tag{4.2.12}$$

where:

$$\mathcal{N}(\eta) = \mathcal{N}^1(\eta) + \mathcal{N}^2(\eta) \tag{4.2.13}$$

and

$$
\begin{aligned}
\mathcal{N}^1(\eta) = {} & \frac{2v}{l^3}\left(\frac{\partial\eta}{\partial S}\right)^2 \frac{\partial^2\eta}{\partial\tau\partial S} + \left[\frac{v^2}{l^4}(1-2S) + \frac{3}{2l^3}\frac{\partial v}{\partial t}(1-S)\right]\left(\frac{\partial\eta}{\partial S}\right)^2 \frac{\partial^2\eta}{\partial S^2} - \\
& \frac{2v^2}{l^4}\left(\frac{\partial\eta}{\partial S}\right)^3 + \frac{1}{l^6}\left[3\,\frac{\partial\eta}{\partial S}\,\frac{\partial^2\eta}{\partial S^2}\,\frac{\partial^3\eta}{\partial S^3} + \left(\frac{\partial^2\eta}{\partial S^2}\right)^3\right] + \\
& \frac{\partial\eta}{\partial S}\int_0^S \Bigg\{\left(\frac{-vS}{l^2}\frac{\partial^2\eta}{\partial S^2} + \frac{1}{l}\frac{\partial^2\eta}{\partial\tau\partial S} - \frac{v}{l^2}\frac{\partial\eta}{\partial S}\right)^2 + \frac{1}{l^2}\frac{\partial\eta}{\partial S} \\
& \qquad \Bigg(\frac{2v^2 - l\,\frac{\partial v}{\partial t}}{l^2}\,\frac{\partial\eta}{\partial S} + \frac{4v^2 S - l\,\frac{\partial v}{\partial t}S}{l^2}\,\frac{\partial^2\eta}{\partial S^2} - \frac{2v}{l}\frac{\partial^2\eta}{\partial\tau\partial S} - \\
& \qquad \frac{2vS}{l}\frac{\partial^3\eta}{\partial\tau\partial S^2} + \frac{v^2 S^2}{l^2}\frac{\partial^3\eta}{\partial S^3}\Bigg) - \qquad\qquad (4.2.14) \\
& \frac{1}{l^2}\Bigg[\frac{2v}{l}(1-S)\frac{\partial\eta}{\partial S}\frac{\partial^3\eta}{\partial\tau\partial S^2} - \frac{2v}{l}\frac{\partial\eta}{\partial S}\frac{\partial^2\eta}{\partial\tau\partial S} - \\
& \qquad \left(\frac{1}{l}\frac{\partial v}{\partial\tau}(1+S) + \frac{4v^2}{l^2}(1-S)\right)\frac{\partial\eta}{\partial S}\frac{\partial^2\eta}{\partial S^2} + \\
& \qquad \left[\frac{1}{l}\frac{\partial v}{\partial\tau} + \frac{v^2}{l^2}(1-S)\right](1-S)\,\frac{\partial\eta}{\partial S}\frac{\partial^3\eta}{\partial S^3} - \\
& \qquad \frac{1}{l^2}\left(l\,\frac{\partial v}{\partial\tau} - 2v^2\right)\left(\frac{\partial\eta}{\partial S}\right)^2 - \frac{1}{l^4}\,\frac{\partial^2\eta}{\partial S^2}\,\frac{\partial^4\eta}{\partial S^4}\Bigg]\Bigg\}\,dS
\end{aligned}
$$

$$
\begin{aligned}
\mathcal{N}^2(\eta) = -\frac{\partial^2\eta}{\partial S^2} \Bigg\{ \int_S^1 \int_0^S \Bigg[ & \left( \frac{-vS}{l^2}\frac{\partial^2\eta}{\partial S^2} + \frac{1}{l}\frac{\partial^2\eta}{\partial\tau\partial S} - \frac{v}{l^2}\frac{\partial\eta}{\partial S} \right)^2 + \frac{1}{l^2}\frac{\partial\eta}{\partial S} \\
& \Bigg( \frac{2v^2 - l\frac{\partial v}{\partial t}}{l^2}\frac{\partial\eta}{\partial S} + \frac{4v^2S - l\frac{\partial v}{\partial t}S}{l^2}\frac{\partial^2\eta}{\partial S^2} - \\
& \frac{2v}{l}\frac{\partial^2\eta}{\partial\tau\partial S} - \frac{2vS}{l}\frac{\partial^3\eta}{\partial\tau\partial S^2} + \frac{v^2S^2}{l^2}\frac{\partial^3\eta}{\partial S^3} \Bigg) - \\
& \frac{1}{l^2}\Bigg( \frac{2v}{l}(1-S)\frac{\partial\eta}{\partial S}\frac{\partial^3\eta}{\partial\tau\partial S^2} - \frac{2v}{l}\frac{\partial\eta}{\partial S}\frac{\partial^2\eta}{\partial\tau\partial S} - \\
& \left( \frac{1}{l}\frac{\partial v}{\partial\tau}(1+S) + \frac{4v^2}{l^2}(1-S) \right)\frac{\partial\eta}{\partial S}\frac{\partial^2\eta}{\partial S^2} + \\
& \left( \frac{1}{l}\frac{\partial v}{\partial\tau} + \frac{v^2}{l^2}(1-S) \right)(1-S)\frac{\partial\eta}{\partial S}\frac{\partial^3\eta}{\partial S^3} - \\
& \frac{1}{l^2}\left( l\frac{\partial v}{\partial\tau} - 2v^2 \right)\left(\frac{\partial\eta}{\partial S}\right)^2 - \frac{1}{l^4}\frac{\partial^2\eta}{\partial S^2}\frac{\partial^4\eta}{\partial S^4} \Bigg) \Bigg] dS\, dS + \\
& \int_S^1 \Bigg[ \frac{1}{2l^3}\frac{\partial v}{\partial\tau}\left(\frac{\partial\eta}{\partial S}\right)^2 + \frac{2v}{l^2}\frac{\partial\eta}{\partial S}\Bigg( \frac{-vS}{l^2}\frac{\partial^2\eta}{\partial S^2} + \frac{1}{l}\frac{\partial^2\eta}{\partial\tau\partial S} - \\
& \frac{v}{l^2}\frac{\partial\eta}{\partial S} \Bigg) + \frac{v^2}{l^4}\frac{\partial\eta}{\partial S}\frac{\partial^2\eta}{\partial S^2} + \frac{1}{l^6}\frac{\partial^2\eta}{\partial S^2}\frac{\partial^3\eta}{\partial S^3} \Bigg] dS \Bigg\}
\end{aligned}
\tag{4.2.15}
$$

To obtain the transient response of the inextensible flexible sliding beams, we need to solve the above integro-differential equation in the fixed domain and transform the response back to the time variable domain.

## 4.2.2 Transformation of the PDE to a set of ODEs: Galerkin's Method

With reference to the discussion in section 4.1.3, one may use the Galerkin's method to solve the governing PDE. Substituting for $\eta$ from equation (4.1.26) in terms of modal functions $\wp_j(\mathcal{S})$ and the corresponding generalized coordinates $q_j(\tau)$ into the governing equation of motion (4.2.12), multiplying by $\wp_i(\mathcal{S})$ and integrating from 0 to 1, we obtain the desired ODEs as:

$$\ddot{q}_i + a_{ij}\,\dot{q}_j + b_{ij}\,q_j + c_{ijkl}\,q_j\,q_k\,q_l + d_{ijkl}\,q_j\,q_k\,\dot{q}_l + e_{ijkl}\,q_j\,\dot{q}_k\,\dot{q}_l = 0 \qquad (4.2.16)$$

where:

$$a_{ij} = \int_0^1 \frac{2v}{l}\,(1-\mathcal{S})\,\wp_i\,\frac{\partial \wp_j}{\partial \mathcal{S}}\,d\mathcal{S} \qquad (4.2.17)$$

and

$$\begin{aligned} b_{ij} = \int_0^1 \wp_i \Bigg\{ & \left[\frac{v^2}{l^2}(1-\mathcal{S})^2 + \frac{1}{l}\,\frac{\partial v}{\partial \tau}(1-\mathcal{S})\right]\frac{\partial^2 \wp_j}{\partial \mathcal{S}^2} - \\ & \frac{1}{l^2}\left[l\,\frac{\partial v}{\partial \tau}\,\mathcal{S} + 2(1-\mathcal{S})\,v^2\right]\frac{\partial \wp_j}{\partial \mathcal{S}} + \frac{1}{l^4}\,\frac{\partial^4 \wp_j}{\partial \mathcal{S}^4}\Bigg\}\,d\mathcal{S} \end{aligned} \qquad (4.2.18)$$

and

$$
\begin{aligned}
c_{ijkl} = \int_0^1 \wp_i \Bigg\{ & \Big[ \frac{v^2}{l^4}(1-2\mathcal{S}) + \frac{3}{2l^3}\frac{\partial v}{\partial \tau}(1-\mathcal{S}) \Big] \frac{\partial \wp_j}{\partial \mathcal{S}} \frac{\partial \wp_k}{\partial \mathcal{S}} \frac{\partial^2 \wp_l}{\partial \mathcal{S}^2} - \\
& \frac{2v^2}{l^4} \frac{\partial \wp_j}{\partial \mathcal{S}} \frac{\partial \wp_k}{\partial \mathcal{S}} \frac{\partial \wp_l}{\partial \mathcal{S}} + \frac{1}{l^6}\Big( 3\, \frac{\partial \wp_j}{\partial \mathcal{S}} \frac{\partial^2 \wp_k}{\partial \mathcal{S}^2} \frac{\partial^3 \wp_l}{\partial \mathcal{S}^3} + \\
& \frac{\partial^2 \wp_j}{\partial \mathcal{S}^2} \frac{\partial^2 \wp_k}{\partial \mathcal{S}^2} \frac{\partial^2 \wp_l}{\partial \mathcal{S}^2} \Big) + \frac{\partial \wp_j}{\partial \mathcal{S}} \int_0^{\mathcal{S}} \Big[ \Big( \frac{v^2 \mathcal{S}^2}{l^4} \frac{\partial^2 \wp_k}{\partial \mathcal{S}^2} \frac{\partial^2 \wp_l}{\partial \mathcal{S}^2} + \\
& \frac{v^2}{l^4} \frac{\partial \wp_k}{\partial \mathcal{S}} \frac{\partial \wp_l}{\partial \mathcal{S}} + \frac{2v^2 \mathcal{S}}{l^4} \frac{\partial^2 \wp_k}{\partial \mathcal{S}^2} \frac{\partial \wp_l}{\partial \mathcal{S}} \Big) + \frac{1}{l^2} \frac{\partial \wp_k}{\partial \mathcal{S}} \Big( \frac{1}{l^2} \Big( l\, \frac{\partial v}{\partial \tau} + 4v^2 \Big) \\
& \frac{\partial^2 \wp_l}{\partial \mathcal{S}^2} + \Big( \frac{v^2 \mathcal{S}^2}{l^2} - \frac{1}{l} \frac{\partial v}{\partial \tau}(1-\mathcal{S}) - \frac{v^2 (1-\mathcal{S})^2}{l^2} \Big) \frac{\partial^3 \wp_l}{\partial \mathcal{S}^3} \Big) + \\
& \frac{1}{l^6} \frac{\partial^2 \wp_k}{\partial \mathcal{S}^2} \frac{\partial^4 \wp_l}{\partial \mathcal{S}^4} \Big] d\mathcal{S} - \frac{\partial^2 \wp_j}{\partial \mathcal{S}^2} \Big[ \int_{\mathcal{S}}^1 \int_0^{\mathcal{S}} \Big( \Big( \frac{v^2 \mathcal{S}^2}{l^4} \frac{\partial^2 \wp_k}{\partial \mathcal{S}^2} \frac{\partial^2 \wp_l}{\partial \mathcal{S}^2} + \\
& \frac{v^2}{l^4} \frac{\partial \wp_k}{\partial \mathcal{S}} \frac{\partial \wp_l}{\partial \mathcal{S}} + \frac{2v^2 \mathcal{S}}{l^4} \frac{\partial^2 \wp_k}{\partial \mathcal{S}^2} \frac{\partial \wp_l}{\partial \mathcal{S}} \Big) + \frac{1}{l^2} \frac{\partial \wp_k}{\partial \mathcal{S}} \Big( \frac{1}{l^2} \Big( l\, \frac{\partial v}{\partial \tau} + 4v^2 \Big) \\
& \frac{\partial^2 \wp_l}{\partial \mathcal{S}^2} + \Big( \frac{v^2 \mathcal{S}^2}{l^2} - \frac{1}{l} \frac{\partial v}{\partial \tau}(1-\mathcal{S}) - \frac{v^2 (1-\mathcal{S})^2}{l^2} \Big) \frac{\partial^3 \wp_l}{\partial \mathcal{S}^3} \Big) + \\
& \frac{1}{l^6} \frac{\partial^2 \wp_k}{\partial \mathcal{S}^2} \frac{\partial^4 \wp_l}{\partial \mathcal{S}^4} \Big) d\mathcal{S}\, d\mathcal{S} + \int_{\mathcal{S}}^1 \Big( \Big( \frac{1}{2l^3} \frac{\partial v}{\partial \tau} - \frac{2v^2}{l^4} \Big) \frac{\partial \wp_k}{\partial \mathcal{S}} \frac{\partial \wp_l}{\partial \mathcal{S}} +
\end{aligned}
\tag{4.2.19}
$$

$$\left.\left.\left.\frac{v^2(1-2S)}{l^4}\frac{\partial \wp_k}{\partial S}\frac{\partial^2 \wp_l}{\partial S^2}+\frac{1}{l^6}\frac{\partial^2 \wp_k}{\partial S^2}\frac{\partial^3 \wp_l}{\partial S^3}\right)dS\right]\right\}dS$$

and

$$d_{ijkl} = \int_0^1 \wp_i \left\{ \frac{2v}{l^3}\frac{\partial \wp_j}{\partial S}\frac{\partial \wp_k}{\partial S}\frac{\partial \wp_l}{\partial S} + \frac{\partial \wp_j}{\partial S}\int_0^S \left[ \frac{-2v\,S}{l^3}\frac{\partial^2 \wp_k}{\partial S^2}\frac{\partial \wp_l}{\partial S} - \right.\right.$$

$$\left. \frac{2v}{l^3}\frac{\partial \wp_k}{\partial S}\frac{\partial \wp_l}{\partial S} - \frac{2v}{l^3}\frac{\partial \wp_k}{\partial S}\frac{\partial^2 \wp_l}{\partial S^2} \right] dS -$$

$$\frac{\partial^2 \wp_j}{\partial S^2}\left[ \int_S^1 \int_0^S \left( \frac{-2v\,S}{l^3}\frac{\partial^2 \wp_k}{\partial S^2}\frac{\partial \wp_l}{\partial S} - \frac{2v}{l^3}\frac{\partial \wp_k}{\partial S}\frac{\partial \wp_l}{\partial S} - \right.\right. \tag{4.2.20}$$

$$\left.\left.\left. \frac{2v}{l^3}\frac{\partial \wp_k}{\partial S}\frac{\partial^2 \wp_l}{\partial S^2} \right) dS\,dS + \int_S^1 \frac{2v}{l^3}\frac{\partial \wp_k}{\partial S}\frac{\partial \wp_l}{\partial S}\,dS \right] \right\} dS$$

and

$$e_{ijkl} = \int_0^1 \wp_i \left( \frac{\partial \wp_j}{\partial S}\int_0^S \frac{1}{l^2}\frac{\partial \wp_k}{\partial S}\frac{\partial \wp_l}{\partial S}\,dS - \frac{\partial^2 \wp_j}{\partial S^2}\int_S^1\int_0^S \frac{1}{l^2}\frac{\partial \wp_k}{\partial S}\frac{\partial \wp_l}{\partial S}\,dS\,dS \right) dS$$

(4.2.21)

Although the coefficients $a_{ij}$, $b_{ij}$, $c_{ijkl}$, $d_{ijkl}$ and $e_{ijkl}$ are time dependent, we may take advantage of the fixed domain by using the space dependent eigenfunctions of the beam. This decreases the computation of these coefficients significantly.

### 4.2.3 Time Integration and Results

Following the discussion in section 4.1.4, we need to define a series of comparison functions satisfying all the boundary conditions.

To study the response of the nonlinear system, we examine two types of constraints the cantilever condition i.e. a sliding beam with fixed-free boundary conditions and a sliding beam with clamped-clamped boundary condition where the sliding beam emerges from a fixed channel and at the other end is attached to a moving channel with the same prescribed motion.

#### 4.2.3.1 Cantilever Condition

In this case we use the same ortho-normal eigenfunctions as given in equation (4.1.30). Substituting these eigenfunctions into relations (4.2.17), (4.2.18), (4.2.19), (4.2.20) and () and using the MAPLE symbolic program, we compute the desired system matrices in terms of the prescribed motion of the beam.

With the discrete equations derived, we integrate the set of ODEs and obtain the transient response.

Following examples illustrate the difference in the response of the linear and the nonlinear systems. No physical damping is included in the system equations.

- **Spaghetti and Reverse Spaghetti Problems: Quadratic Sliding Motion**

A quadratic sliding motion as given in equation (4.1.32) is used for the prescribed sliding motion of the beam. In the test case #1, we consider a constant velocity retraction with the initial length $L_o = 1.5 \quad (m)$ and velocity $V_o = -0.1145 \quad (m/s)$ .

Figure 4.2.1 shows the difference between the linear and the nonlinear time histories of the non-dimensional tip deflection $\eta$ of the sliding beam. The differences in frequencies and amplitudes of oscillations become noticeable when the sliding velocity of the beam is increased (see Figure 4.2.2).

In test case #2, we examine a constant velocity extrusion with the same initial length and at three different sliding speeds: $V_o = 0.041 \quad (m/s)$ , $V_o = 0.123 \quad (m/s)$ and $V_o = 0.205 \quad (m/s)$ . The effect of including the nonlinear terms as well as increasing the extrusion velocity can be seen in the linear and the nonlinear solutions of the system (see Figures 4.2.3, 4.2.4 and 4.2.5).

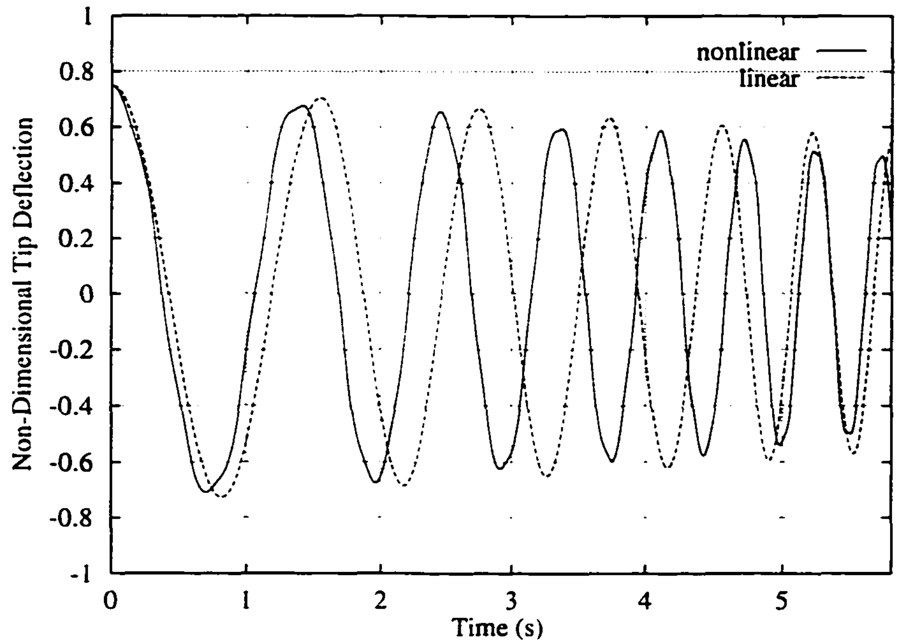


Figure 4.2.1: Test Case #1: Constant Velocity Retraction $V_o = -0.1145 \quad (m/s)$ .

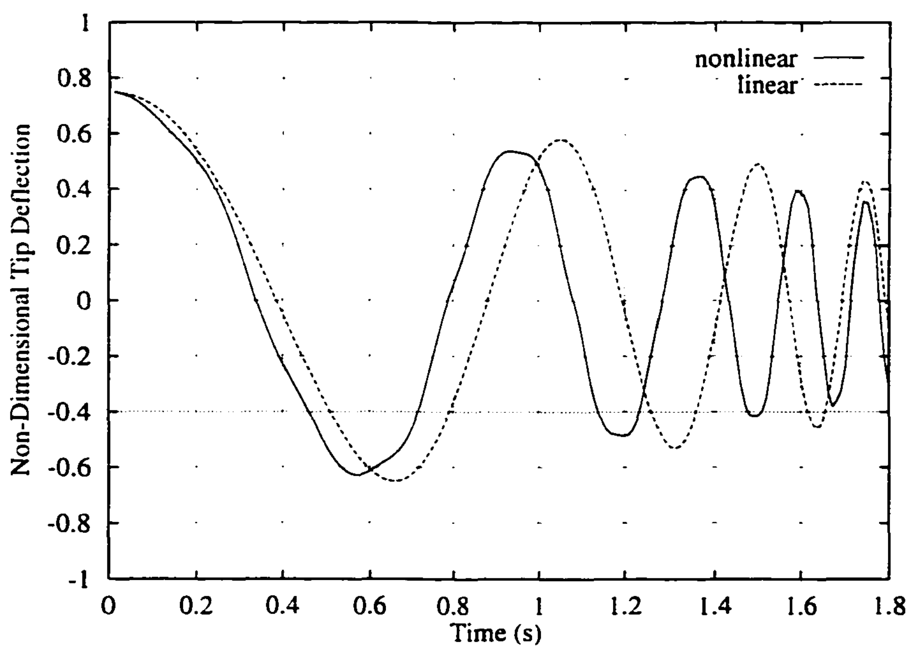


Figure 4.2.2: Test Case #1: Constant Velocity Retraction $V_o = -0.5725 \quad (m/s)$ .

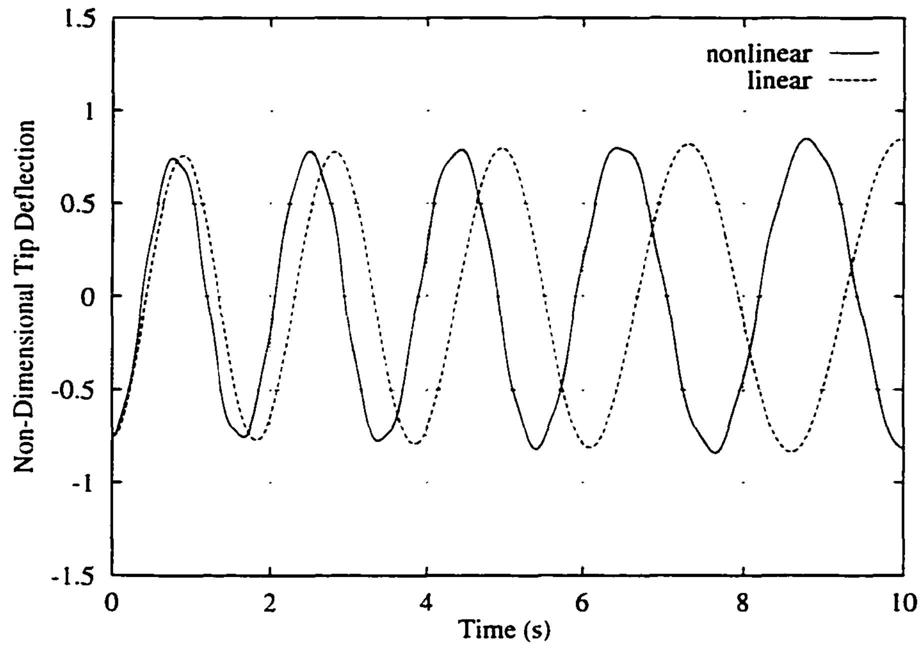


Figure 4.2.3: Test Case #2: Constant Velocity Extrusion $V_o = 0.041 \quad (m/s)$ .

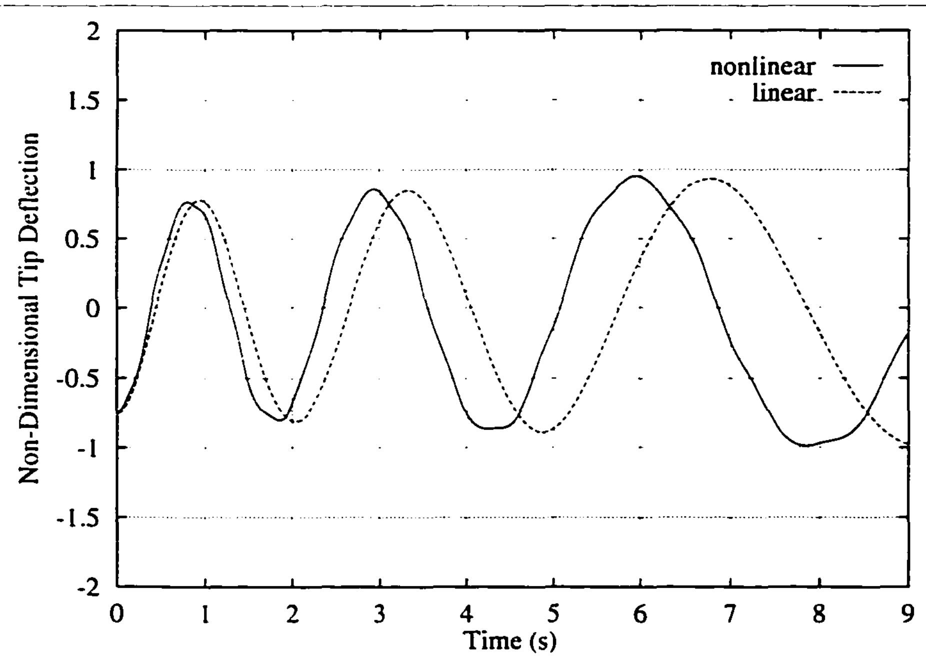


Figure 4.2.4: Test Case #2: Constant Velocity Extrusion $V_o = 0.123 \quad (m/s)$ .

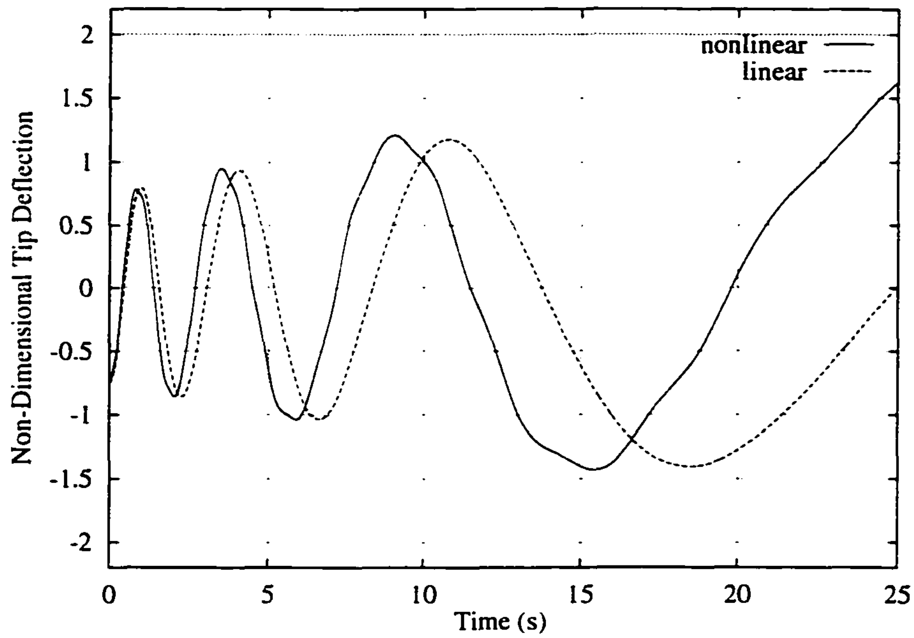


Figure 4.2.5: Test Case #2: Constant Velocity Extrusion $V_o = 0.205\ (m/s)$ .

It is interesting to add a constant acceleration term to the previous reverse spaghetti problem. In this case we consider two different prescribed velocity and acceleration terms for the sliding motion of the beam as follows: $V_o = 0.004\ (m/s)$ , $a_o = 0.0075\ (m/s^2)$ and $V_o = 0.008\ (m/s)$ , $a_o = 0.015\ (m/s^2)$ . The difference between the linear and the nonlinear solutions, both in amplitude and frequency of oscillations, will be noticed in Figures 4.2.6 and 4.2.7.

- **Spaghetti and Reverse Spaghetti Problems: Repositional Motion**

The variable length of the beam is given in equation (4.1.33). In test case #5, we consider a low frequency extrusion $L_o = 1.5\,(m)$ , $c_o = 0.7\,(m)$ and $t_o = 20.8\,(s)$ . Figure 4.2.8 shows the response of the system using the linear and the nonlinear equations. The effect of increasing the prescribed velocity of the sliding and the axial oscillation of the beam can be seen in Figures 4.2.9 and 4.2.10.

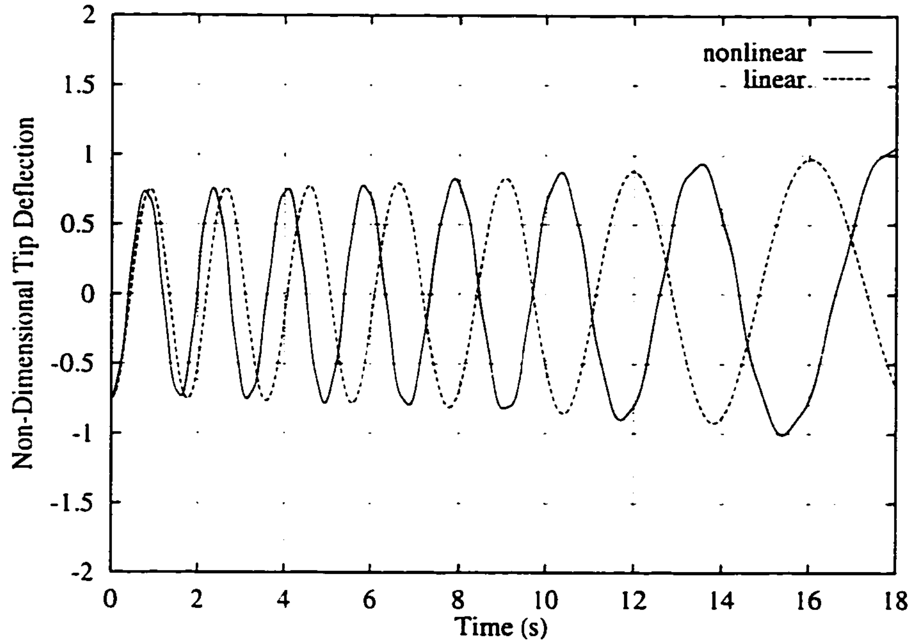


Figure 4.2.6: Test Case #4: Constant Acceleration Extrusion $V_o = 0.004 \quad (m/s)$, $a_o = 0.0075 \quad (m/s^2)$.

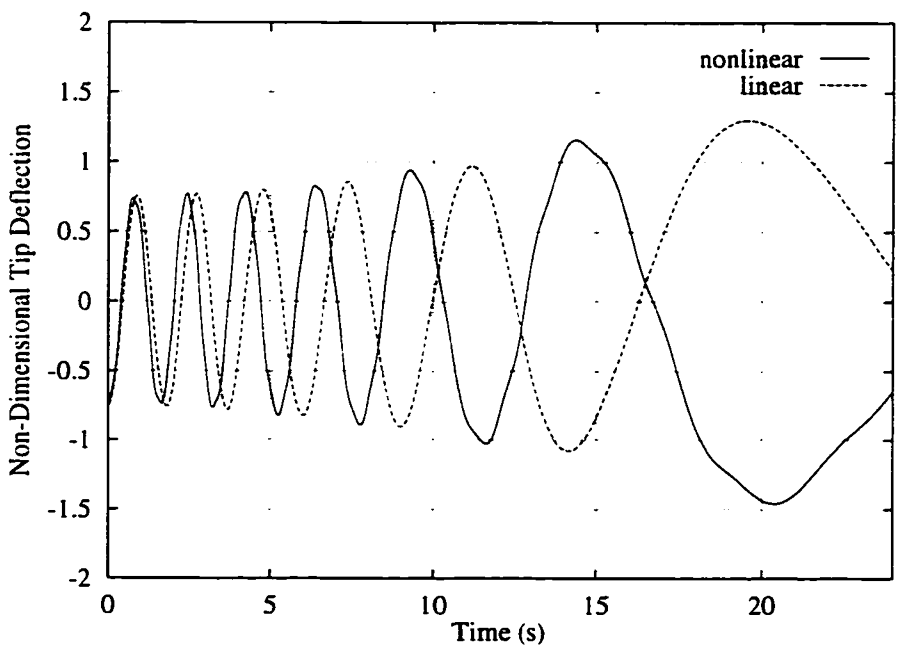


Figure 4.2.7: Test Case #4: Constant Acceleration Extrusion $V_o = 0.008 \quad (m/s)$, $a_o = 0.015 \quad (m/s^2)$.

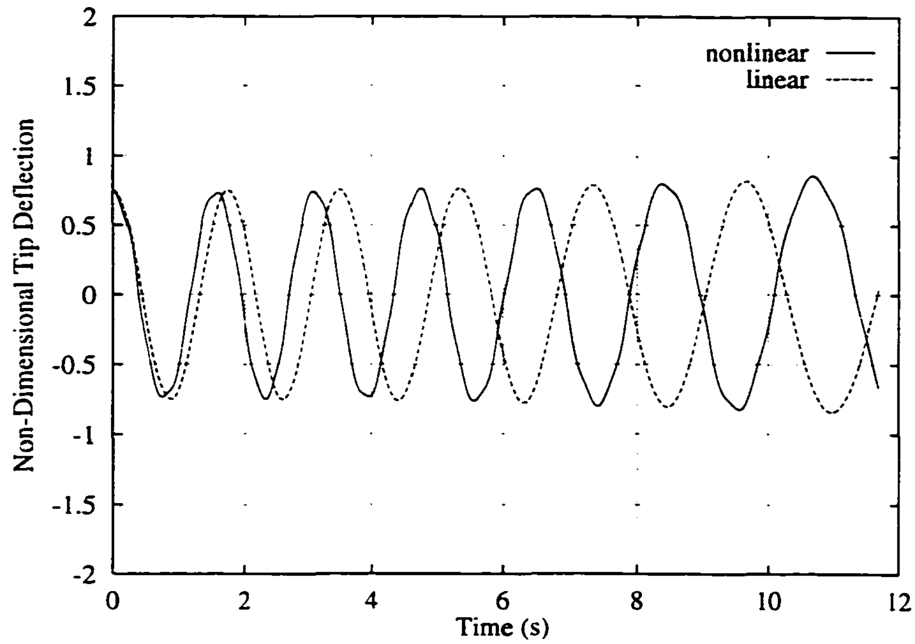


Figure 4.2.8: Test Case #5: Low Frequency Extrusion $c_o = 0.7\ (m)$ .

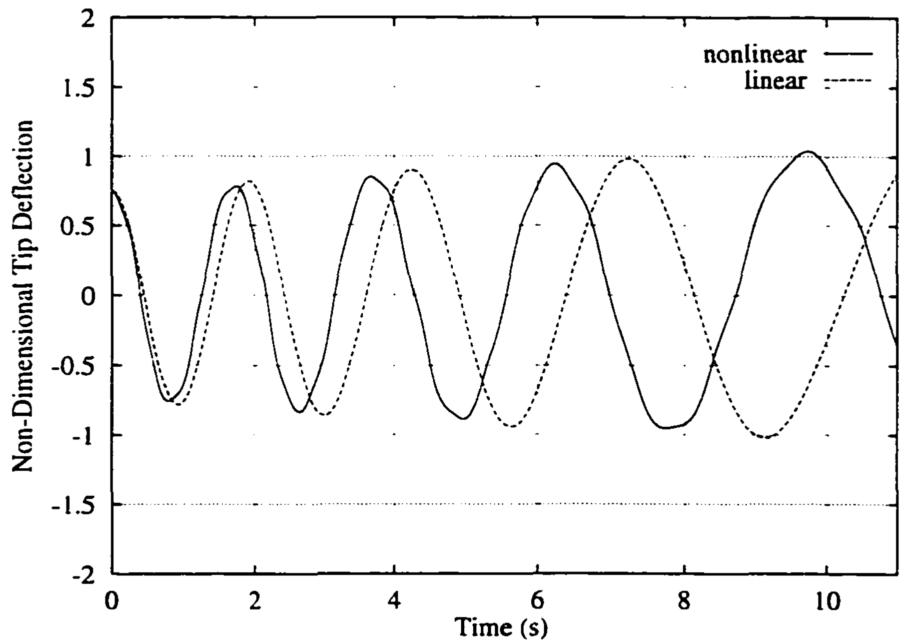


Figure 4.2.9: Test Case #5: Low Frequency Extrusion $c_o = 2.1\ (m)$ .

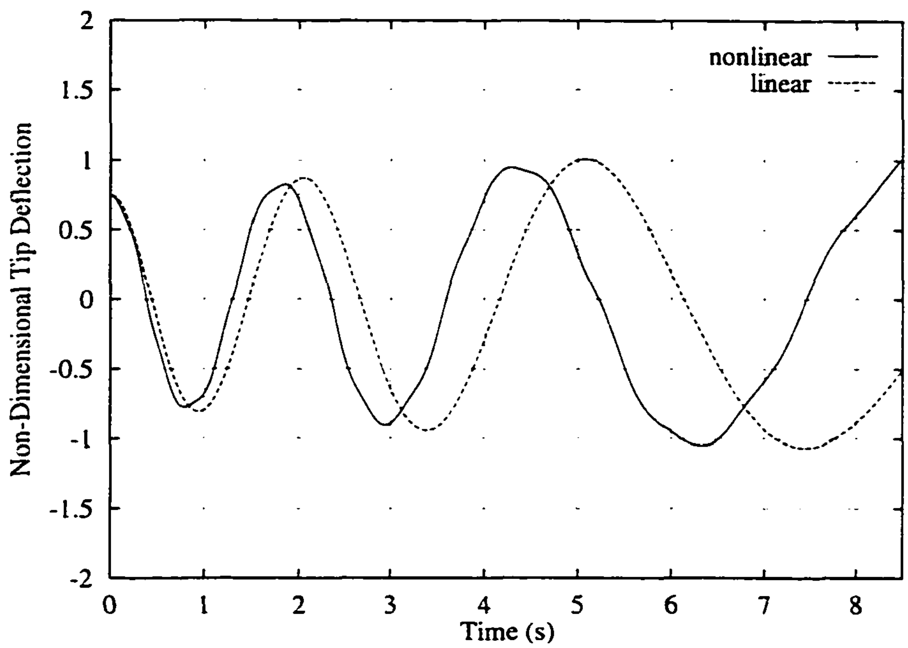


Figure 4.2.10: Test Case #5: Low Frequency Extrusion $c_o = 3.5\,(m)$ .

In test case #6, we examine the high frequency oscillation reverse spaghetti problem. Increasing the frequency, drastically changes the response of the system. In this case we consider $t_o = 0.875\,(s)$ in two different prescribed velocities where $c_o = 0.7\,(m)$ and $c_o = 1.05\,(m)$ . In this case we may notice the considerable difference between the linear response and nonlinear response of the system where increasing the velocity leads to unstable solution for the linear case while the nonlinear solution is bounded (see Figures 4.2.11 and 4.2.12).

In test case #7, we consider the high frequency spaghetti problem with initial length $L_o = 3\,(m)$ and $c_o = -0.7\,(m)$ . Figure 4.2.13 shows the transient response of the system in two different, linear and nonlinear, cases. Increasing the retraction velocity has also significant effect on the system (see Figure 4.2.14).

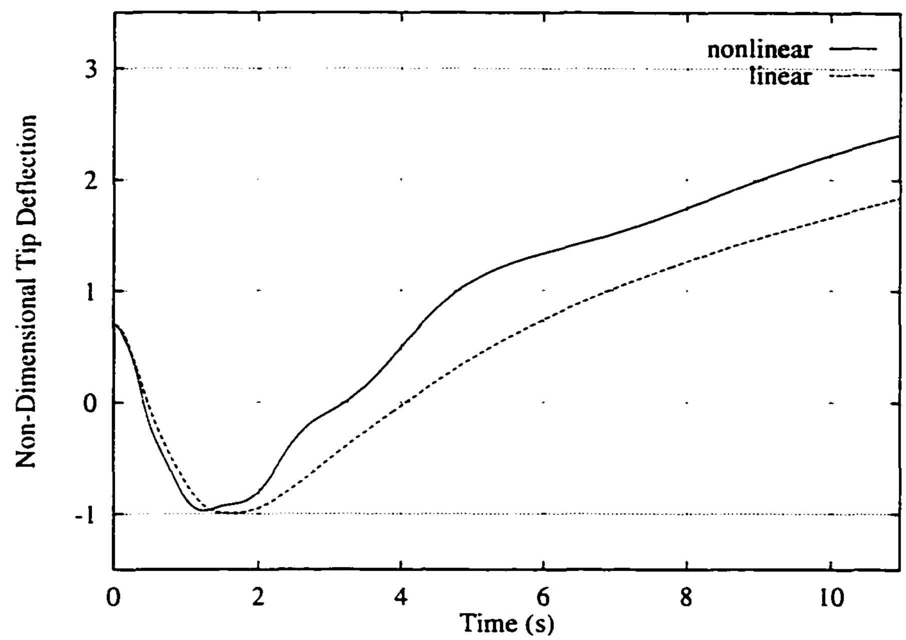


Figure 4.2.11: Test Case #6: High Frequency Extrusion $c_o = 0.7\,(m)$ .

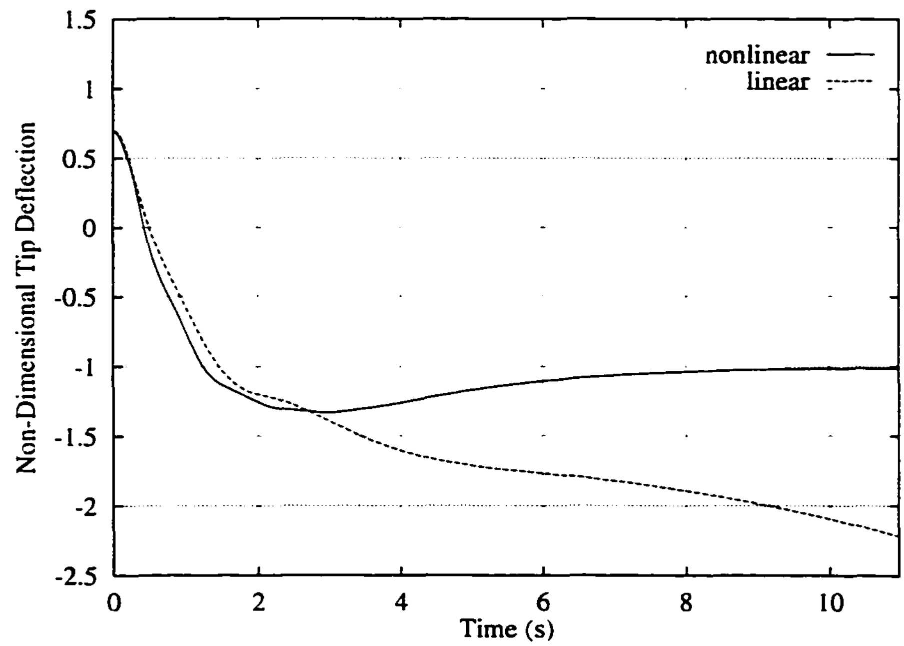


Figure 4.2.12: Test Case #6: High Frequency Extrusion $c_o = 1.05\,(m)$ .

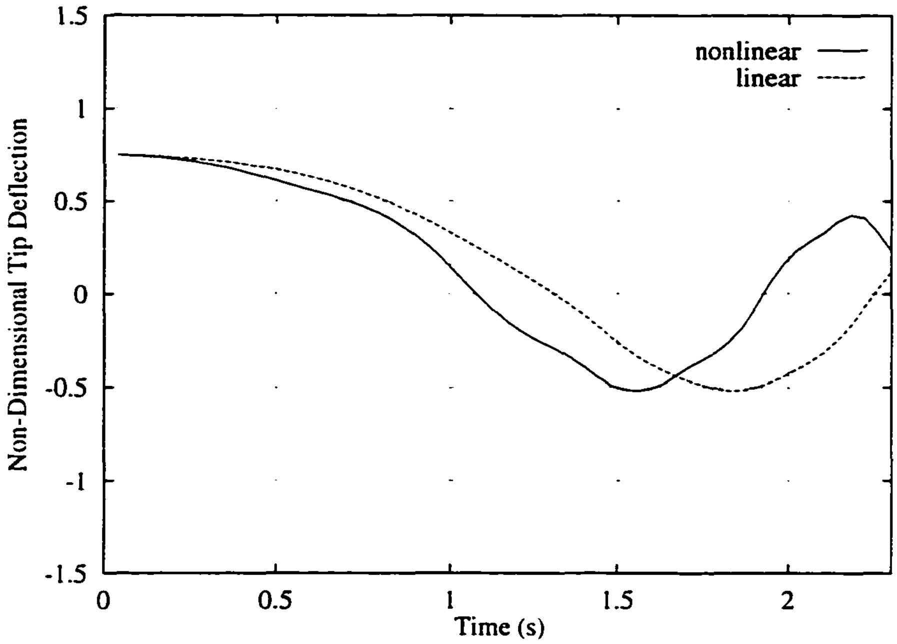


Figure 4.2.13: Test Case #7: High Frequency Retraction $c_o = -0.7\ (m)$ .

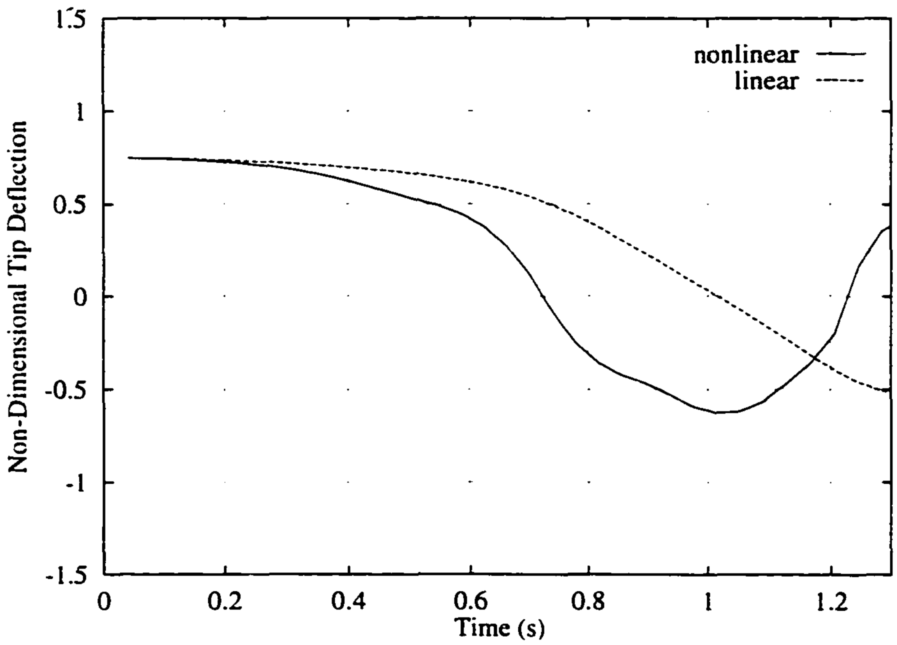


Figure 4.2.14: Test Case #7: High Frequency Retraction $c_o = -2.1\ (m)$ .

- **Reverse Spaghetti Problem: High Frequency Perturbations**

In this case we modify the constant velocity extrusion by introducing an axial perturbation as given in equation (4.1.34).

Here we consider the following parameters to study the effects of nonlinear terms in the response of the system: $L_o = 1.5 \quad (m)$ , $\varepsilon = 0.0133$ and $\hat{\omega} = 11\omega_1$ where $\omega_1$ is the instantaneous fundamental natural frequency of the sliding beam. In this test we include the physical damping as defined in section 4.1.4. Figures 4.2.15 and 4.2.16 show the transient response of the system and the difference between the linear and the nonlinear solutions for the two extruding velocities $V_o = 0.1145 \quad (m/s)$ and $V_o = 0.3435 \quad (m/s)$ .

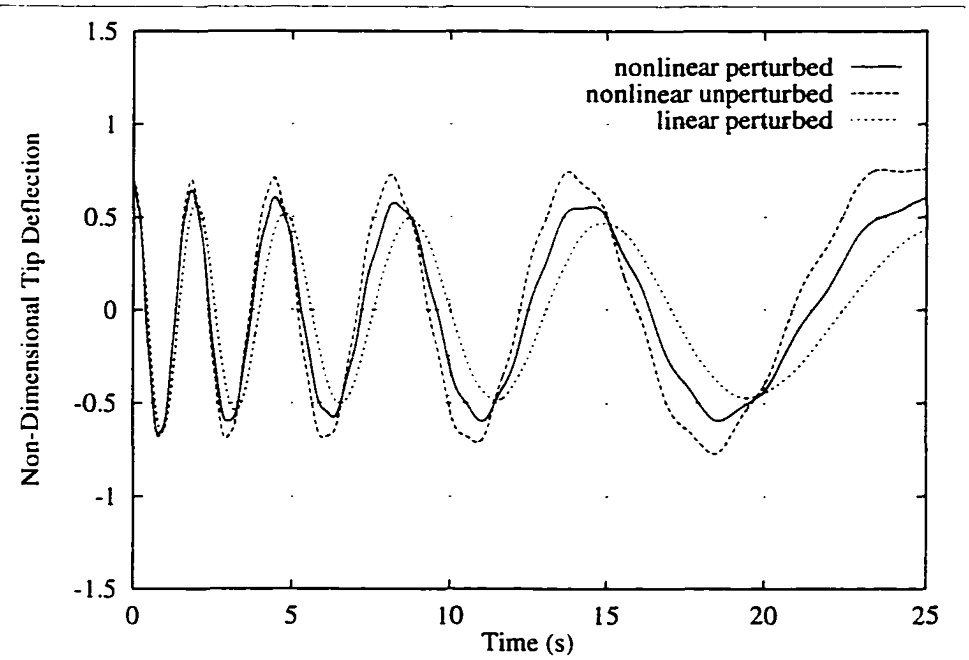


Figure 4.2.15: Test Case #8: High Frequency Perturbation Extrusion $V_o = 0.1145 \quad (m/s)$ .

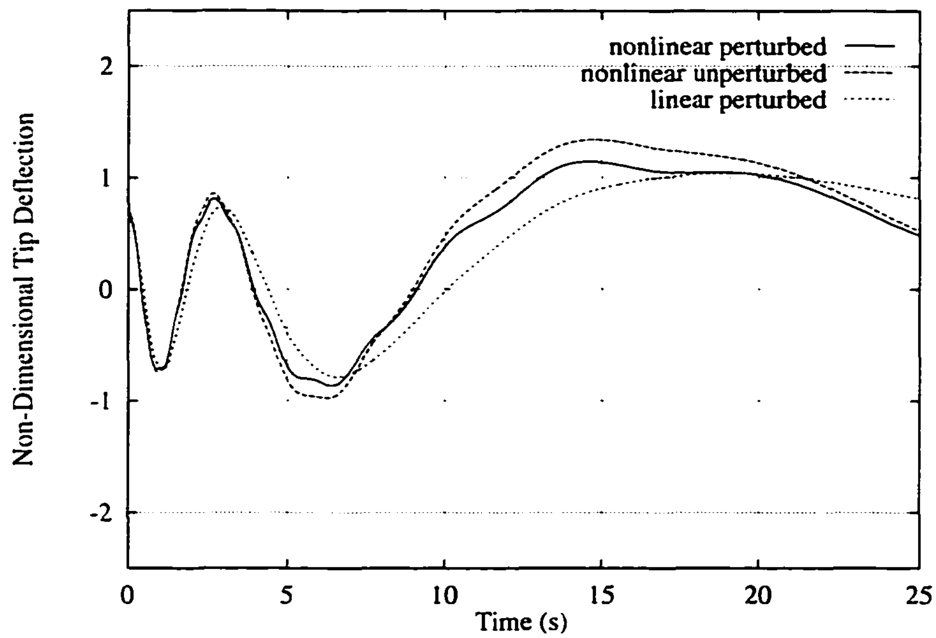


Figure 4.2.16: Test Case #8: High Frequency Perturbation Extrusion $V_o = 0.3435 \ (m/s)$ .

#### 4.2.3.2 Clamped-Clamped Condition

For the clamped-clamped condition, we use the ortho-normal eigenfunctions of the stationary clamped-clamped beam given by:

$$\wp_i = \cosh\beta_i\eta - \cos\beta_i\eta - \frac{\cos\beta_i - \cosh\beta_i}{\sin\beta_i - \sinh\beta_i}(\sinh\beta_i\eta - \sin\beta_i\eta) \qquad (4.2.22)$$

where the eigenvalues $\beta_i$ are the roots of the characteristic equation:

$$\cos\beta_i \ \cosh\beta_i - 1 = 0 \qquad (4.1.23)$$

Using these modal functions we calculate the system matrices as functions of the time varying length and the sliding velocity of the beam.

Figure 4.2.17 shows the non-dimensional mid-span deflection of the beam with initial length $L_o = 1.5 \ (m)$ extruding with constant velocity $V_o = 0.5725 \ (m/s)$ .

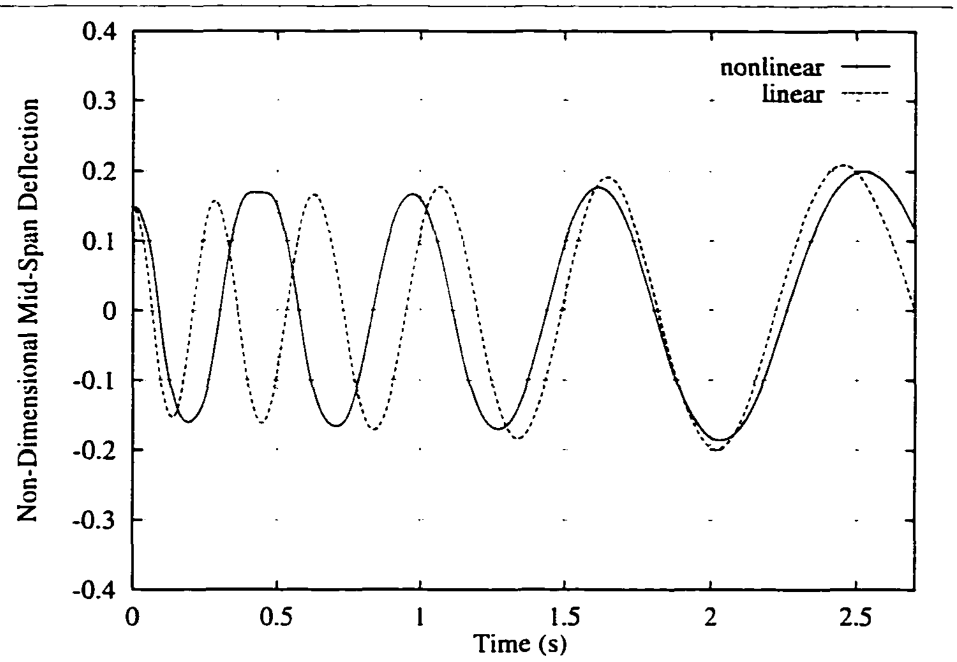


Figure 4.2.17: Test Case #9: Constant Velocity Extrusion $V_o = 0.5725 \quad (m/s)$ .

In another case, we consider the variable length of the beam as defined in equation (4.1.33). For the reverse spaghetti problem, the parameters are chosen as: $L_o = 1.5 \quad (m)$ , $c_o = 0.7 \quad (m)$ and $t_o = 0.875 \quad (s)$ . The response of the system is given in Figure 4.2.18. Increasing the velocity leads to an unstable solution for the linear system (see Figure 4.2.19).

In test case #11, we examine the high frequency retraction case with the initial length of the beam $L_o = 3.0 \quad (m)$ (see Figure 4.2.20). In this test we include the physical damping as defined in section 4.1.4.

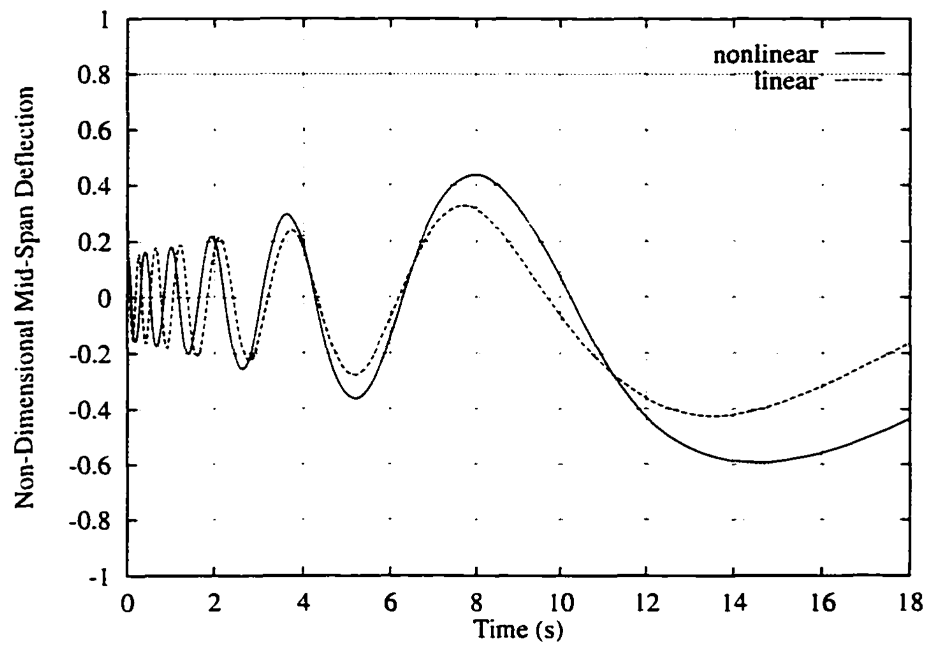


Figure 4.2.18: Test Case #10: High Frequency Extrusion $c_o = 0.7 \quad (m)$ .

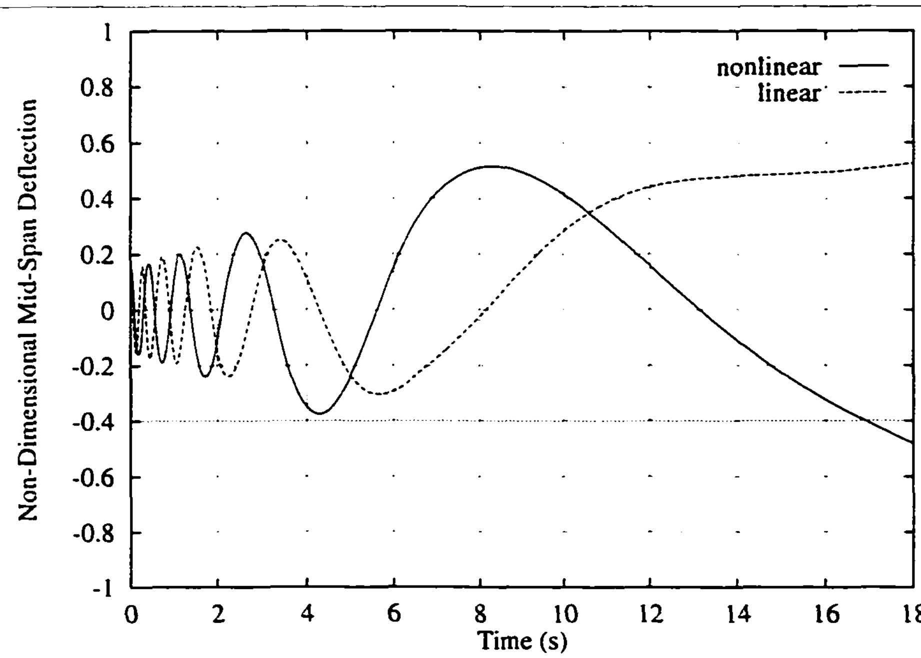


Figure 4.2.19: Test Case #10: High Frequency Extrusion $c_o = 0.931 \quad (m)$ .

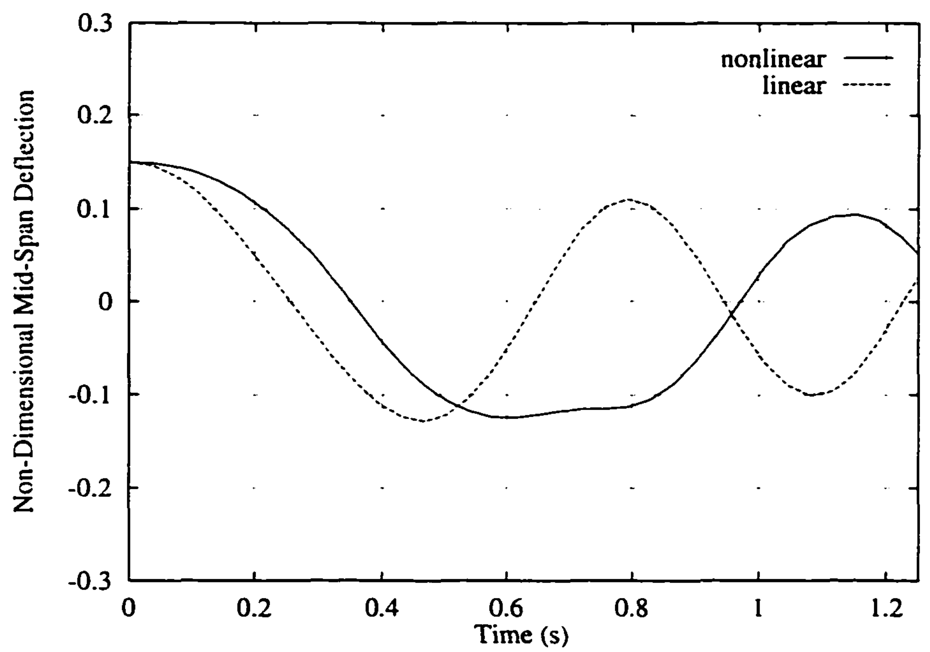


Figure 4.2.20: Test Case #11: High Frequency Retraction $c_o = -0.7 \quad (m)$.

## 4.3 Nonlinear Axially Inextensible Flexible Sliding Beams in Uniform Gravitational Field and in Fixed Domain

Additional terms due to gravity may be obtained as outlined in section 3.1.2.6 and in the fixed domain they may be expressed as:

$$\frac{\rho A g}{l}\frac{\partial \hat{x}_2}{\partial \mathcal{S}}\left[1+\frac{1}{2l^2}\left(\frac{\partial \hat{x}_2}{\partial \mathcal{S}}\right)^2\right]-\frac{\rho A g}{l}(1-\mathcal{S})\left[1+\frac{3}{2l^2}\left(\frac{\partial \hat{x}_2}{\partial \mathcal{S}}\right)^2\right]\frac{\partial^2 \hat{x}_2}{\partial \mathcal{S}^2}$$

Thus the additional linear and nonlinear terms take the form:

$$L_1^G = \frac{\rho A g}{l}\frac{\partial \hat{x}_2}{\partial \mathcal{S}}-\frac{\rho A g}{l}(1-\mathcal{S})\frac{\partial^2 \hat{x}_2}{\partial \mathcal{S}^2} \tag{4.3.1}$$

and

$$N_1^G = \frac{\rho A g}{2l^3}\left(\frac{\partial \hat{x}_2}{\partial \mathcal{S}}\right)^3-\frac{3\rho A g}{2l^3}(1-\mathcal{S})\left(\frac{\partial \hat{x}_2}{\partial \mathcal{S}}\right)^2\frac{\partial^2 \hat{x}_2}{\partial \mathcal{S}^2} \tag{4.3.2}$$

To express the above additional terms in dimensionless form, it is required to define a new non-dimensional term as:

$$\mathcal{G} = \frac{\rho A g}{EI} L_o^3 \tag{4.3.3}$$

Therefore dimensionless additional linear and nonlinear terms become:

$$\mathcal{L}_1^G(\eta) = \frac{\mathcal{G}}{l}\frac{\partial \eta}{\partial \mathcal{S}} - \frac{\mathcal{G}}{l}(1-\mathcal{S})\frac{\partial^2 \eta}{\partial \mathcal{S}^2} \tag{4.3.4}$$

and

$$\mathcal{N}_1^G(\eta) = \frac{\mathcal{G}}{2l^3}\left(\frac{\partial \eta}{\partial \mathcal{S}}\right)^3 - \frac{3\mathcal{G}}{2l^3}(1-\mathcal{S})\left(\frac{\partial \eta}{\partial \mathcal{S}}\right)^2 \frac{\partial^2 \eta}{\partial \mathcal{S}^2} \tag{4.3.5}$$

When transforming from PDE to ODEs, the above additional terms introduce additional linear and nonlinear stiffness matrices derived as:

$$b_{ij}^G = \int_0^1 \wp_i \left[\frac{\mathcal{G}}{l}\frac{\partial \wp_j}{\partial \mathcal{S}} - \frac{\mathcal{G}}{l}(1-\mathcal{S})\frac{\partial^2 \wp_j}{\partial \mathcal{S}^2}\right] d\mathcal{S} \tag{4.3.6}$$

and

$$c_{ijkl}^G = \int_0^1 \wp_i \frac{\partial \wp_j}{\partial \mathcal{S}} \frac{\partial \wp_k}{\partial \mathcal{S}} \left[\frac{\mathcal{G}}{2l^3}\frac{\partial \wp_l}{\partial \mathcal{S}} - \frac{3\mathcal{G}}{2l^3}(1-\mathcal{S})\frac{\partial^2 \wp_l}{\partial \mathcal{S}^2}\right] d\mathcal{S} \tag{4.3.7}$$

With the inclusion of these stiffness matrices in the governing equations of motion obtained in section 4.2, one may study the transient response of the axially rigid sliding beams in a uniform gravitational field.

Here we consider test case #1 under uniform gravitational field. Figures 4.3.1 and 4.3.2 show the necessity of including the nonlinear terms in the solution as well as the effects of uniform gravity field on the response of the system.

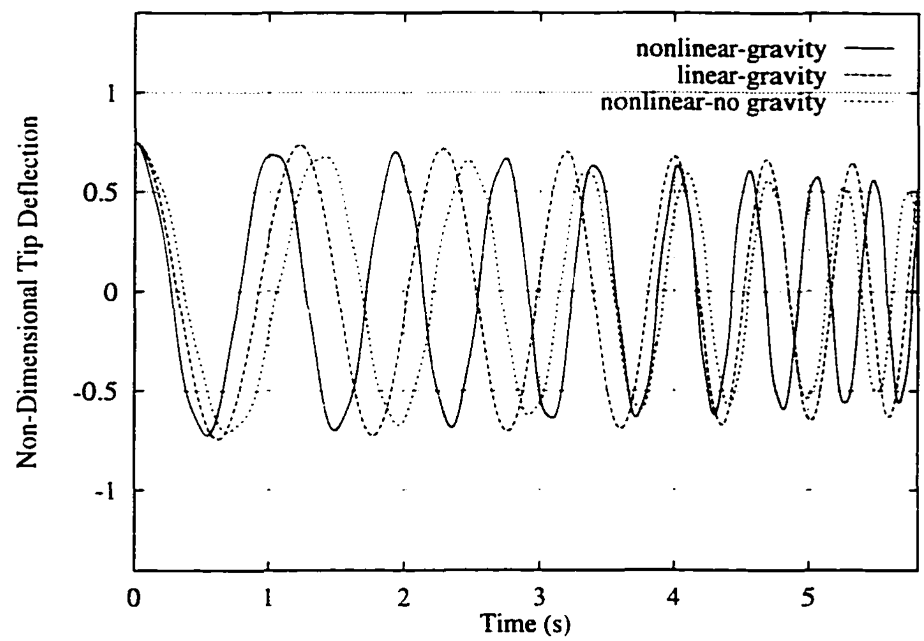


Figure 4.3.1: Spaghetti Problem: Uniform Gravitational Field, Constant Velocity Retraction $V_o = -0.1145 \ (m/s)$ .

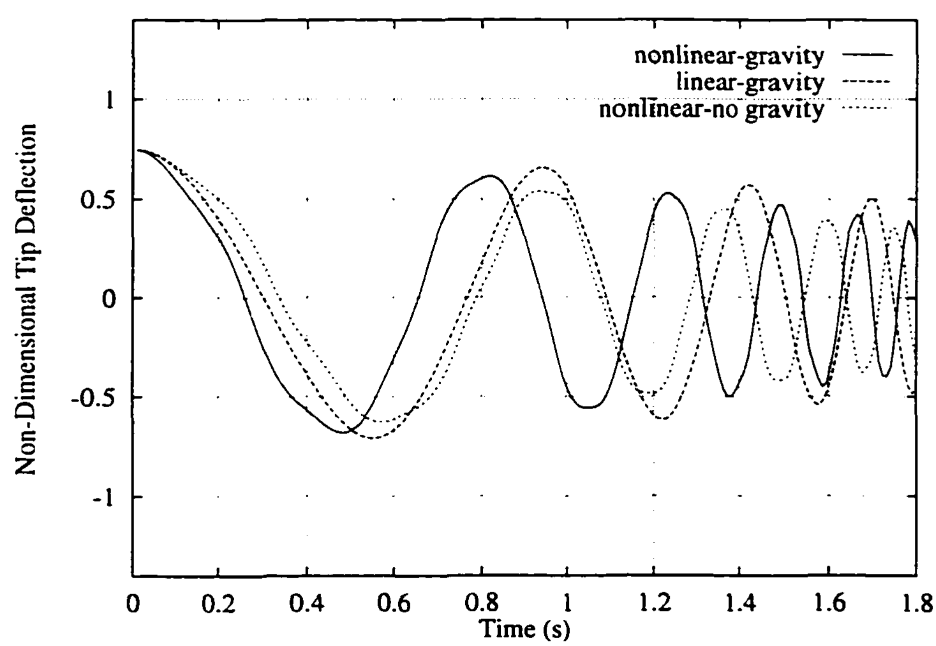


Figure 4.3.2: Spaghetti Problem: Uniform Gravitational Field, Constant Velocity Retraction $V_o = 0.5725 \ (m/s)$ .

## 4.4 Conclusions

In this chapter we computed the transient response of axially inextensible sliding beams. We started with the linear case and transformed the governing equation of motion to the fixed domain. Subsequently we used the Galerkin's method with space dependent modal functions to obtain the system discrete set of ODE's. Numerical solutions of the ODE's were in good agreement with the simulation and experimental work reported by Stylianou,1993, and Yuh and Young, 1991.

We further extended the analysis to the nonlinear case and transformed the system equation obtained in chapter 3 to the fixed domain. Again using the Galerkin's method we obtained a set of nonlinear ODE's which upon solution provided the response of the system. Several illustrative cases were considered and the results exposed the differences between the linear and the nonlinear solutions to these problems. Also the effect of uniform gravitational field on the response of the system was studied.

In this chapter we neglected the effect of axial flexibility which can have a crucial role on the response of the system. This effect has not been considered by other researchers since the large difference between the axial and flexural rigidities of slender beams would indicated that the axial flexibility has negligible effect on the motion of the system. In the following chapters we use the finite element techniques developed in chapter 2 for solution of axially extensible sliding beams.

# Chapter 5

# Incremental FE Discretization of System Equations for Flexible Sliding Beams

We use the finite element method to obtain solutions for geometrically nonlinear flexible sliding beams. The equations of motion for flexible sliding beams have been derived in the time varying domain $(0, \hat{L}(t))$ or $(C(t), L_B)$ in chapter 3. Finite element formulations are normally carried out for fixed domains. Evidently for this problem it is necessary to update the domain in time. This can be done for instance: by using fixed-size elements and increasing the number of elements in time or by using a fixed number of elements with variable lengths (Stylianou, 1993). Another alternative is to transform the system equations to a fixed domain and use a fixed number of elements with fixed lengths. The fixed-size elements formulation with increasing number of elements raises some complications in implementation with respect to the data structures and data flow in conventional finite element programming. The other two formulations do not present such difficulties but need certain considerations in the formulation procedures and implementation. To account for the geometrical nonlinearities in the problem, we may consider either the updated-Lagrangian or the consistent co-rotational nonlinear finite element methods to obtain the discretized governing equations of motion.

## 5.1 Updated Lagrangian Method

This section includes the discretization process for the flexible sliding beam using variable domain beam elements or constant domain stretched beam elements.

### 5.1.1 Variable-Domain Beam Elements

In this formulation we consider a fixed number of elements, with the element lengths changing in time. First we need to obtain the element lagrangian function and discretize it by using the proper time dependent element shape functions. Then by using Hamilton's principle we obtain the discretized form of the governing equations of motion for this problem,

#### 5.1.1.1 Element Lagrangian Function

Consider an element with the length $l(t)$ . In the $i^{th}$ undeformed element located at distance $\hat{L}_i$ form the fixed global coordinates, we consider a material point $M$ along the centerline of the beam element as shown in Figure 5.1.2. The location of this point with respect to the fixed global coordinates can be expressed as:

$$\chi_1 = \hat{L}_i + \chi_{1} \tag{5.1.1}$$

To obtain the rate of change with respect to time of the element coordinate $\chi_1$ , we differentiate the above equation with respect to time and write:

$$\frac{d\chi_1}{dt} = \frac{d\chi_1}{dt} - \frac{d\hat{L}_i}{dt} \tag{5.1.2}$$

Noting that $\frac{d\chi_1}{dt} = \frac{d}{dt}\hat{L}$, we may express equation (5.1.2) as:

$$\frac{d\chi_1}{dt} = \frac{d}{dt}(\hat{L} - \hat{L}_i) = v_i \tag{5.1.3}$$

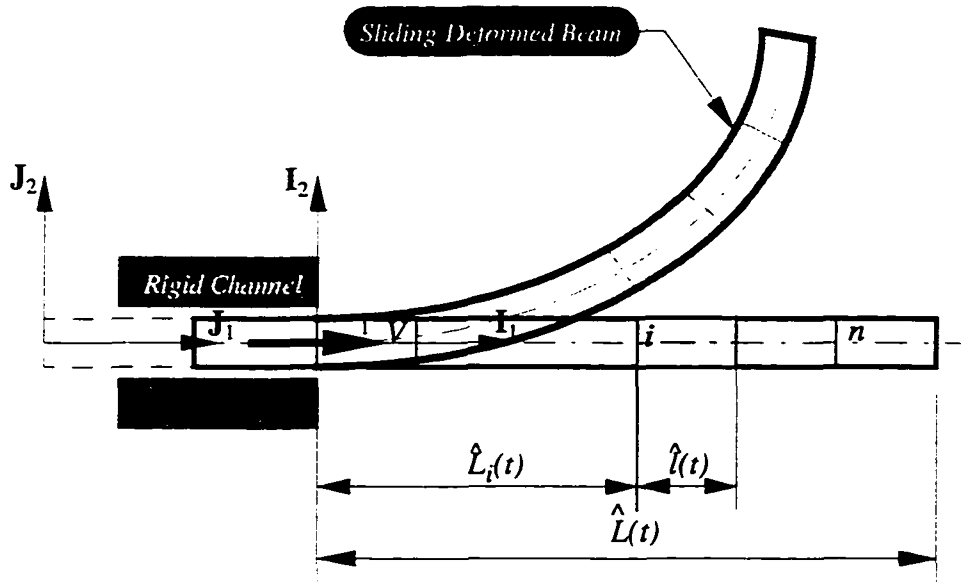


Figure 5.1.1: Variable-Domain Beam Elements.

Also from Figure 5.1.1, we note that:

$$\hat{L} - \hat{L}_i = \hat{L}\,[1 - (i-1)/n] \qquad i = 1, 2, \ldots n \tag{5.1.4}$$

where for convenience we have considered $n$ elements of equal lengths.

Referring to equation (3.1.65) and using the relation (5.1.3), the Lagrangian function for the $i^{th}$ element may be expressed as:

$$\mathcal{L}_i = \int_0^{\hat{l}(t)} \frac{1}{2}\rho_o A \left\{ \left[ \frac{\partial \hat{u}_1}{\partial t} + v_i \left( 1 + \frac{\partial \hat{u}_1}{\partial \chi_1} \right) \right]^2 + \left[ \frac{\partial \hat{u}_2}{\partial t} + v_i \frac{\partial \hat{u}_2}{\partial \chi_1} \right]^2 \right\} d\chi_1 - \Pi \tag{5.1.5}$$

where $\hat{u}_1, \hat{u}_2$ are the element displacements in the inertial frame and $\rho_o$ is the mass density of the undeformed beam element, i.e. $\rho_o(\chi_1, t) = \rho(\hat{x}, t) J(\chi_1, t)$, $J$ being the Jacobian determinant of the deformation map. $\Pi$ is the strain energy of the beam element under large displacements and can be computed from the strain measures of the element as: (see equation 3.1.64)

$$
\begin{aligned}
\Pi = & \int_0^{\hat{l}(t)} \frac{1}{2} EA \left[ \frac{\partial \hat{u}_1}{\partial \chi_1} + \frac{1}{2}\left( \frac{\partial \hat{u}_2}{\partial \chi_1} \right)^2 \right]^2 d\chi_1 + \\
& \int_0^{\hat{l}(t)} \frac{1}{2} EI \left[ \left( \frac{\partial^2 \hat{u}_2}{\partial \chi_1^2} \right)^2 - 2\left( \frac{\partial^2 \hat{u}_2}{\partial \chi_1^2} \right)^2 \frac{\partial \hat{u}_1}{\partial \chi_1} - 2\left( \frac{\partial^2 \hat{u}_2}{\partial \chi_1^2} \right)^2 \left( \frac{\partial \hat{u}_2}{\partial \chi_1} \right)^2 - \right. \\
& \left. 2 \frac{\partial \hat{u}_2}{\partial \chi_1} \frac{\partial^2 \hat{u}_2}{\partial \chi_1^2} \frac{\partial^2 \hat{u}_1}{\partial \chi_1^2} \right] d\chi_1
\end{aligned}
\tag{5.1.6}
$$

It is worth noting that the complementary kinetic energy in the Lagrangian is quadratic while the potential energy has quintic terms. This implies that the momentum velocity relations will be linear while the force displacement relations will be nonlinear. Hence the mass matrix, in the momentum velocity relation, need only be computed once while the stiffness matrix, in the force displacement relation, must be updated in accordance with the equilibrium equations.

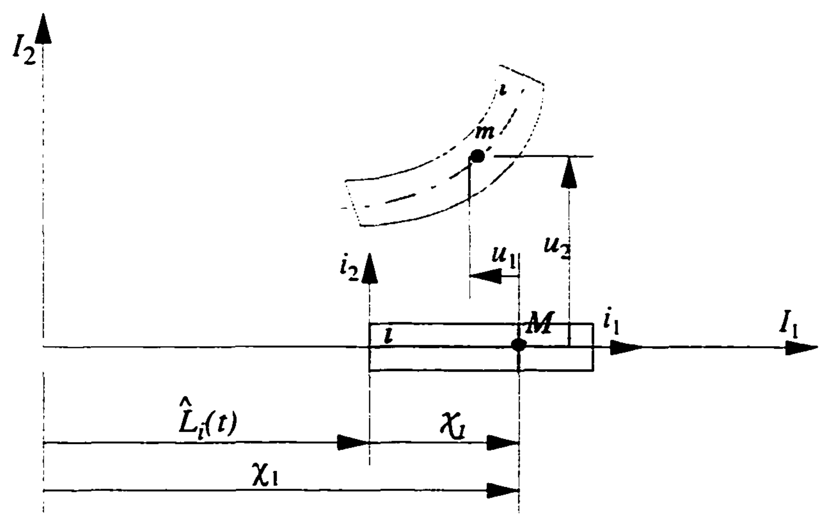


Figure 5.1.2: Element coordinate system.

### 5.1.1.2 Finite element discretization

In customary manner we model the axial and transverse deflections by linear and cubic interpolation functions, respectively, as:

$$\tilde{u}_1 = \lfloor N_1 \rfloor \ \{\tilde{u}\} \tag{5.1.7}$$

and

$$\tilde{u}_2 = \lfloor N_2 \rfloor \ \{\tilde{u}\} \tag{5.1.8}$$

where

$$\lfloor N_1 \rfloor = \left\lfloor \frac{1 - \tilde{x}_1}{\tilde{l}} \quad 0 \quad 0 \quad \frac{\tilde{x}_1}{\tilde{l}} \quad 0 \quad 0 \right\rfloor \tag{5.1.9}$$

and

$$\lfloor N_2 \rfloor = \left\lfloor 0 \quad 1 - \frac{3\tilde{x}_1^2}{\tilde{l}^2} + \frac{2\tilde{x}_1^3}{\tilde{l}^3} \quad \tilde{x}_1 - \frac{2\tilde{x}_1^2}{\tilde{l}} + \frac{\tilde{x}_1^3}{\tilde{l}^2} \quad 0 \quad \frac{3\tilde{x}_1^2}{\tilde{l}^2} - \frac{2\tilde{x}_1^3}{\tilde{l}^3} \quad -\frac{\tilde{x}_1^2}{\tilde{l}} + \frac{\tilde{x}_1^3}{\tilde{l}^2} \right\rfloor \tag{5.1.10}$$

and $\{\tilde{u}\}$ is the nodal variables vector.

It is worth noting that since the length of the beam element varies in time, the shape functions are time dependent. Differentiating equations (5.1.7) and (5.1.8) with respect to space and time, we obtain:

$$\begin{aligned}
\frac{\partial \tilde{u}_j}{\partial t} &= \lfloor N_j \rfloor \ \{\frac{d}{dt}\tilde{u}\} + \left\lfloor \frac{\partial N_j}{\partial t} \right\rfloor \ \{\tilde{u}\} \\
\frac{\partial \tilde{u}_j}{\partial \tilde{x}_1} &= \left\lfloor \frac{\partial N_j}{\partial \tilde{x}_1} \right\rfloor \ \{\tilde{u}\} \\
\frac{\partial^2 \tilde{u}_j}{\partial \tilde{x}_1^2} &= \left\lfloor \frac{\partial^2 N_j}{\partial \tilde{x}_1^2} \right\rfloor \ \{\tilde{u}\} \qquad \text{where } j = 1, 2
\end{aligned} \tag{5.1.11}$$

Returning now to the element Lagrangian function and substituting the expressions (5.1.11) into equation (5.1.5), we obtain:

$$\mathcal{L}_i = \frac{1}{2}\ \{\frac{d}{dt}\hat{u}\}^T\ [m]\ \{\frac{d}{dt}\hat{u}\} - \frac{1}{2}\ \{\hat{u}\}^T\ [k_m]\ \{\hat{u}\} - \Pi +$$
$$\frac{1}{2}\ \{\hat{u}\}^T\ [c_1]\ \{\frac{d}{dt}\hat{u}\} + \frac{1}{2}\ \{\frac{d}{dt}\hat{u}\}^T\ [c_2]\ \{\hat{u}\} + \tag{5.1.12}$$
$$\lfloor f_1 \rfloor\ \{\frac{d}{dt}\hat{u}\} + \lfloor f_2 \rfloor\ \{\hat{u}\} + \frac{1}{2}\ \rho_o A\ \hat{l}\ v_i^2$$

where

$$[m] = \int_0^{\hat{l}(t)} \rho_o A\left(\lfloor N_1 \rfloor^T \lfloor N_1 \rfloor + \lfloor N_2 \rfloor^T \lfloor N_2 \rfloor\right)\ d\chi_1 \tag{5.1.13}$$

$$\begin{aligned}[k_m] = \int_0^{\hat{l}(t)} -\rho_o A \Bigg[ & \left\lfloor \frac{\partial N_1}{\partial t} \right\rfloor^T \left\lfloor \frac{\partial N_1}{\partial t} \right\rfloor + v_i^2 \left\lfloor \frac{\partial N_1}{\partial \chi_1} \right\rfloor^T \left\lfloor \frac{\partial N_1}{\partial \chi_1} \right\rfloor + \\ & v_i \left( \left\lfloor \frac{\partial N_1}{\partial t} \right\rfloor^T \left\lfloor \frac{\partial N_1}{\partial \chi_1} \right\rfloor + \left\lfloor \frac{\partial N_1}{\partial \chi_1} \right\rfloor^T \left\lfloor \frac{\partial N_1}{\partial t} \right\rfloor \right) + \\ & \left\lfloor \frac{\partial N_2}{\partial t} \right\rfloor^T \left\lfloor \frac{\partial N_2}{\partial t} \right\rfloor + v_i^2 \left\lfloor \frac{\partial N_2}{\partial \chi_1} \right\rfloor^T \left\lfloor \frac{\partial N_2}{\partial \chi_1} \right\rfloor + \\ & v_i \left( \left\lfloor \frac{\partial N_2}{\partial t} \right\rfloor^T \left\lfloor \frac{\partial N_2}{\partial \chi_1} \right\rfloor + \left\lfloor \frac{\partial N_2}{\partial \chi_1} \right\rfloor^T \left\lfloor \frac{\partial N_2}{\partial t} \right\rfloor \right) \Bigg]\ d\chi_1 \end{aligned} \tag{5.1.14}$$

$$\begin{aligned}[c_1] = \int_0^{\hat{l}(t)} \rho_o A \Bigg[ & \left\lfloor \frac{\partial N_1}{\partial t} \right\rfloor^T \lfloor N_1 \rfloor + v_i \left\lfloor \frac{\partial N_1}{\partial \chi_1} \right\rfloor^T \lfloor N_1 \rfloor + \\ & \left\lfloor \frac{\partial N_2}{\partial t} \right\rfloor^T \lfloor N_2 \rfloor + v_i \left\lfloor \frac{\partial N_2}{\partial \chi_1} \right\rfloor^T \lfloor N_2 \rfloor \Bigg]\ d\chi_1 \end{aligned} \tag{5.1.15}$$

$$\begin{aligned}[c_2] = \int_0^{\hat{l}(t)} \rho_o A \Bigg[ & \lfloor N_1 \rfloor^T \left\lfloor \frac{\partial N_1}{\partial t} \right\rfloor + v_i \lfloor N_1 \rfloor^T \left\lfloor \frac{\partial N_1}{\partial \chi_1} \right\rfloor + \\ & \lfloor N_2 \rfloor^T \left\lfloor \frac{\partial N_2}{\partial t} \right\rfloor + v_i \lfloor N_2 \rfloor^T \left\lfloor \frac{\partial N_2}{\partial \chi_1} \right\rfloor \Bigg]\ d\chi_1 \end{aligned} \tag{5.1.16}$$

$$\lfloor f_1 \rfloor = \int_0^{\hat{l}(t)} \rho_o A \; v_i \lfloor N_1 \rfloor \; d\chi_1 \tag{5.1.17}$$

$$\lfloor f_2 \rfloor = \int_0^{\hat{l}(t)} \rho_o A \; v_i \left( \left\lfloor \frac{\partial N_1}{\partial t} \right\rfloor + v_i \left\lfloor \frac{\partial N_1}{\partial \chi_1} \right\rfloor \right) \; d\chi_1 \tag{5.1.18}$$

Components of the system matrices and vectors may be obtained explicitly by using the symbolic-computation program MAPLE. It is important to note that all the above matrices are the contribution of the kinetic co-energy of the moving flexible element to the element Lagrangian function. Other contributions, notably due to elastic strain energy, are obtained from $\Pi$ as described in chapter 2.

#### 5.1.1.3 Discretized Equations of Motion

For an element we may write Hamilton's principle as:

$$\delta \int_{t_1}^{t_2} \mathcal{L}_i \; dt = 0 \tag{5.1.19}$$

For the overall system the Lagrangian will be sum of the Lagrangians of individual elements.

Substituting equation (5.1.12) into equation (5.1.19), carrying out the variation and imposing the boundary conditions, we obtain:

$$\delta \int_{t_1}^{t_2} \mathcal{L}_i \; dt = \int_{t_1}^{t_2} - \left( \left[ \frac{dm}{dt} \right] \{ \frac{d}{dt} \hat{u} \} + [m] \{ \frac{d^2}{dt^2} \hat{u} \} + \left[ \frac{dc_2}{dt} \right] \{ \hat{u} \} - [c_2]^T \{ \frac{d}{dt} \hat{u} \} + \right.$$
$$\left. [k_m] \{ \hat{u} \} + \frac{\partial \Pi}{\partial \{ \hat{u} \}^T} - \lfloor f_2 \rfloor^T + \left\lfloor \frac{df_1}{dt} \right\rfloor^T - \{ \hat{r} \} \right) \delta \{ \hat{u} \} \, dt = 0 \tag{5.1.20}$$

where $\{ \hat{r} \}$ is the prescribed element external load vector with potential $\{ \hat{r} \} \{ \hat{u} \}$. Also in the derivation of the above equation, we have taken note of the fact that $[c_1] = [c_2]^T$. Since $\delta \{ \hat{u} \}$ is arbitrary, we deduce that

$$[m]\left\{\frac{d^2}{dt^2}\hat{u}\right\} + [c_{eq}]\left\{\frac{d}{dt}\hat{u}\right\} + \left([k_m] + \left[\frac{dc_2}{dt}\right]\right)\{\hat{u}\} + \frac{\partial\Pi}{\partial\{\hat{u}\}^T} = \{\hat{r}\} + \lfloor f_2 \rfloor^T - \left\lfloor \frac{df_1}{dt} \right\rfloor^T \tag{5.1.21}$$

where

$$[c_{eq}] = \left[\frac{dm}{dt}\right] + [c_2] - [c_2]^T \tag{5.1.22}$$

is the equivalent damping matrix and

$$\frac{\partial\Pi}{\partial\{\hat{u}\}^T} = \{f\} \tag{5.1.23}$$

is the internal force vector. The combination of second and third terms in equation (5.1.22) produces a skew-symmetric matrix, as a result of gyroscopic forces which do no work. On the other hand the term $[dm/dt]$ which arises from the increase (or decrease) of mass in the system, does effect the energy in the system. We have chosen to refer to the combined terms as the "equivalent" damping matrix even though no physical damping has been incorporated into our formulation.

It is important to note that the time dependent inertia forces $\lfloor f_2 \rfloor^T$ and $\lfloor df_1/dt \rfloor^T$, which arise due to the sliding motion of the beam remain directed along the initial undeformed configuration axis $\mathbf{J}_1$ regardless of the large amplitude response of the sliding beam. This can be seen from, for example, the inertia force $\lfloor f_2 \rfloor^T$ given in equation (5.1.18) which requires an integration along $\chi_1$, with unit vector $\mathbf{J}_1$. Also the $v_i$ appearing in this equation is the prescribed velocity along the $\mathbf{J}_1$ axis.

The equation of motion given in (5.1.21) is nonlinear and can be solved through the Newton-Raphson method as described in chapter 2. Using the modified Newton-Raphson technique the element iterational equation with respect to equilibrium configuration at time step $t$ may be expressed as:

$$
{}^{t}_{t}[k_{eq}]\,\{\Delta\hat{u}\}^{i} = -{}^{t}[m]\;{}^{t+\Delta t}\{\frac{d^2}{dt^2}\hat{u}\}^{i} - {}^{t}[c_{eq}]\;{}^{t+\Delta t}\{\frac{d}{dt}\hat{u}\}^{i} + \\
{}^{t+\Delta t}\{\hat{r}\} - {}^{t+\Delta t}_{t+\Delta t}\{f\}^{i-1} + {}^{t}\lfloor f_2 \rfloor^{T} - {}^{t}\left\lfloor \frac{df_1}{dt} \right\rfloor^{T} \tag{5.1.24}
$$

where

$$
{}^{t}_{t}[k_{eq}] = {}^{t}_{t}\left( [k_m] + \left[\frac{dc_2}{dt}\right] + [k_T] \right) \tag{5.1.25}
$$

with

$$
[k_T] = \left[\frac{\partial^2 \Pi}{\partial\hat{u}_m \partial\hat{u}_n}\right] \tag{5.1.26}
$$

defined as the tangent stiffness matrix of the beam element which in general is non-symmetric. Expressions for the element internal force vector and tangent stiffness matrix are given in Appendix F.

Now we may assemble the element incremental equations to obtain the global incremental equations as:

$$
{}^{t}_{t}[K_{eq}]\,\{\Delta u\}^{i} = -{}^{t}[M]\;{}^{t+\Delta t}\left\{\frac{d^2 u}{dt^2}\right\}^{i} - {}^{t}[C_{eq}]\;{}^{t+\Delta t}\{\frac{du}{dt}\}^{i} + \\
{}^{t+\Delta t}\{R\} - {}^{t+\Delta t}_{t+\Delta t}\{F\}^{i-1} + {}^{t}\lfloor F_2 \rfloor^{T} - {}^{t}\left\lfloor \frac{dF_1}{dt} \right\rfloor^{T} \tag{5.1.27}
$$

### 5.1.2 Constant-Domain Stretched Beam Element

The concepts of transforming the system equations to the fixed domain have been extensively discussed in the previous two chapters. In this approach we use such stretched coordinates by using space dependent shape functions (as in conventional finite elements) to discretize the system equations. To achieve this, we may start with the derived Lagrangian function of the alternative formulation (sliding channel) and transform it to the fixed domain. Then by defining the element Lagrangian function in the fixed domain and using the time independent shape functions, we may obtain the discretized Lagrangian function. Finally on substituting the derived Lagrangian into Hamilton's principle we obtain the discretized system equations.

#### 5.1.2.1 Alternative Formulation: Lagrangian in the Fixed Domain

Referring to equation (3.2.14), the Lagrangian function is given by:

$$\mathcal{L} = \int_{C(t)}^{L_B} \frac{1}{2}\rho_o A \left\{ \left[\frac{\partial \bar{u}_1}{\partial t} + V\right]^2 + \left[\frac{\partial \bar{u}_2}{\partial t}\right]^2 \right\} dX_1 - \Pi \tag{5.1.28}$$

where

$$\begin{aligned} \Pi = & \int_{C(t)}^{L_B} \frac{1}{2}EA \left[\frac{\partial \bar{u}_1}{\partial X_1} + \frac{1}{2}\left(\frac{\partial \bar{u}_2}{\partial X_1}\right)^2\right]^2 dX_1 + \\ & \int_{C(t)}^{L_B} \frac{1}{2}EI \left[\left(\frac{\partial^2 \bar{u}_2}{\partial X_1^2}\right)^2 - 2\left(\frac{\partial^2 \bar{u}_2}{\partial X_1^2}\right)^2 \frac{\partial \bar{u}_1}{\partial X_1} - 2\left(\frac{\partial^2 \bar{u}_2}{\partial X_1^2}\right)^2 \left(\frac{\partial \bar{u}_2}{\partial X_1}\right)^2 - \right. \\ & \left. 2\frac{\partial \bar{u}_2}{\partial X_1} \frac{\partial^2 \bar{u}_2}{\partial X_1^2} \frac{\partial^2 \bar{u}_1}{\partial X_1^2} \right] dX_1 \end{aligned} \tag{5.1.29}$$

is the strain energy of the system.

To map the Lagrangian to the fixed domain, we need to define the following transformations: (see equation (3.3.6))

$$\begin{aligned} \eta_1 &= \frac{X_1 - C}{L} & \text{where } (0 < \eta_1 \le 1) \\ \eta_2 &= X_2 & \text{where } \left(-\frac{h}{2} < \eta_2 \le \frac{h}{2}\right) \end{aligned} \tag{5.1.30}$$

where $L = \hat{L}(t)$ and $C = C(t)$ are the time varying lengths of the beam outside and inside the channel, respectively, and $X_1$ and $t$ are the independent variables. From equation (5.1.30), we may express the following relations at time $t$:

$$dX_1 = L \; d\eta_1$$

$$\frac{\partial \bar{u}_i}{\partial X_1} = \frac{\partial \hat{u}_i}{\partial \eta_1} \frac{\partial \eta_1}{\partial X_1} = \frac{1}{L} \frac{\partial \hat{u}_i}{\partial \eta_1}$$

$$\frac{\partial^2 \bar{u}_i}{\partial X_1^{\,2}} = \frac{\partial}{\partial X_1}\left(\frac{1}{L} \frac{\partial \hat{u}_i}{\partial \eta_1}\right) = \frac{1}{L^2} \frac{\partial^2 \hat{u}_i}{\partial \eta_1^{\,2}} \qquad (5.1.31)$$

where

$$\bar{u}_i (X_1, t) \equiv \hat{u}_i (\eta_1 (X_1, t), t) \qquad (5.1.32)$$

and $i = 1, 2$. Also from equation (5.1.30), we deduce that:

$$\frac{\partial \eta_1}{\partial t} = \frac{V}{L} \; (1 - \eta_1) \qquad (5.1.33)$$

and

$$\frac{\partial^2 \eta_1}{\partial t^2} = \frac{L \dfrac{\partial V}{\partial t} (1 - \eta_1) - 2V^2 (1 - \eta_1)}{L^2} \qquad (5.1.34)$$

Now, as in equation (4.1.13), we may also write:

$$\frac{\partial \bar{u}_i}{\partial t} = \frac{V}{L} (1 - \eta_1) \; \frac{\partial \hat{u}_i}{\partial \eta_1} + \frac{\partial \hat{u}_i}{\partial t} \qquad i = 1, 2 \qquad (5.1.35)$$

Substituting the relations (5.1.31) and (5.1.35) into equation (5.1.28), the Lagrangian in the fixed domain may be expressed as:

$$\hat{\mathcal{L}} = \int_0^1 \frac{1}{2} \rho_o A \; \left\{ \left[ V + \frac{V}{L} (1 - \eta_1) \; \frac{\partial \hat{u}_1}{\partial \eta_1} + \frac{\partial \hat{u}_1}{\partial t} \right]^2 + \left[ \frac{V}{L} (1 - \eta_1) \; \frac{\partial \hat{u}_2}{\partial \eta_1} + \frac{\partial \hat{u}_2}{\partial t} \right]^2 \right\} L d\eta_1 - \hat{\Pi} \qquad (5.1.36)$$

where

$$\hat{\Pi} = \int_0^1 \frac{1}{2L} EA \left[\frac{\partial \hat{u}_1}{\partial \eta_1} + \frac{1}{2L}\left(\frac{\partial \hat{u}_2}{\partial \eta_1}\right)^2\right]^2 d\eta_1 +$$
$$\int_0^1 \frac{1}{2L^3} EI \left[\left(\frac{\partial^2 \hat{u}_2}{\partial \eta_1^2}\right)^2 - \frac{2}{L}\left(\frac{\partial^2 \hat{u}_2}{\partial \eta_1^2}\right)^2 \frac{\partial \hat{u}_1}{\partial \eta_1} - \frac{2}{L^2}\left(\frac{\partial^2 \hat{u}_2}{\partial \eta_1^2}\right)^2 \left(\frac{\partial \hat{u}_2}{\partial \eta_1}\right)^2 - \right. \tag{5.1.37}$$
$$\left. \frac{2}{L} \frac{\partial \hat{u}_2}{\partial \eta_1} \frac{\partial^2 \hat{u}_2}{\partial \eta_1^2} \frac{\partial^2 \hat{u}_1}{\partial \eta_1^2}\right] d\eta_1$$

### 5.1.2.2 Element Lagrangian Function

The Lagrangian function (5.1.37) is obtained in the fixed domain allowing us to discretize the equations in the conventional finite element procedure. Let us consider $n$ qual size beam elements with the length of $\frac{1}{n}$ (see Figure 5.1.3). The location of a point on the center line of the $i^{th}$ beam element with respect to the global coordinate system may be defined as:

$$\eta_1 = \hat{l}_i + \xi \tag{5.1.38}$$

where $0 \le \eta_1 \le 1$ and $0 \le \xi \le \frac{1}{n}$.

Using equations (5.1.36) and (5.1.38), one may express the element Lagrangian function as:

$$\hat{\mathcal{L}}_i = \int_0^{\frac{1}{n}} \frac{1}{2}\rho_o A \left\{\left[V + \frac{V}{L}(1 - l_i - \xi) \frac{\partial \hat{u}_1}{\partial \xi} + \frac{\partial \hat{u}_1}{\partial t}\right]^2 + \right. \tag{5.1.39}$$
$$\left. \left[\frac{V}{L}(1 - l_i - \xi) \frac{\partial \hat{u}_2}{\partial \xi} + \frac{\partial \hat{u}_2}{\partial t}\right]^2\right\} L d\xi - \hat{\Pi}$$

where $\hat{\Pi}$ is the strain energy of the beam element: (see equation (5.1.37))

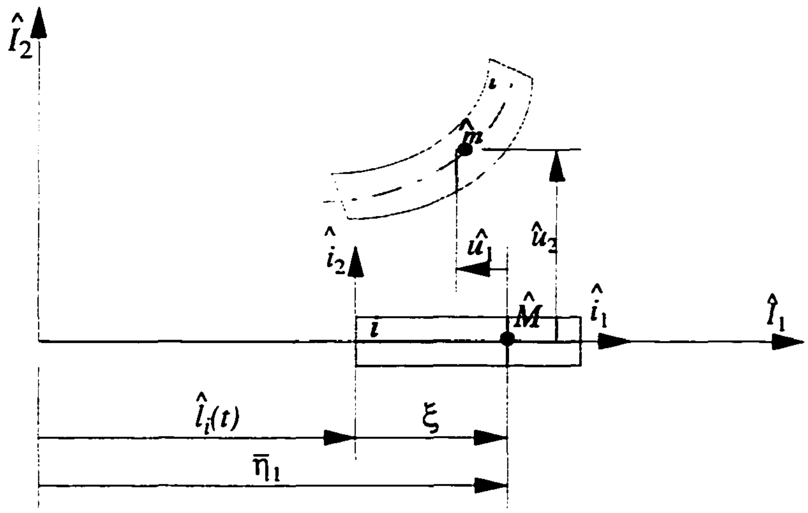


Figure 5.1.3: constant domain stretched beam element.

$$\hat{\Pi} = \int_0^{\frac{1}{n}} \frac{1}{2L} EA \left[ \frac{\partial \hat{u}_1}{\partial \xi} + \frac{1}{2L} \left( \frac{\partial \hat{u}_2}{\partial \xi} \right)^2 \right]^2 d\xi + \int_0^{\frac{1}{n}} \frac{1}{2L^3} EI \left[ \left( \frac{\partial^2 \hat{u}_2}{\partial \xi^2} \right)^2 - \frac{2}{L} \left( \frac{\partial^2 \hat{u}_2}{\partial \xi^2} \right)^2 \frac{\partial \hat{u}_1}{\partial \xi} - \frac{2}{L^2} \left( \frac{\partial^2 \hat{u}_2}{\partial \xi^2} \right)^2 \left( \frac{\partial \hat{u}_2}{\partial \xi} \right)^2 - \frac{2}{L} \frac{\partial \hat{u}_2}{\partial \xi} \frac{\partial^2 \hat{u}_2}{\partial \xi^2} \frac{\partial^2 \hat{u}_1}{\partial \xi^2} \right] d\xi \tag{5.1.40}$$

### 5.1.2.3 Finite Element Discretization

The axial and transverse deflections are modelled by linear and cubic interpolation functions, respectively, as:

$$\hat{u}_1 = \lfloor H_1 \rfloor \ \{\hat{u}\} \tag{5.1.41}$$

and

$$\hat{u}_2 = \lfloor H_2 \rfloor \ \{\hat{u}\} \tag{5.1.42}$$

where

$$\lfloor H_1 \rfloor = \lfloor 1 - n\xi \quad 0 \quad 0 \quad n\xi \quad 0 \quad 0 \rfloor \tag{5.1.43}$$

and

$$\lfloor H_2 \rfloor = \lfloor 0 \quad 1-3n^2\xi^2 + 2n^3\xi^3 \quad \xi-2n\xi^2 + n^2\xi^3 \quad 0 \quad 3n^2\xi^2 - 2n^3\xi^3 \quad n^2\xi^3 - n\xi^2 \rfloor \tag{5.1.44}$$

and $\{\hat{u}\}$ is the nodal variables vector.

In this case shape functions are only space dependent and we have then:

$$\begin{aligned} \frac{\partial \hat{u}_j}{\partial t} &= \lfloor H_j \rfloor \ \{\frac{d}{dt}\hat{u}\} \\ \frac{\partial \hat{u}_j}{\partial \xi} &= \left\lfloor \frac{\partial H_j}{\partial \xi} \right\rfloor \ \{\hat{u}\} \\ \frac{\partial^2 \hat{u}_j}{\partial \xi^2} &= \left\lfloor \frac{\partial^2 H_j}{\partial \xi^2} \right\rfloor \ \{\hat{u}\} \qquad\qquad j = 1, 2 \end{aligned} \tag{5.1.45}$$

Substituting equation (5.1.45) into the element Lagrangian function (5.1.39), we obtain:

$$\begin{aligned} \hat{\mathcal{L}}_i = & \frac{1}{2} \ \{\frac{d}{dt}\hat{u}\}^T \ [\hat{m}] \ \{\frac{d}{dt}\hat{u}\} - \frac{1}{2} \ \{\hat{u}\}^T \ [\hat{k}_m] \ \{\hat{u}\} - \hat{\Pi} + \\ & \frac{1}{2} \ \{\hat{u}\}^T \ [\hat{c}_1] \ \{\frac{d}{dt}\hat{u}\} + \frac{1}{2} \ \{\frac{d}{dt}\hat{u}\}^T \ [\hat{c}_2] \ \{\hat{u}\} + \\ & \lfloor \hat{f}_1 \rfloor \ \{\frac{d}{dt}\hat{u}\} + \lfloor \hat{f}_2 \rfloor \ \{\hat{u}\} + \frac{1}{2n} \ \rho_o A \ l_i \ V^2 \end{aligned} \tag{5.1.46}$$

where

$$[\hat{m}] = \int_0^{\frac{1}{n}} \rho_o A L \left( \lfloor H_1 \rfloor^T \lfloor H_1 \rfloor + \lfloor H_2 \rfloor^T \lfloor H_2 \rfloor \right) d\xi \tag{5.1.47}$$

$$[\hat{k}_m] = \int_0^{\frac{1}{n}} -\frac{\rho_o A}{L}\left[V^2(1-l_i-\xi)^2\left\lfloor\frac{dH_1}{d\xi}\right\rfloor^T\left\lfloor\frac{dH_1}{d\xi}\right\rfloor + V^2(1-l_i-\xi)^2\left\lfloor\frac{dH_2}{d\chi_1}\right\rfloor^T\left\lfloor\frac{dH_2}{d\chi_1}\right\rfloor\right]d\xi \tag{5.1.48}$$

$$[\hat{c}_1] = \int_0^{\frac{1}{n}} \rho_o A V(1-l_i-\xi)\left[\left\lfloor\frac{dH_1}{d\xi}\right\rfloor^T\lfloor H_1\rfloor + \left\lfloor\frac{dH_2}{d\xi}\right\rfloor^T\lfloor H_2\rfloor\right]d\xi \tag{5.1.49}$$

$$[\hat{c}_2] = \int_0^{\frac{1}{n}} \rho_o A V(1-l_i-\xi)\left[\lfloor H_1\rfloor^T\left\lfloor\frac{dH_1}{d\xi}\right\rfloor + \lfloor H_2\rfloor^T\left\lfloor\frac{dH_2}{d\xi}\right\rfloor\right]d\xi \tag{5.1.50}$$

$$\lfloor\hat{f}_1\rfloor = \int_0^{\frac{1}{n}} \rho_o A\ L\ V\lfloor H_1\rfloor\, d\xi \tag{5.1.51}$$

$$\lfloor\hat{f}_2\rfloor = \int_0^{\frac{1}{n}} \rho_o A\ V^2(1-l_i-\xi)\left\lfloor\frac{dH_1}{d\xi}\right\rfloor d\xi \tag{5.1.52}$$

Using the symbolic-computation program MAPLE, we may obtain the components of the system matrices and inertia force vectors explicitly.

#### 5.1.2.4 Discretized Equations of Motion

Again by using Hamilton's principle, the discretized equation of motion may be expressed as: (see section 5.1.1.3)

$$[\hat{m}]\{\frac{d^2}{dt^2}\hat{u}\} + [\hat{c}_{eq}]\{\frac{d}{dt}\hat{u}\} + \left([\hat{k}_m] + \left[\frac{d\hat{c}_2}{dt}\right]\right)\{\hat{u}\} + \frac{\partial\hat{\Pi}_i}{\partial\{\hat{u}\}^T} = \{\hat{r}\} + \lfloor\hat{f}_2\rfloor^T - \left\lfloor\frac{d\hat{f}_1}{dt}\right\rfloor^T \tag{5.1.53}$$

where

$$[\hat{c}_{eq}] = \left[\frac{d}{dt}\hat{m}\right] + [\hat{c}_2] - [\hat{c}_2]^T \tag{5.1.54}$$

is the equivalent damping matrix in the fixed domain,

$$\frac{\partial \hat{\Pi}_i}{\partial \{\hat{u}\}^T} = \{\hat{f}\} \tag{5.1.55}$$

is the internal force vector and $\{\hat{r}\}$ is the element external force vector.

The Newton-Raphson method can be used to obtain the solution for the system. We choose the modified Newton-Raphson method to obtain the element iterational equation of motion with respect to transformed equilibrium configuration at time $t$, i.e.:

$$\begin{aligned} {}^t_t[\hat{k}_{eq}]\,\{\Delta\hat{u}\}^i = {} & -{}^t[\hat{m}]\;{}^{t+\Delta t}\{\frac{d^2}{dt^2}\hat{u}\}^i - {}^t[\hat{c}_{eq}]\;{}^{t+\Delta t}\{\frac{d}{dt}\hat{u}\}^i + \\ & {}^{t+\Delta t}\{\hat{r}\} - {}^{t+\Delta t}_{t+\Delta t}\{\hat{f}\}^{i-1} + {}^t\lfloor\hat{f}_2\rfloor^T - {}^t\left\lfloor\frac{d\hat{f}_1}{dt}\right\rfloor^T \end{aligned} \tag{5.1.56}$$

where

$${}^t_t[\hat{k}_{eq}] = {}^t_t\left([\hat{k}_m] + \left[\frac{d\hat{c}_2}{dt}\right] + [\hat{k}_T]\right) \tag{5.1.57}$$

with

$$[\hat{k}_T] = \left[\frac{\partial^2}{\partial\hat{u}_m\partial\hat{u}_n}\hat{\Pi}\right] \tag{5.1.58}$$

defined as the tangent stiffness matrix of the sliding beam element in the fixed domain.

To obtain the incremental equations in the global coordinate system, we need to assemble the element incremental equations which yield:

$$\begin{aligned} {}^t_t[\hat{K}_{eq}]\,\{\Delta u\}^i = {} & -{}^t[\hat{M}]\;{}^{t+\Delta t}\left\{\frac{d^2u}{dt^2}\right\}^i - {}^t[\hat{C}_{eq}]\;{}^{t+\Delta t}\{\frac{du}{dt}\}^i + \\ & {}^{t+\Delta t}\{\hat{R}\} - {}^{t+\Delta t}_{t+\Delta t}\{\hat{F}\}^{i-1} + {}^t\lfloor\hat{F}_2\rfloor^T - {}^t\left\lfloor\frac{d\hat{F}_1}{dt}\right\rfloor^T \end{aligned} \tag{5.1.59}$$

### 5.1.3 Comparison of Two Formulations

Equations (5.1.24) and (5.1.56) show that both formulations have many features in common. In one case we use variable domain beam elements, i.e. the length of the beam element is time dependent and therefore the shape functions which are used to form the system matrices become time dependent; hence at each time step we need to update the system matrices.

In the other case, we transform the system equations to the constant domain at each instant of time and use the stretched beam element with fixed lengths. Here it is reasonable to use the time independent shape functions as in conventional finite element formulations and obtain the system matrices. But it is obvious that still we need to form the system matrices at each time step since these matrices are still time dependent due to their relations to the prescribed sliding motion of the beam. Therefore the perceived advantages of the constant-domain stretched beam element is questionable.

On the other hand in the second formulation, since the calculated response of the system is in the fixed domain, one needs to postprocess the solution and return to the physical system. Therefore to obtain the response of the system further computations are necessary.

In this respect, we question the statement made by Vu-Quoc and Li, 1995, that the use of the constant domain and the stretched coordinate system will reduce the difficulties of this problem and has advantages over the other techniques.

## 5.2 Consistent Co-Rotational Method

In this section we use the excellent technique of consistent co-rotational method which accounts for the geometric nonlinearities developed in chapter 2 to obtain the discretized equation of motion. The discretization procedure is carried out on the variable domain beam element, using both the sliding channel and the sliding beam formulations (see chapter 3) which lead to the same discretized system equations.

### 5.2.1 The sliding Channel Formulation

Let us consider the beam to be spatially fixed with a moving boundary as the channel slides. Then the structural deformation may be described by a time dependent map from the material configuration to the spatial configuration.

The material configuration, $\Upsilon_o$, is parameterized by the coordinates $(X_1, X_2)$ with the unit vectors $(\mathbf{J}_1, \mathbf{J}_2)$ and origin $O$.

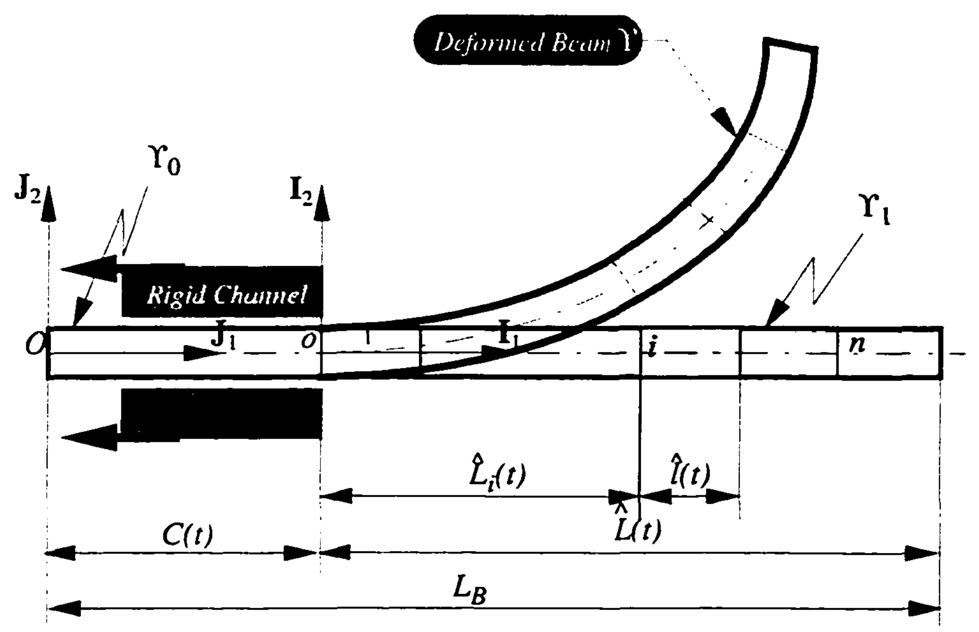


Figure 5.2.1: Sliding Channel Formulation: Kinematics Description.

We assume that the part inside the channel is rigid and the part outside the channel is deformable and can undergo large rotations and small deformations. Thus the deformable part of the material configuration which is outside the channel may be described as $\Upsilon_1$ , (see Figure 5.2.1).

We also may define the length of the material beam inside the channel as:

$$C(t) = L_B - \hat{L}(t) \tag{5.2.1}$$

where $\hat{L}(t)$ is the prescribed time dependent length of the beam outside the channel.

In co-rotational method, the deformation map from material configuration $\Upsilon_o$ to spatial configuration $\Upsilon$ may be decomposed into rigid body translation and rotation and small deformation.

Let the spatial point $m$ be the image of the material point $M$ on the centerline of the beam outside the channel under the deformation map; hence the position vector of this point at a given time $t$ with respect to the observer on the moving channel may be defined as (see Figure 5.2.2):

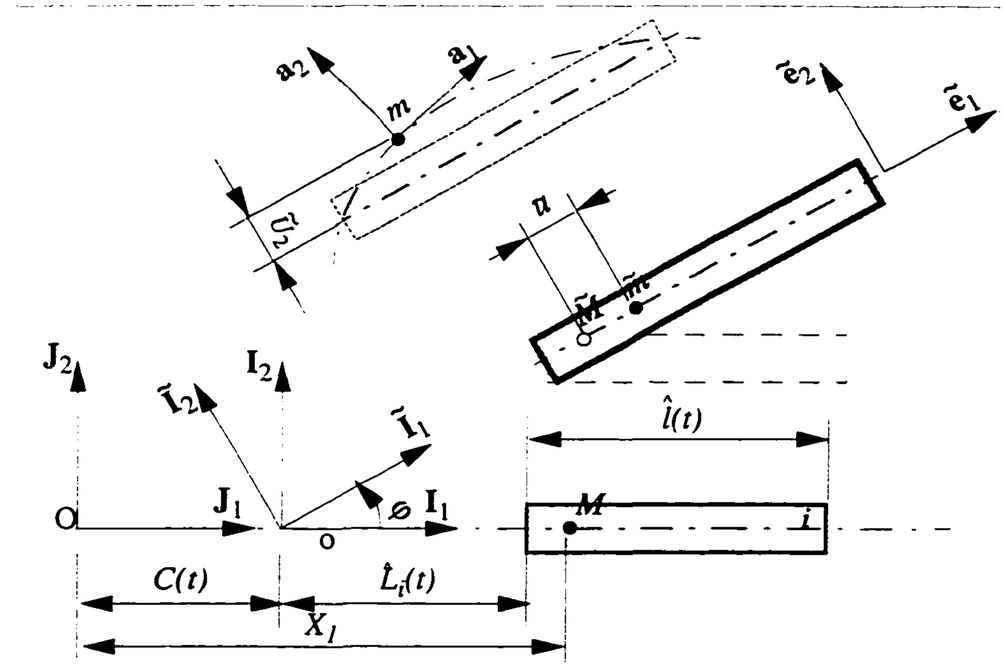


Figure 5.2.2: Sliding Channel Formulation: Co-rotational Axes.

$$\mathbf{R}_m = \left(X_1 - C - \hat{L}_i\right)\mathbf{I}_1 + \mathbf{u} \tag{5.2.2}$$

or

$$\mathbf{R}_m = D_i\ \mathbf{I}_1 + \mathbf{u} \tag{5.2.3}$$

where

$$D_i = X_1 - C - \hat{L}_i \tag{5.2.4}$$

and $\mathbf{u}$ corresponds to element coordinate system.

#### 5.2.1.1 Complementary Kinetic Energy

Time derivative of $\mathbf{R}_m$ leads to the velocity of the material point $m$, i.e.:

$$\begin{aligned} \frac{\partial \mathbf{R}_m}{\partial t} &= \frac{\partial D_i}{\partial t} \mathbf{I}_1 + \frac{\partial}{\partial t}\hat{\mathbf{u}} \\ &= v_i \mathbf{I}_1 + \frac{\partial}{\partial t}\hat{\mathbf{u}} \end{aligned} \tag{5.2.5}$$

The kinetic co-energy of the $i^{th}$ element may now be expressed as:

$$T_i^* = \frac{1}{2} \int_0^{\hat{l}(t)} \rho_o A \left( \frac{\partial \mathbf{R}_m}{\partial t} \cdot \frac{\partial \mathbf{R}_m}{\partial t} \right) dX_1 \tag{5.2.6}$$

Substituting equation (5.2.5) to equation (5.2.6), we obtain:

$$T_i^* = \frac{1}{2} \int_0^{\hat{l}(t)} \rho_o A \left( v_i \mathbf{I}_1 + \frac{\partial}{\partial t}\hat{\mathbf{u}} \right) \cdot \left( v_i \mathbf{I}_1 + \frac{\partial}{\partial t}\hat{\mathbf{u}} \right) dX_1 \tag{5.2.7}$$

Now let us introduce the co-rotational axis of this element with its origin at the moving observer $o$ and following the rigid body rotation of this element; then the displacement vector $\hat{\mathbf{u}}$ can be transformed to this axis as follows:

$$\hat{\mathbf{u}} = \mathbf{T}\tilde{\mathbf{u}} \tag{5.2.8}$$

where $\mathbf{T}$ is the rotation matrix from the co-rotational configuration to the initial material configuration defined as:

$$T_{jk} = \begin{bmatrix} \cos\varphi & -\sin\varphi \\ \sin\varphi & \cos\varphi \end{bmatrix} \tag{5.2.9}$$

Also we have:

$$\frac{\partial}{\partial t}\hat{\mathbf{u}} = \mathbf{T}\frac{\partial}{\partial t}\tilde{\mathbf{u}} + \frac{d\mathbf{T}}{dt}\tilde{\mathbf{u}} \tag{5.2.10}$$

Substituting equations (5.2.8) and (5.2.10) into equation (5.2.7), kinetic co-energy of the beam element may be expressed as:

$$T_i^* = \frac{1}{2}\int_0^{\hat{l}(t)} \rho_o A \left(\mathbf{T}\frac{\partial}{\partial t}\tilde{\mathbf{u}} + \frac{d\mathbf{T}}{dt}\tilde{\mathbf{u}}\right)\cdot\left(\mathbf{T}\frac{\partial}{\partial t}\tilde{\mathbf{u}} + \frac{d\mathbf{T}}{dt}\tilde{\mathbf{u}}\right)dX_1 + \int_0^{\hat{l}(t)} \rho_o A\,(v_i\ \mathbf{I}_1)\cdot\left(\mathbf{T}\frac{\partial}{\partial t}\tilde{\mathbf{u}} + \frac{d\mathbf{T}}{dt}\tilde{\mathbf{u}}\right)\,dX_1 + \frac{1}{2}\int_0^{\hat{l}(t)} \rho_o A\,(v_i\ \mathbf{I}_1)\cdot(v_i\ \mathbf{I}_1)\ dX_1 \tag{5.2.11}$$

To express the kinetic co-energy of the beam element in terms of the nodal variables, we model the axial and transverse deflection by linear and cubic interpolation functions, respectively, i.e.:

$$\tilde{u}_1 = \lfloor \mathcal{H}_1 \rfloor\ \{\tilde{u}\} \tag{5.2.12}$$

and

$$\tilde{u}_2 = \lfloor \mathcal{H}_2 \rfloor\ \{\tilde{u}\} \tag{5.2.13}$$

where for $-1 \le \zeta \le 1$

$$\lfloor \mathcal{H}_1 \rfloor = \left\lfloor \frac{1}{2}(1-\zeta) \quad 0 \quad 0 \quad \frac{1}{2}(1+\zeta) \quad 0 \quad 0 \right\rfloor \tag{5.2.14}$$

and

$$\lfloor \mathcal{H}_2 \rfloor = \left\lfloor 0 \quad \frac{\zeta^3}{4} - \frac{3}{4}\zeta + \frac{1}{2} \quad \frac{\hat{l}}{8}\left(\zeta^3 - \zeta^2 - \zeta + 1\right) \quad 0 \quad -\frac{\zeta^3}{4} + \frac{3}{4}\zeta + \frac{1}{2} \quad \frac{\hat{l}}{8}\left(\zeta^3 + \zeta^2 - \zeta - 1\right) \right\rfloor \tag{5.2.15}$$

and $\{\tilde{u}\}$ is the vector of the nodal variables. Also we should note that since we are using variable beam elements, shape functions are time dependent so that:

$$\frac{\partial \tilde{u}_j}{\partial t} = \lfloor \mathcal{H}_j \rfloor\ \{\frac{d}{dt}\tilde{u}\} + \left\lfloor \frac{\partial \mathcal{H}_j}{\partial t} \right\rfloor\ \{\tilde{u}\} \qquad j = 1, 2 \tag{5.2.16}$$

Now we may substitute the above expressions into the first term on the right hand side of equation (5.2.11) and obtain:

$$T_{i1}{}^* = \frac{1}{2}\ \{\frac{d}{dt}\tilde{u}\}^T\ [\tilde{m}]\ \{\frac{d}{dt}\tilde{u}\} - \frac{1}{2}\ \{\tilde{u}\}^T\ [\tilde{k}_m]\ \{\tilde{u}\}\ +$$
$$\frac{1}{2}\ \{\tilde{u}\}^T\ [\tilde{c}_1]\ \{\frac{d}{dt}\tilde{u}\} + \frac{1}{2}\ \{\frac{d}{dt}\tilde{u}\}^T\ [\tilde{c}_2]\ \{\tilde{u}\} \tag{5.2.17}$$

where

$$[\tilde{m}] = \int_0^{\hat{l}(t)} \rho_o A\, [\mathcal{H}]^T [\mathcal{H}]\ dX_1 \tag{5.2.18}$$

$$[\tilde{k}_m] = \int_0^{\hat{l}(t)} -\ \rho_o A \Bigg( [\mathcal{H}]^T \left[\frac{dT}{dt}\right]^T \left[\frac{dT}{dt}\right] [\mathcal{H}] + [\mathcal{H}]^T \left[\frac{dT}{dt}\right]^T [T] \left[\frac{d\mathcal{H}}{dt}\right] +$$
$$\left[\frac{d\mathcal{H}}{dt}\right]^T [T]^T \left[\frac{dT}{dt}\right] [\mathcal{H}] + \left[\frac{d\mathcal{H}}{dt}\right]^T \left[\frac{d\mathcal{H}}{dt}\right] \Bigg)\ dX_1 \tag{5.2.19}$$

$$[\tilde{c}_1] = \int_0^{\hat{l}(t)} \rho_o A \Bigg( [\mathcal{H}]^T \left[\frac{dT}{dt}\right]^T [T]\ [\mathcal{H}] + \left[\frac{d\mathcal{H}}{dt}\right]^T [\mathcal{H}] \Bigg)\ dX_1 \tag{5.2.20}$$

$$[\tilde{c}_2] = \int_0^{\hat{l}(t)} \rho_o A \Bigg( [\mathcal{H}]^T [T]^T \left[\frac{dT}{dt}\right] [\mathcal{H}] + [\mathcal{H}]^T \left[\frac{d\mathcal{H}}{dt}\right] \Bigg)\ dX_1 \tag{5.2.21}$$

where the components of $[\mathcal{H}]$ are given in equations (5.2.14) and (5.2.15). In equation (5.2.17), the nodal variables in the co-rotational frame may be transformed to the global coordinate system using the transformation:

$$\{\tilde{u}\} = [Q]\ \{\hat{u}\} \tag{5.2.22}$$

The time derivative of $\{\tilde{u}\}$ is then obtained as:

$$\{\frac{d}{dt}\tilde{u}\} = [Q]\ \{\frac{d}{dt}\hat{u}\} + \left[\frac{dQ}{dt}\right] \{\hat{u}\} \tag{5.2.23}$$

where

$$[Q] = \begin{bmatrix} \cos\varphi & \sin\varphi & 0 & 0 & 0 & 0 \\ -\sin\varphi & \cos\varphi & 0 & 0 & 0 & 0 \\ 0 & 0 & 1 & 0 & 0 & 0 \\ 0 & 0 & 0 & \cos\varphi & \sin\varphi & 0 \\ 0 & 0 & 0 & -\sin\varphi & \cos\varphi & 0 \\ 0 & 0 & 0 & 0 & 0 & 1 \end{bmatrix} \tag{5.2.24}$$

Substituting equations (5.2.22) and (5.2.23) into equation (5.2.17), we obtain:

$$\begin{aligned} T_{i1}{}^* = \frac{1}{2}\ \{\frac{d}{dt}\hat{u}\}^T\ [m]\ \{\frac{d}{dt}\hat{u}\} - \frac{1}{2}\ \{\hat{u}\}^T\ [k_m]\ \{\hat{u}\}\ + \\ \frac{1}{2}\ \{\hat{u}\}^T\ [c_1]\ \{\frac{d}{dt}\hat{u}\} + \frac{1}{2}\ \{\frac{d}{dt}\hat{u}\}^T\ [c_2]\ \{\hat{u}\} \end{aligned} \tag{5.2.25}$$

where

$$[m] = [Q]^T [\tilde{m}]\, [Q] \tag{5.2.26}$$

$$[c_1] = \left[\frac{dQ}{dt}\right]^T [\tilde{m}]\, [Q] + [Q]^T [\tilde{c}_1]\, [Q] \tag{5.2.27}$$

$$[c_2] = [Q]^T [\tilde{m}] \left[\frac{dQ}{dt}\right] + [Q]^T [\tilde{c}_2]\, [Q] \tag{5.2.28}$$

$$\begin{aligned} [k_m] = \left[\frac{dQ}{dt}\right]^T [\tilde{m}] \left[\frac{dQ}{dt}\right] + [Q]^T [\tilde{c}_1] \left[\frac{dQ}{dt}\right] \\ \left[\frac{dQ}{dt}\right]^T [\tilde{c}_2]\, [Q] + [Q]^T [\tilde{k}_m]\, [Q] \end{aligned} \tag{5.2.29}$$

Now we need to obtain the second term in the right hand side of equation (5.2.11) which causes the sliding inertia force. By substituting equations (5.2.22) and (5.2.23) into equations (5.2.12), (5.2.13) and (5.2.16), we obtain:

$$\{\tilde{u}_j\} = [\mathcal{H}]\, [Q]\, \{\hat{u}\} \tag{5.2.30}$$

and

$$\left\{\frac{\partial \tilde{u}_j}{\partial t}\right\} = \left[\frac{\partial \mathcal{H}}{\partial t}\right] [Q]\, \{\hat{u}\} + [\mathcal{H}] \left[\frac{dQ}{dt}\right] \{\hat{u}\} + [\mathcal{H}]\, [Q]\, \{\frac{d}{dt}\hat{u}\} \tag{5.2.31}$$

where $j = 1,2$. Substituting equations (5.2.30) and (5.2.31) into the second term on the right hand side of equation (5.2.11), we obtain:

$$T_{i2}^* = \lfloor f_1 \rfloor \ \{\frac{d}{dt}\dot{u}\} + \lfloor f_2 \rfloor \ \{\dot{u}\} \tag{5.2.32}$$

where

$$\lfloor f_1 \rfloor = \int_0^{\hat{l}(t)} \rho_o A\Big( v_i \ \lfloor I_1 \rfloor \Big) [T] \ [\mathcal{H}] \ [Q] \ dX_1 \tag{5.2.33}$$

and

$$\lfloor f_2 \rfloor = \int_0^{\hat{l}(t)} \rho_o A\Big( v_i \ \lfloor I_1 \rfloor \Big) \left( \left[\frac{dT}{dt}\right] [\mathcal{H}] \ [Q] + [T] \ [\mathcal{H}] \left[\frac{dQ}{dt}\right] + [T] \left[\frac{d\mathcal{H}}{dt}\right] [Q] \right) dX_1 \tag{5.2.34}$$

Equations (5.2.33) and (5.2.34) show that the inertia forces due to the sliding motion of the beam, remain directed along the initial undeformed axis.

Since the third term in equation (5.2.11) is prescribed, it does not contribute to the discretized equations of motion of the system.

### 5.2.1.2 Element Lagrangian Function

The element Lagrangian function may be defined by using the element kinetic co-energy and strain energy due to large rotations and small deformations, i.e.:

$$\begin{aligned} \mathcal{L}_i = {} & \frac{1}{2} \ \{\frac{d}{dt}\dot{u}\}^T \ [m] \ \{\frac{d}{dt}\dot{u}\} - \frac{1}{2} \ \{\dot{u}\}^T \ [k_m] \ \{\dot{u}\} - \Pi_i + \\ & \frac{1}{2} \ \{\dot{u}\}^T \ [c_1] \ \{\frac{d}{dt}\dot{u}\} + \frac{1}{2} \ \{\frac{d}{dt}\dot{u}\}^T \ [c_2] \ \{\dot{u}\} + \\ & \lfloor f_1 \rfloor \ \{\frac{d}{dt}\dot{u}\} + \lfloor f_2 \rfloor \ \{\dot{u}\} + pr \end{aligned} \tag{5.2.35}$$

where $\Pi_i$ is the element strain energy and $pr$ is the prescribed part of the kinetic co-energy.

### 5.2.1.3 Discretized Equations of Motion

Substituting the element Lagrangian function into Hamilton's principle (equation (5.1.19)), we may obtain the discretized equations of motion of the system. These equations are nonlinear and may be piece-wise linearized via the full Newton-Raphson method and solved to obtain the system response at the $i^{th}$ iteration and time step $t + \Delta t$ as (see section 5.1.1.3):

$$
\begin{aligned}
{}^{t+\Delta t}[m]\,{}^{t+\Delta t}\left\{\frac{d^2}{dt^2}\hat{u}\right\}^i + {}^{t+\Delta t}[c_{eq}]\,{}^{t+\Delta t}\left\{\frac{d}{dt}\hat{u}\right\}^i + {}^{t+\Delta t}[k_{eq}]\,\{\Delta\hat{u}\}^i = \\
{}^{t+\Delta t}\{\hat{r}\} - {}^{t+\Delta t}\{f\}^{i-1} + {}^{t+\Delta t}\{f_{eq}\}
\end{aligned}
\qquad (5.2.36)
$$

where

$$[c_{eq}] = \left[\frac{dm}{dt}\right] + [c_2] - [c_2]^T \qquad (5.2.37)$$

is the equivalent damping matrix and

$$[k_{eq}] = [k_m] + [k_T] + \left[\frac{dc_2}{dt}\right] \qquad (5.2.38)$$

is the equivalent stiffness matrix. The tangent stiffness matrix $[k_T]$ is given by:

$$[k_T] = \left[\frac{\partial^2 \Pi}{\partial \hat{u}_m \partial \hat{u}_n}\right] \qquad (5.2.39)$$

The equivalent sliding inertia force vector is obtained from:

$$\{f_{eq}\} = \lfloor f_2 \rfloor^T - \left\lfloor \frac{df_1}{dt} \right\rfloor^T \qquad (5.2.40)$$

and the element internal force vector $\{f\}$ is derived from;

$$\{f\} = \left[\frac{\partial \Pi}{\partial \{\hat{u}\}}\right] \qquad (5.2.41)$$

To form the sum total of all the elements, equation (5.2.36) may be assembled yielding:

$$
\begin{aligned}
{}^{t+\Delta t}[M]\;{}^{t+\Delta t}\{\frac{d^2}{dt^2}u\}^{i} + {}^{t+\Delta t}[C_{eq}]\;{}^{t+\Delta t}\{\frac{d}{dt}u\}^{i} + {}^{t+\Delta t}[K_{eq}]\,\{\Delta u\}^{i} &= \\
{}^{t+\Delta t}\{R\} - {}^{t+\Delta t}\{F\}^{i-1} + {}^{t+\Delta t}\{F_{eq}\}
\end{aligned}
\tag{5.2.42}
$$

### 5.2.2 The Sliding Beam Formulation

In this formulation, the rigid channel is fixed and the beam has prescribed sliding motion and undergoing large rotations and small deformations. The basis of this formulation has been extensively discussed in chapter 3.

The inertially fixed intermediate configuration which has a moving boundary may be described as $\Im$ (see Figure 5.2.3).

The sliding rigid body motion of a material point $M$ on the centerline of the beam along the channel axis that coincides and passes by inertially fixed point $\bar{m}$ in this configuration may be defined as:

$$
\begin{aligned}
\chi_1 &= X_1 - L_B + \hat{L}(t) \\
\chi_2 &= X_2
\end{aligned}
\tag{5.2.43}
$$

In the co-rotational method, the large deflection of a material point in the intermediate configuration to the deformed configuration may be decomposed into a rigid body translation and rotation and small deformations.

Now we divide the beam outside the channel by $n$ time variable domain beam elements. The position vector of a material point $m$ in the deformed configuration with respect to point $o$ with the origin on the fixed coordinate system in the intermediate configuration, may be expressed as (see Figure 5.2.4):

$$
\mathbf{R}_m = \left(\chi_1 - \hat{L}_i\right)\mathbf{I}_1 + \grave{\mathbf{u}}
\tag{5.2.44}
$$

where $\grave{\mathbf{u}}$ is the displacement vector corresponding to the element coordinate system.

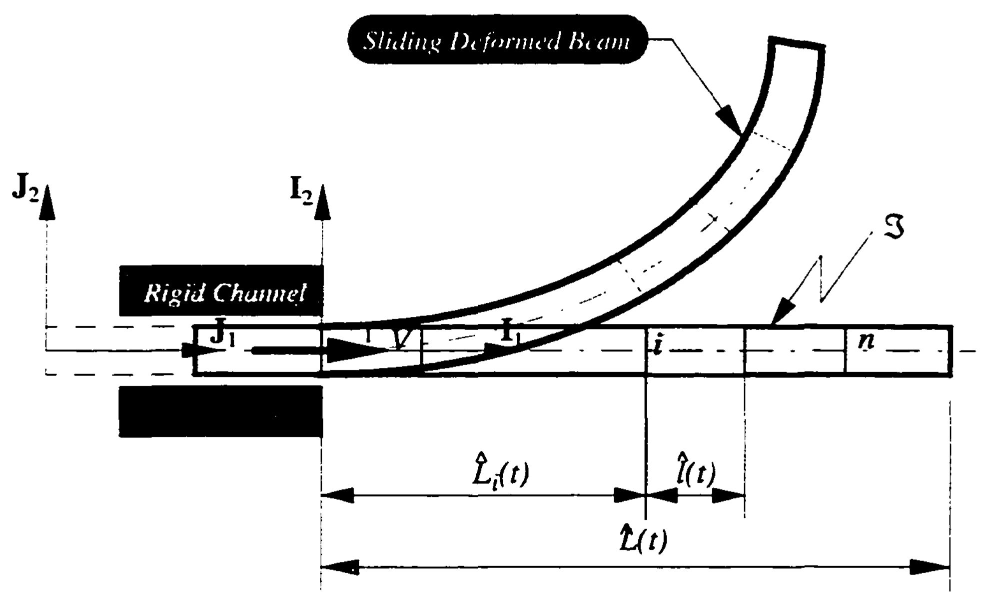


Figure 5.2.3: Sliding Beam Formulation: Kinematics Description.

#### 5.2.2.1 Complementary Kinetic Energy

The velocity of the material point $m$ is obtained from differentiation of $\mathbf{R}_m$ with respect to time, i.e.:

$$\begin{aligned} \frac{d\mathbf{R}_m}{dt} &= v_i\ \mathbf{I}_1 + \frac{d\mathbf{u}}{dt} \\ &= v_i\ \mathbf{I}_1 + v_i\ \frac{\partial \mathbf{u}}{\partial \chi_1} + \frac{\partial \mathbf{u}}{\partial t} \end{aligned} \tag{5.2.45}$$

where $v_i$ is defined in equation (5.1.3).

Using equation (5.2.45), one may express the kinetic co-energy of the beam element as:

$$T_i^* = \frac{1}{2} \int_0^{\hat{l}(t)} \rho_o A \left( v_i\ \mathbf{I}_1 + v_i\ \frac{\partial \mathbf{u}}{\partial \chi_1} + \frac{\partial \mathbf{u}}{\partial t} \right) \cdot \left( v_i\ \mathbf{I}_1 + v_i\ \frac{\partial \mathbf{u}}{\partial \chi_1} + \frac{\partial \mathbf{u}}{\partial t} \right) d\chi_1 \tag{5.2.46}$$

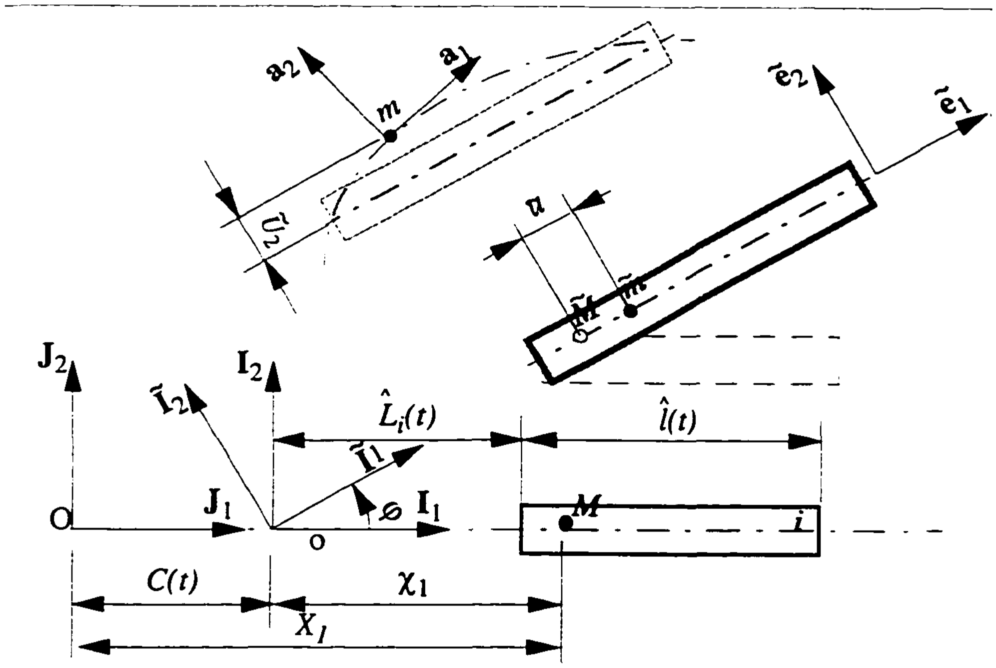


Figure 5.2.4: Sliding Beam Formulation: Co-rotational element.

After transforming the displacement vector **u** into the co-rotational axis and using the shape functions defined in equations (5.2.12) and (5.2.13), one may obtain the element kinetic co-energy in terms of the nodal variables as:

$$T_i^* = \frac{1}{2}\ \{\frac{d}{dt}\tilde{u}\}^T\ [\tilde{m}]\ \{\frac{d}{dt}\tilde{u}\} - \frac{1}{2}\ \{\tilde{u}\}^T\ [\tilde{k}_m]\ \{\tilde{u}\}\ +$$
$$\frac{1}{2}\ \{\tilde{u}\}^T\ [\tilde{c}_1]\ \{\frac{d}{dt}\tilde{u}\} + \frac{1}{2}\ \{\frac{d}{dt}\tilde{u}\}^T\ [\tilde{c}_2]\ \{\tilde{u}\}\ + \tag{5.2.47}$$
$$\lfloor f_1 \rfloor\ \{\frac{d}{dt}\tilde{u}\} + \lfloor f_2 \rfloor\ \{\tilde{u}\} + pr$$

where

$$[\tilde{m}] = \int_0^{\hat{l}(t)} \rho_o A\, [\mathcal{H}]^T [\mathcal{H}]\ d\chi_1 \tag{5.2.48}$$

$$[\tilde{k}_m] = \int_0^{\hat{l}(t)} -\rho_o A\Big( [\mathcal{H}]^T\left[\frac{dT}{dt}\right]^T\left[\frac{dT}{dt}\right][\mathcal{H}] + [\mathcal{H}]^T\left[\frac{dT}{dt}\right]^T[T]\left[\frac{\partial\mathcal{H}}{\partial t}\right] +$$

$$v_i[\mathcal{H}]^T\left[\frac{dT}{dt}\right]^T[T]\left[\frac{\partial\mathcal{H}}{\partial\chi_1}\right] + \left[\frac{\partial\mathcal{H}}{\partial t}\right]^T[T]^T\left[\frac{dT}{dt}\right][\mathcal{H}] +$$

$$v_i\left[\frac{\partial\mathcal{H}}{\partial\chi_1}\right]^T[T]^T\left[\frac{dT}{dt}\right][\mathcal{H}] + v_i\left[\frac{\partial\mathcal{H}}{\partial\chi_1}\right]^T\left[\frac{\partial\mathcal{H}}{\partial t}\right] + v_i\left[\frac{\partial\mathcal{H}}{\partial t}\right]^T\left[\frac{\partial\mathcal{H}}{\partial\chi_1}\right] \tag{5.2.49}$$

$$v_i^2\left[\frac{\partial\mathcal{H}}{\partial\chi_1}\right]^T\left[\frac{\partial\mathcal{H}}{\partial\chi_1}\right] + \left[\frac{\partial\mathcal{H}}{\partial t}\right]^T\left[\frac{\partial\mathcal{H}}{\partial t}\right]\Big)\, d\chi_1$$

$$[\tilde{c}_1] = \int_0^{\hat{l}(t)} \rho_o A\Big( [\mathcal{H}]^T\left[\frac{dT}{dt}\right]^T[T]\,[\mathcal{H}] + \left[\frac{\partial\mathcal{H}}{\partial t}\right]^T[\mathcal{H}] +$$

$$v_i\left[\frac{\partial\mathcal{H}}{\partial\chi_1}\right]^T[\mathcal{H}]\Big)\, d\chi_1 \tag{5.2.50}$$

$$[\tilde{c}_2] = \int_0^{\hat{l}(t)} \rho_o A\Big( [\mathcal{H}]^T[T]^T\left[\frac{dT}{dt}\right][\mathcal{H}] + [\mathcal{H}]^T\left[\frac{\partial\mathcal{H}}{\partial t}\right] +$$

$$v_i\,[\mathcal{H}]^T\left[\frac{\partial\mathcal{H}}{\partial\chi_1}\right]\Big)\, d\chi_1 \tag{5.2.51}$$

$$\lfloor\tilde{f}_1\rfloor = \int_0^{\hat{l}(t)} \rho_o A\lfloor v_i \quad 0\rfloor\,[\mathcal{H}]\, d\chi_1 \tag{5.2.52}$$

$$\lfloor\tilde{f}_2\rfloor = \int_0^{\hat{l}(t)} \rho_o A\Big(\lfloor v_i \quad 0\rfloor\,[T]^T\left[\frac{dT}{dt}\right][\mathcal{H}] + \lfloor v_i \quad 0\rfloor\left[\frac{\partial\mathcal{H}}{\partial t}\right] +$$

$$\lfloor v_i^2 \quad 0\rfloor\left[\frac{\partial\mathcal{H}}{\partial\chi_1}\right]\Big)\, d\chi_1 \tag{5.2.53}$$

Now one may follow the procedures in section 5.2.1 to obtain the discretized system equations in the global coordinates.

Evidently the shape functions defined for the beam elements in the sliding channel formulation are space and time dependent as seen by the observer on the sliding channel and therefore we have:

$$\left[\frac{d\mathcal{H}}{dt}\right] = \left[\frac{\partial\mathcal{H}}{\partial t}\right] + v_i \left[\frac{\partial\mathcal{H}}{\partial \chi_1}\right] \quad (5.2.54)$$

Expression for $[d\mathcal{H}/dt]$ is given in Appendix G.

It is interesting to note that the above relation can be used in the system matrices and equations in the sliding channel formulation to obtained the same expressions for the sliding beam formulation.

## 5.3 Conclusions

In the foregoing we have used two methods previously discussed in chapter 2, i.e. the updated Lagrangian method and the consistent co-rotational method to solve the non-linear flexible sliding channel problem.

To discretize the system equations, two types of beam elements: variable domain elements and constant domain stretched elements were introduced. It was found that since the system matrices are time dependent in both approaches, there is little advantage of one approach over the other. Further, additional computational work is needed in the fixed domain approach to transform back to the real physical system. Therefore we have chosen the variable domain elements to implement and obtain the time response of the system.

In the consistent co-rotational finite element, we used the sliding channel and the sliding beam formulations, described in chapter 3, to obtain the discretized equations of motion. Finally we showed that through proper transformations the two formulations are related and describe the same physical problem.

In the next chapter we integrate the discretized equations of motion obtained in this chapter and determine the response of the system in time.

# Chapter 6

# Transient Response of Flexible Sliding Beams

In this chapter we obtain solutions for the discretized incremental system equations, obtained in chapter 5, under certain initial and boundary conditions and/or specified applied loads, using the variable domain beam element. In the absence of known theoretical or experimental results for such a system, we rely on the plausibility of the results on physical grounds to support our findings. As a check on the validity of implementation, we first use the program as a linear solver and obtain results for the axially inextensible sliding beams which we compare with the results reported in the literature. Second we set the axial velocity to zero and solve some special cases when the length of the beam is constant. In this case we check the formulation and its implementation for nonlinearities in the system due to large displacements. Finally we solve the sliding beam problems for small amplitude oscillations (linear range), with the nonlinear solver and compare the results with those obtained by the linear solver used for inextensible sliding beams.

With these preliminary comparisons completed, we obtain the transient response of the free and forced large amplitude vibrations of the flexible sliding beam and demonstrate the need for using a nonlinear analysis for this complex system. Finally we consider the stability of the motion of periodically time varying flexible sliding beams and show that in the case of parametric resonance, the unstable regions obtained in the linear analysis, which imply unbounded amplitudes, are indeed stable and bounded when nonlinear terms are taken into account.

## 6.1 Inextensible Flexible Sliding Beams: Linear Analysis

In this section we use the codes developed for the updated Lagrangian (UL) and the consistent co-rotational (CC) methods, but we deactivate the nonlinear parts of these codes and render them suitable for the dynamic analysis of inextensible flexible sliding beams. Then we solve some problems in the linear range and verify the obtained results by comparisons with those reported in the literature. To make quantitative comparisons, we need to introduce structural damping forces in the form of the so called Rayleigh-type damping and add their effects to the equivalent damping obtained in chapter 5 (see e.g. Petyt, 1990, and Bathe, 1982). To obtain the damping coefficients, we use the experimentally-obtained modal damping functions used by Yuh and Young, 1991, namely:

$$\begin{aligned} \zeta_1 &= \frac{0.4874}{4L^2\omega_1} \\ \zeta_2 &= \frac{3.124}{4L^2\omega_2} \end{aligned} \tag{6.1.1}$$

where $\omega_1$ and $\omega_2$ are the instantaneous first and second natural frequencies of a cantilever sliding beam of length $L(t)$ .

### 6.1.1 Spaghetti and Reverse Spaghetti Problems: Quadratic Sliding Motion

We use 4 elements to model the sliding beam. The quadratic sliding motion of the beam may be expressed as:

$$L(t) = L_o + V_o\ t + \frac{A_o\ t^2}{2} \tag{6.1.2}$$

Let us consider a constant velocity spaghetti problem with the initial length of 0.525 ($m$) and constant sliding velocity of $-0.1145$ ($m/s$). The beam properties are: mass density = 3144.3858 ($kg/m^3$), Young's modulus = $68.96 \times 10^9$ ($N/m^2$), area = $4.3434 \times 10^{-5}$ ($m^2$) and second moment of area = $1.059 \times 10^{-11}$ ($m^4$). For this problem we test the UL formulation and obtain the time history of the tip deflection as given in Figure 6.1.1. This result is identical to that obtained in test case #1 by Stylianou, 1993, and in the Figure the two sets of results are superimposed.

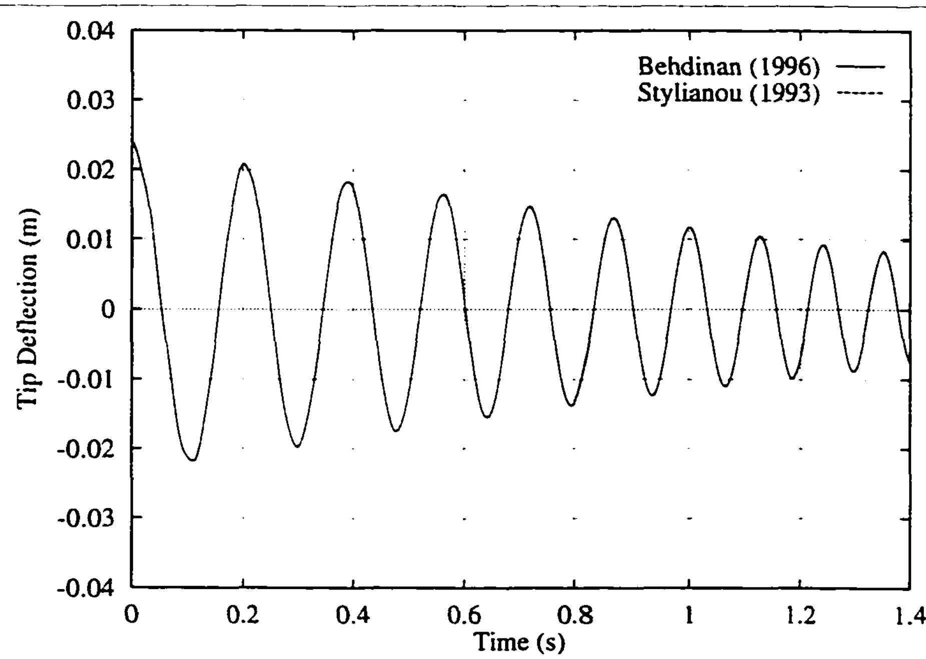


Figure 6.1.1: Spaghetti Problem: Constant Velocity Retraction, UL Program.

For the case of constant velocity reverse spaghetti problem we consider a beam extruding from a rigid channel with the initial length of 0.4255 ($m$) and velocity of 0.0410 ($m/s$). This case is solved using the consistent co-rotational formulation where the transient response of the beam is shown in Figure 6.1.2 and is identical to the test case #2 reported by Stylianou, 1993.

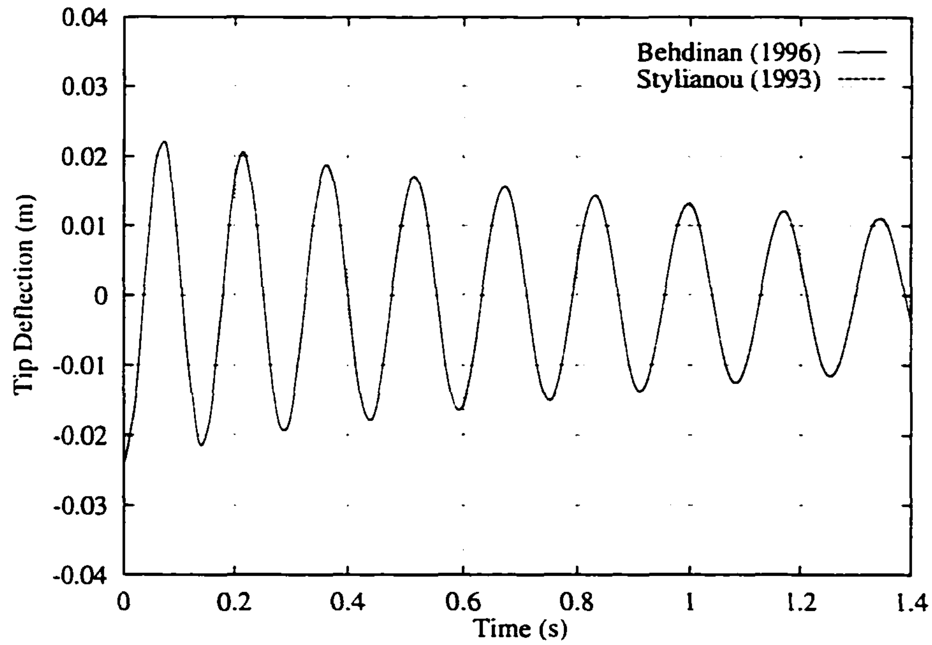


Figure 6.1.2: Reverse Spaghetti Problem: Constant Velocity Extrusion, C.C. Formulation.

The case of accelerated spaghetti problem may also be checked using the CC formulation. In this case we consider a beam with initial length of 0.525 (*m*) and initial sliding velocity of -0.03 (*m/s*) retracting from a rigid fixed channel with constant axial acceleration of -0.054 ($m/s^2$). The transient response shown in Figure 6.1.3 is found to be identical to the test case #3 reported by Stylianou, 1993.

For the case of constant accelerated extrusion we use a sliding beam with the initial length of 0.44 (*m*) and sliding extruding initial velocity of 0.008 (*m/s*) and constant acceleration of 0.015 ($m/s^2$). Using the UL method, again, the time history of the tip deflection is identical to the one obtained in test case #4 by Stylianou, 1993 (see Figure 6.1.4).

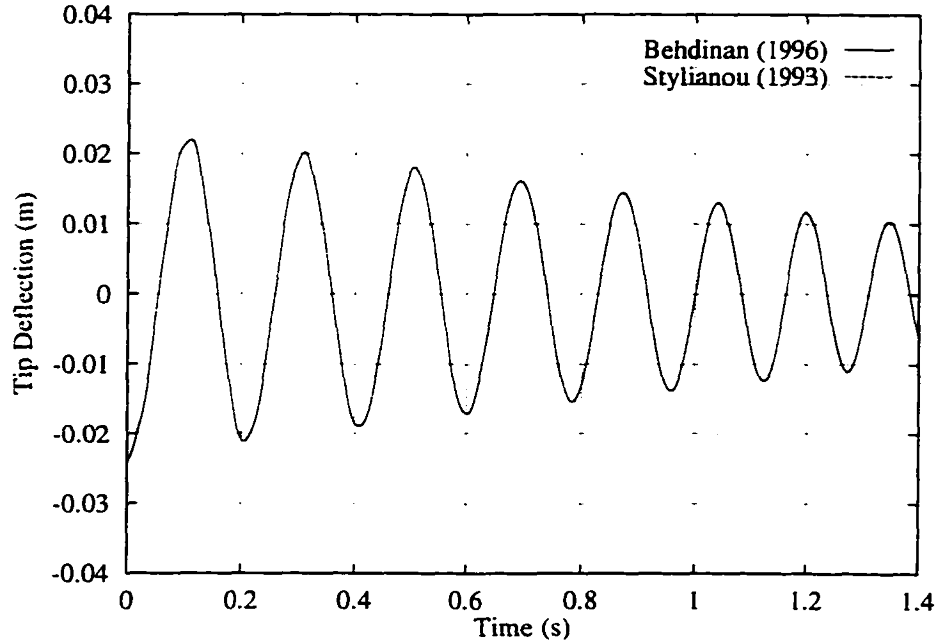


Figure 6.1.3: Spaghetti Problem: Constant Accelerated Retraction, CC Formulation.

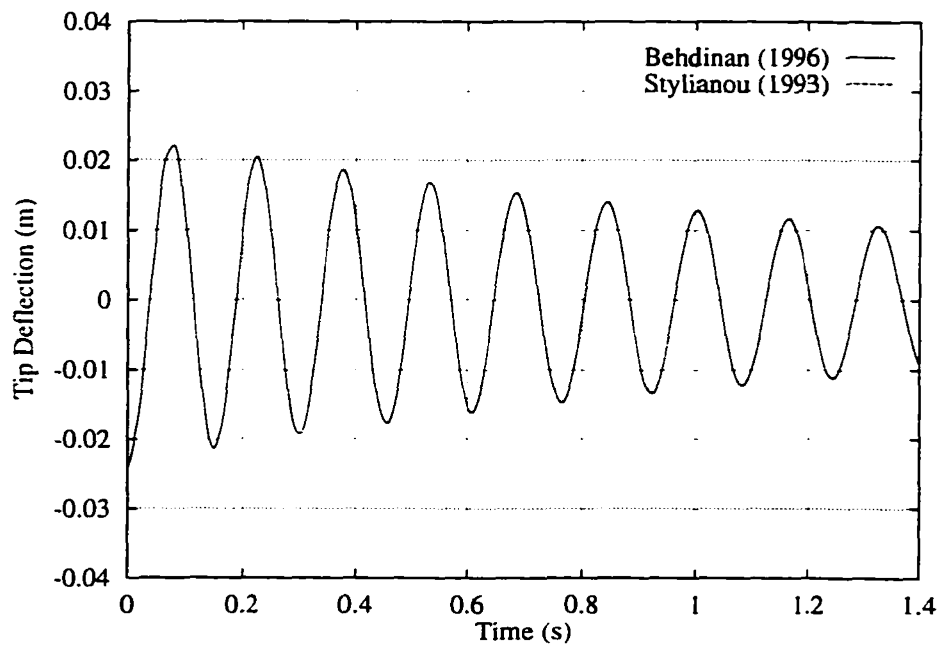


Figure 6.1.4: Reverse Spaghetti Problem: Constant Accelerated Extrusion, UL Formulation.

### 6.1.2 Spaghetti and Reverse Spaghetti Problems: Repositional Motion

For these simulations the prescribed length of the beam is taken as:

$$L(t) = L_o + \frac{c_o}{t_o}\left[t - \frac{t_o}{2\pi}\sin\left(\frac{2\pi t}{t_o}\right)\right] \tag{6.1.3}$$

In this case, first we consider a low frequency extrusion of $t_o = 1.2$ $(s)$ with the initial beam length of $L_o = 0.35$ $(m)$ and $c_o = 0.7$ $(m)$. It should be noted that equation (6.1.3) consists of a constant and an oscillatory part. The result obtained using the CC formulation is identical to the simulation #1 reported by Stylianou, 1993 (see Figure 6.1.5).

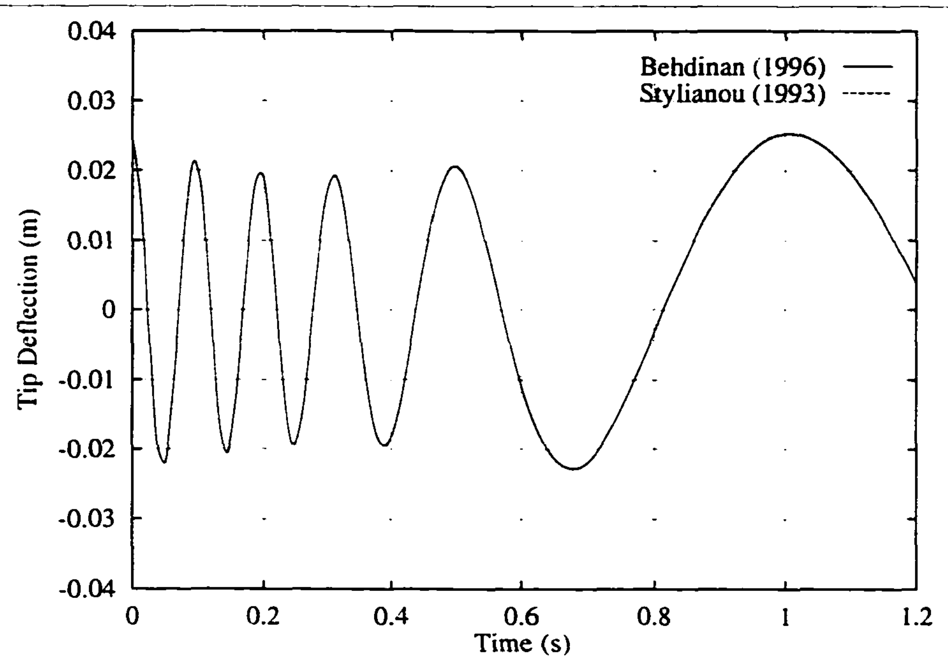


Figure 6.1.5: Low Frequency Reverse Spaghetti Problem: CC Formulation.

Now we may examine the low frequency spaghetti problem using the UL method. In this case we consider a beam with initial length of 1.05 $(m)$ and constant $c_o$ as -0.7 $(m)$. Tip deflection history shown in Figure 6.1.6 is also identical with the one reported by Stylianou, 1993, simulation #3.

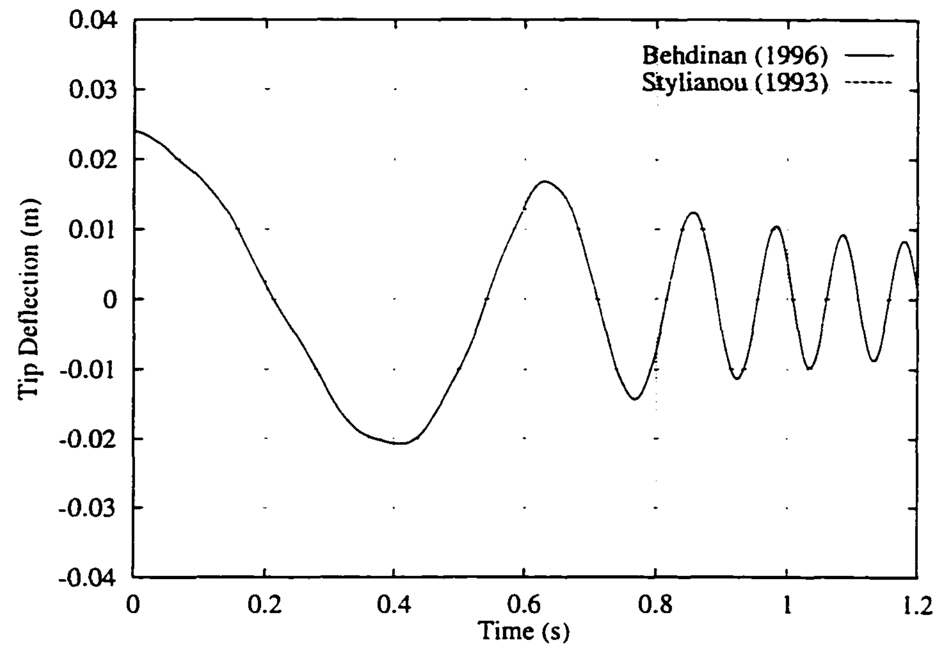


Figure 6.1.6: Low Frequency Spaghetti Problem: UL Technique.

Next let us consider the high frequency extrusion. In this case $t_o = 0.2$ ($s$), $L_o = 0.35$ ($m$) and $c_o = 0.7$ ($m$). This problem can also be solved by the UL formulation. The obtained results are identical to those obtained by Stylianou, 1993, simulation case #5 (see Figure 6.1.7).

In the case of high frequency spaghetti problem we consider the initial beam length of 1.05 ($m$) and the constant $c_o = -0.7$ ($m$). Using the CC formulation we compute the time response of the free end of the beam. Again the results shown in Figure 6.1.8 are identical to the simulation case #7 reported by Stylianou, 1993.

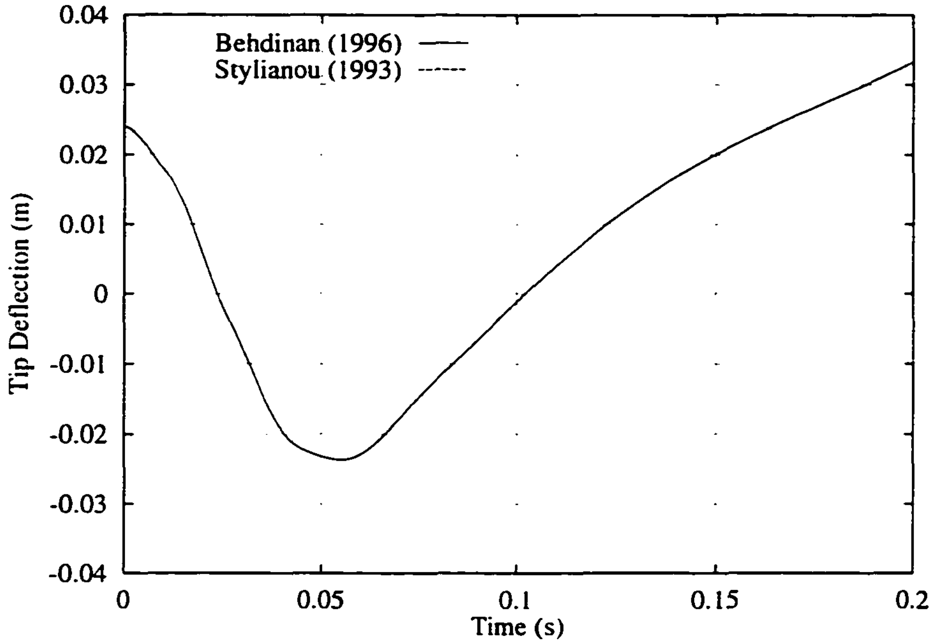


Figure 6.1.7: High Frequency Reverse Spaghetti Problem: UL Formulation.

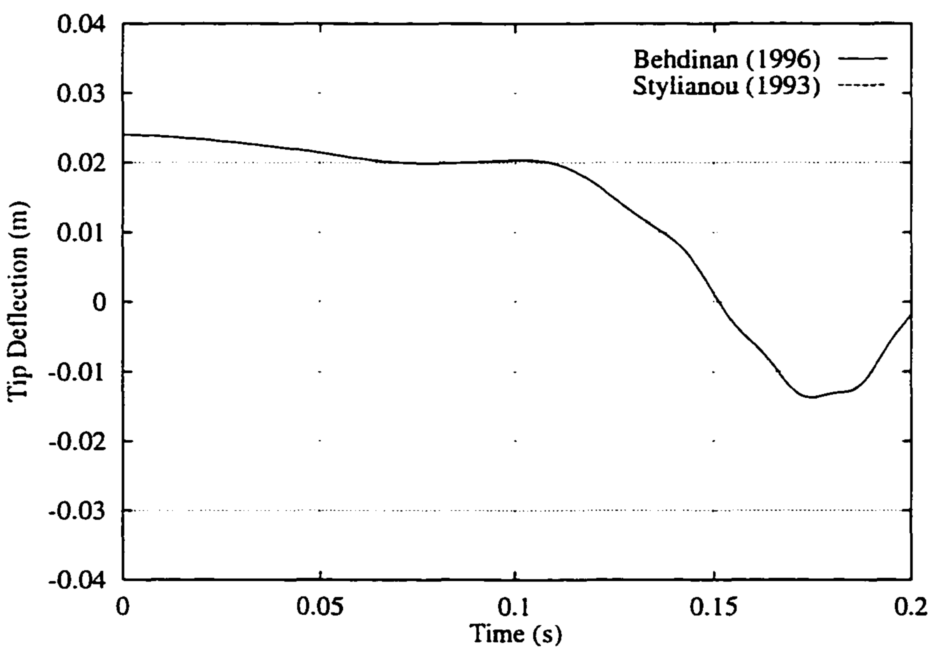


Figure 6.1.8: High Frequency Spaghetti Problem: CC Formulation.

### 6.1.3 Spaghetti and Reverse Spaghetti Problem: High Frequency Perturbation

The effect of high frequency low amplitude perturbations, to the otherwise constant velocity axial motion, was discussed in chapter 4, and was shown to attenuate the transverse oscillations of flexible sliding beams. As in chapter 4 we use the prescribed motion of the beam as:

$$L(t) = L_o(1 + \varepsilon \sin\hat{\omega}t) + V_o t \tag{6.1.4}$$

Let us consider a flexible sliding beam with an initial length of 0.525 ($m$) and constant retraction velocity -0.1145 ($m/s$). The perturbation factor and the frequency of perturbation are taken as 0.0133 and $11\omega_1$, respectively, where $\omega_1$ is the instantaneous fundamental natural frequency of the flexible sliding beam. Using the UL formulation, the result obtained are in good agreement with those obtained by Stylianou, 1993, see Figure 6.1.9.

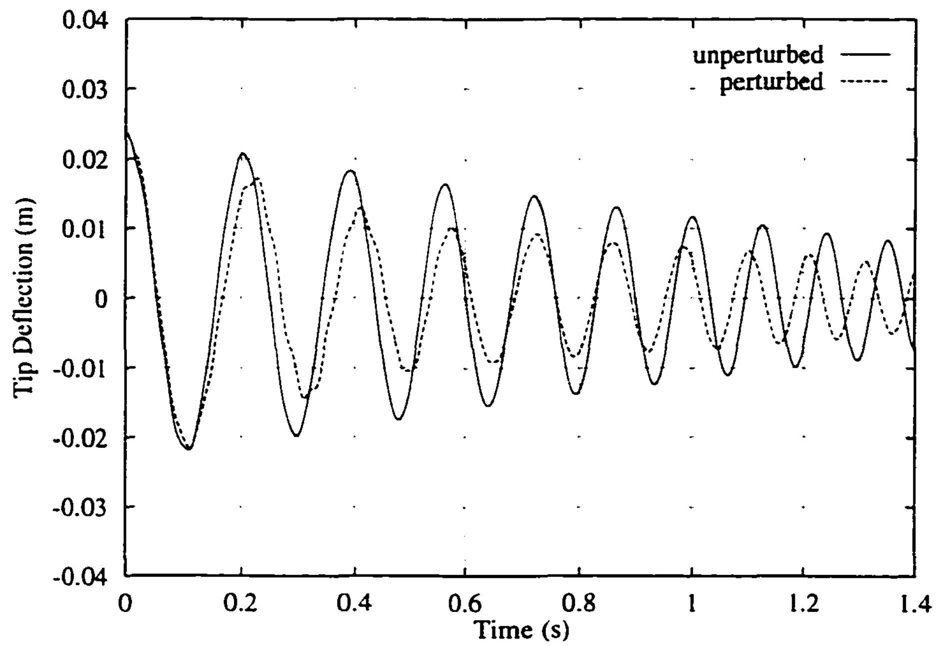


Figure 6.1.9: Spaghetti Problem: High Frequency Perturbation, UL Formulation.

For the case of the reverse spaghetti problem, we consider a beam with initial length of 0.4255 ($m$) extruding from a rigid-fixed channel with a constant velocity of 0.041 ($m/$

$s$). The perturbation factor is chosen as 0.0165. To solve, we use the program based on the CC formulation. Figure 6.1.10 shows the resulting suppression of the oscillations and is in good agreement with the results reported by Stylianou, 1993.

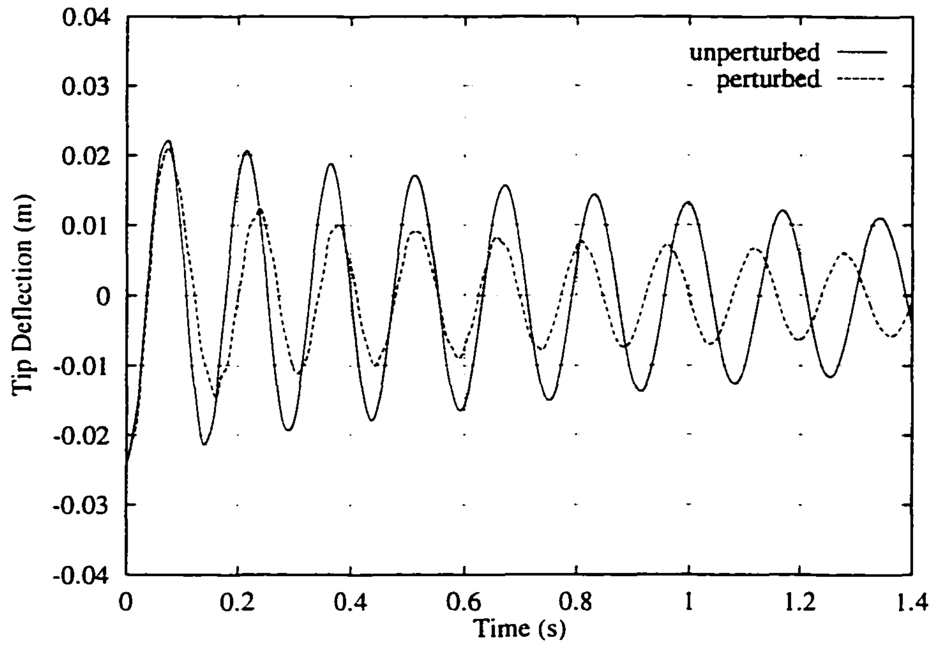


Figure 6.1.10: Reverse Spaghetti Problem: High Frequency Perturbation, CC Formulation.

### 6.1.4 Parabolic Extrusion

For the linear analysis of inextensible flexible sliding beams, Tabarrok et al., 1974, showed that there exists a similarity solution in the special case when the beam extrudes from a rigid-fixed wall with a prescribed axial velocity such that:

$$L(t) = \hat{\alpha} \sqrt{t} \tag{6.1.5}$$

Stylianou, 1993, extensively studied this case and stated that the beam will not oscillate throughout its extrusion history. This indicates that the parabolic extrusion is a severe test for the formulation and implementation procedures. Here we use two finite element models, one with 4 elements and the other with 10 elements. The beam properties are: E = 200 x $10^9$ (Pa), $\rho$ = 7000.0 ($kg/m^3$), I = 20 x $10^{-9}$ ($m^4$) and A = 250 x

$10^{-6}$ ($m^2$). We used both formulations and obtained identical results which are found to be in good agreement with the results reported by Stylianou, 1993, see Figure 6.1.11.

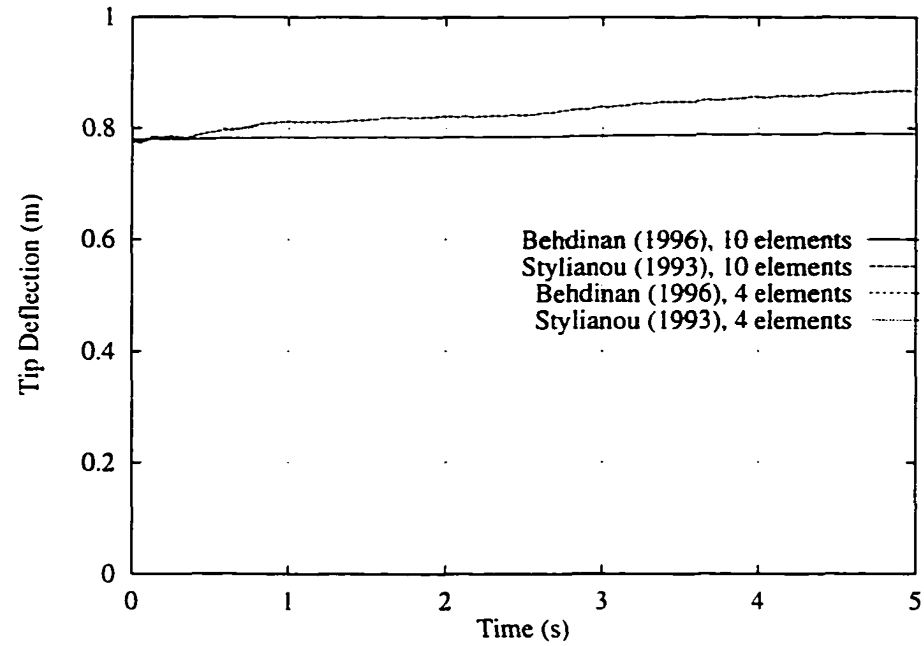


Figure 6.1.11: Similarity Simulation: Tip Deflection History.

## 6.2 Flexible Constant Length Beam: Nonlinear Analysis

Having ensured that in the absence of nonlinear effects, both programs, in the range of linear deformation, produce the same results and that these results are identical to those reported in the literature, we now consider the dynamics of large amplitude oscillations of flexible constant length beams. In this case the beam can have large overall motions requiring a nonlinear solver for its analysis.

First we use the UL method to solve the damped cantilever oscillations under a ramp-ramp loading defined in chapter 2. In this case we use the program for sliding beams and its axial velocity equal to zero. Figure 6.2.1 shows the results obtained which are identical to those presented in chapter 2 using a different program developed for fixed length beams.

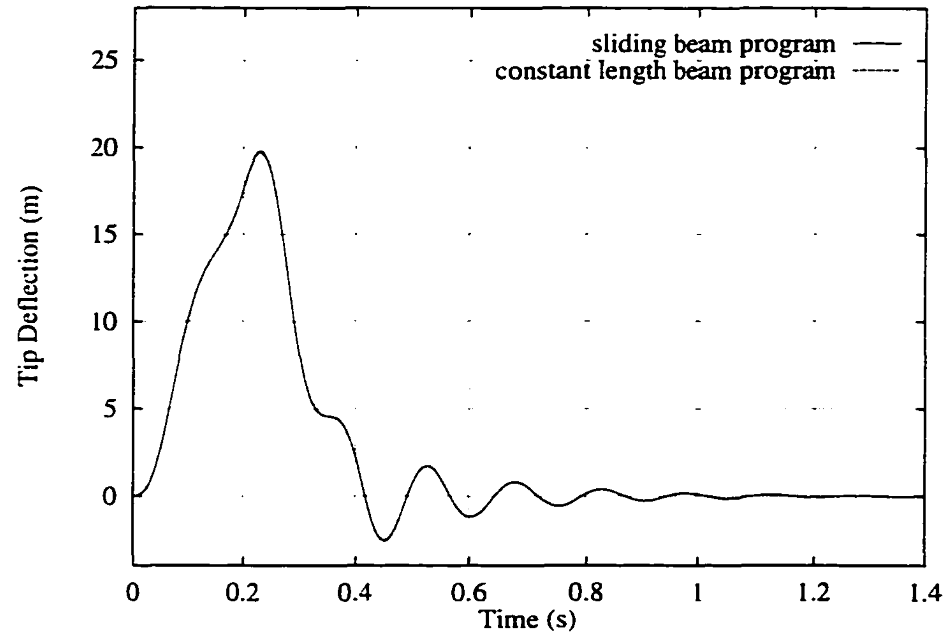


Figure 6.2.1: Tip Displacement History: UL formulation.

We also consider the cantilever subjected to infinite duration load defined in chapter 2 and use the CC formulation for its solution. The results obtained are again identical to those obtained in chapter 2 (see Figure 6.2.2).

## 6.3 Free Vibration Test Cases

Initially we will analyse the motion of sliding beams with small amplitude oscillations. The effects of shortening and extensibility will be included in these cases and a comparison with results in section 6.1 will reveal the importance of these additional effects. Subsequently we will allow for large amplitudes, that is, we will account for full nonlinearities. For initial conditions we will take the static deflection of the beam under a tip load. At the beginning of motion the tip load will be removed and at the same time the beam will begin to slide through the channel.

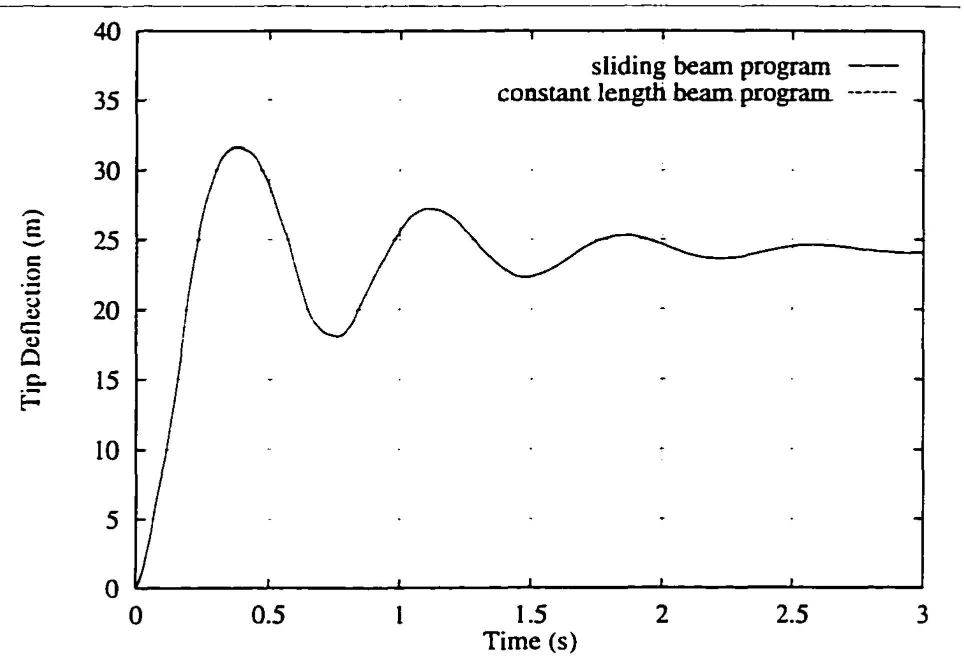


Figure 6.2.2: Tip Displacement History: CC Formulation.

### 6.3.1 Small Amplitude Motions

Let us consider the case of constant velocity retraction as described in section 6.1. Figure 6.3.1 shows the response of the beam using the CC formulation (nonlinear analysis) compared with the result for inexetensible beam (linear analysis). This difference is due to fact that for the linear analysis, the shortening effect and the axial extensibility are neglected. These effects are included in the more comprehensive nonlinear formulation. It is interesting to note that as the beam retracts in the rigid fixed wall the nonlinear solution exhibits period elongation relative to the linear solution and it also shows higher amplitudes. Since the amplitudes in both cases are small, these differences must be attributed to axial flexibility and foreshortening effects. As noted already these effects are ignored in the linear analysis. To identify the dominant effect by the nonlinear solver further calculations were completed with increasing axial stiffness. The results obtained were only slightly different from those depicted in Figure 6.3.1 showing that the period elongation and the amplitude growth is largely due to the foreshortening effect.

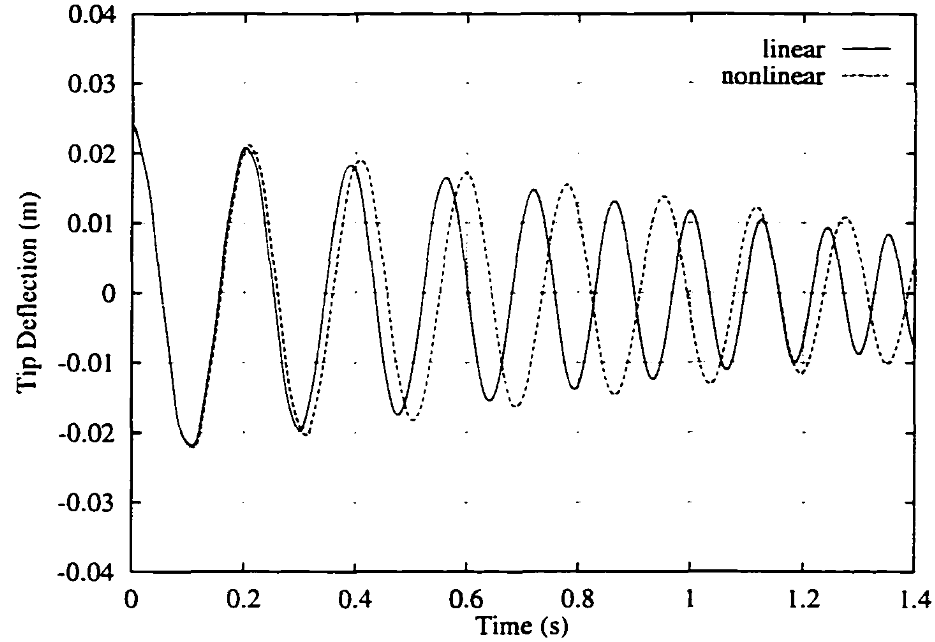


Figure 6.3.1: Spaghetti Problem: Constant Velocity Retraction.

We may also check the other cases of quadratic prescribed motion of flexible sliding beams, i.e. accelerated retraction and accelerated extrusion, and compare the results with those obtained in section 6.1. It can be easily seen that there are always differences between the solutions obtained by linear and the nonlinear solvers and they become significant when the sliding velocity and acceleration become relatively large (see Figures 6.3.2 and 6.3.3).

Now we consider the low frequency repositional motion extrusion, as described in section 6.1. It can be seen that using the linear solver, the transient response of the tip deflection becomes unbounded whereas for the nonlinear analysis the response remains bounded (see Figure 6.3.4).

For the case of low frequency spaghetti problem, Figure 6.3.5 shows the differences between the solutions obtained by the linear and the nonlinear solvers.

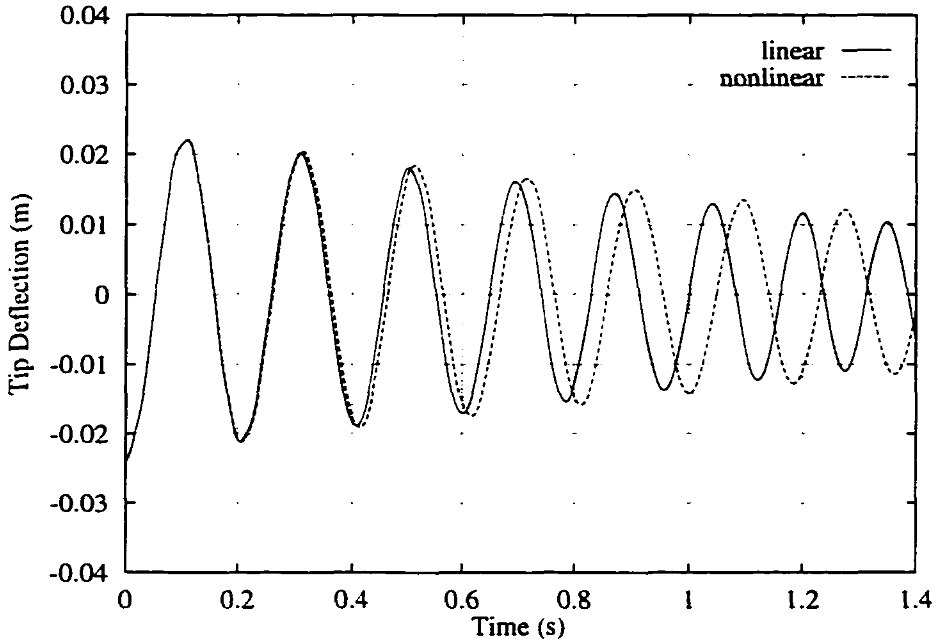


Figure 6.3.2: Spaghetti Problem: Accelerated Retraction.

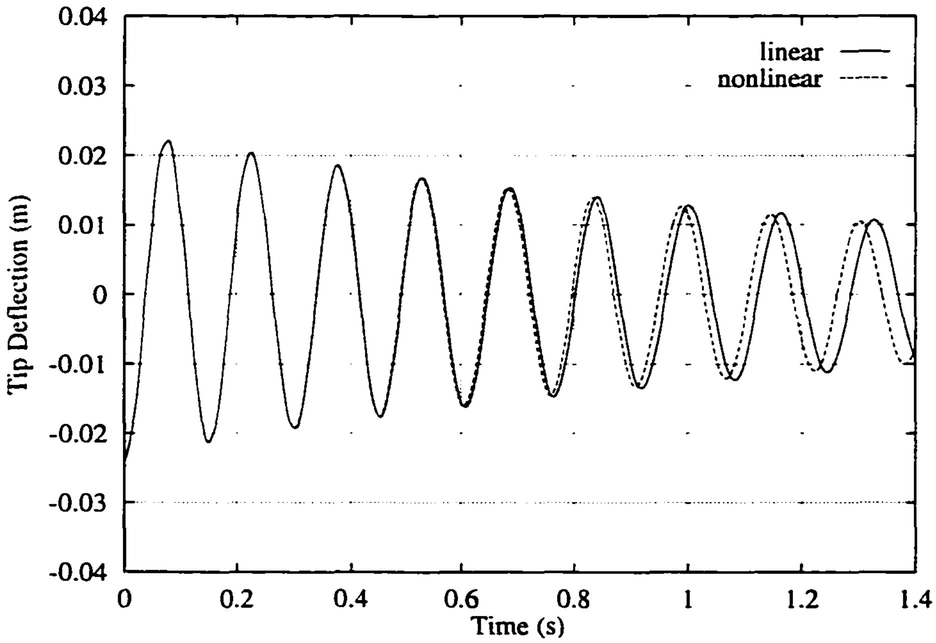


Figure 6.3.3: Reverse Spaghetti Problem: Accelerated Extrusion.

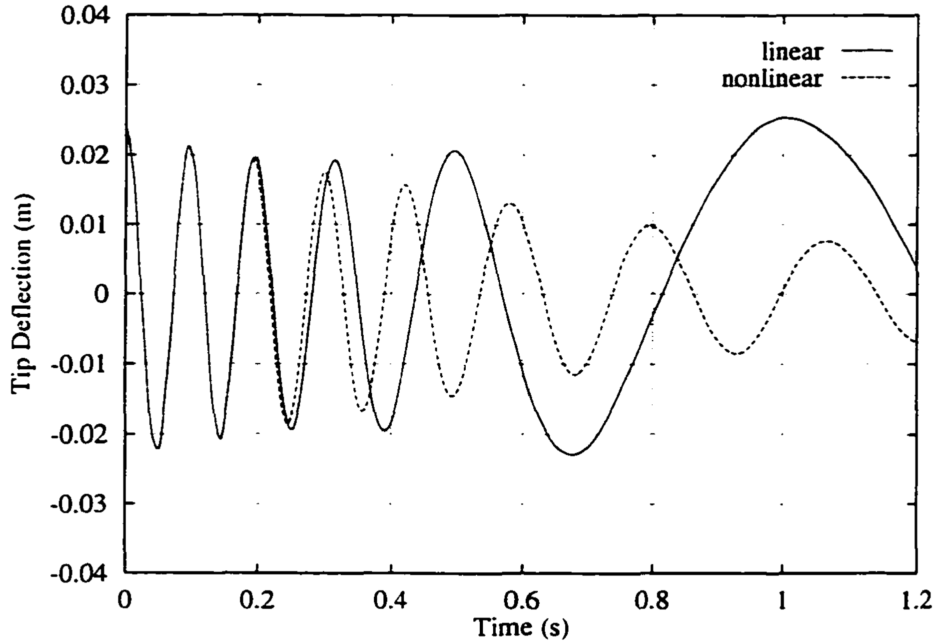


Figure 6.3.4: Reverse Spaghetti Problem: Low Frequency Extrusion.

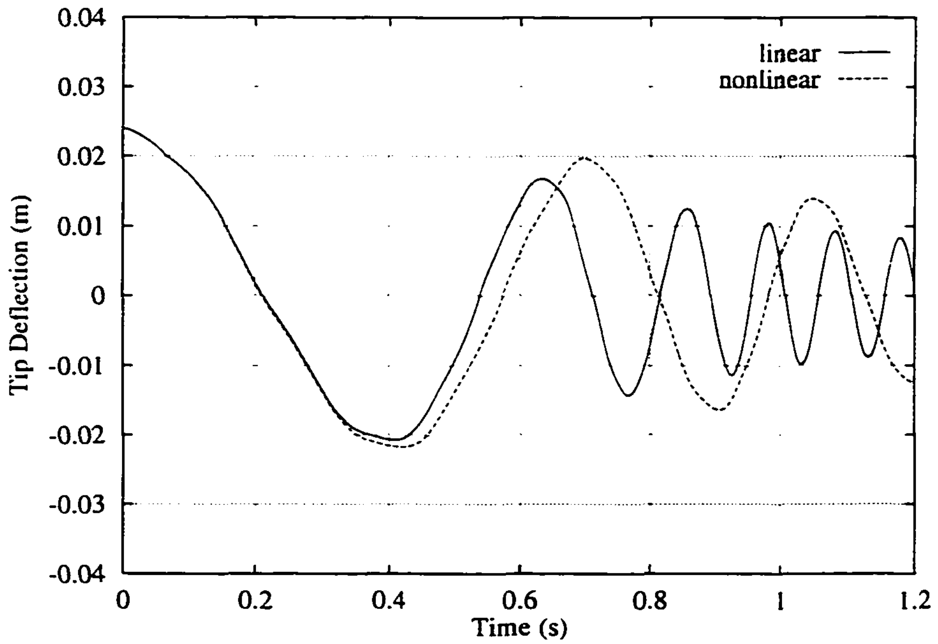


Figure 6.3.5: Spaghetti Problem: Low Frequency Retraction.

Finally, we check for the case of high frequency extrusion, where we find the nonlinear solver provides a bounded response for the system, Figure 6.3.6.

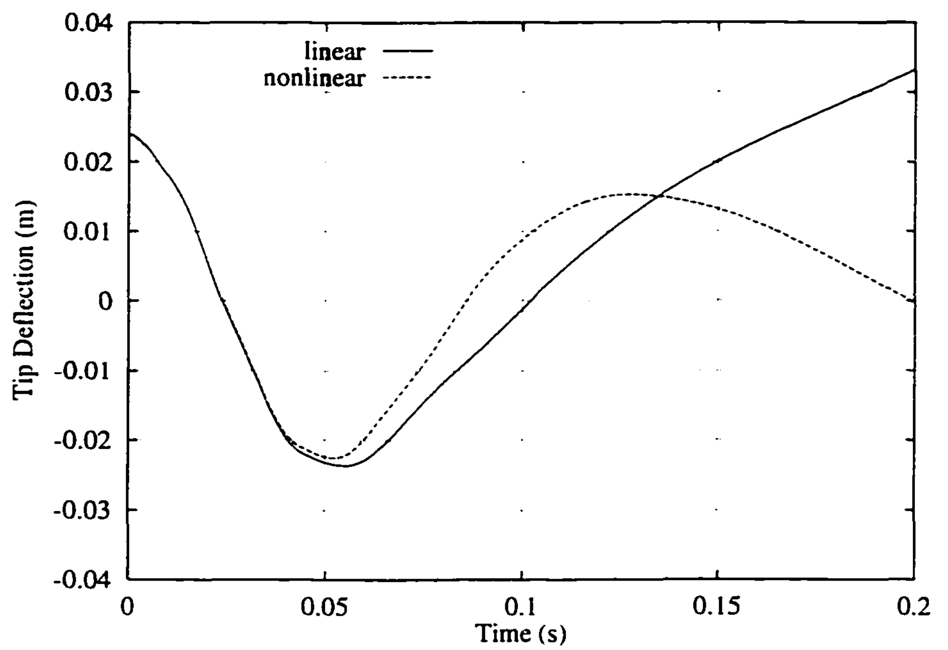


Figure 6.3.6: Reverse Spaghetti Problem: High Frequency Extrusion.

From the foregoing examples we may conclude that in the case of flexible sliding beams it is important to account for nonlinearities associated with the shortening effect and the axial flexibility even when the vibration amplitudes are small.

### 6.3.2 Large Amplitude Motions

In the following examples, we examine the large amplitude vibrations of flexible sliding beams with the initial tip deflection of about 33.5% of the initial length of the beam. For the following examples the initial length of the beam is taken as 0.525 ($m$).

We start with the constant velocity spaghetti problem with the parameters as given in section 6.1. Figure 6.3.7 shows the transient response of the free end of the beam obtained by the nonlinear and the linear solvers.

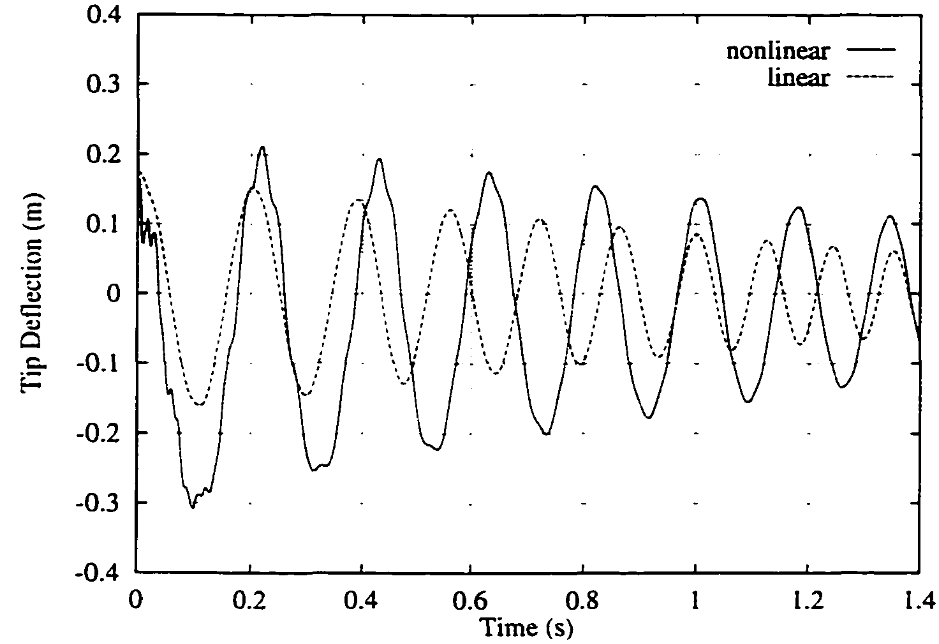


Figure 6.3.7: Spaghetti Problem: Constant velocity Retraction.

To examine the effect of increasing the sliding velocity, we double the constant velocity and again compare the results with those obtained by the linear solver (see Figure 6.3.8).

Next we consider the accelerated extrusion as defined in section 6.1. For large amplitude vibrations, linear and nonlinear solvers show significant differences (Figure 6.3.9).

Figure 6.3.10 shows the effect of doubling the axial initial velocity and constant extruding acceleration.

In the next test we consider a low frequency extrusion with the parameters as defined in section 6.1. Figure 6.3.11 shows the nonlinear and the linear responses. Again one can see that the nonlinear response is bounded whereas the linear response exhibits amplitude growth.

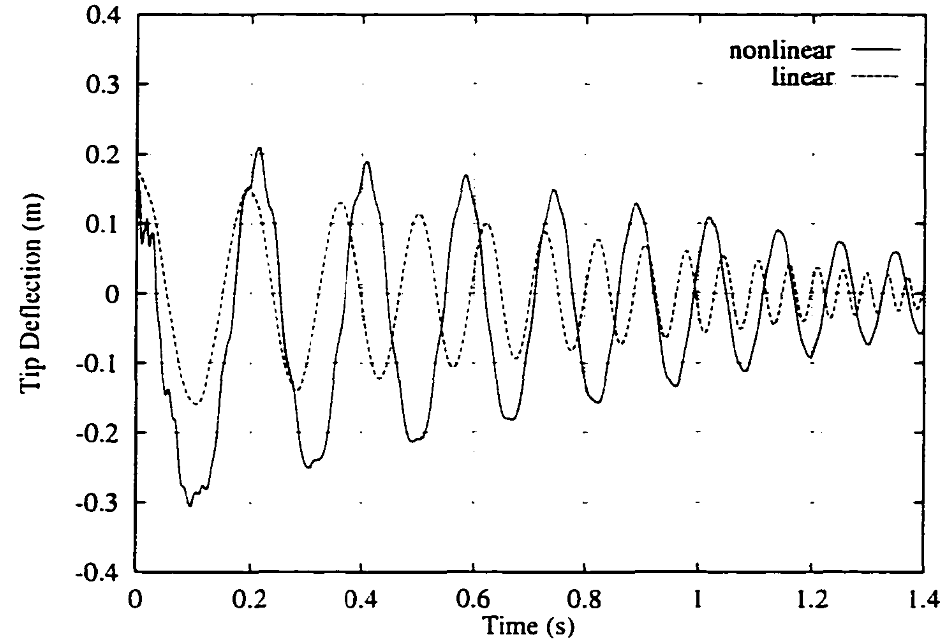


Figure 6.3.8: Spaghetti Problem: High Speed Constant Retraction.

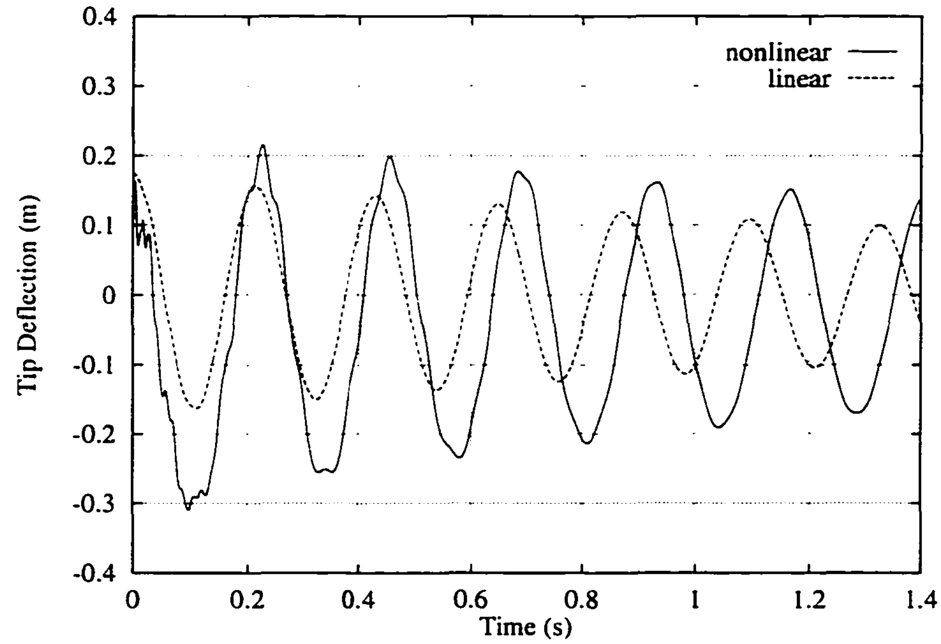


Figure 6.3.9: Reverse Spaghetti Problem: Accelerated Extrusion.

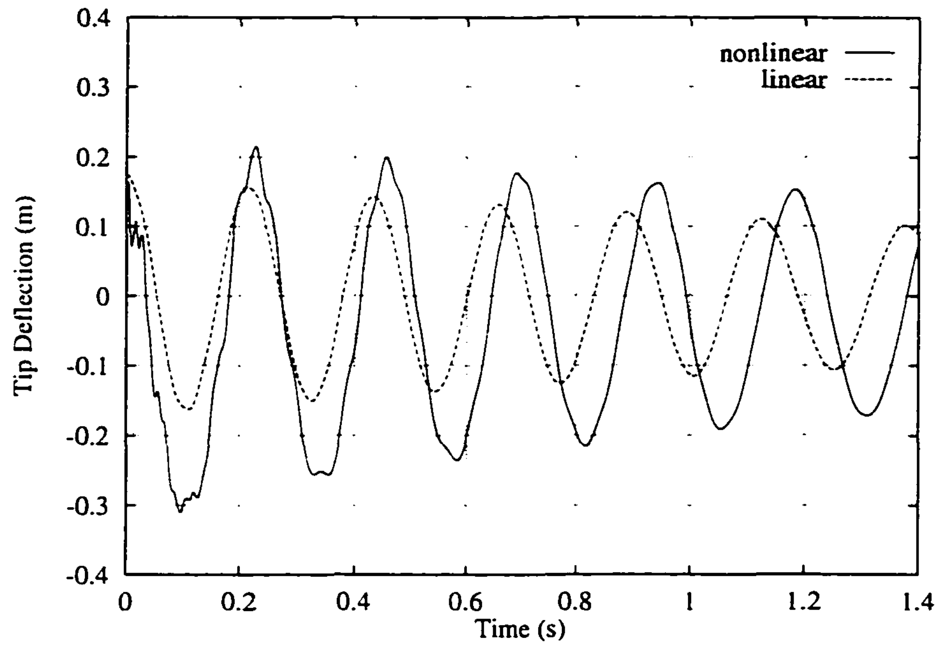


Figure 6.3.10: Reverse Spaghetti Problem: High Speed Extrusion.

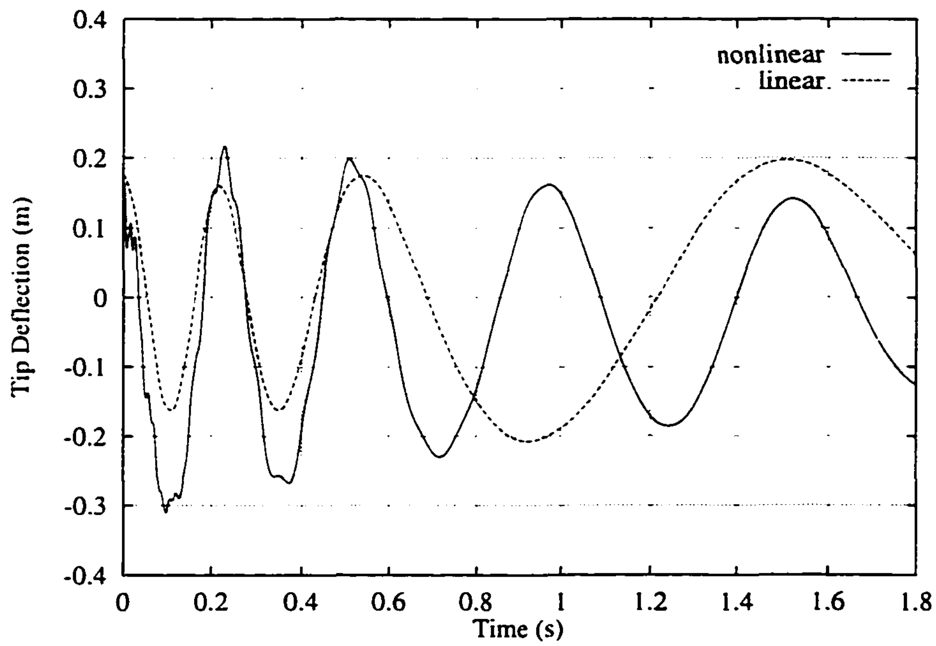


Figure 6.3.11: Reverse Spaghetti Problem: Low Frequency Extrusion.

We also consider the high frequency reverse spaghetti problem with $t_o = 0.4$ ($s$). The results obtained show a stable response when the nonlinear solver is used whereas the linear solver depicts an unstable response.

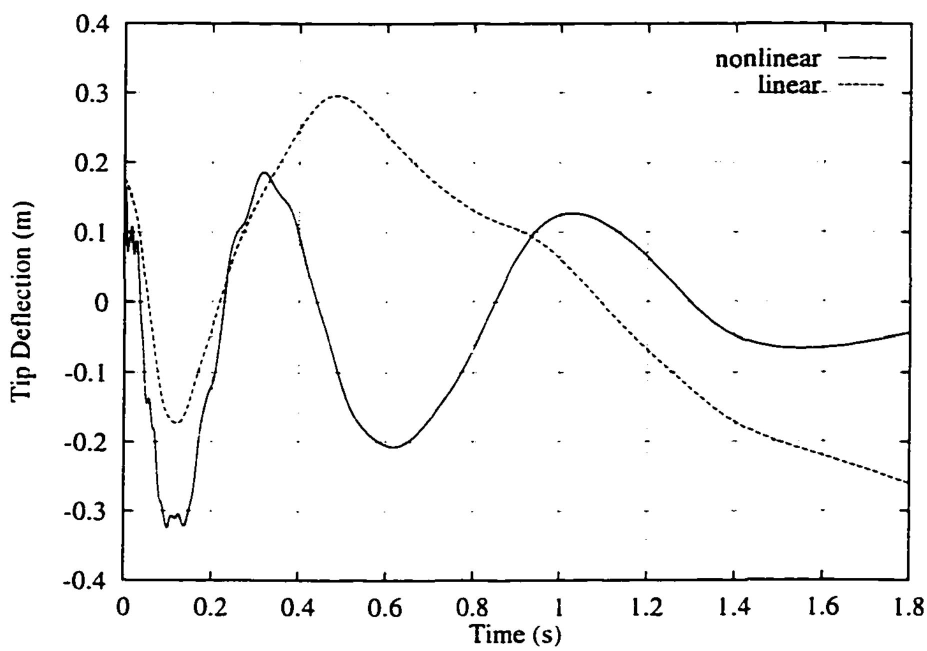


Figure 6.3.12: Reverse Spaghetti Problem: High Frequency Extrusion.

## 6.4 Forced Vibration Illustrative Examples

In the first two examples we consider a quadratic prescribed sliding motion for the flexible sliding beam under a tip infinite duration force and compare the responses obtained by the CC, UL and the linear formulations. Then we use the CC formulation to investigate some other cases with different natural boundary conditions. For the following examples the initial length of the beam is taken as 0.525 ($m$).

### 6.4.1 Constant Velocity Spaghetti Problem: Infinite Duration Concentrated Tip Load

In this problem we consider a beam retracting from a rigid channel with a constant velocity as given in section 6.1. We model the beam as shown in Figure 6.4.1 and use a Rayleigh type damping as described in the previous test cases.

The obtained results shown in Figure 6.4.2, show significant differences between the solutions obtained from the linear and the nonlinear solvers. Also differences can be seen between the solutions obtained by CC and the UL formulations. This latter difference is due to the effects discussed in chapter 2.

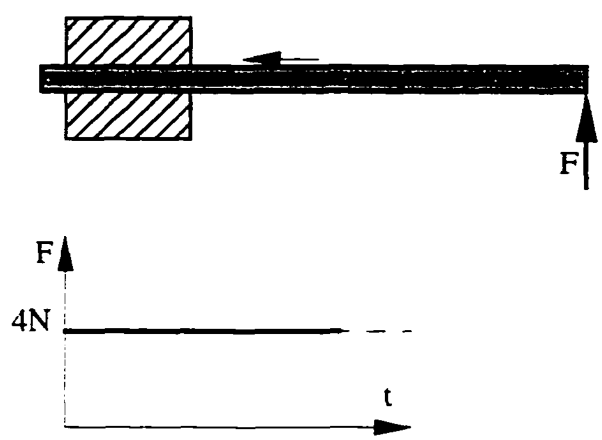


Figure 6.4.1: Concentrated Tip Load History.

### 6.4.2 Accelerated Reverse Spaghetti Problem: Infinite Duration Concentrated Tip Load

For this case the load history is given in Figure 6.4.1. The beam extrudes from a rigid channel with a constant acceleration as given in section 6.1. Figure 6.4.3 shows the differences in the responses computed by the CC, UL and the linear formulations, respectively.

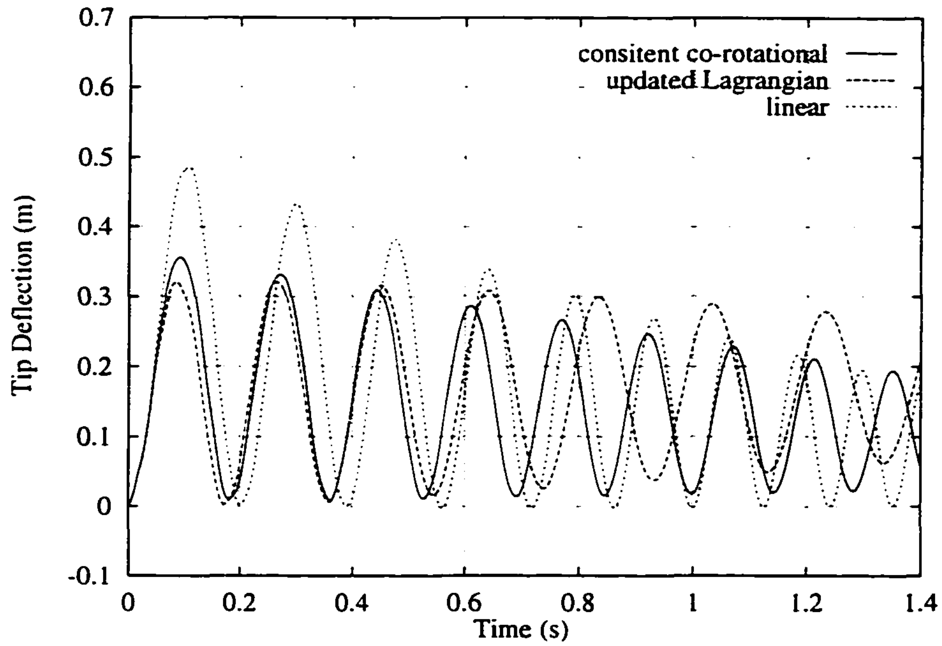


Figure 6.4.2: Spaghetti Problem: Constant Velocity Retraction.

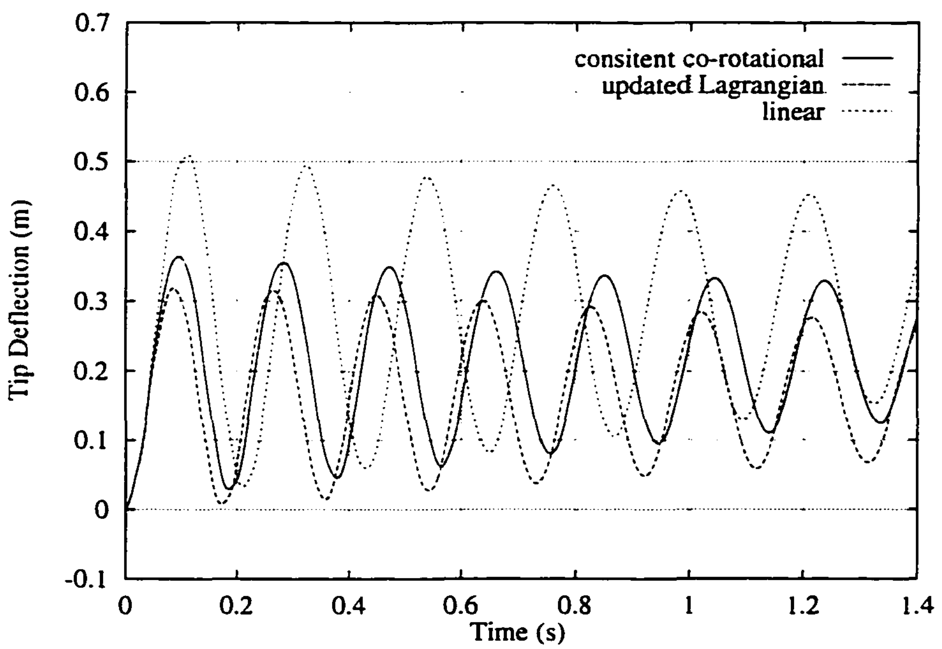


Figure 6.4.3: Reverse Spaghetti Problem: Accelerated Extrusion.

### 6.4.3 Constant Velocity Spaghetti Problem: Further Examples

Here, we first consider two types of concentrated tip load histories as given in Figures 6.4.4 and 6.4.6. In both cases the transient responses obtained from the CC formulation show significant differences with the results obtained from the linear formulation (see Figures 6.4.5 and 6.4.7).

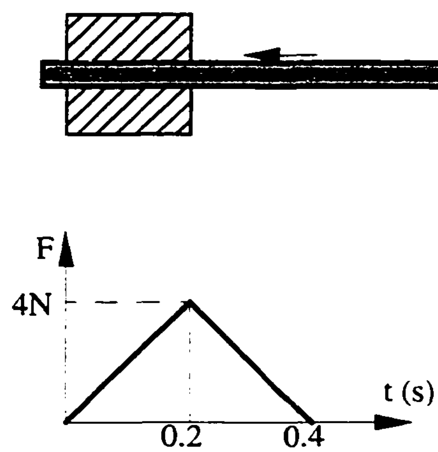


Figure 6.4.4: Concentrated Tip Load History.

Next we examine the sliding beam with a concentrated tip pure moment. The load time history and transient response of the beam are given in Figures 6.4.8 and 6.4.9.

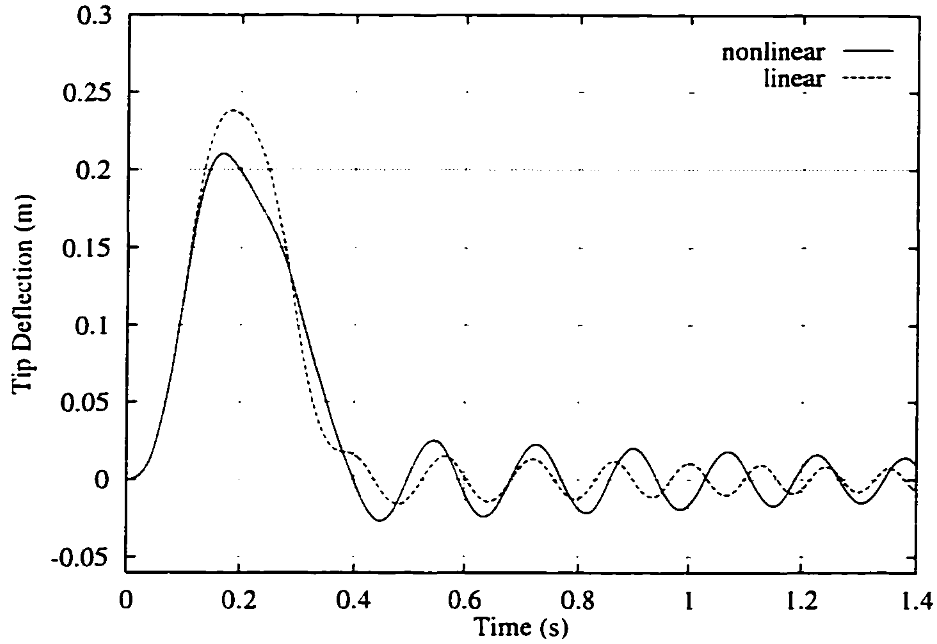


Figure 6.4.5: Spaghetti Problem: Constant Velocity Retraction, Ramp-Ramp Load.

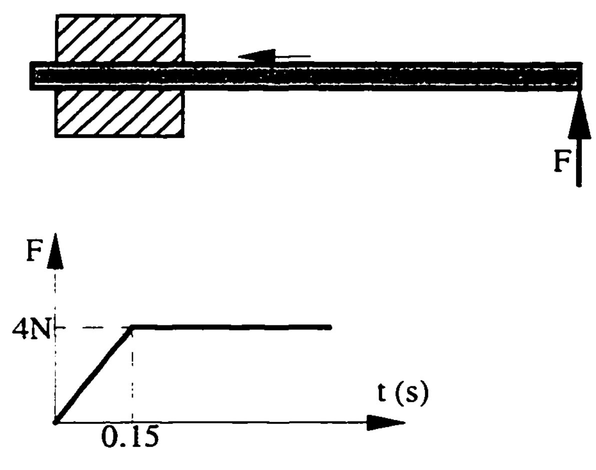


Figure 6.4.6: Concentrated Tip Load History.

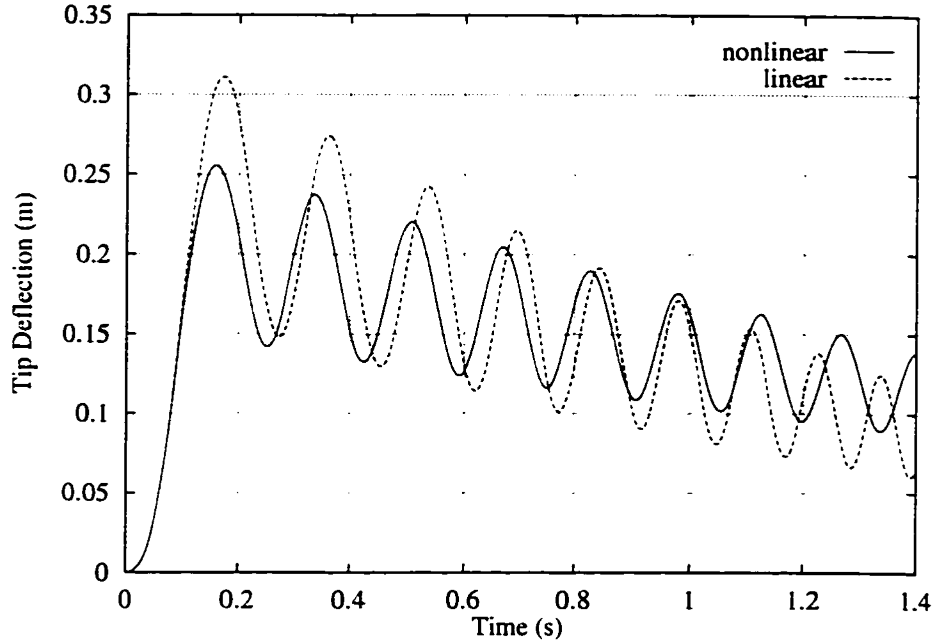


Figure 6.4.7: Spaghetti Problem: Constant Velocity Retraction, Ramp-constant Load.

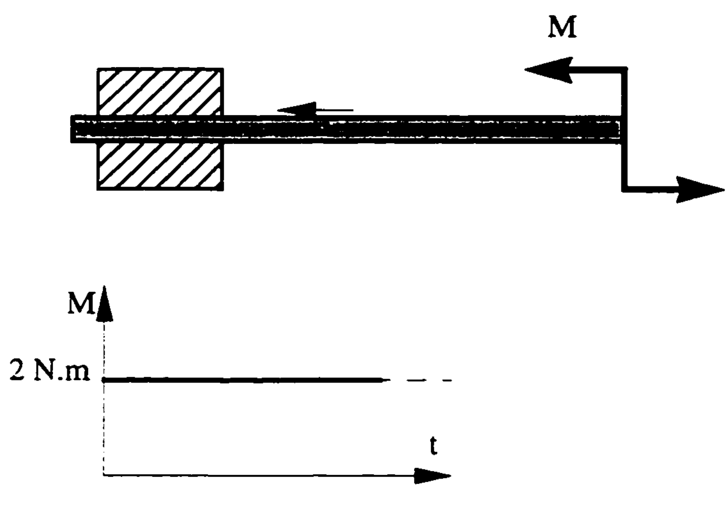


Figure 6.4.8: Concentrated Tip Load History.

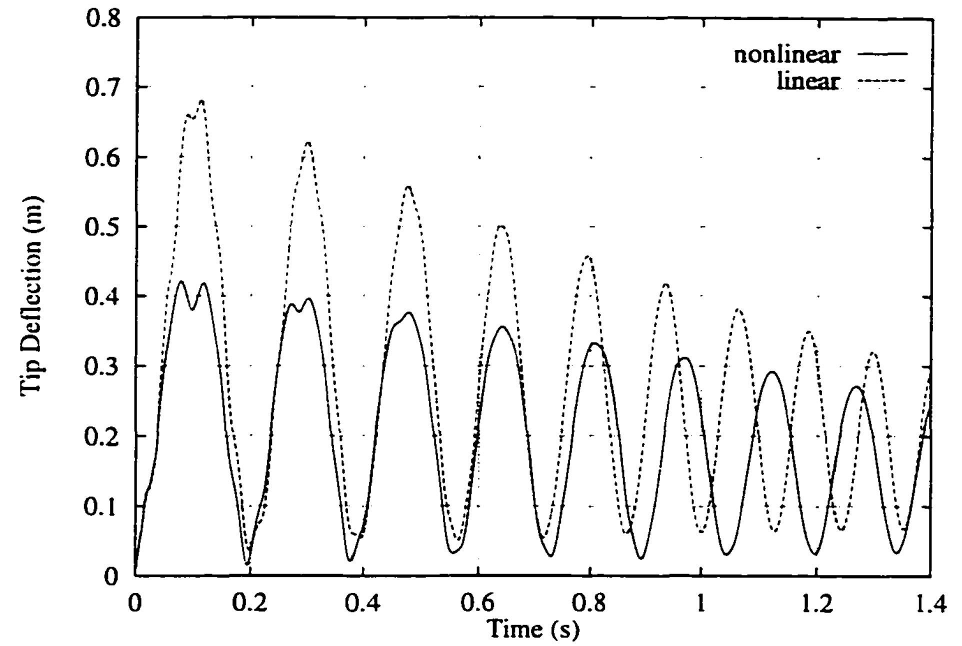


Figure 6.4.9: Spaghetti Problem: Constant Velocity Retraction.

### 6.4.4 Accelerated Reverse Spaghetti Problem: Concentrated Ramp-Ramp Tip Load

The load time history is given in Figure 6.4.10. The beam accelerates from a rigid channel with parameters as given in section 6.1. The differences between the transient response of the system using the CC and the linear formulations is again in evidence.

### 6.4.5 Spaghetti and Reverse Spaghetti Problem: Repositional Motion

We now examine some problems with prescribed axial motions as given by equation (6.1.3). For these problems the initial length of the beam is taken as 0.525 ($m$) and the other parameters are as used in section 6.2.

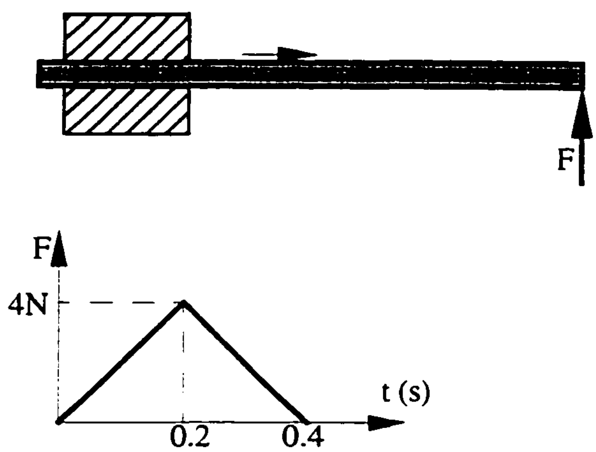


Figure 6.4.10: Concentrated Tip Load History.

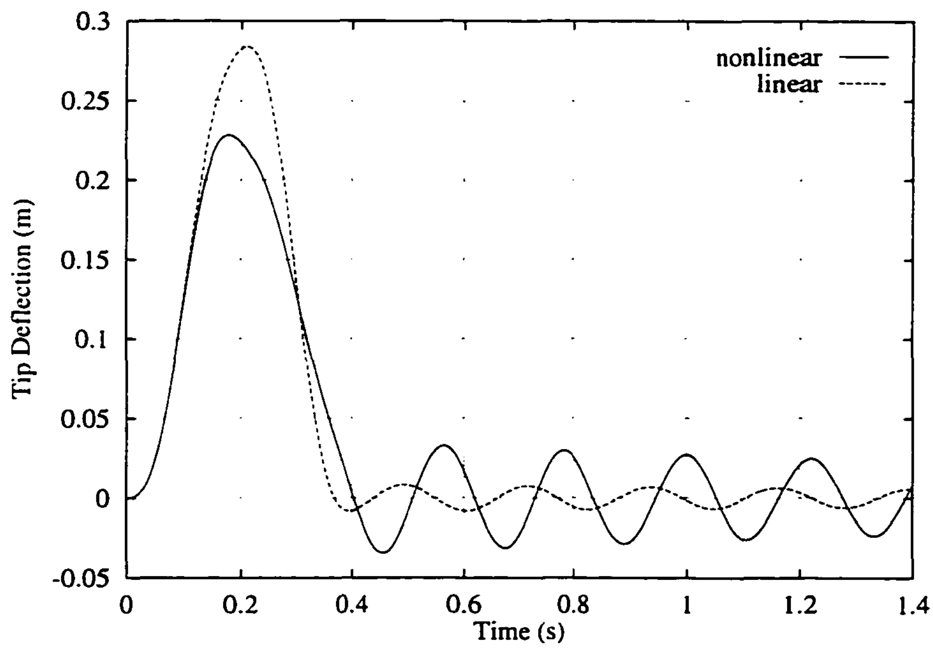


Figure 6.4.11: Reverse Spaghetti Problem: Accelerated Extrusion.

#### 6.4.5.1 Low Frequency Extrusion

In this case, we consider the beam extruding from a rigid channel under a finite duration tip load as shown in Figure 6.4.12. The transient response of the tip is given in Figure 6.4.13 which shows stable response for the nonlinear analysis whereas the linear solution describes an unstable motion. If we double the extruding velocity, the nonlinear response still remains stable whereas the linear response clearly shows unbounded response, see Figure 6.4.14.

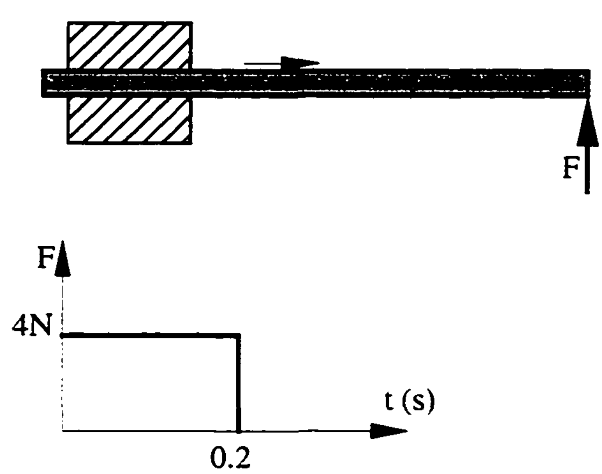


Figure 6.4.12: Concentrated Tip Load History.

#### 6.4.5.2 Low Frequency Spaghetti Problem

In this case we consider a beam retracting from a rigid channel under a ramp-ramp concentrated tip load (see Figure 6.4.15). Also we increase the retracting velocity by five fold as compared with the velocity considered in section 6.1, that is in equation (6.1.3) we let $c_o = 3.5\ (m)$, $(t_o = 1.2\ (s))$. Figure 6.4.16 shows the transient response of the system as determined from the linear and the nonlinear solvers.

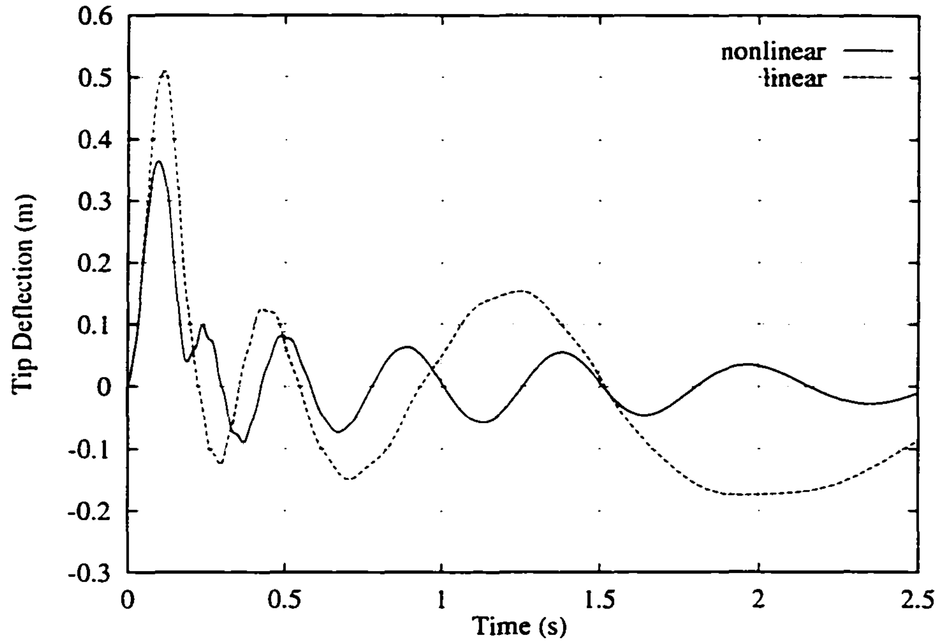


Figure 6.4.13: Reverse Spaghetti Problem: Low Frequency Extrusion.

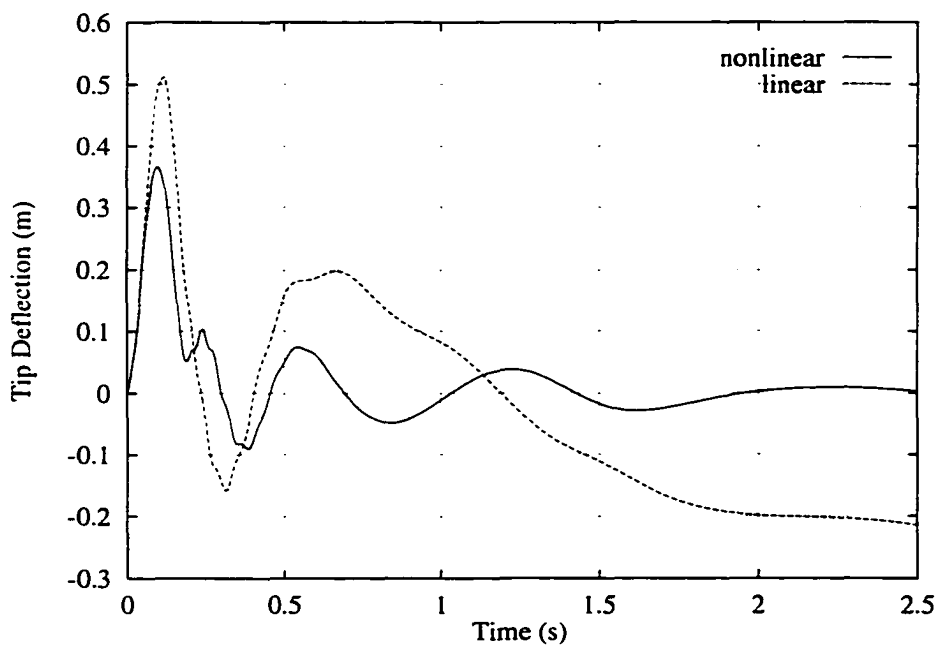


Figure 6.4.14: Reverse Spaghetti Problem: High Speed Low Frequency Extrusion.

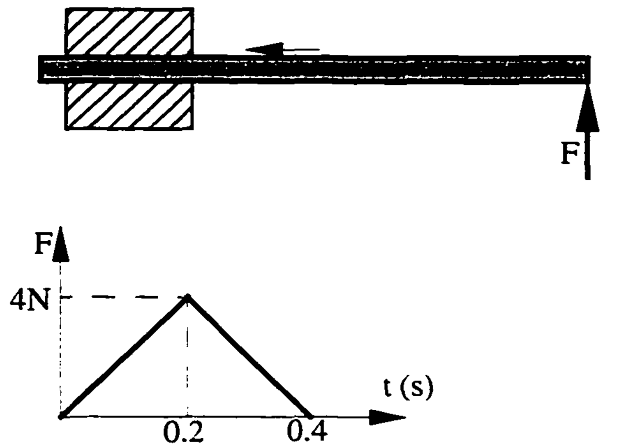


Figure 6.4.15: Concentrated Tip Load History.

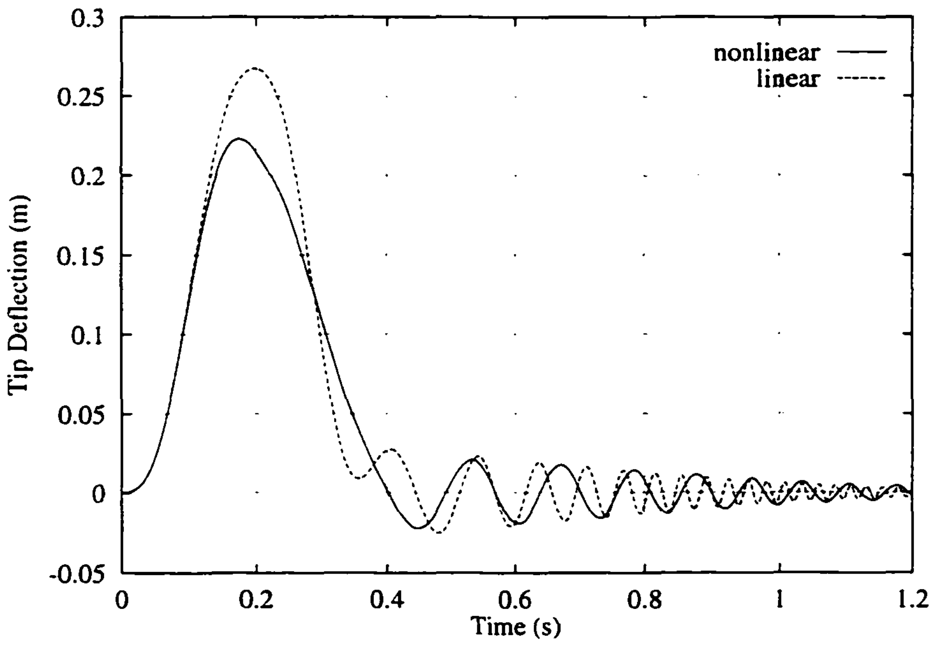


Figure 6.4.16: Spaghetti Problem: Low Frequency Retraction.

#### 6.4.5.3 High Frequency Extrusion

Here we use the same parameters as given in section 6.1 but we let $t_o = 0.4\,(s)$. The load history is given in Figure 6.4.17. The transient response of the system, using non-linear analysis, shows stable behaviour whereas the linear formulation predicts unstable response (see Figure 6.4.18).

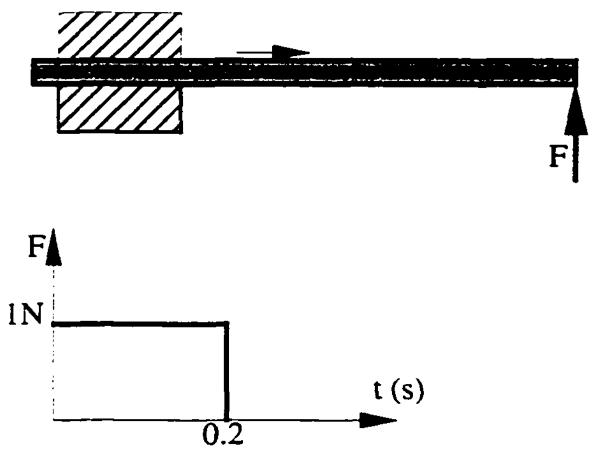


Figure 6.4.17: Concentrated Tip Load History.

#### 6.4.5.4 High Frequency Retraction

In this problem we consider two types of loads applied at the tip as give by Figures 6.4.19 and 6.4.21. Time responses of the tip are given in Figures 6.4.20 and 6.4.22 where the linear and nonlinear formulations are compared.

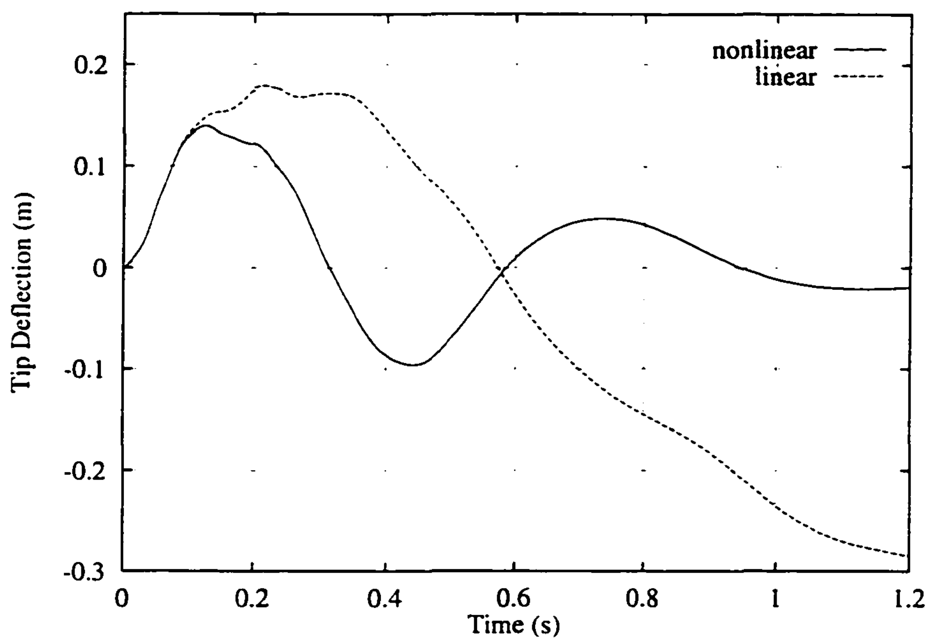


Figure 6.4.18: Reverse Spaghetti Problem: High Frequency Extrusion.

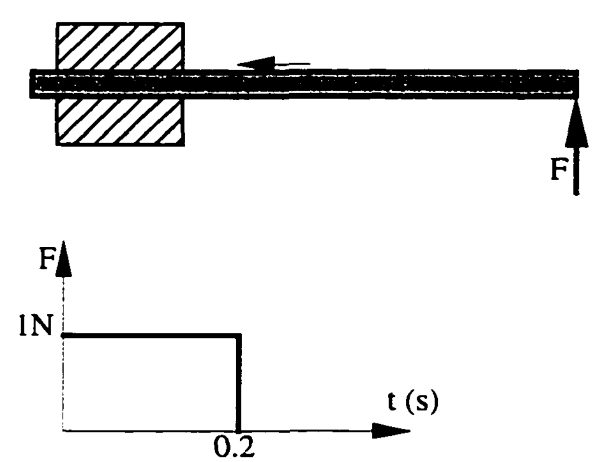


Figure 6.4.19: Concentrated Tip Load History.

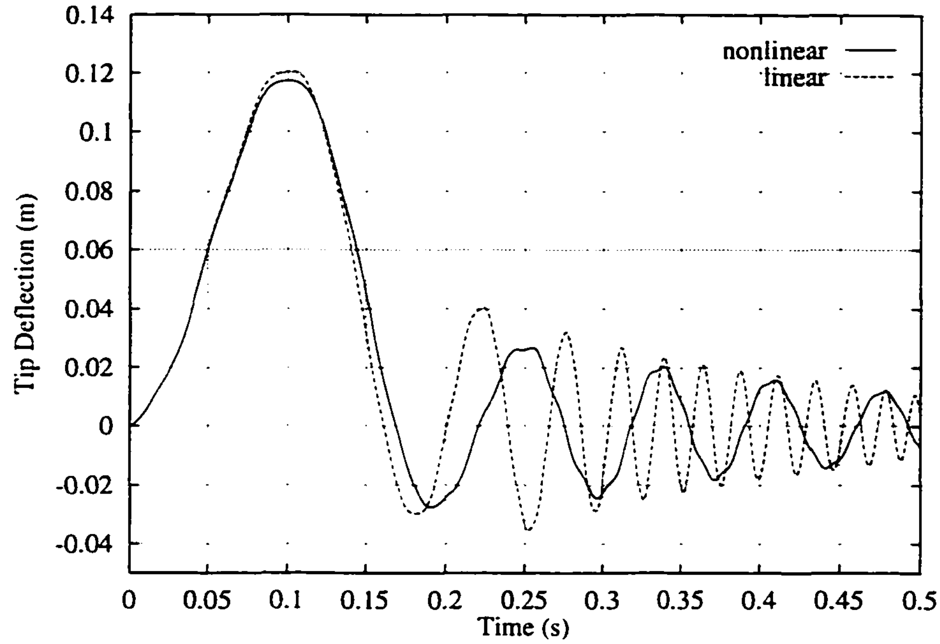


Figure 6.4.20: Spaghetti Problem: High Frequency Retraction, Finite Duration Load.

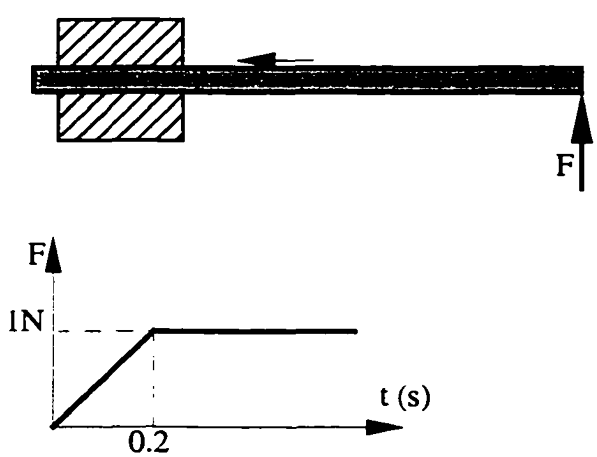


Figure 6.4.21: Concentrated Tip Load History.

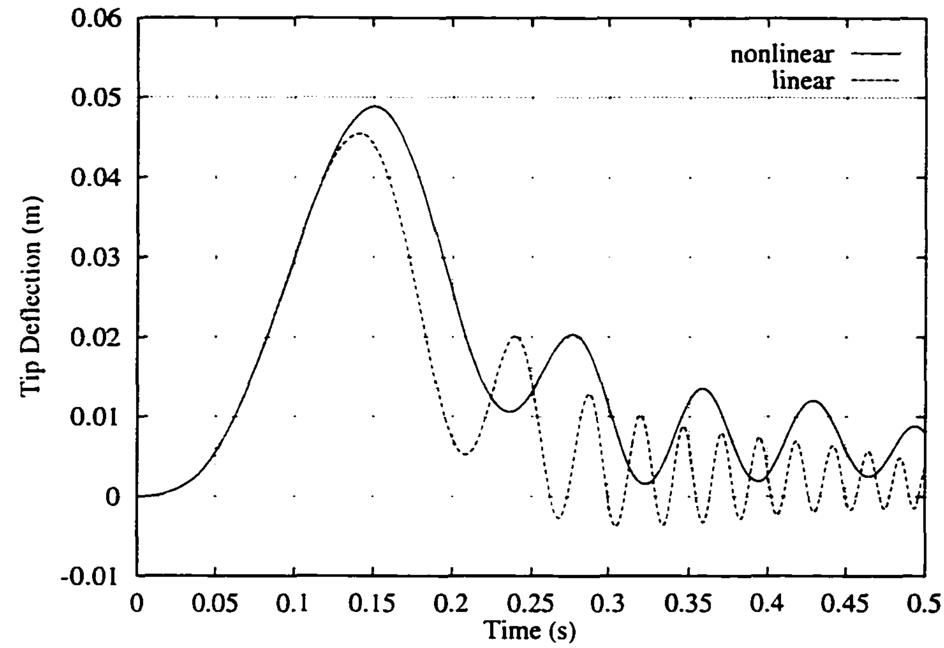


Figure 6.4.22: Spaghetti Problem: High Frequency Retraction, Ramp-Constant Load.

## 6.5 Instability of the Motion for Periodically Varying Length: Parametric Resonance

The problem of instability of motion for sliding beams of periodically varying length, as given in equation (6.5.1), has been addressed by Zajaczkowski and Lipinski, 1979.

$$L(t) = L_o(1 - a\cos\omega t) \tag{6.5.1}$$

They showed that depending on the parameters $a$ and $\omega$, stable or unstable regions are obtained and they plotted the boundaries of the unstable regions in the parameter plane of $\sqrt{\omega/(2\bar{\omega}_1)}$ and $a$ where $\bar{\omega}_1$ is the first natural frequency of the beam with initial length $L_o$. Damping forces were not considered in their analysis. The following examples show that in some regions of instability, as obtained by the linear analysis of Zajaczkowski and Lipinski the response of the physical system as described by the proper nonlinear formulation has bounded amplitude oscillations, i.e. it is stable. Vu-Quoc and Li, 1995, who also considered these cases experienced difficulties in time integration of equations of motion. In the present analysis such difficulties were not encountered. This may be due to the advantages of the consistent co-rotational method over the geometrically-exact beam theory used by them.

In the following we consider a beam with an initial length of 0.525 (m) in the stable region (linear analysis) with $a = 0.2$ and $\sqrt{\omega/(2\varpi_1)} = 0.67$. Figure 6.5.1 confirms stable responses for both the linear and the nonlinear formulations.

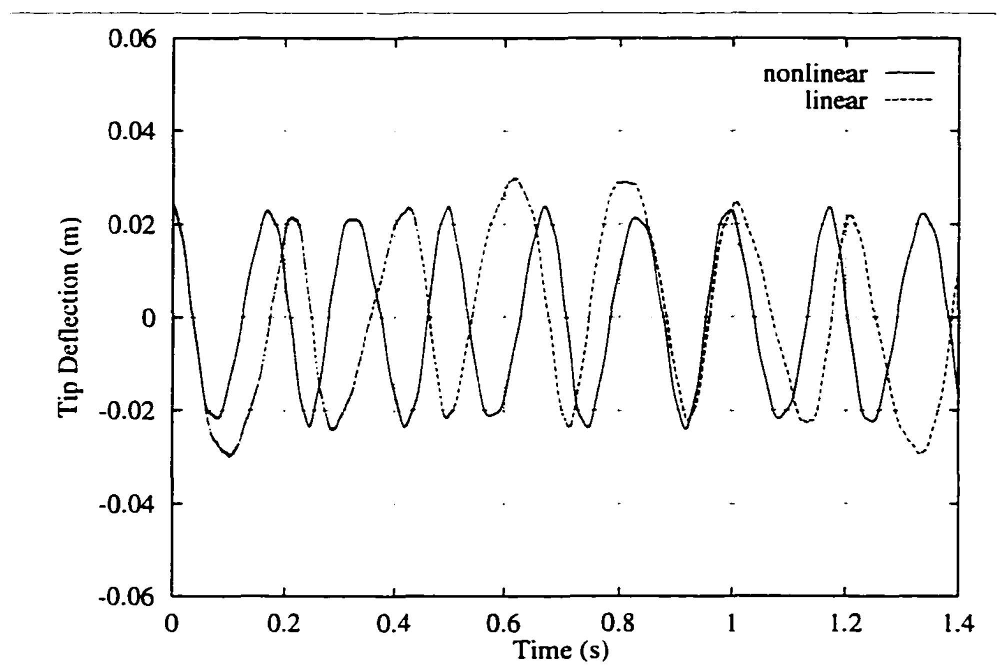


Figure 6.5.1: Periodically Varying Length Beam: Stable Region, $\sqrt{\dfrac{\omega}{2\varpi_1}} = 0.67$.

Now we consider $\sqrt{\omega/(2\varpi_1)} = 1.0$ which is in the unstable region (see Zajaczkowski and Lipinski, 1979). Using the linear analysis we find resonance in the response of the beam where as the nonlinear analysis indicates bounded response in the tip deflection (see Figures 6.5.2 and 6.5.3).

In another test we consider $\sqrt{\omega/(2\varpi_1)} = 1.7$ which still is in the unstable region. Figure 6.5.4 shows instability in the solution when a linear analysis is used. Such instabilities can not be observed when the nonlinear analysis is used (see Figure 6.5.5).

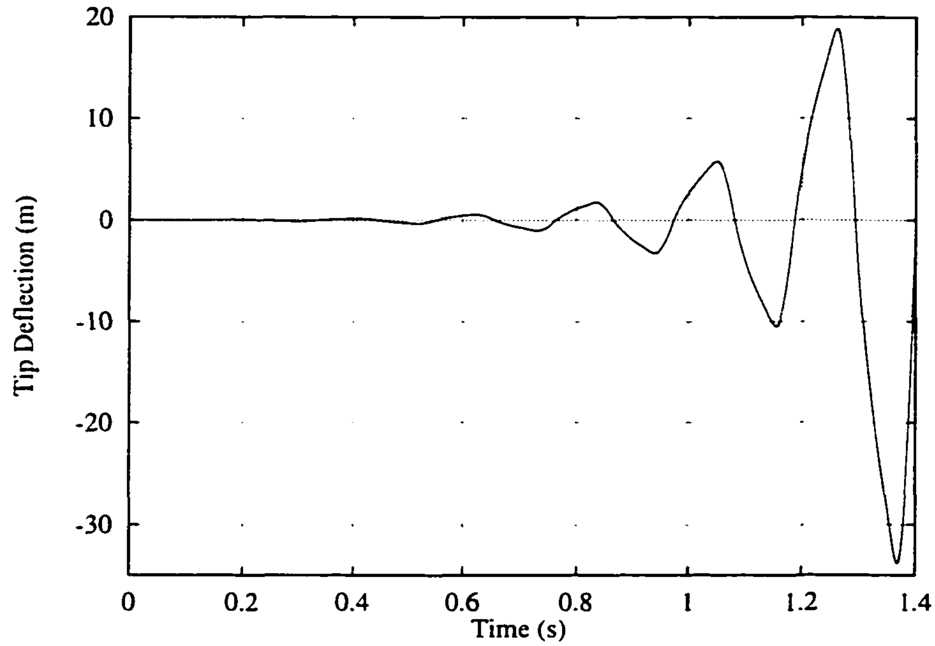


Figure 6.5.2: Periodically Varying Length Beam: Linear Analysis, $\sqrt{\dfrac{\omega}{2\varpi_1}} = 1$.

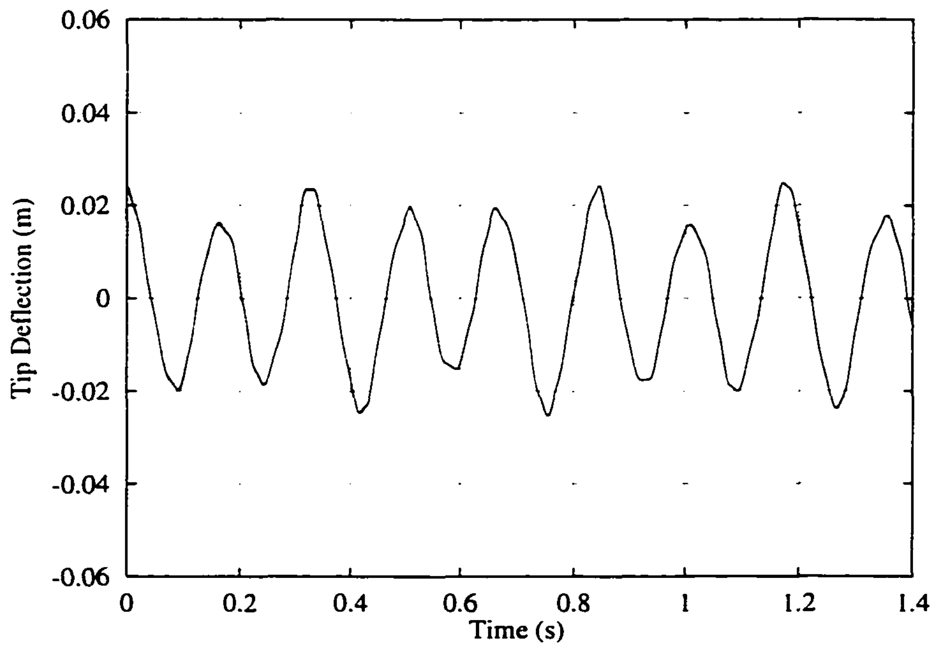


Figure 6.5.3: Periodically Varying Length Beam: Nonlinear Analysis, $\sqrt{\dfrac{\omega}{2\varpi_1}} = 1$.

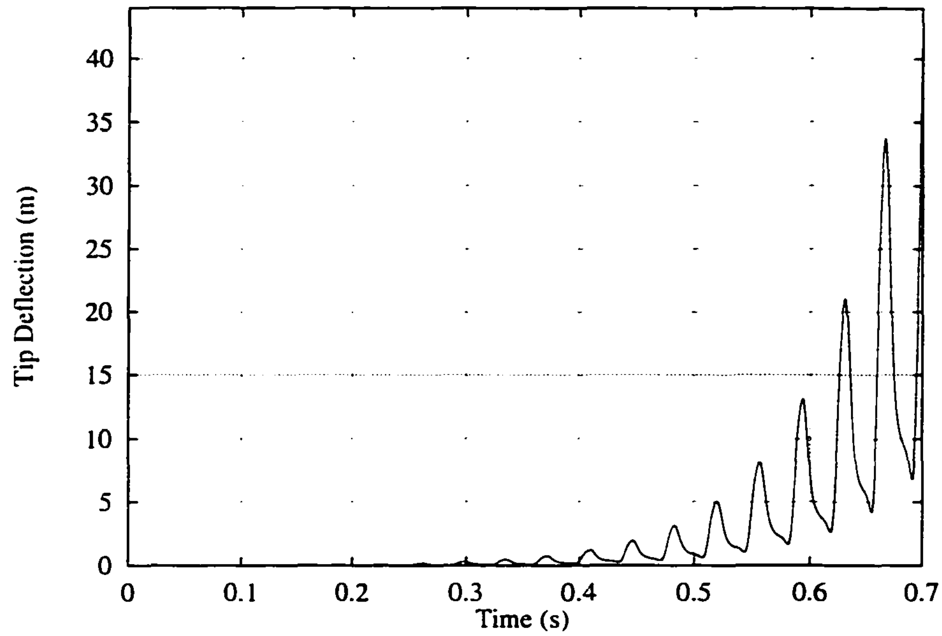


Figure 6.5.4: Periodically Varying Length Beam: Linear Analysis, $\sqrt{\frac{\omega}{2\varpi_1}} = 1.7$.

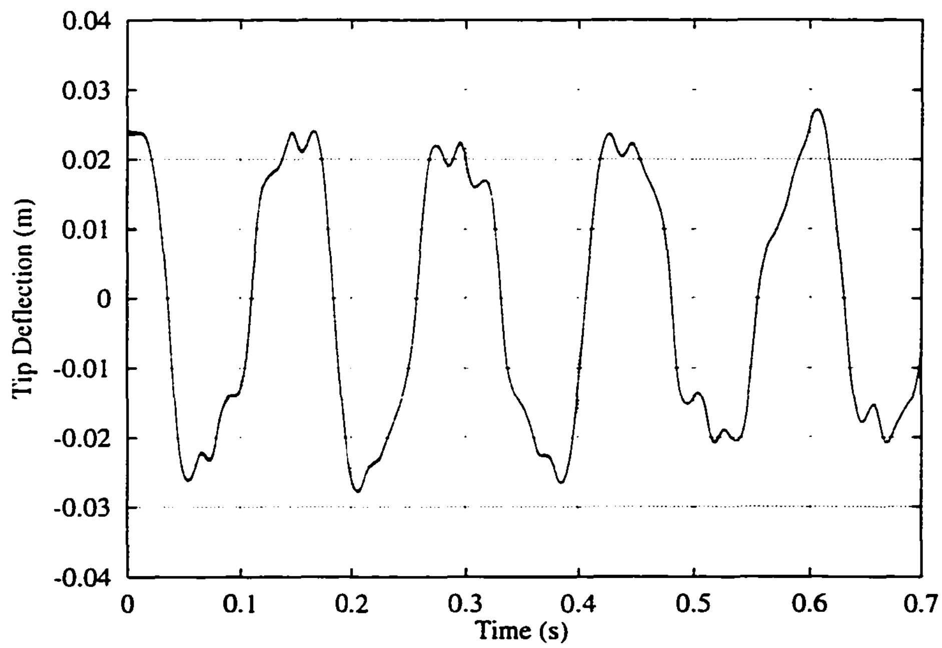


Figure 6.5.5: Periodically Varying Length Beam: Nonlinear Analysis, $\sqrt{\frac{\omega}{2\varpi_1}} = 1.7$.

## 6.6 Conclusions

In this chapter we used the formulations derived in chapter 5 in conjunction with the technique of geometrical nonlinearities developed in chapter 2, to obtain the transient response of flexible sliding beams.

We started with small amplitude oscillations and showed that both formulations lead to the same results when the nonlinear part of the code is not active (UL and CC). Those results are in agreement with those reported in the literature. Then we solved some examples of large amplitude oscillations for beams of fixed lengths. In these cases we showed that the two nonlinear programs produced similar results.

Next we solved some problems in the linear range with the nonlinear solvers and compared the results with those obtained by the linear analysis and we observed the differences in the transient response of the system. From these tests, we concluded that a nonlinear analysis that accounts for foreshortening and axial flexibility of the beam is necessary for the analysis of flexible sliding beams even when the amplitudes of oscillations are small.

Further we examined some large displacement problems in free and forced vibrations of flexible sliding beams. On comparing the results we noted the significant differences between the responses computed by the linear and the nonlinear solvers.

Finally we considered the problem of beams with periodically time varying lengths and showed that in regions of instability, as obtained by the linear analysis and reported in the literature, nonlinear analysis frequently shows bounded, i.e. stable, solutions.

# Chapter 7

# Closing Comments

In this work we pursued an extensive research program on the dynamics of flexible sliding beams in which the protruding part of the beam can undergo large rotations but small strains.

First we carried out a preliminary study on the general problem of static and dynamic analysis of geometrically nonlinear beams. We used two important geometrically nonlinear formulations, namely the updated Lagrangian and the consistent co-rotational formulations to study the statics of beams and then we extended these formulations to dynamic analysis. To this end we developed a new formulation for consistent co-rotational method in dynamic analysis and we showed that this method has distinct advantages over the updated Lagrangian method both in terms of accuracy and efficiency.

We provided a comprehensive formulation for the sliding beam and supported it by an alternative formulation. Nonlinearities due to large deflections were taken into account and the governing equations of motion were obtained through an extension of Hamilton's principle. We also showed that the two formulations with time varying domain can be transformed to a common fixed domain.

Next we computed the transient response of the inextensible flexible sliding beam. We started with the linear case and transformed the equations of motion to the fixed domain. Then we used Galerkin's method with space dependent beam modal functions and obtained the system discrete set of ODE's in time. Several example were solved and the results were compared with those reported in the literature. Good agreement in these comparisons supported the validity of the presented formulations. We further extended the problem to nonlinear analysis and via the same procedure we obtained a set of nonlinear ODE's which upon solution provided the response of the system. The differences between the linear and the nonlinear analysis were exposed through several illustrative examples. Also we examined the effect of uniform gravitational field on the response of the system.

To obtain the transient response of flexible sliding beams, we used two methods developed in our preliminary study of large deflection analysis of beams. In the discretization procedures, we developed two types of beam elements, namely, a variable domain element and a constant domain stretched element. The formulations showed that in both approaches the system matrices are time dependent leaving little advantage of one approach over the other. However, additional computational work is required in the fixed domain approach to transform the solution back to the physical system. Hence, we chose the variable domain elements for our further investigations. Also in the discretization procedures we developed the consistent co-rotational finite element for the sliding beam and its alternative formulation and obtained the discretized equations of motion and showed that the two formulations are related and describe the same physical problem.

Finally we integrated the discretized governing equations in time and we solved several illustrative examples to expose the effect of the nonlinear terms on the transient response of flexible sliding beams. We showed that the consistent co-rotational method offers advantages over the other methods in terms of accuracy and efficiency. Also we showed the differences between the linear and nonlinear analysis even when the amplitudes of oscillations are small. We concluded that for this dynamically rich problem, a comprehensive nonlinear analysis is essential.

It is hoped that the present work will encourage further studies on sliding beams. The following are suggestions for future work:

- Further investigation is needed to identify the external work required to maintain the prescribed axial motion which brings about a convection of mass out of (into) the domain of interest.

- In the foregoing research, our formulations were based on the Euler-Bernoulli beam theory which is valid for slender beams. When the beam is close to the fixed channel, it can not be considered slender. In such situations we need to use other beam theories, e.g. Timoshenko or Reissner beam theories, to obtain more accurate response. This will require further modifications to the consistent co-rotational method presented in this study.

- Stability analysis of flexible sliding beams presents a challenging problem. Since the beam's equations of motion, even in the linear case, include time varying coefficients, its stability analysis does not fall within the existing structural stability theories. In the special case of beams with periodically varying lengths, it is possible to use Bolotin's method to study the stability of inextensible sliding beams in general.

- It is highly likely that under certain conditions the motion of a sliding beam may become chaotic. Païdoussis et al., 1993, have shown that for pipes conveying fluid chaotic motions do arise under particular conditions. The problem of flow in pipes and the sliding beam problem, while different, have much in common particularly in regards to changing mass.

- There is room for improvement in the time integration routines used for nonlinear structural dynamics problems.

- The formulations presented here for motion in a plane can be readily extended to three dimensions. The co-rotational method will require description of rigid body motions in 3D space. Quaternions provide a useful tool for this task.

- The developed flexible sliding beam element may be used in a chain of multibody systems for other applications such as in robotics and space based articulating systems.

- Problems of flow through curved pipes (as in condenser tubes) and flow over twisted beams (as in turbine blades) can be studied by modifying the nonlinear variable domain beam element developed in this research.

- Finally the way is now open to extend the present work to problems of sliding plates and shells.

# References

Abrate, S., 1992, "Vibrations of Belts and Belt Drives", *Mech. Mach. Theory*, **27, 6**, pp. 645-659.

Al-Bedoor, B.O., and Khulief, Y.A., 1996, "Vibrational Motion of an Elastic Beam with Prismatic and Revolute Joints", *J. of Sound and Vibration*, **190, 2**, pp. 195-206.

Al-Bedoor, B.O., and Khulief, Y.A., 1996, "Finite Element Dynamic Modeling of a Translating and Rotating Flexible Link", *Comput. Meth. Appl. Mech. Engng*, **131**, pp. 173-189.

Argyris, J.H., Hilpert, O., Malejannakis, G.A., and Scharpf, D.W., 1979, "On the Geometrical Stiffness of a Beam in Space-A Consistent V.W. Approach", *Comput. Meth. Appl. Mech. Engng*, **20**, pp. 105-131.

Argyris, J., and Mlejnek, H.P., 1991, *Texts on Computational Mechanics, V, Dynamics of Structures*, Elsevier Science, North-Holland.

Bathe, K.J., Ramm, E., and Wilson, E.L., 1975, "Finite Element Formulations for Large Deformation Dynamic Analysis", *Int. J. Numer. Meth. Engng*, **9**, pp. 353-386.

Bathe, K.J., and Bolourchi, S., 1979, "Large Displacement Analysis of Three-Dimensional Beam Structures", *Int. J. Numer. Meth. Engng*, **14**, pp. 961-986.

Bathe, K.J., 1982, *Finite Element Procedures in Engineering Analysis*, Prentice-Hall, Inc., Toronto.

Bathe, K.J., 1986, *Finite Element Procedures for Solid and Structures-Nonlinear Analysis*, MIT Centre for Advanced Engineering Studies.

Belytschko, T., and Hsieh, B.J., 1973, "Nonlinear Transient Finite Element Analysis with Convected Coordinates", *Int. J. Numer. Meth. Engng*, **7**, pp. 255-271.

Belytschko, T., and Glaum, L.W., 1979, "Application of Higher Order Co-rotational Stretch Theories to Nonlinear Finite Element Analysis", *Computers & Structures*, **10**, pp. 175-182.

Belytschko, T., and Hughes, T.J.R., 1983, "An Overview of Semi-discretisation and Time Integration Procedures", Computational Methods for Transient Analysis, Elsevier Science, North-Holland, pp. 1-65.

Bolotin, V.V., 1964, *The Dynamic Stability of Elastic Systems*, Holden Day, San Francisco.

Buffinton, K.W., 1992, "Dynamics of Elastic Manipulators with Prismatic Joints", *ASME J. of Dynamic Syst. Measurements Control*, **114**, pp. 41-49.

Chang, T.-P., and Liu, Y.-N., 1996, "Dynamic Finite Element Analysis of a Nonlinear Beam Subjected to a Moving Load", *Int. J. Solids Structures*, **33**, **12**, pp. 1673-1688.

Chen, Z.Q., and Agar, T.J.A., 1993, "Geometric Nonlinear Analysis of Flexible Spatial Beam Structures", *Computers & Structures*, **49**, **6**, pp. 1083-1094.

Cherchas, D.B., and Gossain, D.M., 1974, "Dynamics of a Flexible Solar Array During Deployment from a Spinning Spacecraft", *J. of Sound and Vibration*, **7**, pp. 10-18.

Chung, J., and Lee, J.M., 1994, "A New Family of Explicit Time Integration Methods for Linear and Nonlinear Structural Dynamics", *Int. J. Numer. Meth. Engng*, **37**, pp. 3961-3976.

Cleghorn, W.L., Fenton, R.G., and Tabarrok, B., 1981, "Finite Element Analysis of High-Speed Flexible Mechanisms", *Mechanism and Machine Theory*, **16**, **4**, pp. 407-424.

Cole, G., 1990, *Consistent Co-rotational Formulation for Geometrically Nonlinear Beam Elements with Special Reference to Large Rotations*, Ph.D. Thesis, School of Civil Engineering, Kingston Polytechnic, England.

Cook, R.D., 1981, *Concepts and Applications of Finite Element Analysis*, John Wiley & Sons, Inc., U.S.A.

Crisfield, M.A., 1990, "A Consistent Co-rotational Formulation for Nonlinear, Three-Dimensional, Beam-Elements", *Comput. Meth. Appl. Mech. Engng*, **81**, pp. 131-150.

Crisfield, M.A., and Peng, X., 1992, "Efficient Nonlinear Shell Formulations with Large Rotations and Plasticity", In Computational Plasticity, Fundamentals & Applications, Part 2 (Eds D.R.J. Owen et al.), Pineridge Press, Swansea, pp. 1979-1996.

Crisfield, M.A., and Shi, J., 1994, "A Co-rotational Element/Time-Integration Strategy for Nonlinear Dynamics", *Int. J. Numer. Meth. Engng*, **37**, pp. 1897-1913.

Crisfield, M.A., Moita, G.F., 1996, "A Unified Co-rotational Framework for Solids, Shells and Beams", *Int. J. Solids Structures*, **33**, **20**, pp. 2969-2992.

Dokainish, M.A., and Subbaraj, K., 1989, "Asurvey of Direct Time-Integration Methods in Computational Structural Dynamics-I. Explicit Methods", *Computers & Structures*, **32**, **6**, pp. 1371-1386.

Dost, S., and Tabarrok, B., 1979, "Application of Hamilton's Principle to Large Deformation and Flow Problems", *ASME J. Appl. Mech.*, **46**, pp. 285-290.

Dvorkin, E.N., Onate, E., and Oliver, J., 1988, "On a Nonlinear Formulation for Curved Timoshenko Beam Elements Considering Large Displacement/Rotation Increments", *Int. J. Numer. Meth. Engng*, **26**, pp. 1597-1613.

Elkaranshawy, H.A., Dokainish, M.A., 1995, "Co-rotational Finite Element Analysis of Planar Flexible Multibody Systems", *Computers & Structures*, **54**, **5**, pp. 881-890.

Elmaraghy, R., and Tabarrok, B., 1975, "On the Dynamic Stability of an Axially Oscillating Beam", *J. of Franklin Institute*, **300**, pp. 25-39.

Fredriksson, B., and Mackerle, J., 1983, "Partial List of Major Finite Element Programs and Description of Some of Their Capabilities", *ASME State-of-Art Survey on Finite Element Technology*, pp. 363-404.

Frisch-Fay, R., 1962, *Flexible Bars*, ButterWorths, London.

Geradin, M., and Cardona, A., 1989, "Kinematics and Dynamics of Rigid and Flexible Mechanisms Using Finite Element and Quarternion Algebra", *Comput. Mech.*, pp. 115-136.

Golnaraghi, M.F., 1991, "Vibration Suppression of Flexible Structures Using Internal Resonance", *Mechanics Research Communications*, **8**, **2/3**, pp. 135-143.

Haug, E., Nguyen, O.S., and De Rouvary, A.L., 1977, "*An Improved Energy Conserving Implicit Time, Integration Algorithm for Nonlinear Dynamic Structural Analysis*", Proc. 4th Int. Conf. on Mech. in Reactor Tech., San Francisco.

Hilber, H.M., Hughes, T.J.R., and Taylor, R.L., 1977, "Improved Numerical Dissipation for Time Integration Algorithms in Structural Dynamics", *Earthquake Engineering and Structural Dynamics*, **5**, pp. 283-292.

Holden, J.T., 1972, "On the Finite Deflections of Thin Beams", *Int. J. Solids Structures*, **8**, pp. 1051-1055.

Hsiao, K.M., 1987, "Nonlinear Analysis of General Shell Structures by Flat Triangular Shell Element", *Computers & Structures*, **25**, pp. 665-675.

Hsiao, K.M., and Jang, J., 1991, "Dynamic Analysis of Planar Flexible Mechanisms by Co-rotational Formulation", *Comput. Meth. Appl. Mech. Engng*, **24**, pp. 359-381.

Hughes, T.J.R., 1976, "Stability, Convergence and Growth and Decay of Energy of the Average Acceleration Method in Nonlinear Structural Dynamics", *Computers & Structures*, **6**, pp. 313-324.

Hughes, T.J.R., Liu, W.K., and Caughy, 1978, "Transient Finite Element Formulations that Preserve Energy", *ASME J. Appl. Mech.*, **45**, pp. 366-370.

Hwang, S.-J., and Perkins, N.C., 1994, "High Speed Stability of Coupled Band/Wheel Systems: Theory and Experiment", *J. of Sound and Vibration*, **169**, **4**, pp. 459-483.

Iura, M., 1994, "Effects of Coordinate System on the Accuracy of Co-rotational Formulation for Bernoulli-Euler's Beam", *Int. J. Solids Structures*, **31**, **20**, pp. 2793-2806.

Iura, M., and Atluri, S.N., 1995, "Dynamic Analysis of Planar Flexible Beams with Finite Rotations by Using Inertial and Rotating Frames", *Computers & Structures*, **55**, **3**, pp. 453-462.

Kane, T.R., and Levinson, D.A., 1981, "Simulation of Large Motions of Nonuniform Beams in Orbit: Part II-The Unrestrained Beam", *The J. of the Astronautical Science*, **29**, **3**, pp. 245-276.

Kim, Y.K., 1988, *Adaptive Control of a Robotic Manipulator with a Sliding Flexible Link*, Ph.D. Thesis, University of California, Los Angeles.

Kim, Y.K., and Gibson, J.S., 1991, "A Variable-Order Adaptive Controller of a Manipulator with a Sliding Flexible Link", *IEEE Robotics and Automation*, **7**, pp. 818-827.

Lau, J.H., 1982, "*Large Deflections of Beams with Combined Loads*", Proceedings of the American Society of Civil Engineering ASCE, 108, EM1, pp. 180-185.

Leech, C.M., 1977, "Hamilton's Principle Applied to Fluid Mechanics", *Quart. J. of Mech. and Appl. Math*, **XXX**, pp. 107-130.

Leong, L.K., 1992, *Dynamic Stability of Suddenly Loaded Structures*, M.Sc. Thesis, Dept. of Aeronautics, Imperial College, London.

Leung, A.Y.T., and Mao, S.G., 1995, "Symplectic Integration of an Accurate Beam Finite Element in Nonlinear Vibration", *Computers & Structures*, **54**, **6**, pp. 1135-1147.

Levinson, D.A., and Kane, T.R., 1981, "Simulation of Large Motions of Nonuniform Beams in Orbit: Part I-The Cantilever Beam", *The J. of the Astronautical Science*, **29**, **3**, pp. 213-244.

Li, G.X., and Païdoussis, M.P., 1994, "Stability, Double Degeneracy and Chaos in Cantilevered Pipes Conveying Fluid", *Int. J. Non-linear Mechanics*, **29**, **1**, pp. 83-107.

Lopez-Almansa, F., Barbat, A.H., and Rodellar, J., 1988, "SSP Algorithm for Linear and Nonlinear Dynamic Response Simulation", *Int. J. Numer. Meth. Engng*, **26**, pp.- 2687-2706.

Mattiasson, K., 1981, "Numerical Results from Large Deflection Beam and Frame Problems Analysed by Means of Elliptic Integrals", *Int. J. Numer. Meth. Engng.*, **17**, pp. 145-153.

McIver, D.B., 1973, "Hamilton's Principle for Systems of Changing Mass", *J. of Engng Math.*, **7**, pp. 249-261.

Meek, J.L., and Loganathan, S., 1989, "Large Displacement Analysis of Space-Frame Structures", *Comput. Meth. Appl. Mech. Engng*, **72**, pp. 57-75.

Meirovitch, L., 1967, *Analytical Methods in Vibrations*, Macmillan, co., New-York.

Modi, V.J., and Marom, I., 1993, "*A Dynamical Study and Control of Flexible Space Based Deployable Manipulator*", Proceeding of the IRIS Workshop, Vancouver, Canada.

Mote, C.D., Jr., 1972, "*Dynamic Stability of Axial Moving Material*", Shock and Vibration Digest, U.S. Naval Research Laboratory, **4**, pp. 2-11.

Mote, C.D., Jr., and Wu, W.Z., 1985, "Vibration Coupling in Continuous Belt and Band System", *J. of Sound and Vibration*, **102, 1**, pp. 1-9.

Nour-Omid, B., and Rankin, C.C., 1991, "Finite Rotation Analysis and Consistent Linearisation Using Projectors", *Comput. Meth. Appl. Mech. Engng*, **93**, pp. 353-384.

Orth, F.J., and Surana, K.S., 1994, "p-Version Two-Dimensional Beam Element for Geometrically Nonlinear Analysis", *Computers & Structures*, **50**, **3**, pp. 383-392.

Owren, B., and Simonsen, H.H., 1995, "Alternative Integration Methods for Problems in Structural Dynamics", *Comput. Meth. Appl. Mech. Engng*, **122**, pp. 1-10.

Pai, P.F., and Palazotto, A.N., 1996, "Large Deformation Analysis of Flexible Beams", *Int. J. Solids Structures*, **33**, **9**, pp. 1335-1353.

Païdoussis, M.P., 1991, "*Pipes Conveying Fluid: A Model Dynamical Problem*", CANCAM Proceedings, pp. 1-33.

Païdoussis, M.P., and Semler, C., 1993, "Nonlinear and Chaotic Oscillations of a Constrained Cantilevered Pipe Conveying Fluid: A Full Nonlinear Analysis", *Nonlinear Dynamics*, **4**, pp. 655-670.

Pan, Y.C., Scott, R.A., and Ulsoy, A.G., 1990, "Experimental Model Validation for a Flexible Robot with Prismatic Joints", *J. Mech. Des.*, **112**, pp. 307-314.

Petrolito, J., 1995, "Stiffness Analysis of Beams Using a Higher-Order Theory", *Computers & Structures*, **55**, 1, pp. 33-39.

Petyt, M., 1990, *Introduction to Finite Element Vibration Analysis*, Cambridge University Press, Cambridge.

Rankin, C.C., and Brogan, F.A., 1986, "An Element Independent Co-rotational Procedure for the Treatment of Large Rotations", *J. of Pressure Vessel Technology*, **108**, pp. 165-174.

Rankin, C.C., and Nour-Omid, B., 1988, "The use of Projectors to Improve Finite Element Performance", *Computers & Structures*, **30**, **1/2**, pp. 257-267.

Rice, D.L., and Ting, E.C., 1993, "Large Displacement Transient Analysis of Flexible Structures", *Int. J. Numer. Meth. Engng*, **36**, pp. 1541-1562.

Saje, M., 1990, "A Variational Principle for Finite Planar Deformation of Straight Slender Elastic Beams", *Int. J. Solids Structures*, **26**, **8**, pp. 887-900.

Schmidt, R., and DaDeppo, D.A., 1971, "A Survey of Literature on Large Deflections of Nonshallow Arches. Bibliography of Finite Deflections of Straight and Curved Beams, Rings, and Shallow Arches.", *J. of the Industrial Mathematics Society*, **21**, pp. 91-114.

Semler, C., Li, G.X., and Païdoussis, M.P., 1994, "The Nonlinear Equations of Motion of Pipes Conveying Fluid", *J. of Sound and Vibration*, **169**, **5**, pp. 577-599.

Semler, C., 1991, *Nonlinear Dynamics and Chaos of a Pipe Conveying Fluid*, Master's Thesis, Faculty of Engineering, McGill University, Montreal, Quebec, Canada.

Simo, J.C., Vu-Quoc, L., 1986, "On the Dynamics of Flexible Beams Under Large Overall Motions-The Plane Case: Part I", *ASME J. Appl. Mech.*, **53,4**, pp. 849-854.

Simo, J.C., Vu-Quoc, L., 1986, "On the Dynamics of Flexible Beams Under Large Overall Motions-The Plane Case: Part II", *ASME J. Appl. Mech.*, **53,4**, pp. 855-863.

Simo, J.C., 1985, "A Finite Strain Beam Formulation. The Three Dimensional Dynamic Problem. Part I", *Comput. Meth. Appl. Mech. Engng*, **49**, pp. 55-70.

Simo, J.C., Vu-Quoc, L., 1986, "A Three-Dimensional Finite-Strain Rod Model. Part II: Computational Aspects", *Comput. Meth. Appl. Mech. Engng*, **58**, pp. 79-116.

Simo, J.C., Vu-Quoc, L., 1988, "On the Dynamics in Space of Rods Undergoing Large Motions-A Geometrically Exact Approach", *Comput. Meth. Appl. Mech. Engng*, **66**, pp. 125-161.

Subbaraj, K., and Dokainish, M.A., 1989, "Asurvey of Direct Time-Integration Methods in Computational Structural Dynamics-II. Implicit Methods", *Computers & Structures*, **32**, **6**, pp. 1387-1401.

Simo, J.C., and Wong, K.K., 1991, "Unconditionally Stable Algorithms for Rigid Body Dynamics that Exactly Preserve Energy and Momentum", *Int. J. Numer. Meth. Engng*, **31**, pp. 19-52.

Simo, J.C., Tarnow, N., and Wong, K.K., 1992, "Exact Energy-Momentum Conserving Algorithms and Symplectic Schemes for Nonlinear Dynamics", *Comput. Meth. Appl. Mech. Engng*, **100**, pp. 63-116.

Simo, J.C., Rifai, M.S., and Fox, D.D., 1992, "On a Stress Resultant Geometrically Exact Shell Model. Part VI: Conserving Algorithms for Nonlinear Dynamics", *Int. J. Numer. Meth. Engng*, **34**, pp. 117-164.

Simo, J.C., and Tarnow, N., 1992, "The Discrete Energy-Momentum Method. Conserving Algorithms for Nonlinear Elastodynamics", *Z Angew Math. Phys.*, **43**, pp. 757-792.

Simo, J.C., and Tarnow, N., 1994, "A New Energy and Momentum Conserving Algorithm for the Nonlinear Dynamics of Shells", *Int. J. Numer. Meth. Engng*, **37**, pp. 2527-2549.

Simo, J.C., Tarnow, N., and Doblare, M., 1995, "Nonlinear Dynamics of Three Dimensional Rods: Exact Energy and Momentum Conserving Algorithms", *Int. J. Numer. Meth. Engng*, **38**, pp. 1431-1473.

Spillers, W.R., 1990, "Geometric Stiffness Matrix for Space Frames", *Computers & Structures*, **36**, **1**, pp. 29-37.

Stoker, J.J., 1968, *Nonlinear Elasticity*, Gordon and Breach, New York.

Stylianou, M.C., 1993, *Dynamics of Flexible Extendible Beam*, Ph.D. Thesis, Dept. of Mech. Engng, University of Victoria, Canada.

Stylianou, M.C., and Tabarrok, B., 1994, "Finite Element Analysis of an Axially Moving Beam, Part I: Time Integration", *J. of Sound and Vibration*, **178**, pp. 433-453.

Tabarrok, B., Leech, C.M., and Kim, Y.I., 1974, "On the Dynamics of an Axially Moving Beam", *J. of Franklin Institute*, **297**, pp. 201-220.

Tadikonda, S.S.K., and Baruh, H., 1992, "Dynamics and Control of a Translating Flexible Beam with a Prismatic Joint", *ASME J. of Dynamic Syst. Measurements Control*, **114**, pp. 422-427.

Tarnow, N., and Simo, J.C., 1994, "How to render Second Order Accurate Time-Stepping Algorithms Fourth Order Accurate while Retaining the Stability and Conservation Properties", *Comput. Meth. Appl. Mech. Engng*, **115**, pp. 233-252.

Veubeke, B.F., 1974, "*Variational Principle in Fluid Mechanics and Finite Element Applications*", Laboratoire de Techniques Aeromautiques et Spatiales, FA.1, Universite de Liege, Liege, Belgique.

Vu-Quoc, L., and Olssom, M., 1993, "High-Speed Vehicle Models Based on a New Concept of Vehicle/Structure Interaction Component: Part I-Formulation", *ASME J. of Dynamic Syst. Measurements Control*, **115**, pp. 140-147.

Vu-Quoc, L., and Olssom, M., 1993, "High-Speed Vehicle Models Based on a New Concept of Vehicle/Structure Interaction Component: Part II-Algorithmic Treatment and Results for Multispan Guideways", *ASME J. of Dynamic Syst. Measurements Control*, **115**, pp. 148-155.

Vu-Quoc, L., and Li, S., 1995, "Dynamics of Sliding Geometrically-Exact Beams: Large Angle Maneuver and Parametric Resonance", *Comput. Meth. Appl. Mech. Engng*, **120**, pp. 65-118.

Wang, P.K.C., and Wei, J., 1987, "Vibration in a Moving Flexible Robot Arm", *J. of Sound and Vibration*, **116**, pp. 149-160.

Wempner, G., 1969, "Finite Element, Finite Rotations and Small Strains of Flexible Shells", *Int. J. Solids Structures*, **5**, pp. 117-153.

Wickert, J.A., and Mote, C.D., 1988, "Current Research on the Vibration and Stability of Axially-Moving Materials", *The Shock and Vibration Digest*, **20**, pp. 3-13.

Yang, Y.B., Leu, L.J., 1994, "Nonlinear Stiffnesses in Analysis of Planar Frames", *Comput. Meth. Appl. Mech. Engng*, **117**, pp. 233-247.

Yuh, J., and Young, T., 1991, "Dynamic Modelling of an Axially Moving Beam in Rotation: Simulation and Experiment", *ASME J. of Dynamic Syst. Measurements Control*, **113**, pp. 34-40.

Zajaczkowski, J., and Lipinski, J., 1979, "Instability of the Motion of a Beam of Periodically Varying Length", *J. of Sound and Vibration*, **63**, pp. 9-18.

Zajaczkowski, J., and Yamada, G., 1980, "Further Results on Instability of the Motion of a Beam of Periodically Varying Length", *J. of Sound and Vibration*, **68**, **2**, pp. 173-180.

Zienkiewicz, O.C., Wood, W.L., and Taylor, R.L., 1980, "An Alternative Single-Step Algorithm for Dynamic Problems", *Earthquake Engineering and Structural Dynamics*, **8**, pp. 31-40.

# Appendices

## Appendix A: The Equation of Motion for Axially Inextensible Flexible Sliding Beams

Starting with equation (3.1.48) for the kinetic co-energy for the sliding beam:

$$T^* = \int_0^{L(t)} \frac{1}{2}\rho A \left[\left(\frac{\partial x_1}{\partial t} + V\frac{\partial x_1}{\partial S}\right)^2 + \left(\frac{\partial x_2}{\partial t} + V\frac{\partial x_2}{\partial S}\right)^2\right] dS \tag{1}$$

We compute its variation and obtain:

$$\begin{aligned}\delta\int_{t_1}^{t_2} T^*\, dt = \int_{t_1}^{t_2}\int_0^{L(t)} \rho A &\left[\left(\frac{\partial x_1}{\partial t} + V\frac{\partial x_1}{\partial S}\right)\left(\delta\left(\frac{\partial x_1}{\partial t}\right) + V\,\delta\left(\frac{\partial x_1}{\partial S}\right)\right) + \right.\\ &\left.\left(\frac{\partial x_2}{\partial t} + V\frac{\partial x_2}{\partial S}\right)\left(\delta\left(\frac{\partial x_2}{\partial t}\right) + V\,\delta\left(\frac{\partial x_2}{\partial S}\right)\right)\right] dS\, dt\end{aligned} \tag{2}$$

Using the Leibniz rule and carrying out integration by parts, after simplification and taking out the boundary terms, we find:

$$\begin{aligned}\delta\int_{t_1}^{t_2} T^*\, dt = &-\int_{t_1}^{t_2}\int_0^{L(t)} \rho A\left[\frac{\partial^2 x_1}{\partial t^2} + \frac{\partial V}{\partial t}\frac{\partial x_1}{\partial S} + 2V\frac{\partial^2 x_1}{\partial t\partial S} + V^2\frac{\partial^2 x_1}{\partial S^2}\right](\delta x_1)\, dSdt - \\ &\int_{t_1}^{t_2}\int_0^{L(t)} \rho A\left[\frac{\partial^2 x_2}{\partial t^2} + \frac{\partial V}{\partial t}\frac{\partial x_2}{\partial S} + 2V\frac{\partial^2 x_2}{\partial t\partial S} + V^2\frac{\partial^2 x_2}{\partial S^2}\right](\delta x_2)\, dSdt\end{aligned} \tag{3}$$

We now may obtain the variation of the strain energy in the same manner. To this end first we consider the strain energy of the system expressed in equation (3.1.50) as:

$$\Pi = \int_0^{L(t)} \frac{EI}{2} \left(\frac{\partial^2 x_2}{\partial S^2}\right)^2 \left[1 + \left(\frac{\partial x_2}{\partial S}\right)^2\right] dS \tag{4}$$

The variation of equation (4) yields:

$$\begin{aligned} \delta\int_{t_1}^{t_2} \Pi \, dt &= \int_{t_1}^{t_2} \int_0^{L(t)} \frac{EI}{2} \, \delta\left\{ \left(\frac{\partial^2 x_2}{\partial S^2}\right)^2 \left[1 + \left(\frac{\partial x_2}{\partial S}\right)^2\right]\right\} dS dt \\ &= \int_{t_1}^{t_2} \int_0^{L(t)} EI \left(\frac{\partial^2 x_2}{\partial S^2}\right) \left[1 + \left(\frac{\partial x_2}{\partial S}\right)^2\right] \delta\left(\frac{\partial^2 x_2}{\partial S^2}\right) dS dt + \\ &\quad \int_{t_1}^{t_2} \int_0^{L(t)} EI \left(\frac{\partial^2 x_2}{\partial S^2}\right)^2 \left(\frac{\partial x_2}{\partial S}\right) \delta\left(\frac{\partial x_2}{\partial S}\right) dS dt \end{aligned} \tag{5}$$

After carrying out integrations by parts, simplifications and taking out the boundary terms, we find:

$$\delta\int_{t_1}^{t_2} \Pi dt = \int_{t_1}^{t_2}\int_0^{L(t)} EI\left[\frac{\partial^4 x_2}{\partial S^4} + \left(\frac{\partial^2 x_2}{\partial S^2}\right)^3 + \frac{\partial^4 x_2}{\partial S^4}\left(\frac{\partial x_2}{\partial S}\right)^2 + 4\frac{\partial x_2}{\partial S}\,\frac{\partial^2 x_2}{\partial S^2}\,\frac{\partial^3 x_2}{\partial S^3}\right] (\delta x_2)\, dS dt \tag{6}$$

Now we use the inextensibility condition to express all the terms in equation (3) which include $x_1$, in terms of $x_2$ (see Semler et al., 1994). To this end we use the inextensibility condition to write:

$$\frac{\partial x_1}{\partial S} = \sqrt{1 - \left(\frac{\partial x_2}{\partial S}\right)^2} \cong 1 - \frac{1}{2}\left(\frac{\partial x_2}{\partial S}\right)^2 \tag{7}$$

Also we have that:

$$\frac{\partial x_1}{\partial S}\,\delta\left(\frac{\partial x_1}{\partial S}\right) = -\,\frac{\partial x_2}{\partial S}\,\delta\left(\frac{\partial x_2}{\partial S}\right) \tag{8}$$

Substituting equation (7) into equation (8), we obtain:

$$\begin{aligned}\delta\left(\frac{\partial x_1}{\partial S}\right) &= - \frac{\dfrac{\partial x_2}{\partial S}}{\sqrt{1-\left(\dfrac{\partial x_2}{\partial S}\right)^2}}\ \delta\left(\frac{\partial x_2}{\partial S}\right) \\ &\cong - \frac{\partial x_2}{\partial S}\left[1+\frac{1}{2}\left(\frac{\partial x_2}{\partial S}\right)^2\right]\delta\left(\frac{\partial x_2}{\partial S}\right)\end{aligned} \tag{9}$$

Hence we may have:

$$\delta x_1 \cong - \int_0^S \left\{\frac{\partial x_2}{\partial S}\left[1+\frac{1}{2}\left(\frac{\partial x_2}{\partial S}\right)^2\right]\delta\left(\frac{\partial x_2}{\partial S}\right)\right\} dS \tag{10}$$

Considering the geometrical boundary condition and doing the integration by part, we may express equation (10) as:

$$\delta x_1 \cong - \left[\frac{\partial x_2}{\partial S}+\frac{1}{2}\left(\frac{\partial x_2}{\partial S}\right)^3\right]\delta x_2 + \int_0^S \left[\frac{\partial^2 x_2}{\partial S^2}+\frac{3}{2}\left(\frac{\partial x_2}{\partial S}\right)^2\frac{\partial^2 x_2}{\partial S^2}\right]\delta x_2\ dS \tag{11}$$

Also from equation (9), we obtain:

$$\frac{\partial^2 x_1}{\partial S \partial t} \cong - \frac{\partial x_2}{\partial S}\left[1+\frac{1}{2}\left(\frac{\partial x_2}{\partial S}\right)^2\right]\frac{\partial^2 x_2}{\partial S \partial t} \tag{12}$$

Next we differentiate equation (12) with respect to time and integrate the result from 0 to $S$. Then we have:

$$\frac{\partial^2 x_1}{\partial t^2} = - \int_0^S \left\{\frac{\partial^3 x_2}{\partial t^2 \partial S}\frac{\partial x_2}{\partial S}\left[1+\frac{1}{2}\left(\frac{\partial x_2}{\partial S}\right)^2\right]+\left(\frac{\partial^2 x_2}{\partial t \partial S}\right)^2\right\} dS \tag{13}$$

For further simplifications, we also need to use the following relation (see Semler, 1991):

$$\int_0^L g(S)\left(\int_0^S f(S)\,\delta x_2\ dS\right) dS = \int_0^L \left(\int_S^L g(S)\ dS\right) f(S)\,\delta x_2\ dS \tag{14}$$

Relations (11), (12), (13) and (14) may now be used to obtain the variation of kinetic co-energy, expressed in equation (3), in terms of $x_2$. Hence after some manipulations, the terms inside the first integral of equation (3) may be expressed as:

$$\int_0^{L(t)} \rho A\left[\frac{\partial^2 x_1}{\partial t^2}\right]\delta x_1 dS \equiv \int_0^{L(t)} \left\{\rho A\frac{\partial x_2}{\partial t}\int_0^S\left[\frac{\partial^3 x_2}{\partial t^2 \partial S}\frac{\partial x_2}{\partial S} + \left(\frac{\partial^2 x_2}{\partial t \partial S}\right)^2\right]dS\right\}\delta x_2 \; dS -$$
$$\int_0^{L(t)}\left\{\rho A\int_S^{L(t)}\left(\int_0^S\left[\frac{\partial^3 x_2}{\partial t^2 \partial S}\frac{\partial x_2}{\partial S} + \left(\frac{\partial^2 x_2}{\partial t \partial S}\right)^2\right]\right)dS \; dS\right\} \tag{15}$$
$$\frac{\partial^2 x_2}{\partial S^2}\;\delta x_2 \; dS$$

$$\int_0^{L(t)} \rho A\left[\frac{\partial V}{\partial t}\frac{\partial x_1}{\partial S}\right](\delta x_1)\,dS \equiv \int_0^{L(t)} - \rho A\left[\frac{\partial V}{\partial t}\frac{\partial x_2}{\partial S}\right](\delta x_2)\,dS +$$
$$\int_0^{L(t)} \rho A\left\{\frac{\partial V}{\partial t}(L-S)\left[1+\frac{3}{2}\left(\frac{\partial x_2}{\partial S}\right)^2\right] - \right. \tag{16}$$
$$\left.\frac{1}{2}\frac{\partial V}{\partial t}\left(\frac{\partial x_2}{\partial S}\right)^2\right\}\frac{\partial^2 x_2}{\partial S^2}\;\delta x_2 \; dS$$

$$\int_0^{L(t)} \rho A\left[2V\frac{\partial^2 x_1}{\partial t \partial S}\right](\delta x_1)\,dS \equiv \int_0^{L(t)} \rho A\left[2V\frac{\partial^2 x_2}{\partial t \partial S}\left(\frac{\partial x_2}{\partial S}\right)^2\right](\delta x_2)\,dS -$$
$$\int_0^{L(t)} \rho A\left\{\int_S^{L(t)}\left[2V\frac{\partial^2 x_2}{\partial t \partial S}\frac{\partial x_2}{\partial S}\right]\right\}\frac{\partial^2 x_2}{\partial S^2}(\delta x_2)\,dS \tag{17}$$

$$\int_0^{L(t)} \rho A\left[V^2\frac{\partial^2 x_1}{\partial S^2}\right](\delta x_1)\,dS \equiv \int_0^{L(t)} \rho A\left[V^2\left(\frac{\partial x_2}{\partial S}\right)^2\frac{\partial^2 x_2}{\partial S^2}\right](\delta x_2)\,dS -$$
$$\int_0^{L(t)} \rho A\left\{\int_S^{L(t)}\left[V^2\frac{\partial x_2}{\partial S}\frac{\partial^2 x_2}{\partial S^2}\right]\right\}\frac{\partial^2 x_2}{\partial S^2}(\delta x_2)\,dS \tag{18}$$

Now on substituting the above relations in equation (3) an expression for the variation of kinetic co-energy may be obtained. Finally using $\delta T^*$ and $\delta\Pi$ in the extended

Hamilton's principle introduced in chapter 3, leads to the governing equation of motion as expressed in equation (3.1.52).

# Appendix B: Euler-Lagrange Equations for a Second Order Lagrangian Function with Two Dependent and Two Independent Variables

Hamilton's principle for a second order Lagrangian function with two dependent and two independent variables may be expressed as:

$$\delta\int_{t_1}^{t_2}\int_{X_1}^{X_2}\mathcal{L}(t,X,Y,\dot{Y},Y',\dot{Y}',\ddot{Y},Y'',Z,\dot{Z},Z',\dot{Z}',\ddot{Z},Z'')\;dX\;dt = 0 \qquad (19)$$

where $t$, $X$ are the independent variables and $Y(X,t)$, $Z(X,t)$ are the dependent functions and $X_1$ and $X_2$ are in general time dependent. Here, also $(\dot{\ })$ and $(\ )'$ denote the derivatives with respect to $t$ and $X$, respectively.

Carrying out the variation in equation (19), we obtain:

$$\begin{aligned}
&\int_{t_1}^{t_2}\int_{X_1}^{X_2}\left(\frac{\partial\mathcal{L}}{\partial Y}\,\delta Y+\frac{\partial\mathcal{L}}{\partial Z}\,\delta Z\right)dX\;dt+\int_{t_1}^{t_2}\int_{X_1}^{X_2}\left(\frac{\partial\mathcal{L}}{\partial\dot{Y}}\,\delta\dot{Y}+\frac{\partial\mathcal{L}}{\partial\dot{Z}}\,\delta\dot{Z}\right)dX\;dt+\\
&\int_{t_1}^{t_2}\int_{X_1}^{X_2}\left(\frac{\partial\mathcal{L}}{\partial Y'}\,\delta Y'+\frac{\partial\mathcal{L}}{\partial Z'}\,\delta Z'\right)dX\;dt+\int_{t_1}^{t_2}\int_{X_1}^{X_2}\left(\frac{\partial\mathcal{L}}{\partial\dot{Y}'}\,\delta\dot{Y}'+\frac{\partial\mathcal{L}}{\partial\dot{Z}'}\,\delta\dot{Z}'\right)dX\;dt+\\
&\int_{t_1}^{t_2}\int_{X_1}^{X_2}\left(\frac{\partial\mathcal{L}}{\partial\ddot{Y}}\,\delta\ddot{Y}+\frac{\partial\mathcal{L}}{\partial\ddot{Z}}\,\delta\ddot{Z}\right)dX\;dt+\int_{t_1}^{t_2}\int_{X_1}^{X_2}\left(\frac{\partial\mathcal{L}}{\partial Y''}\,\delta Y''+\frac{\partial\mathcal{L}}{\partial Z''}\,\delta Z''\right)dX\;dt = 0
\end{aligned} \qquad (20)$$

Using the Leibniz rule, the second integral on the left hand side of equation (20) may be written as:

$$\int_{t_1}^{t_2}\int_{X_1}^{X_2}\left(\frac{\partial\mathcal{L}}{\partial\dot{Y}}\ \delta\dot{Y}+\frac{\partial\mathcal{L}}{\partial\dot{Z}}\ \delta\dot{Z}\right)dX\ \ dt = \int_{t_1}^{t_2}\frac{d}{dt}\left[\int_{X_1}^{X_2}\frac{\partial\mathcal{L}}{\partial\dot{Y}}\ \delta Y\ \ dX+\int_{X_1}^{X_2}\frac{\partial\mathcal{L}}{\partial\dot{Z}}\ \delta Z\ \ dX\right]\ dt -$$
$$\int_{t_1}^{t_2}\left[\dot{X}_2\frac{\partial\mathcal{L}}{\partial\dot{Y}}\ \delta Y\Big|_{X_2}+\dot{X}_2\frac{\partial\mathcal{L}}{\partial\dot{Z}}\ \delta Z\Big|_{X_2}\right]dt +$$
$$\int_{t_1}^{t_2}\left[\dot{X}_1\frac{\partial\mathcal{L}}{\partial\dot{Y}}\ \delta Y\Big|_{X_1}+\dot{X}_1\frac{\partial\mathcal{L}}{\partial\dot{Z}}\ \delta Z\Big|_{X_1}\right]dt - \tag{21}$$
$$\int_{t_1}^{t_2}\int_{X_1}^{X_2}\left[\frac{\partial}{\partial t}\left(\frac{\partial\mathcal{L}}{\partial\dot{Y}}\right)\ \delta Y+\frac{\partial}{\partial t}\left(\frac{\partial\mathcal{L}}{\partial\dot{Z}}\right)\ \delta Z\right]dX\ \ dt$$

The Leibniz rule can also be used on the fifth integral; Therefore we obtain:

$$\int_{t_1}^{t_2}\int_{X_1}^{X_2}\left(\frac{\partial\mathcal{L}}{\partial\ddot{Y}}\ \delta\ddot{Y}+\frac{\partial\mathcal{L}}{\partial\ddot{Z}}\ \delta\ddot{Z}\right)dX\ \ dt = \int_{t_1}^{t_2}\frac{d}{dt}\left[\int_{X_1}^{X_2}\frac{\partial\mathcal{L}}{\partial\ddot{Y}}\ \delta\dot{Y}\ \ dX+\int_{X_1}^{X_2}\frac{\partial\mathcal{L}}{\partial\ddot{Z}}\ \delta\dot{Z}\ \ dX\right]\ dt -$$
$$\int_{t_1}^{t_2}\frac{d}{dt}\left[\int_{X_1}^{X_2}\frac{\partial}{\partial t}\left(\frac{\partial\mathcal{L}}{\partial\ddot{Y}}\right)\delta Y dX+\int_{X_1}^{X_2}\frac{\partial}{\partial t}\left(\frac{\partial\mathcal{L}}{\partial\ddot{Z}}\right)\delta Z dX\right]dt +$$
$$\int_{t_1}^{t_2}\left[\dot{X}_2\frac{\partial}{\partial t}\left(\frac{\partial\mathcal{L}}{\partial\ddot{Y}}\right)\ \delta Y\Big|_{X_2}+\dot{X}_2\frac{\partial}{\partial t}\left(\frac{\partial\mathcal{L}}{\partial\ddot{Z}}\right)\ \delta Z\Big|_{X_2}\right]dt -$$
$$\int_{t_1}^{t_2}\left[\dot{X}_2\frac{\partial\mathcal{L}}{\partial\ddot{Y}}\ \delta\dot{Y}\Big|_{X_2}+\dot{X}_2\frac{\partial\mathcal{L}}{\partial\ddot{Z}}\ \delta\dot{Z}\Big|_{X_2}\right]dt - \tag{22}$$
$$\int_{t_1}^{t_2}\left[\dot{X}_1\frac{\partial}{\partial t}\left(\frac{\partial\mathcal{L}}{\partial\ddot{Y}}\right)\ \delta Y\Big|_{X_1}+\dot{X}_1\frac{\partial}{\partial t}\left(\frac{\partial\mathcal{L}}{\partial\ddot{Z}}\right)\ \delta Z\Big|_{X_1}\right]dt +$$
$$\int_{t_1}^{t_2}\left[\dot{X}_1\frac{\partial\mathcal{L}}{\partial\ddot{Y}}\ \delta\dot{Y}\Big|_{X_2}+\dot{X}_1\frac{\partial\mathcal{L}}{\partial\ddot{Z}}\ \delta\dot{Z}\Big|_{X_2}\right]dt +$$
$$\int_{t_1}^{t_2}\int_{X_1}^{X_2}\left[\frac{\partial^2}{\partial t^2}\left(\frac{\partial\mathcal{L}}{\partial\ddot{Y}}\right)\ \delta Y+\frac{\partial^2}{\partial t^2}\left(\frac{\partial\mathcal{L}}{\partial\ddot{Z}}\right)\ \delta Z\right]dX\ \ dt$$

Carrying out integration by part, the third and sixth integrals on the left hand side of equation (20) can be written as:

$$\int_{t_1}^{t_2}\int_{X_1}^{X_2}\left(\frac{\partial \mathcal{L}}{\partial Y'}\,\delta Y' + \frac{\partial \mathcal{L}}{\partial Z'}\,\delta Z'\right)dX\;dt = \int_{t_1}^{t_2}\left[\frac{\partial \mathcal{L}}{\partial Y'}\,\delta Y\Big|_{X_1}^{X_2} + \frac{\partial \mathcal{L}}{\partial Z'}\,\delta Z\Big|_{X_1}^{X_2}\right]dt - \int_{t_1}^{t_2}\int_{X_1}^{X_2}\left[\frac{\partial}{\partial X}\left(\frac{\partial \mathcal{L}}{\partial Y'}\right)\,\delta Y + \frac{\partial}{\partial X}\left(\frac{\partial \mathcal{L}}{\partial Z'}\right)\,\delta Z\right]dX\;dt \tag{23}$$

and

$$\int_{t_1}^{t_2}\int_{X_1}^{X_2}\left(\frac{\partial \mathcal{L}}{\partial Y''}\,\delta Y'' + \frac{\partial \mathcal{L}}{\partial Z''}\,\delta Z''\right)dX\;dt = \int_{t_1}^{t_2}\left[\frac{\partial \mathcal{L}}{\partial Y''}\,\delta Y'\Big|_{X_1}^{X_2} + \frac{\partial \mathcal{L}}{\partial Z''}\,\delta Z'\Big|_{X_1}^{X_2}\right]dt - \int_{t_1}^{t_2}\left[\frac{\partial}{\partial X}\left(\frac{\partial \mathcal{L}}{\partial Y''}\right)\delta Y\Big|_{X_1}^{X_2} + \frac{\partial}{\partial X}\left(\frac{\partial \mathcal{L}}{\partial Z''}\right)\delta Z\Big|_{X_1}^{X_2}\right]dt + \int_{t_1}^{t_2}\int_{X_1}^{X_2}\left[\frac{\partial^2}{\partial X^2}\left(\frac{\partial \mathcal{L}}{\partial Y''}\right)\delta Y + \frac{\partial^2}{\partial X^2}\left(\frac{\partial \mathcal{L}}{\partial Z''}\right)\delta Z\right]dX\;dt \tag{24}$$

Finally, using the Leibniz rule and carrying out integration by part, the fourth integral on the left hand side of equation (20) may be written as:

$$\int_{t_1}^{t_2}\int_{X_1}^{X_2}\left(\frac{\partial\mathcal{L}}{\partial\dot{Y}}\delta\dot{Y}+\frac{\partial\mathcal{L}}{\partial\dot{Z}}\delta\dot{Z}\right)dXdt = -\int_{t_1}^{t_2}\frac{d}{dt}\left[\int_{X_1}^{X_2}\frac{\partial}{\partial X}\left(\frac{\partial\mathcal{L}}{\partial\dot{Y}}\right)\delta YdX+\frac{\partial}{\partial X}\left(\frac{\partial\mathcal{L}}{\partial\dot{Z}}\right)\delta ZdX\right]dt +$$

$$\int_{t_1}^{t_2}\left[\frac{\partial\mathcal{L}}{\partial\dot{Y}}\delta\dot{Y}\Big|_{X_1}^{X_2}+\frac{\partial\mathcal{L}}{\partial\dot{Z}}\delta\dot{Z}\Big|_{X_1}^{X_2}\right]dt +$$

$$\int_{t_1}^{t_2}\int_{X_1}^{X_2}\left[\frac{\partial^2}{\partial X\partial t}\left(\frac{\partial\mathcal{L}}{\partial\dot{Y}}\right)\delta Y+\frac{\partial^2}{\partial X\partial t}\left(\frac{\partial\mathcal{L}}{\partial\dot{Z}}\right)\delta Z\right]dX\ \ dt + \qquad (25)$$

$$\int_{t_1}^{t_2}\left[\dot{X}_2\frac{\partial}{\partial X}\left(\frac{\partial\mathcal{L}}{\partial\dot{Y}}\right)\ \delta Y\Big|_{X_2}+\dot{X}_2\frac{\partial}{\partial X}\left(\frac{\partial\mathcal{L}}{\partial\dot{Z}}\right)\ \delta Z\Big|_{X_2}\right]dt -$$

$$\int_{t_1}^{t_2}\left[\dot{X}_1\frac{\partial}{\partial X}\left(\frac{\partial\mathcal{L}}{\partial\dot{Y}}\right)\ \delta Y\Big|_{X_1}+\dot{X}_1\frac{\partial}{\partial X}\left(\frac{\partial\mathcal{L}}{\partial\dot{Z}}\right)\ \delta Z\Big|_{X_1}\right]dt$$

Now, by substituting equations (21) to (25) into equation (20), and requiring the vanishing of variation of $Y$, $Z$, $\dot{Y}$ and $\dot{Z}$ at $t_1$ and $t_2$ and noting the arbitrariness of $\delta Y$ and $\delta Z$, one concludes that for the stationary conditions the functional in (19), the following equations must be satisfied:

In the domain:

$$\frac{\partial\mathcal{L}}{\partial Y}-\frac{\partial}{\partial t}\left(\frac{\partial\mathcal{L}}{\partial\dot{Y}}\right)-\frac{\partial}{\partial X}\left(\frac{\partial\mathcal{L}}{\partial Y'}\right)+\frac{\partial^2}{\partial t^2}\left(\frac{\partial\mathcal{L}}{\partial\ddot{Y}}\right)+\frac{\partial^2}{\partial X^2}\left(\frac{\partial\mathcal{L}}{\partial Y''}\right)+\frac{\partial^2}{\partial t\partial X}\left(\frac{\partial\mathcal{L}}{\partial\dot{Y}'}\right) = 0 \qquad (26)$$

$$\frac{\partial\mathcal{L}}{\partial Z}-\frac{\partial}{\partial t}\left(\frac{\partial\mathcal{L}}{\partial\dot{Z}}\right)-\frac{\partial}{\partial X}\left(\frac{\partial\mathcal{L}}{\partial Z'}\right)+\frac{\partial^2}{\partial t^2}\left(\frac{\partial\mathcal{L}}{\partial\ddot{Z}}\right)+\frac{\partial^2}{\partial X^2}\left(\frac{\partial\mathcal{L}}{\partial Z''}\right)+\frac{\partial^2}{\partial t\partial X}\left(\frac{\partial\mathcal{L}}{\partial\dot{Z}'}\right) = 0 \qquad (27)$$

and along the boundaries:

$$\left[\dot{X}_2\frac{\partial}{\partial X}\left(\frac{\partial\mathcal{L}}{\partial\dot{Y}}\right)-\dot{X}_2\frac{\partial\mathcal{L}}{\partial\dot{Y}}+\dot{X}_2\frac{\partial}{\partial t}\left(\frac{\partial\mathcal{L}}{\partial\ddot{Y}}\right)+\frac{\partial\mathcal{L}}{\partial Y'}-\frac{\partial}{\partial X}\left(\frac{\partial\mathcal{L}}{\partial Y''}\right)\right]\delta Y = 0 \qquad \text{at } X = X_2 \qquad (28)$$

$$\left[\dot{X}_1\frac{\partial}{\partial X}\left(\frac{\partial\mathcal{L}}{\partial\dot{Y}}\right)-\dot{X}_1\frac{\partial\mathcal{L}}{\partial\dot{Y}}+\dot{X}_1\frac{\partial}{\partial t}\left(\frac{\partial\mathcal{L}}{\partial\ddot{Y}}\right)+\frac{\partial\mathcal{L}}{\partial Y'}-\frac{\partial}{\partial X}\left(\frac{\partial\mathcal{L}}{\partial Y''}\right)\right]\delta Y = 0 \qquad \text{at } X = X_1 \qquad (29)$$

$$\left[\frac{\partial\mathcal{L}}{\partial\ddot{Y}}-\frac{\partial\mathcal{L}}{\partial\dot{Y}'}\right]\delta\dot{Y} = 0 \qquad \text{at } X = X_2 \ \text{ and } \ X = X_1 \qquad (30)$$

$$\left[\frac{\partial \mathcal{L}}{\partial Y'}\right]\delta Y' = 0 \qquad \text{at } X = X_2 \quad \text{and} \quad X = X_1 \tag{31}$$

Similar relations at the boundaries can be written for $Z$.

# Appendix C: The Equation of Motion Obtained from the Alternative Formulation

Consider again the expression for the kinetic co-energy given in equation (3.2.7):

$$T^* = \int_{C(t)}^{L_B} \frac{1}{2}\rho A \left[\left(\frac{\partial \bar{x}_1}{\partial t}\right)^2 + \left(\frac{\partial \bar{x}_2}{\partial t}\right)^2\right] dS \tag{32}$$

Carrying out the variation of equation (32), we obtain:

$$\delta\int_{t_1}^{t_2} T^* \; dt = \int_{t_1}^{t_2} \int_{C(t)}^{L_B} \rho A \left[\frac{\partial \bar{x}_1}{\partial t}\, \delta\left(\frac{\partial \bar{x}_1}{\partial t}\right) + \frac{\partial \bar{x}_2}{\partial t}\, \delta\left(\frac{\partial \bar{x}_2}{\partial t}\right)\right] dS \; dt \tag{33}$$

Using the Leibniz rule and carrying out the integrations by parts, after simplification and taking out the boundary terms, one may express equation (33) as:

$$\begin{aligned}\delta\int_{t_1}^{t_2} T^* \; dt = &- \int_{t_1}^{t_2} \int_{C(t)}^{L_B} \rho A \frac{\partial^2 \bar{x}_1}{\partial t^2}\, \delta(\bar{x}_1)\, dS \; dt - \\ &\int_{t_1}^{t_2} \int_{C(t)}^{L_B} \rho A \frac{\partial^2 \bar{x}_2}{\partial t^2}\, \delta\bar{x}_2 \; dS \; dt\end{aligned} \tag{34}$$

We obtain the variation of the strain energy in the same manner. To this end from equation (3.2.8) we obtain:

$$\Pi = \int_{C(t)}^{L_B} \frac{EI}{2} \left(\frac{\partial^2 \bar{x}_2}{\partial S^2}\right)^2 \left[1 + \left(\frac{\partial \bar{x}_2}{\partial S}\right)^2\right] dS \tag{35}$$

Hence:

$$\delta\int_{t_1}^{t_2} \Pi \ dt = \int_{t_1}^{t_2} \int_{C(t)}^{L_B} \frac{EI}{2} \delta\left\{ \left(\frac{\partial^2 \bar{x}_2}{\partial S^2}\right)^2 \left[1+\left(\frac{\partial \bar{x}_2}{\partial S}\right)^2\right]\right\} dSdt$$

$$= \int_{t_1}^{t_2} \int_{C(t)}^{L_B} EI \left(\frac{\partial^2 \bar{x}_2}{\partial S^2}\right) \left[1+\left(\frac{\partial \bar{x}_2}{\partial S}\right)^2\right] \delta\left(\frac{\partial^2 \bar{x}_2}{\partial S^2}\right) dSdt + \tag{36}$$

$$= \int_{t_1}^{t_2} \int_{C(t)}^{L_B} EI \left(\frac{\partial^2 \bar{x}_2}{\partial S^2}\right)^2 \left(\frac{\partial \bar{x}_2}{\partial S}\right) \delta\left(\frac{\partial \bar{x}_2}{\partial S}\right) dSdt$$

After carrying out the integrations by parts, simplifications and taking out the boundary terms, we may express the variation of strain energy of the system as:

$$\delta\int_{t_1}^{t_2} \Pi dt = \int_{t_1}^{t_2} \int_{C(t)}^{L_B} EI\left[\frac{\partial^4 \bar{x}_2}{\partial S^4} + \left(\frac{\partial^2 \bar{x}_2}{\partial S^2}\right)^3 + \frac{\partial^4 \bar{x}_2}{\partial S^4}\left(\frac{\partial \bar{x}_2}{\partial S}\right)^2 + 4\frac{\partial \bar{x}_2}{\partial S} \frac{\partial^2 \bar{x}_2}{\partial S^2} \frac{\partial^3 \bar{x}_2}{\partial S^3}\right] (\delta\bar{x}_2)\, dSdt \tag{37}$$

Now we use the inextensibility condition to express all the terms in equation (34) which include $\bar{x}_1$, in terms of $\bar{x}_2$. To this end we write the inetensibility condition as:

$$\left[\frac{\partial \bar{x}_1}{\partial S}\right]^2 + \left[\frac{\partial \bar{x}_2}{\partial S}\right]^2 = 1 \tag{38}$$

Hence we have (see Appendix A):

$$\delta\left(\frac{\partial \bar{x}_1}{\partial S}\right) \equiv - \frac{\partial \bar{x}_2}{\partial S} \left[1+\frac{1}{2}\left(\frac{\partial \bar{x}_2}{\partial S}\right)^2\right] \delta\left(\frac{\partial \bar{x}_2}{\partial S}\right) \tag{39}$$

Also we may write (see Appendix A):

$$\delta\bar{x}_1 \equiv - \left[\frac{\partial \bar{x}_2}{\partial S} + \frac{1}{2}\left(\frac{\partial \bar{x}_2}{\partial S}\right)^3\right]\delta\bar{x}_2 + \int_{C(t)}^{S} \left[\frac{\partial^2 \bar{x}_2}{\partial S^2} + \frac{3}{2}\left(\frac{\partial \bar{x}_2}{\partial S}\right)^2 \frac{\partial^2 \bar{x}_2}{\partial S^2}\right]\delta\bar{x}_2 \ dS \tag{40}$$

and

$$\frac{\partial^2 \bar{x}_1}{\partial t^2} = -\int_{C(t)}^{S} \left\{ \frac{\partial^3 \bar{x}_2}{\partial t^2 \partial S} \frac{\partial \bar{x}_2}{\partial S} \left[ 1 + \frac{1}{2} \left( \frac{\partial \bar{x}_2}{\partial S} \right)^2 \right] + \left( \frac{\partial^2 \bar{x}_2}{\partial t \partial S} \right)^2 \right\} dS \tag{41}$$

Relations (39), (40) and (41) may now be used to obtain the variation of the kinetic co-energy expressed in equation (34) in terms of $\bar{x}_2$. Hence after some manipulations, the term inside the first integral of equation (34) may be expressed as:

$$\begin{aligned}\int_{C(t)}^{L_B} \rho A \left[ \frac{\partial^2 \bar{x}_1}{\partial t^2} \right] \delta \bar{x}_1 dS \equiv & \int_{C(t)}^{L_B} \left\{ \rho A \frac{\partial \bar{x}_2}{\partial S} \int_{C(t)}^{S} \left[ \frac{\partial^3 \bar{x}_2}{\partial t^2 \partial S} \frac{\partial \bar{x}_2}{\partial S} + \left( \frac{\partial^2 \bar{x}_2}{\partial t \partial S} \right)^2 \right] \right. \\ & \left. dS \right\} \delta \bar{x}_2 \, dS - \\ & \int_{C(t)}^{L_B} \left\{ \rho A \int_{S}^{L_B} \left( \int_{C(t)}^{S} \left[ \frac{\partial^3 \bar{x}_2}{\partial t^2 \partial S} \frac{\partial \bar{x}_2}{\partial S} + \left( \frac{\partial^2 \bar{x}_2}{\partial t \partial S} \right)^2 \right] \right) \right. \\ & \left. dS \, dS \right\} \frac{\partial^2 \bar{x}_2}{\partial S^2} \delta \bar{x}_2 \, dS \end{aligned} \tag{42}$$

Now one may substitute the above relations in equation (34) and obtain an expression for the variation of kinetic co-energy. Then substitution $\delta T^*$ and $\delta \Pi$ into the extended Hamilton's principle introduced in chapter 3, will lead to the governing equation of motion as expressed in equation (3.2.10).

# Appendix D: Sliding Beam and Alternative Formulations in the Fixed Domain

To map equations (3.1.66) and (3.1.67) onto the fixed domain, we use the transformation given in equation (3.3.4), i.e.:

$$\begin{aligned} \eta_1 &= \frac{\chi_1}{L(t)} && \text{where } (0 < \eta_1 \le 1) \\ \eta_2 &= \chi_2 && \text{where } \left(-\frac{h}{2} < \eta_2 \le \frac{h}{2}\right) \end{aligned} \tag{43}$$

From equation (43) it can be seen that:

$$\begin{aligned} d\chi_1 &= L\ d\eta_1 \\ \frac{\partial u_i}{\partial \chi_1} &= \frac{\partial \hat{u}_i}{\partial \eta_1}\frac{\partial \eta_1}{\partial \chi_1} = \frac{1}{L}\frac{\partial \hat{u}_i}{\partial \eta_1} \\ \frac{\partial^2 u_i}{\partial {\chi_1}^2} &= \frac{\partial}{\partial \eta_1}\left(\frac{1}{L}\frac{\partial \hat{u}_i}{\partial \eta_1}\right) = \frac{1}{L^2}\frac{\partial^2 \hat{u}_i}{\partial {\eta_1}^2} \end{aligned} \tag{44}$$

where $i = 1, 2$ and

$$u_i(\chi_1(X_1, t), t) \rightarrow \hat{u}_i(\eta_1(X_1, t), t) \tag{45}$$

Also we have (see chapter 4):

$$\frac{\partial u_i}{\partial t} = \frac{\partial \hat{u}_i}{\partial \eta_1}\frac{\partial \eta_1}{\partial t} + \frac{\partial \hat{u}_i}{\partial t} \tag{46}$$

and

$$\frac{\partial^2 u_i}{\partial t^2} = \frac{\partial^2 \eta_1}{\partial t^2}\frac{\partial \hat{u}_i}{\partial \eta_1} + 2\frac{\partial \eta_1}{\partial t}\frac{\partial^2 \hat{u}_i}{\partial t \partial \eta_1} + \left(\frac{\partial \eta_1}{\partial t}\right)^2 \frac{\partial^2 \hat{u}_i}{\partial {\eta_1}^2} + \frac{\partial^2 \hat{u}_i}{\partial t^2} \tag{47}$$

where $i = 1, 2$. Substituting equations (4.1.11) and (4.1.12) into equations (46) and (47), we obtain:

$$\frac{\partial u_i}{\partial t} = -\frac{V}{L}\eta_1 \frac{\partial \hat{u}_i}{\partial \eta_1} + \frac{\partial \hat{u}_i}{\partial t} \tag{48}$$

and

$$\frac{\partial^2 u_i}{\partial t^2} = \frac{2V^2\eta_1 - L\frac{\partial V}{\partial t}\eta_1}{L^2} \frac{\partial \hat{u}_i}{\partial \eta_1} + 2\left(-\frac{V}{L}\eta_1\right)\frac{\partial^2 \hat{u}_i}{\partial t \partial \eta_1} + \left(-\frac{V}{L}\eta_1\right)^2 \frac{\partial^2 \hat{u}_i}{\partial \eta_1^{\,2}} + \frac{\partial^2 \hat{u}_i}{\partial t^2} \tag{49}$$

where $i = 1, 2$. Also using relation (44), we may write:

$$\begin{aligned}\frac{\partial^2 u_i}{\partial t \partial \chi_1} &= \frac{\partial}{\partial \eta_1}\left(\frac{1}{L}\frac{\partial \hat{u}_i}{\partial \eta_1}\right)\frac{\partial \eta_1}{\partial t} + \frac{\partial}{\partial t}\left(\frac{1}{L}\frac{\partial \hat{u}_i}{\partial \eta_1}\right) \\ &= -\frac{V}{L^2}\eta_1 \frac{\partial^2 \hat{u}_i}{\partial \eta_1^{\,2}} + \frac{1}{L}\frac{\partial^2 \hat{u}_i}{\partial t \partial \eta_1} - \frac{V}{L^2}\frac{\partial \hat{u}_i}{\partial \eta_1}\end{aligned} \tag{50}$$

where $i = 1, 2$. By substituting equations (44), (48), (49) and (50) into equation (3.1.66), we obtain the first governing equation of motion in the fixed domain as:

$$\begin{aligned}&\rho_o A\left[L^2\frac{\partial^2 \hat{u}_1}{\partial t^2} + L^2\frac{\partial V}{\partial t} + 2LV(1-\eta_1)\frac{\partial^2 \hat{u}_2}{\partial t \partial \eta_1} + V^2(1-\eta_1)^2\frac{\partial^2 \hat{u}_1}{\partial \eta_1^2} + \right. \\ &\left.(1-\eta_1)\left(L\frac{\partial V}{\partial t} - 2V^2\right)\frac{\partial \hat{u}_1}{\partial \eta_1}\right] - \\ &EA\left[\frac{\partial^2 \hat{u}_1}{\partial \eta_1^{\,2}} + \frac{1}{L}\left(\frac{\partial \hat{u}_2}{\partial \eta_1}\frac{\partial^2 \hat{u}_2}{\partial \eta_1^{\,2}}\right)\right] - \frac{EI}{L^3}\left[\frac{\partial^2 \hat{u}_2}{\partial \eta_1^{\,2}}\frac{\partial^3 \hat{u}_2}{\partial \eta_1^{\,3}} + \frac{\partial \hat{u}_2}{\partial \eta_1}\frac{\partial^4 \hat{u}_2}{\partial \eta_1^{\,4}}\right] = 0\end{aligned} \tag{51}$$

In the same way we obtain the second equation as given in (3.3.9).

Next let us transform the alternative equations of motion to the fixed domain. Thus we need to use the transformation introduced in equation (3.3.6) as:

$$\begin{aligned}\eta_1 &= \frac{X_1 - C(t)}{L(t)} & &\text{where } (0 < \eta_1 \le 1) \\ \eta_2 &= X_2 & &\text{where } \left(-\frac{h}{2} < \eta_2 \le \frac{h}{2}\right)\end{aligned} \tag{52}$$

From equation (52), we may express the following relations at time $t$:

$$dX_1 = L\ d\eta_1$$

$$\frac{\partial \bar{u}_i}{\partial X_1} = \frac{\partial \hat{u}_i}{\partial \eta_1}\frac{\partial \eta_1}{\partial X_1} = \frac{1}{L}\frac{\partial \hat{u}_i}{\partial \eta_1} \tag{53}$$

$$\frac{\partial^2 \bar{u}_i}{\partial X_1{}^2} = \frac{\partial}{\partial X_1}\left(\frac{1}{L}\frac{\partial \hat{u}_i}{\partial \eta_1}\right) = \frac{1}{L^2}\frac{\partial^2 \hat{u}_i}{\partial \eta_1{}^2}$$

where

$$\bar{u}_i(X_1, t) \equiv \hat{u}_i(\eta_1(X_1, t), t) \tag{54}$$

and $i = 1, 2$. Also from equation (52), we deduce that:

$$\frac{\partial \eta_1}{\partial t} = \frac{V}{L}\ (1 - \eta_1) \tag{55}$$

and

$$\frac{\partial^2 \eta_1}{\partial t^2} = \frac{L\dfrac{\partial V}{\partial t}(1-\eta_1) - 2V^2(1-\eta_1)}{L^2} \tag{56}$$

Now as in equations (4.1.9) and (4.1.10), we may also write:

$$\frac{\partial \bar{u}_i}{\partial t} = \frac{V}{L}(1-\eta_1)\ \frac{\partial \hat{u}_i}{\partial \eta_1} + \frac{\partial \hat{u}_i}{\partial t} \qquad i = 1, 2 \tag{57}$$

and

$$\frac{\partial^2 \bar{u}_i}{\partial t^2} = \frac{L\dfrac{\partial V}{\partial t}(1-\eta_1) - 2V^2(1-\eta_1)}{L^2}\ \frac{\partial \hat{u}_i}{\partial \eta_1} + 2\left[\frac{V}{L}\ (1-\eta_1)\right]\ \frac{\partial^2 \hat{u}_i}{\partial t \partial \eta_1} + \left[\frac{V}{L}\ (1-\eta_1)\right]^2\ \frac{\partial^2 \hat{u}_i}{\partial \eta_1{}^2} + \frac{\partial^2 \hat{u}_i}{\partial t^2} \qquad i = 1, 2 \tag{58}$$

On substituting equations (53), (57) and (58) into equation (3.2.15) the first equation of motion for the alternative formulation in fixed domain may be obtained as:

$$\rho_o A \left[ L^2 \frac{\partial^2 \hat{\bar{u}}_1}{\partial t^2} + L^2 \frac{\partial V}{\partial t} + 2LV(1-\eta_1)\frac{\partial^2 \hat{\bar{u}}_2}{\partial t \partial \eta_1} + V^2 (1-\eta_1)^2 \frac{\partial^2 \hat{\bar{u}}_1}{\partial \eta_1^2} + \right.$$

$$\left. (1-\eta_1)\left( L \frac{\partial V}{\partial t} - 2V^2 \right) \frac{\partial \hat{\bar{u}}_1}{\partial \eta_1} \right] - \tag{59}$$

$$EA \left[ \frac{\partial^2 \hat{\bar{u}}_1}{\partial {\eta_1}^2} + \frac{1}{L} \left( \frac{\partial \hat{\bar{u}}_2}{\partial \eta_1} \frac{\partial^2 \hat{\bar{u}}_2}{\partial {\eta_1}^2} \right) \right] - \frac{EI}{L^3} \left[ \frac{\partial^2 \hat{\bar{u}}_2}{\partial {\eta_1}^2} \frac{\partial^3 \hat{\bar{u}}_2}{\partial {\eta_1}^3} + \frac{\partial \hat{\bar{u}}_2}{\partial \eta_1} \frac{\partial^4 \hat{\bar{u}}_2}{\partial {\eta_1}^4} \right] = 0$$

which is identical to equation (51). In the same way we obtain the second equation of motion in the fixed domain and show that it is identical to that obtained in the sliding beam formulation in the fixed domain.

# Appendix E: Equation of Motion for Linear Axially Inextensible Flexible Sliding Beams in Fixed Domain

Consider the Lagrangian given in equation (4.1.17) as:

$$\mathcal{L}_{oL} = \int_0^1 \left\{ \frac{1}{2}\rho A \left[ \frac{V}{L}(1-\mathcal{S})\frac{\partial \hat{x}_2}{\partial \mathcal{S}} + \frac{\partial \hat{x}_2}{\partial t} \right]^2 - \frac{EI}{2L^4}\left( \frac{\partial^2 \hat{x}_2}{\partial \mathcal{S}^2} \right)^2 \right\} L d\mathcal{S} \tag{60}$$

Now the variation of equation (60) can be written as:

$$\begin{aligned} \delta\int_{t_1}^{t_2} \mathcal{L}_{oL}\, dt = \int_{t_1}^{t_2}\int_0^1 \Bigg\{ &\rho A \left[ \frac{V}{L}(1-\mathcal{S})\frac{\partial \hat{x}_2}{\partial \mathcal{S}} + \frac{\partial \hat{x}_2}{\partial t} \right] \delta\left[ \frac{V}{L}(1-\mathcal{S})\frac{\partial \hat{x}_2}{\partial \mathcal{S}} + \frac{\partial \hat{x}_2}{\partial t} \right] - \\ &\frac{EI}{L^4}\frac{\partial^2 \hat{x}_2}{\partial \mathcal{S}^2}\,\delta\left( \frac{\partial^2 \hat{x}_2}{\partial \mathcal{S}^2} \right) \Bigg\} L\, d\mathcal{S}\, dt \end{aligned} \tag{61}$$

Carrying out the integrations by parts and taking out the geometric and natural boundary conditions, we may express all terms on the right hand side of equation (61) as:

$$\begin{aligned} \int_0^1 \rho A \frac{V^2}{L^2}(1-\mathcal{S})^2 \frac{\partial \hat{x}_2}{\partial \mathcal{S}}\,\delta\left( \frac{\partial \hat{x}_2}{\partial \mathcal{S}} \right) L d\mathcal{S} = &\int_0^1 2\rho A \frac{V^2}{L^2}(1-\mathcal{S})\,\frac{\partial \hat{x}_2}{\partial \mathcal{S}}\,(\delta\hat{x}_2)\, L d\mathcal{S} - \\ &\int_0^1 \rho A \frac{V^2}{L^2}(1-\mathcal{S})^2\,\frac{\partial^2 \hat{x}_2}{\partial \mathcal{S}^2}\,(\delta\hat{x}_2)\, L d\mathcal{S} \end{aligned} \tag{62}$$

and

$$\begin{aligned} \int_0^1 \rho A \frac{V}{L}(1-\mathcal{S})\,\frac{\partial \hat{x}_2}{\partial t}\,\delta\left( \frac{\partial \hat{x}_2}{\partial \mathcal{S}} \right) L d\mathcal{S} = &\int_0^1 \rho A \frac{V}{L}\,\frac{\partial \hat{x}_2}{\partial t}\,(\delta\hat{x}_2)\, L d\mathcal{S} - \\ &\int_0^1 \rho A \frac{V}{L}(1-\mathcal{S})\,\frac{\partial^2 \hat{x}_2}{\partial t\partial \mathcal{S}}\,(\delta\hat{x}_2)\, L d\mathcal{S} \end{aligned} \tag{63}$$

and

$$\int_0^1 \rho A \frac{V}{L}(1-S)\ \frac{\partial \hat{x}_2}{\partial S}\ \delta\left(\frac{\partial \hat{x}_2}{\partial t}\right) L dS = -\int_0^1 \frac{\rho A}{L}\ \frac{\partial V}{\partial t}(1-S)\ \frac{\partial \hat{x}_2}{\partial S}\ (\delta \hat{x}_2)\, L dS - \int_0^1 \rho A \frac{V}{L}(1-S)\ \frac{\partial^2 \hat{x}_2}{\partial t \partial S}\ (\delta \hat{x}_2)\, L dS \tag{64}$$

and

$$\int_0^1 \rho A L\ \frac{\partial \hat{x}_2}{\partial t}\ \delta\left(\frac{\partial \hat{x}_2}{\partial t}\right) dS = -\int_0^1 \rho A \frac{V}{L}\ \frac{\partial \hat{x}_2}{\partial t}\ (\delta \hat{x}_2)\, L dS - \int_0^1 \rho A\ \frac{\partial^2 \hat{x}_2}{\partial t^2}\ (\delta \hat{x}_2)\, L dS \tag{65}$$

and

$$\int_0^1 \frac{EI}{L^4}\ \frac{\partial^2 \hat{x}_2}{\partial S^2}\ \delta\left(\frac{\partial^2 \hat{x}_2}{\partial S^2}\right) L dS = \int_0^1 \frac{EI}{L^4}\ \frac{\partial^4 \hat{x}_2}{\partial S^4}\ (\delta \hat{x}_2)\, L dS \tag{66}$$

On substituting equations (62) to (66) into the extended Hamilton's principle given in equation (4.1.18), and noting the arbitrariness of $\delta \hat{x}_2$, we obtain the governing equation of motion for the linear axially inextensible flexible sliding beam, in the fixed domain and in the absence of shortening effect as:

$$\rho A \left\{ \frac{\partial^2 \hat{x}_2}{\partial t^2} + \frac{2V}{L}(1-S)\frac{\partial^2 \hat{x}_2}{\partial t \partial S} + \frac{V^2}{L^2}(1-S)^2\ \frac{\partial^2 \hat{x}_2}{\partial S^2} + \left[\frac{2V^2}{L^2}S - \frac{2V^2}{L^2} + \frac{1}{L}\ \frac{\partial V}{\partial t} - \frac{1}{L}\ \frac{\partial V}{\partial t} S\right] \frac{\partial \hat{x}_2}{\partial S} \right\} + \frac{EI}{L^4}\ \frac{\partial^4 \hat{x}_2}{\partial S^4} = 0 \tag{67}$$

# Appendix F: Element Internal Force Vector and Tangent Stiffness Matrix

To express the internal force vector and the tangent stiffness matrix of the sliding beam in terms of the nodal variables, first we use relations (5.1.7), (5.1.8), (5.1.9), (5.1.10) and (5.1.11) to obtain the strain energy of the system as introduced in equation (5.1.6) in terms of the nodal variables. Then we substitute the resulting discretized strain energy of the system into equations (5.1.23) and (5.1.26) which leads to the desired internal force vector and tangent stiffness matrix.

In the following the internal force vector is given and for simplicity it is divided into several vectors:

Internal forces due to axial strain:

$$\{f_1\} = EA \int_0^{\hat{l}(t)} \left\lfloor \frac{\partial N_1}{\partial \chi_1} \right\rfloor^T \left\lfloor \frac{\partial N_1}{\partial \chi_1} \right\rfloor \{\hat{u}\}\, d\chi_1 \,. \tag{68}$$

$$\{f_2\} = \frac{EA}{2} \int_0^{\hat{l}(t)} \left\lfloor \frac{\partial N_1}{\partial \chi_1} \right\rfloor^T \left( \left\lfloor \frac{\partial N_2}{\partial \chi_1} \right\rfloor \{\hat{u}\} \right)^2 d\chi_1 \,. \tag{69}$$

$$\{f_3\} = EA \int_0^{\hat{l}(t)} \left\lfloor \frac{\partial N_2}{\partial \chi_1} \right\rfloor^T \left( \{\hat{u}\}^T \left\lfloor \frac{\partial N_1}{\partial \chi_1} \right\rfloor^T \right) \left( \left\lfloor \frac{\partial N_2}{\partial \chi_1} \right\rfloor \{\hat{u}\} \right) d\chi_1 \tag{70}$$

and

$$\{f_4\} = \frac{EA}{2} \int_0^{\hat{l}(t)} \left\lfloor \frac{\partial N_2}{\partial \chi_1} \right\rfloor^T \left( \left\lfloor \frac{\partial N_2}{\partial \chi_1} \right\rfloor \{\hat{u}\} \right)^3 d\chi_1 \tag{71}$$

Internal forces due to curvature:

$$\{f_5\} = EI \int_0^{\hat{l}(t)} \left\lfloor \frac{\partial^2 N_2}{\partial \chi_1^2} \right\rfloor^T \left\lfloor \frac{\partial^2 N_2}{\partial \chi_1^2} \right\rfloor \{\hat{u}\}\, d\chi_1 \,. \tag{72}$$

$$\{f_6\} = -2EI\int_0^{\hat{l}(t)} \left\lfloor\frac{\partial^2 N_2}{\partial x_1^2}\right\rfloor^T \left(\left\lfloor\frac{\partial N_1}{\partial x_1}\right\rfloor \{\hat{u}\}\right)\left(\left\lfloor\frac{\partial^2 N_2}{\partial x_1^2}\right\rfloor \{\hat{u}\}\right)dx_1, \tag{73}$$

$$\{f_7\} = -\ EI\int_0^{\hat{l}(t)} \left\lfloor\frac{\partial N_1}{\partial x_1}\right\rfloor^T \left(\left\lfloor\frac{\partial^2 N_2}{\partial x_1^2}\right\rfloor \{\hat{u}\}\right)^2 dx_1, \tag{74}$$

$$\{f_8\} = -2EI\int_0^{\hat{l}(t)} \left\lfloor\frac{\partial^2 N_2}{\partial x_1^2}\right\rfloor^T \left(\left\lfloor\frac{\partial N_2}{\partial x_1}\right\rfloor \{\hat{u}\}\right)\left(\left\lfloor\frac{\partial N_2}{\partial x_1}\right\rfloor \{\hat{u}\}\right)^2 dx_1 \tag{75}$$

and

$$\{f_9\} = -2EI\int_0^{\hat{l}(t)} \left\lfloor\frac{\partial N_2}{\partial x_1}\right\rfloor^T \left(\left\lfloor\frac{\partial^2 N_2}{\partial x_1^2}\right\rfloor \{\hat{u}\}\right)^2 \left(\left\lfloor\frac{\partial N_2}{\partial x_1}\right\rfloor \{\hat{u}\}\right)dx_1 \tag{76}$$

We may also split the tangent stiffness matrix of the system into several matrices and express them as:

The tangent stiffness matrices due to axial strain:

$$[K_1] = EA\int_0^{\hat{l}(t)} \left\lfloor\frac{\partial N_1}{\partial x_1}\right\rfloor^T \left\lfloor\frac{\partial N_1}{\partial x_1}\right\rfloor dx_1. \tag{77}$$

$$[K_2] = EA\int_0^{\hat{l}(t)} \left\lfloor\frac{\partial N_1}{\partial x_1}\right\rfloor^T \left\lfloor\frac{\partial N_2}{\partial x_1}\right\rfloor \left(\left\lfloor\frac{\partial N_2}{\partial x_1}\right\rfloor \{\hat{u}\}\right)dx_1. \tag{78}$$

$$\begin{aligned}[K_3] = EA\int_0^{\hat{l}(t)} \left\lfloor\frac{\partial N_2}{\partial x_1}\right\rfloor^T \left\lfloor\frac{\partial N_1}{\partial x_1}\right\rfloor \left(\left\lfloor\frac{\partial N_2}{\partial x_1}\right\rfloor \{\hat{u}\}\right)dx_1 + \\ EA\int_0^{\hat{l}(t)} \left\lfloor\frac{\partial N_2}{\partial x_1}\right\rfloor^T \left\lfloor\frac{\partial N_2}{\partial x_1}\right\rfloor \left(\left\lfloor\frac{\partial N_1}{\partial x_1}\right\rfloor \{\hat{u}\}\right)dx_1\end{aligned} \tag{79}$$

and

$$[K_4] = \frac{3}{2}EA\int_0^{\hat{l}(t)} \left\lfloor\frac{\partial N_2}{\partial x_1}\right\rfloor^T \left\lfloor\frac{\partial N_2}{\partial x_1}\right\rfloor \left(\left\lfloor\frac{\partial N_2}{\partial x_1}\right\rfloor \{\hat{u}\}\right)^2 dx_1 \tag{80}$$

The tangent stiffness matrices due to curvature:

$$[K_5] = EI \int_0^{\hat{l}(t)} \left\lfloor \frac{\partial^2 N_2}{\partial \chi_1^2} \right\rfloor^T \left\lfloor \frac{\partial^2 N_2}{\partial \chi_1^2} \right\rfloor d\chi_1 . \tag{81}$$

$$\begin{aligned}[K_6] = &-2EI \int_0^{\hat{l}(t)} \left\lfloor \frac{\partial^2 N_2}{\partial \chi_1^2} \right\rfloor^T \left\lfloor \frac{\partial N_1}{\partial \chi_1} \right\rfloor \left( \left\lfloor \frac{\partial^2 N_2}{\partial \chi_1^2} \right\rfloor \{\hat{u}\} \right) d\chi_1 - \\ &2EI \int_0^{\hat{l}(t)} \left\lfloor \frac{\partial^2 N_2}{\partial \chi_1^2} \right\rfloor^T \left\lfloor \frac{\partial^2 N_2}{\partial \chi_1^2} \right\rfloor \left( \left\lfloor \frac{\partial N_1}{\partial \chi_1} \right\rfloor \{\hat{u}\} \right) d\chi_1\end{aligned} \tag{82}$$

$$[K_7] = -2EI \int_0^{\hat{l}(t)} \left\lfloor \frac{\partial N_1}{\partial \chi_1} \right\rfloor^T \left\lfloor \frac{\partial^2 N_2}{\partial \chi_1^2} \right\rfloor \left( \left\lfloor \frac{\partial^2 N_2}{\partial \chi_1^2} \right\rfloor \{\hat{u}\} \right) d\chi_1 . \tag{83}$$

$$\begin{aligned}[K_8] = &-2EI \int_0^{\hat{l}(t)} \left\lfloor \frac{\partial^2 N_2}{\partial \chi_1^2} \right\rfloor^T \left\lfloor \frac{\partial^2 N_2}{\partial \chi_1^2} \right\rfloor \left( \left\lfloor \frac{\partial N_2}{\partial \chi_1} \right\rfloor \{\hat{u}\} \right)^2 d\chi_1 - \\ &2EI \int_0^{\hat{l}(t)} \left\lfloor \frac{\partial^2 N_2}{\partial \chi_1^2} \right\rfloor^T \left\lfloor \frac{\partial N_2}{\partial \chi_1} \right\rfloor \left( \left\lfloor \frac{\partial^2 N_2}{\partial \chi_1^2} \right\rfloor \{\hat{u}\} \right) \left( \left\lfloor \frac{\partial N_2}{\partial \chi_1} \right\rfloor \{\hat{u}\} \right) d\chi_1\end{aligned} \tag{84}$$

and

$$\begin{aligned}[K_9] = &-4EI \int_0^{\hat{l}(t)} \left\lfloor \frac{\partial N_2}{\partial \chi_1} \right\rfloor^T \left\lfloor \frac{\partial^2 N_2}{\partial \chi_1^2} \right\rfloor \left( \left\lfloor \frac{\partial^2 N_2}{\partial \chi_1^2} \right\rfloor \{\hat{u}\} \right) \left( \left\lfloor \frac{\partial N_2}{\partial \chi_1} \right\rfloor \{\hat{u}\} \right) d\chi_1 - \\ &2EI \int_0^{\hat{l}(t)} \left\lfloor \frac{\partial N_2}{\partial \chi_1} \right\rfloor^T \left\lfloor \frac{\partial N_2}{\partial \chi_1} \right\rfloor \left( \left\lfloor \frac{\partial^2 N_2}{\partial \chi_1^2} \right\rfloor \{\hat{u}\} \right)^2 d\chi_1\end{aligned} \tag{85}$$

# Appendix G: Expression for the Rate of Change of $[\mathcal{H}]$ in Time

From equation (5.2.54):

$$\left[\frac{d\mathcal{H}}{dt}\right] = \left[\frac{\partial \mathcal{H}}{\partial t}\right] + v_i \left[\frac{\partial \mathcal{H}}{\partial \chi_1}\right] \tag{86}$$

We know from equations (5.2.18) and (5.2.19) that the shape functions are in terms of natural coordinate where:

$$\zeta = -1 + \frac{2\chi_1}{\hat{l}(t)} \tag{87}$$

Thus we have:

$$\frac{\partial \zeta}{\partial \chi_1} = \frac{2}{\hat{l}(t)} \tag{88}$$

and

$$\frac{\partial \zeta}{\partial t} = 2\chi_1 \left( - \frac{\frac{\partial}{\partial t}\hat{l}}{\hat{l}^2} \right) = - \frac{\partial}{\partial t}\hat{l} \, \frac{(1+\zeta)}{\hat{l}} \tag{89}$$

Now we may write equation (86) in the following form:

$$\left[\frac{d\mathcal{H}}{dt}\right] = \left[\frac{\partial \mathcal{H}}{\partial \zeta}\frac{\partial \zeta}{\partial t}\right] + \left[\frac{\partial \mathcal{H}}{\partial \hat{l}}\frac{\partial}{\partial t}\hat{l}\right] + v_i \left[\frac{\partial \mathcal{H}}{\partial \zeta}\frac{\partial \zeta}{\partial \chi_1}\right] \tag{90}$$

Substituting relations (88) and (89) into equation (90), we obtain:

$$\left[\frac{d\mathcal{H}}{dt}\right] = \left( \frac{2v_i - \frac{\partial}{\partial t}\hat{l} \, (1+\zeta)}{\hat{l}} \right) \left[\frac{\partial \mathcal{H}}{\partial \zeta}\right] + \left[\frac{\partial \mathcal{H}}{\partial \hat{l}}\frac{\partial}{\partial t}\hat{l}\right] \tag{91}$$

# Appendix H: The Nonlinear Dependence of the Out of Balance Force $\phi$ in the Orientation of Axis $\varphi$

To show the nonlinear dependency of the out of balance force vector on the rigid body rotation of the co-rotational axis, we need to calculate the $\mathbf{G}$ matrix given by:

$$\mathbf{G}^T = \begin{bmatrix} \mathbf{g}_1^T \\ \mathbf{g}_2^T \end{bmatrix} \tag{92}$$

where

$$\mathbf{g}_1^T = \begin{bmatrix} -\cos\varphi & -\sin\varphi & 0 & \cos\varphi & \sin\varphi & 0 \end{bmatrix} \tag{93}$$

and

$$\mathbf{g}_2 = \begin{bmatrix} -\dfrac{1}{\cos\tilde{\theta}_1}\,\mathbf{g}_{21}^T, & -\dfrac{1}{\cos\tilde{\theta}_2}\,\mathbf{g}_{22}^T \end{bmatrix} \tag{94}$$

Let us first expand the row vector $\mathbf{g}_{21}^T$ in equation (2.1.68). Using equations (2.1.65), (2.1.53) and (2.1.54):

$$\begin{aligned} \mathbf{a}_2\ \mathbf{A} &= \mathbf{a}_2\ \left\{\frac{1}{l_c}[\mathbf{I} - \tilde{\mathbf{e}}_1 \otimes \tilde{\mathbf{e}}_1]\right\} = \frac{1}{l_c}\ [\mathbf{a}_2\ \mathbf{I} - (\mathbf{a}_2 \cdot \tilde{\mathbf{e}}_1)\,\tilde{\mathbf{e}}_1] \\ &= \frac{1}{l_c}\ \lfloor -\sin\alpha \quad \cos\alpha \rfloor + \frac{1}{l_c}\ \sin\tilde{\theta}_1\ \lfloor \cos\varphi \quad \sin\varphi \rfloor \end{aligned} \tag{95}$$

Knowing that $\alpha = \varphi + \tilde{\theta}_1$, after some manipulations we obtain:

$$\mathbf{a}_2\ \mathbf{A} = \frac{1}{l_c}\ \lfloor -\sin\varphi\ \cos\tilde{\theta}_1 \qquad \cos\varphi\ \cos\tilde{\theta}_1 \rfloor \tag{96}$$

Also from Figure 2.1.15, we have:

$$-\tilde{\mathbf{e}}_1 \cdot \mathbf{a}_1 = -\cos\tilde{\theta}_1 \tag{97}$$

Hence we obtain:

$$\mathbf{g}_{21}^{T} = \cos\tilde{\theta}_1 \left[\frac{1}{l_c}\sin\varphi,\ -\frac{1}{l_c}\cos\varphi,\ -1,\ -\frac{1}{l_c}\sin\varphi,\ \frac{1}{l_c}\cos\varphi,\ 0\right] \tag{98}$$

The expanded form of $\mathbf{g}_{22}^{T}$ can also be found in the same way and we have:

$$\mathbf{g}_{22}^{T} = \cos\tilde{\theta}_2 \left[\frac{1}{l_c}\sin\varphi,\ -\frac{1}{l_c}\cos\varphi,\ 0,\ -\frac{1}{l_c}\sin\varphi,\ \frac{1}{l_c}\cos\varphi,\ -1\right] \tag{99}$$

Substituting equations (93) and (98) into equation (94) and the result with equation (99) into equation (92), we find:

$$\mathbf{G} = \begin{bmatrix} -\cos\varphi & -\frac{1}{l_c}\sin\varphi & -\frac{1}{l_c}\sin\varphi \\ -\sin\varphi & \frac{1}{l_c}\cos\varphi & \frac{1}{l_c}\cos\varphi \\ 0 & 1 & 0 \\ \cos\varphi & \frac{1}{l_c}\sin\varphi & \frac{1}{l_c}\sin\varphi \\ \sin\varphi & -\frac{1}{l_c}\cos\varphi & -\frac{1}{l_c}\cos\varphi \\ 0 & 0 & 1 \end{bmatrix} \tag{100}$$

Now using equation (100) and referring to equation (2.1.77), one can see that the out of balance force vector is a nonlinear function of the rigid body rotation of the co-rotational frame.